INSTITUTO TECNOLOGICO Y DE ESTUDIOS SUPERIORES DE MONTERREY

CAMPUS MONTERREY

DIVISION DE INGENIERIA Y ARQUITECTURA

PROGRAMA DE GRADUADOS EN INGENIERIA

TECNOLÓGICO DE MONTERREY®

"MODIFICATION OF THE PTT MODEL AND ITS APPLICATION FOR THE PREDICTIONS OF ELONGATIONAL VISCOSITY OF POLYPROPYLENES"

TESIS

PRESENTADA COMO REQUISITO PARCIAL PARA OBTENER EL GRADO ACADEMICO DE:

MAESTRO EN CIENCIAS

CON ESPECIALIDAD EN SISTEMAS AMBIENTALES

POR:

LEONARDO FEDERICO CORTES RODRIGUEZ

MONTERREY, N. L. MAYO 2004

INSTITUTO TECNOLOGICO Y DE ESTUDIOS SUPERIORES DE MONTERREY

CAMPUS MONTERREY

DIVISION DE INGENIERIA Y ARQUITECTURA
PROGRAMA DE GRADUADOS EN INGENIERIA

TECNOLÓGICO
DE MONTERREY.

"MODIFICATION OF THE PTT MODEL AND ITS APPLICATION FOR THE PREDICTIONS OF ELONGATIONAL VISCOSITY OF POLYPROPYLENES"

TESIS
PRESENTADA COMO REQUISITO PARCIAL PARA
OBTENER EL GRADO ACADEMICO DE:

MAESTRO EN CIENCIAS
CON ESPECIALIDAD EN SISTEMAS AMBIENTALES

POR:
LEONARDO FEDERICO CORTES RODRIGUEZ

MONTERREY, N. L. MAYO 2004

ABSTRACT

A comprehensive rheological study of four pairs of isotactic and syndiotactic polypropylene resins with similar MFI was conducted. The study also includes the standard quality properties commonly used in the industry. The rheological tests included double bore capillary rheometry, frequency sweeps and creep and recovery compliance. The standard quality properties tested were percentage of Xylene Solubles (XS), Gel Permation Chromatography (GPC), Nuclear Magnetic Resonance (NMR) and Differential Scanning Calorimetry (DSC). It was found that the viscoelastic behavior is significantly different between these two types of resins.

On the other hand, the PTT (Phan Thien and Tanner, 1977) and XPP (Verbeeten, 2001) models were analyzed and evaluated using the experimental data of the resins under study. It was found that the PTT model fails to predict accurately the elongational response of the syndiotactic resins.

In addition, a modified PTT model is proposed and evaluated with satisfactory results. The parameters of this new model were found to be related to molecular weight distributions features such as Mz and Me.

Additionally, an innovative approach using fractals theory is proposed for the development of a new fundamental constitutive equation. Further study is recommended to this topic as well as to the modified PTT model.

DEDICATION

To my grandmother and greatest person

Fili

To my parents

Oscar Federico and Ana María

for all your love, support, patience, wisdom and confidence received in my early and present days. Thank you for all the positive examples and good familiar principles. You have taught me to challenge new opportunities in my life and become a better human being.

To my fiancée

Karla Janet

the love and understanding you gave me was the engine for accomplishing this goal in my life. Thank you for your beautiful smile, your support and your patience.

ACKNOWLEDGMENTS

First of all, I want to thank **God** for giving me the health and strength to accomplish this goal in my life.

To Jaime Bonilla Ríos, Ph.D.

Thank you for offering me the Research Assistant position in the first place, and for the opportunity and privilege of being your student. Thank you for your continuous and invaluable advices during the course of this research and for the countless hours you spent teaching me how to improve my technical skills, and for increasing my general knowledge and not only in the field of rheology. Thank you for directing me to be consistent and for offering me your knowledge and experience.

I want to thank you also for introducing me to Total's research team and for the exposure to the industrial applied research environment. It was a great pleasure for me to work in an international environment on such an exciting subject under your supervision.

Furthermore, I want to thank you for the demand for academic excellence through my Master studies, and for proof-reading this document.

To Michel Daumarie, Ph.D.

Thank you for the support, time and trust received for doing this project. I will forever appreciate the unique opportunity you gave me and the exposure to the industrial applied research environment.

To Joaquin Acevedo, Ph.D.

Thank you for accepting being Member of the Committee, for your teachings and for your helpful comments.

I would like to thank all those at **I.T.E.S.M.** who made possible my Masters Degree:

To all my professors for your teachings and for sharing your knowledge and experience.

To Elva Cavazos, Genaro Tamez, Manuel Ramos, Ester Niño and Dolores Coronado for all your assistance and administrative support.

I would like to thank also the team that made possible the work done in this thesis at **Total's Research and Technology Center**:

To Dorothy Bartol, Jeff Nairn, Juan Jose Aguirre, Rodolfo Mier, and Greg Kaase for their time, interest, support, technical advises, attentions, and for helping me getting things done during my internships.

To Rodolfo Mier, Jeff Nairn, Bobby Stokes, Theresa Lewis and Michael Schmidt for teaching me how to use the rheometers. Jeff's interest on the area was always very important.

Furthermore, I am grateful to Jordan Koniski, Ph.D., Enrique Barrera, Ph.D., Kay McStay, Judith Farhat, Susan Massey, Sandra Bloem, Adria Baker and all those who made possible the academic exchange at **Rice University**.

Special gratitude to all **my Family. My parents, Oscar Federico and Ana María,** thank you for all your love, patience, wisdom and confidence received in my early and present days. Thank you also for the financial support for all these years. **My brothers, Oscar Francisco and Hugo Fernando,** thank you for your friendship and invaluable support. **My fiancée, Karla Janet**, thank you for all your love and understanding.

I would like to thank Jesus Valencia, Rocío Hernandez, Mónica Macías, Raziel Cazares, Carlos Moráles and all colleagues of the institute for the pleasant time I spent at Monterrey Tech. I would also like to thank Juan Aguirre, Rodolfo Mier, Julio Hernandez, Daniel Amador and all those who helped me during my internships in Houston.

Finally, I want to thank the **INSTITUTO TECNOLOGICO Y DE ESTUDIOS SUPERIORES DE MONTERREY** (Monterrey, N.L., México) for the excellence scholarship that covered the graduate program tuition, and **TOTAL PETROCHEMICALS** (Houston, TX., USA) for providing the financial support.

NOMENCLATURE

a	Yasuda or Cross model parameter
a_i	Giesekus model parameters a_1 , a_2 , a_3
a_k	Weighting factor for the exponential terms of the memory function $\eta_k / (\lambda_k)^2$
a_T	Horizontal temperature shift factor
A	Modified PTT model parameter.
b_T	Vertical temperature shift factor
B	Finger strain tensor or die swell
B	Modified PTT model parameter.
BHT	2-6 di-tert-butyl-p-cresol
B^{-1}	Cauchy finite strain tensor
C	Modified PTT model parameter.
D	Capillary diameter in capillary rheometry
D_p	Diameter of the extrudate after die swell
DSC	Differential scanning calorimeter
E_H	Horizontal activation energy for flow
E_V	Vertical activation energy for flow
f_1 , f_2	Weighting factor for damping function
G'(ω)	Storage modulus
G"(ω)	Loss modulus
G*(ω)	Complex modulus G'(ω) + *i*G"(ω)
G(t)	Relaxation modulus
G_N^o	Plateau modulus
GPC	Gel permeation chromatography
$G_x(\omega_x)$	Cross-over modulus
G_i	Shear modulus η_i / λ_i in relaxation spectra
G_0	Plateau Modulus
$h(I_1, I_2)$	Damping function
HDPE	High density polyethylene
I	Identity tensor
I_1	First scalar invariant of the Finger tensor
I_2	Second scalar invariant of the Finger tensor
I_3	Third scalar invariant of the Finger tensor
"i"	As a subscript refers to the contribution for the stress tensor of the i-th relaxation element

"i"	As a superscript refers to the component of the stress tensor
iPP	Isotactic polypropylene
J(t)	Creep compliance
J_e^o	Steady state recoverable compliance
Jmax	Maximum compliance $J(t_o)$
Jr(t)	Recoverable compliance at any time after the stress ceased
Je(t)	Elastic compliance $J_r(0) - J_r(t)$
L	Length of the capillary die or spinning
L_L	Length of the long capillary die in the double barrel rheometer (Rosand)
L_S	Length of the short capillary die in the double barrel rheometer (Rosand)
L / D	Length to diameter ratio for capillary die
LDPE	Low density polyethylene
MFI	Melt flow index
Mn	Average number molecular weight
Mw	Average molecular weight
MWD	Molecular weight distribution
Mz	Third moment of the molecular weight
M(t-t')	Memory function
m	Consistency (power law parameter)
m'	Parameter for Hershel-Bulkley model
N	Number of relaxation elements
NMR	Nuclear Magnetic Resonance
$N_1(t,\dot{\gamma})$	First normal stress difference
n_1, n_2	Damping function strain sensitive parameters
n	Power-law model parameter
n'	Parameter for Hershel-Bulkley model
PDI	Polydispersity index Mw/Mn
PTT	Phan-Thien and Tanner
p	Isotropic pressure
q	Dangling arms in a pom-pom molecule
Q	Volumetric flow rate through die
RAA	Rheometrics asphalt analyzer
RDA	Rheometrics dynamic analyzer
RS5000	Rheometrics stress rheometer
R_b	Radius of the barrel or reservoir
R^2	Correlation coefficient

S	Second moment of the orientation distribution of backbone segments in XPP model
$S_{(1)}$	Convected time derivative of S tensor.
sPP	Syndiotactic Polypropylene
SQP	Standard quality properties
T	Temperature
Tg	Glass transition temperature
Tm	Melting temperature
To	Reference temperature
TTS	Time-Temperature Superposition
t	Time
t'	Time relative to the position at time t
t_o	Time at which stress ceases in a creep test
tan $\delta(\omega)$	Loss tangent, ratio of G''(ω)/G'(ω)
u	Dimensionless axial velocity $u = \upsilon / \upsilon_o$
$W(I_1,I_2)$	Potential Function in Wagner Model
XPP	Extended Pom-Pom
XS	Percentage of xylene solubles
$Z(tr\tau_i)$	Rate of destruction of junctions function of the PTT model corresponding to the i-th contribution to the stress

Greek Symbols

α	PTT model elongational parameter.
α	XPP model parameter defining the amount of anisotropy.
$\gamma(t)$	Imposed shear strain $\gamma(t) = \gamma_o \sin(\omega t)$
γ_o	Strain amplitude in an oscillatory test
γ_r	Recovered shear strain in a creep test
$\dot{\gamma}$	Rate of strain (deformation) tensor
$\dot{\gamma}_o$	Imposed shear rate
$\dot{\gamma}_a$	Apparent shear rate $(32Q)/(\pi D^3)$
$\dot{\gamma}_t$	Corrected shear rate $\left[\frac{3n+1}{4n}\right]\dot{\gamma}_a$
$\dot{\gamma}_{ii}$	Shear rate tensor component
ΔP_E	Pressure drop due to elasticity of the melt
ΔP_L	Long capillary die pressure drop
ΔP_S	Short capillary die pressure drop

ΔP_T	Total pressure drop ΔP_V + ΔP_E
ΔP_V	Pressure drop due to viscosity of the melt
ε	Elongational (Henky) strain
$\dot{\varepsilon}$	Extension rate
$\dot{\varepsilon}_{max}$	Maximum extension rate
η_a	Apparent shear viscosity $\eta_a = \tau_w / \dot{\gamma}_a$
η_i or η_k	Relaxation spectrum viscosity
η_o	Zero shear viscosity
$\eta(t, \dot{\gamma})$	Shear viscosity
$\bar{\eta}_1(\dot{\varepsilon}, b)$	Shear free viscosity function
$\bar{\eta}_2(\dot{\varepsilon}, b)$	Shear free viscosity function
$\eta_e(\dot{\varepsilon})$	Elongational viscosity $\bar{\eta}_1(\dot{\varepsilon}, 0)$
η_t	True shear viscosity from capillary data
$\eta'(\omega)$	Dynamic viscosity G''(ω) / ω
$\eta''(\omega)$	Imaginary component of complex viscosity
$\eta^*(\omega)$	Complex viscosity
θ	Capillary die entrance angle: Flat entrance θ = 180° = π radian Cone entrance θ = 90° = π /2 radian
λ_C	Cross model characteristic time
λ_i or λ_k	Relaxation spectrum time
λ_{0b}	Relaxation time of the backbone tube orientation in the XPP model.
λ_s	Stretch relaxation time.
Λ	Stretch ratio of the backbone in XPP model
ν	Measure of the influence of surroundings polymer chains on the backbone tube stretch
μ	Newtonian viscosity
ξ	PTT model shear parameter.
ρ	Density
σ_e	Extensional (elongational) stress
σ_o	Stress amplitude
$\sigma(t)$	Sinusoidal stress $\sigma_o \sin(\omega t + \delta)$
σ_{ii}	Extensional stress component
τ	Stress tensor
τ^i_{kk}	Component (kk) of the stress tensor corresponding to the i-th relaxation element contribution to the stress tensor.

τ_o Imposed stress in a creep test

τ_w Shear stress at the wall

τ_i i-th contribution to the stress tensor

τ_{ii} Stress tensor component

τ_t True shear stress

$\tau_{1/2}$ Value of τ_{yx} when $\eta = \eta_o / 2$

$\tau_{(1)}$ Convected time derivative of the stress tensor

$$\boldsymbol{\tau}_{(1)} = \frac{D}{Dt}\boldsymbol{\tau} - \left\{(\nabla \upsilon)^t \cdot \boldsymbol{\tau} + \boldsymbol{\tau} \cdot (\nabla \upsilon)\right\}$$

υ Piston velocity in a capillary test

Ω Wagner's (1976) damping function parameter

Φ Wagner's (1976) damping function parameter

Ξ Wagner's (1979) damping function parameter

$\Psi_1(\dot{\gamma})$ First normal stress coefficient

$\Psi_2(\dot{\gamma})$ Second normal stress coefficient

$\boldsymbol{\omega}$ Vorticity tensor

$$\nabla \upsilon - (\nabla \upsilon)^t = 2\nabla \upsilon - \dot{\gamma}$$

ω Frequency (rad/sec)

ω_x Cross-over frequency (rad/sec)

$\nabla \upsilon$ Velocity gradient tensor

TABLE OF CONTENTS

List of Figures

List of Tables

CHAPTER I. Introduction

The polyolefins business is a commodity market where profit can be made only by mass production. In order to maintain a financial performance, the competitive strategy is to develop technological innovations and faster characterization techniques, so the polyolefins can be processed faster and sold at higher prices. However, any innovation requires large amounts of polymer in order to determine its performance in the processing lines.

The manufacturing process of polymers has a large influence on the resulting mechanical and optical properties of the end product. For instance, dimensional stability in precision injection molding or yield strength, Young's modulus and even tear strength of blown films are affected by the viscoelastic properties of the polymer melt.

Therefore, a necessary requirement in the design of polymer processing operations is a fundamental understanding of the rheology of the polymer melt. Then, the industry needs both absolute quantitative information and also inexpensive testing for multiple samples in order to understand polymer melt's behavior. The difficulty in recovering research and development costs has made some producers to think about modeling polymer processes to understand and establish the processability of a new polymer. Therefore, experimentation demands the greatest quantity of accurate information at a minimum cost in order to have a fast ROI regarding the research and development costs and to be able to increase the market shore.

Research and development departments have considered that the rheological models (constitutive equations) are very important because they could predict melt flow behavior in a wide range of deformation histories; however, the usefulness of a constitutive equation lies in its ability to make accurate predictions for as many

polymer systems with as few adjustable parameters as possible. In addition, to simulate polymer melt processing realistically, the model must be able to describe material behavior in the linear and in the nonlinear regime. Particularly, the study of the elongational behavior is very important because the flow behavior of polymer melts in economically important processes like fiber spinning and film blowing is governed rather by elongational than by shear properties of the melt. Furthermore, processes such as extrusion, though primarily governed by shear properties, may also be influenced by elongational properties. (Laun, 1976).

This thesis is a contribution to the predictive modeling of viscoelastic materials. The PTT model (Phan Thien and Tanner, 1977) and XPP model (Verbeeten, 2001) are analyzed and evaluated using the experimental data of eight polypropylene resins. A modified PTT model is proposed as well as an innovative approach using fractals theory.

A. Problem Statement

Previous work (Mier, 2000) proved that PTT model (Phan Thien and Tanner, 1977) predicts rheological properties accurately in the steady state, but the predictions in the transient state are not that accurate. Besides, several authors (Larson, 1987; Stephenson, 1989) had showed some important limitations for this model. These limitations of PTT model and other constitutive equations have caused the creation of new constitutive equations, like the POM-POM model (McLeish and Larson, 2000).

On the other hand, most rheological models use empirical parameters to fit the experimental data. Those parameters have no theoretical explanation; therefore the models cannot relate the polymer behavior in extensional flow to their molecular features, or to other fundamental aspects.

B. Research Proposal and Objectives

The primary objective of this research is *to improve the existing constitutive equations by reducing the number of empirical parameters, to better explain polymer melt's behavior in extensional flow during transient state*. In addition, there are the following particular objectives:

1. Rheological characterization of isotactic and syndiotactic polypropylene resins.
2. Identification of rheological differences between similar isotactic and syndiotactic resins
3. Modification of the PTT model in order to obtain better predictions of elongational behavior of polyolefins.
4. Build the basis for a new model that explains satisfactorily the rheological behavior of polymer melts using fractals theory.

C. Justification

There are several rheological analytical techniques used in the characterization of polymers, however such techniques not always discriminate resins with similar quality control data but with different processing behavior. An example of a technique typically used for discrimination of resins with similar steady state viscoelastic data is the Cogswell analysis. Such technique is time consuming, requires the use of costly equipment and uses empirical parameters not necessarily related to typical molecular weight distribution features. Therefore, there is a need for a constitutive equation capable of predicting the elongational transient behavior of a polymer based on the fewest number of steady state linear viscoelastic data, on molecular weight and/or other physical parameters. Based on Mier's (2000) results, it sounds reasonable to propose a modification to the PTT model in which the compressibility effect can be taken into consideration and in which the deformation tensor might need a modification altogether.

It is worth to remember that the PTT model presents a relationship between strain and elastic energy in addition to the inclusion of a set of multiple relaxation times, which can easily be obtained in the laboratory.

D. General Methodology

To guarantee the accuracy of the results generated in this project, special care was taken in materials preparation, standard quality control tests, rheological techniques and validation of the constitutive equations.

1. Materials Preparation

All resins were prepared using the same conditions and with the same additive package, so that any variations observed could be associated to changes in the polymer's molecular structure and MWD and not to other factors.

2. Standard Quality Control Techniques

Information on reproducibility on the quality control techniques was included to determine if reported differences were significant or not.

3. Rheological Techniques

Standard well-documented and proven procedures were followed in each rheological test. Conditions previously documented were used (Aguirre, 1999; Mier, 2000).

E. General Organization

This thesis is divided in thirteen chapters, including the present one. Chapter II presents a literature review as a theoretical background. Chapter III explains the principles behind the standard quality control techniques and the rheological tests.

The experimental data is presented in Chapters IV through VII. Chapter IV presents the resins' typical quality control properties (standard properties). Such properties are the melt flow index (MFI), xylenes solubles percentage analysis (PS), molecular weight distribution (MWD), differential scanning calorimetry (DSC), and isotacticity analysis (NMR). Chapter V presents the oscillatory data and Chapter VI presents the shear and elongational viscosity from capillary data. Chapter VII presents the creep and recovery compliance experimental data.

Chapter VIII presents the development of the PTT model, as well as its rheological functions predictions. Chapter IX shows the mathematical modification of the model and its rheological functions predictions. Chapter X presents the development of the POM-POM model and its rheological functions predictions.

Chapter XI presents a discussion of results in addition to several empirical relationships that were found among the rheological parameters and the standard quality properties. Chapter XII presents a new way of modeling polymer's melt using a fractals approach. Finally, Chapter XIII presents the conclusions of the project as well as a summary of findings and recommendations for future work.

CHAPTER II. Theoretical Background

This chapter presents a complete literature review. It is divided in four sections. Section A presents an introduction to rheology, section B shows some empirical models while section C presents constitutive equations, and finally section D shows an introduction to fractals theory.

In some cases, the nomenclature used by the original consulted articles is changed to avoid confusions. The reader can look at the nomenclature list given in the first pages of this thesis.

A. Introduction to Rheology

Rheology is the science that deals with the way materials deform when forces are applied to them. The term is most commonly applied to the study of liquids and liquid-like materials such as paint, catsup, oil well drilling mud, blood, polymer solutions and molten plastics. However, rheology also includes the study of the deformation of solids such as occurs in metal forming and the stretching of rubber. (Dealy, 1990).

To learn anything about the rheological properties of a material, we must either measure the deformation resulting from a given force or measure the force required to produce a given deformation. (Dealy, 1990).

There are two principal aspects of rheology. One involves the development of quantitative relationships between deformation and force for a material of interest. The information for the development of such a relationship is obtained from experimental measurements. For a linear elastic material or a Newtonian fluid, such simple observations are sufficient to establish a general equation describing

how such material will respond to any type of deformation. Such an equation is called a "constitutive equation" or a "rheological equation of state". (Dealy, 1990).

The second aspect of rheology is the development of relationships that show how rheological behavior is influenced by the structure and composition of the material and the temperature and pressure. Ideally, one would like to know how these parameters affect the constitutive equation, but this has not been accomplished at the present time, except for very simple materials such as Newtonian fluids. (Dealy, 1990).

Molten plastics are rheologically complex materials that can exhibit both viscous flow and elastic recoil. A truly general constitutive equation has not been developed for these materials, and our present knowledge of their rheological behavior is largely empirical. (Dealy, 1990).

1. Strain and Stress Tensors (Bird, 1987)

The velocity field for *simple shear flow* is given by the velocity field:

$$\upsilon_x = \dot{\gamma}_{yx} y , \tag{2. 1}$$

$$\upsilon_y = \upsilon_z = 0 . \tag{2. 2}$$

The velocity field for *extensional flows* (shear free flows) is given by generalized forms:

$$\upsilon_x = -\frac{1}{2}\dot{\varepsilon}(1+b)x , \tag{2. 3}$$

$$\upsilon_y = -\frac{1}{2}\dot{\varepsilon}(1-b)y , \tag{2. 4}$$

$$\upsilon_z = +\dot{\varepsilon} z , \tag{2. 5}$$

where $\dot{\varepsilon}$ is the extension rate and b is a constant that is either 0 or 1. When b = 0 and $\dot{\varepsilon} > 0$, the flow is a *uniaxial extensional flow*. When b = 0 and $\dot{\varepsilon} < 0$, the flow is an *equibiaxial extensional flow*. When b = 1, the flow is a planar *extensional flow*.

In uniaxial extensional flow, the system is stretched along the z axis while it contracts uniformly along the x and y axis in such a manner that the volume is kept constant. The elongational (Henky) strain is given by $\varepsilon = \dot{\varepsilon}(t - t')$. In biaxial extension flow, the differential element is stretched equally along the x and y axis, but contracts in the z direction. In planar extensional flow, the system is stretched along the z direction, but is constrained only in the x direction.

The different elongational flows have different effects on the orientation of the macromolecules, for example the uniaxial extensional flow impart significant molecular orientation (compared to shear flow), while biaxial extensional flow does not lead to a strong degree of molecular orientation.

For *shear flow*, the components of the rate of strain (deformation) tensor are:

$$\dot{\gamma}_{ij} = \dot{\gamma}(t)\begin{pmatrix} 0 & 1 & 0 \\ 1 & 0 & 0 \\ 0 & 0 & 0 \end{pmatrix}. \qquad (2.6)$$

For *extensional* (shear free) flow, the components of the rate of strain tensor are:

$$\dot{\gamma}_{ij} = \begin{pmatrix} -\dot{\varepsilon}(1+b) & 0 & 0 \\ 0 & -\dot{\varepsilon}(1-b) & 0 \\ 0 & 0 & 2\dot{\varepsilon} \end{pmatrix}. \qquad (2.7)$$

For a viscoelastic fluid in *shear flow*, the components of the stress tensor are:

$$\tau = \begin{pmatrix} \tau_{xx} + p & \tau_{xy} & 0 \\ \tau_{yx} & \tau_{yy} + p & 0 \\ 0 & 0 & \tau_{zz} + p \end{pmatrix}. \qquad (2.\ 8)$$

For a viscoelastic fluid in *extensional* flow, the components of the stress tensor are:

$$\tau = \begin{pmatrix} \tau_{xx} + p & 0 & 0 \\ 0 & \tau_{yy} + p & 0 \\ 0 & 0 & \tau_{zz} + p \end{pmatrix}. \qquad (2.\ 9)$$

where p is the isotropic pressure. For Newtonian fluids, $\tau_{xx} = \tau_{yy} = \tau_{zz} = 0.$

Some other continuum mechanics tensors components for shear and shear free flows can be found in appendix C of the monography by Bird et al. (1987).

2. Materials Functions

The stresses that are customarily used with *shear flow* are:

$$\tau_{yx} = -\eta(\dot{\gamma})\dot{\gamma}_{yx}, \qquad (2.\ 10)$$

$$\tau_{xx} - \tau_{yy} = -\Psi_1(\dot{\gamma})\dot{\gamma}_{yx}^2, \qquad (2.\ 11)$$

$$\tau_{yy} - \tau_{zz} = -\Psi_2(\dot{\gamma})\dot{\gamma}_{yx}^2, \qquad (2.\ 12)$$

where $\Psi_1(\dot{\gamma})$ and $\Psi_2(\dot{\gamma})$ are the first and second normal stress coefficients, respectively.

The stresses that are customarily used with shear free flow are:

$$\tau_{zz} - \tau_{xx} = -\bar{\eta}_1(\dot{\varepsilon}, b)\dot{\varepsilon}, \tag{2. 13}$$

$$\tau_{yy} - \tau_{xx} = -\bar{\eta}_2(\dot{\varepsilon}, b)\dot{\varepsilon}, \tag{2. 14}$$

where $\bar{\eta}_1(\dot{\varepsilon}, b)$ and $\bar{\eta}_2(\dot{\varepsilon}, b)$ are shear free viscosity functions. For the special case when b = 0, $\bar{\eta}_2(\dot{\varepsilon}, 0) = 0$, and $\bar{\eta}_1(\dot{\varepsilon}, 0)$ is equal to the *elongational viscosity:*

$$\eta_e(\dot{\varepsilon}) = \bar{\eta}_1(\dot{\varepsilon}, 0), \tag{2. 15}$$

$$\bar{\eta}_2(\dot{\varepsilon}, 0) = 0. \tag{2. 16}$$

For $\dot{\varepsilon} > 0$, η_e describes elongational flow, and for $\dot{\varepsilon} < 0$, η_e describes biaxial stretching.

3. Convected Derivative Tensors

It is important to define some tensors used frequently in constitutive modeling:

Velocity gradient tensor: $\nabla \upsilon$ (2. 17)

Rate-of-strain tensor: $\dot{\gamma} = \nabla \upsilon + (\nabla \upsilon)^t$ (2. 18)

Vorticity tensor: $\omega = \nabla \upsilon - (\nabla \upsilon)^t = 2\nabla \upsilon - \dot{\gamma}$ (2. 19)

First rate-of-strain tensor: $\gamma_{(1)} \equiv \dot{\gamma}$ (2. 20)

Nth rate-of-strain tensor: $\gamma_{(n+1)} = \frac{D}{Dt}\gamma_{(n)} - \left\{(\nabla \upsilon)^t \cdot \gamma_{(n)} + \gamma_{(n)} \cdot (\nabla \upsilon)\right\}$ (2. 21)

Contravariant convected time derivative of the stress tensor:

$$\tau_{(1)} = \frac{D}{Dt}\tau - \left\{(\nabla \upsilon)^t \cdot \tau + \tau \cdot (\nabla \upsilon)\right\} \tag{2. 22}$$

For convenience, the components of $\nabla \upsilon$, $\dot{\gamma}$, and ω in four coordinate systems are completely given in appendices A and B of the monography by Bird *et. al.* (1987); while τ and $\tau_{(1)}$ for shear and shear free flows are given in appendix C of the same monography.

Finger strain tensor: $B(r,t,t') = \{E \cdot E^t\}$, (2. 23)

Cauchy finite strain tensors: $B^{-1}(r,t,t') = \{\Delta^t \cdot \Delta\}$, (2. 24)

Relative finite strain tensors: $\gamma^{[0]}(r,t,t') = \{\Delta^t \cdot \Delta\} - \delta$, (2. 25)

$\gamma_{[0]}(r,t,t') = \delta - \{E \cdot E^t\}$, (2. 26)

First scalar invariant of the Finger strain tensor: $I_1 = \text{tr } \boldsymbol{B}$, (2. 27)

Second scalar invariant of the Finger strain tensor:

$I_2 = (1/2)[(\text{tr } \boldsymbol{B})^2 - \text{tr } (\boldsymbol{B}^2)]$, (2. 28)

Third scalar invariant of the Finger strain tensor: $I_3 = \det \boldsymbol{B}$, (2. 29)

where Δ_{ij} are measures of the displacements at time t' relative to the positions at time t, whereas $\boldsymbol{E}_{ij}$ are measures of the displacements at time t relative to the positions at time t', and δ is the unit tensor. Whenever components of Δ, $\boldsymbol{E}$, $\gamma^{[0]}$, and $\gamma_{[0]}$ the reader can find complete tabulations for general deformations in rectangular, cylindrical, and spherical coordinate systems in appendices B and C of Bird et al. (1987) work. In addition, appendix C of the same work (Bird et al. 1987) gives expressions for Δ, $\boldsymbol{E}$, $\gamma^{[0]}$, $\gamma_{[0]}$, I_1, I_2, and I_3 in rectangular coordinates worked out specifically for simple shear flows and for shear-free flows.

B. Measurements and Empirical Models

1. Die Swell

A viscoelastic correlation can be useful for estimating the extrudate swell, which is the recovery expansion that a polymer exhibits on leaving a die. It has been suggested that die swell can be correlated to the primary normal stress difference N_1 and to the shear stress at the wall, τ_w. The most common is that proposed by Tanner (1970):

$$B = \frac{D_p}{D_o} = 0.1 + \left[1.0 + \frac{1}{2}\left(\frac{N_{1,w}}{2\tau_w}\right)^2\right]^{1/6}, \qquad (2.30)$$

where D_p is the diameter of the extrudate and D_o is the capillary diameter. The capillary die swell, B, is also a function of the capillary L/D_o, the entrance geometry, the exit geometry, the time after a fluid element leaves the die, the time required for the melt to pass through the die, and the longest relaxation time (λ) of the fluid (Baird, 1998).

2. Polidispersity Index

Zeichner and Patel (1981) found that the breadth of the MWD (PDI) for a family of polypropylene resins was related to the value of the crossover modulus G_c ; which is the value of G' and G" are equal at the crossover frequency ω_c.

$$PDI = \frac{10^5}{G_c(\omega_c)[=]Pa} \qquad (2.31)$$

Shang (1993) questioned the Zeichner-Patel correlation arguing that the crossover point is sensitive to the strain at which the oscillatory data is obtained. He suggested using 5% strain for resins with MFI > 30 and 15% for resins with MFI < 30.

Chambon (1995) used the Zeichner-Patel correlation and found that it predicted the same PDI for several resins, while the GPC data reported different PDI values for those resins. They suggested estimating PDI by the reciprocal of the slope of plots of tan δ versus frequency. The PDI should be estimated from specific regions of the plot: for resins with MFR < 8, the slope in the region $1 < \tan\delta < 4$ should be used; while for resins with MFR > 8, $2 < \tan\delta < 10$ region should be used.

3. Steady Shear Properties

Dynamic oscillatory properties are easier to measure and can be obtained over a wide range of frequencies compared to the range of shear rates that can be obtained using a rheometer. With the following relations, is then possible to obtain steady shear rheological data from linear viscoelastic data over a wide range of shear rates.

It has been observed experimentally for many polymers that the magnitude of the complex viscosity, and the shear viscosity are identical (at least for flexible polymers) if they are evaluated at the same values of ω and $\dot{\gamma}$. This relation is known as the Cox-Merz rule (Cox and Merz, 1958).

$$\eta(\dot{\gamma}) = \left|\eta^*(\omega)\right|_{\omega=\dot{\gamma}} = \eta'(\omega)\left[1+\left(\frac{\eta''(\omega)}{\eta'(\omega)}\right)^2\right]^{0.5}\Bigg|_{\omega=\dot{\gamma}}, \qquad (2.\ 32)$$

where $\eta'(\omega)$ and $\eta''(\omega)$ are the components of the complex viscosity $\eta^*(\omega)$.

A second, no less important, Cox-Merz rule relates the slope of the viscosity curve to the dynamic viscosity (Cox and Merz, 1958):

$$\frac{d\tau_{yx}(\dot{\gamma})}{d\dot{\gamma}} = \eta'(\omega)\Big|_{\omega=\dot{\gamma}} \qquad (2.\ 33)$$

Laun (1986) proposed a relationship between the first normal stress coefficient and the storage and loss modulus:

$$\Psi_1(\dot{\gamma}) = 2\frac{G'}{\omega^2}\left[1+\left(\frac{G'}{G''}\right)^2\right]^{0.7}_{\omega=\dot{\gamma}} = \frac{2\eta'(\omega)}{\omega}\left[1+\left(\frac{\eta''(\omega)}{\eta'(\omega)}\right)^2\right]^{0.7}\Bigg|_{\omega=\dot{\gamma}}. \qquad (2.\ 34)$$

An alternative form relating the mechanical loss angle and the in-phase component of the complex viscosity is (Laun, 1986):

$$\Psi_1(\dot{\gamma}) = 2\eta'(\sec\delta)^{1.4}\,\omega\Big|_{\omega=\dot{\gamma}} \qquad (2.\ 35)$$

4. Time-Temperature Superposition Principle

Material functions (rheological properties) taken at several temperatures can be brought together on a single master curve. This simplifies the description of the effect of temperature and it makes possible to present the material function in a much broader range of time or frequency than can ever be measured at a single temperature. This principle is named *Time-Temperature-Superposition* (TTS) and is useful for the analysis of non-isothermal flows as happens, for example, in industrial melt spinning.

The linear viscoelastic behavior of a polymer melt can be described using a model made of N Maxwell elements in parallel. Each of them is defined by the rigidity of the spring G_i and the relaxation time λ_i which is the ratio between the viscosity of the dashpot and the rigidity of the spring ($\lambda_i = \eta_i / G_i$). Such model is called the generalized Maxwell model and their λ_i at a different temperature T are related to the reference temperature T_0:

$$\lambda_i(T) = a_T \lambda_i(T_o) \qquad (2.\ 36)$$

where a_T is called the horizontal shift factor. The coefficients G_i are altered by a change in temperature by:

$$G_i(T) = G_i(T_o)T\rho / T_o\rho_o \qquad (2.\ 37)$$

Using the above two relationships, the relaxation modulus of the generalized Maxwell fluid is:

$$G(t,T)=\frac{T\rho}{T_o\rho_o}\sum_{i=1}^{N}G_i(T_o)\exp[-t/(\lambda_i(T_o)a_T)] \qquad (2.\ 38)$$

Defining $G_r(t)\equiv G(t,T)T_o\rho_o/T\rho$ and $t_r=t/a_T$:

$$G(t_r)=\sum_{i=1}^{N}G_i(T_o)\exp[-t_r/\lambda_i(T_o)] \qquad (2.\ 39)$$

Thus, if G_r is plotted as a function of t_r, the data taken at various temperatures should fall on the same master curve as those taken at the reference temperature T_o.

All *linear* viscoelastic properties obey a time-temperature superposition principle. It is found that the shift factor is given by:

$$a_T=\frac{\eta_o(T)T_o\rho_o}{\eta_o(T_o)T\rho} \qquad (2.\ 40)$$

Since the ratio $T_o\rho_o/T\rho$ has almost no change at ordinary temperature ranges.

$$a_T=\frac{\eta_o(T)}{\eta_o(T_o)}. \qquad (2.\ 41)$$

Two types of exponential functions have been used for describing the temperature dependence of a_T. The WLF equation (Hamed, 1988) holds in the range of temperatures Tg to Tg + 100 °C, where Tg is the glass transition temperature for the polymer.

$$a_T=\frac{\eta_o(T)}{\eta_o(T_o)}=\frac{-C_1^o(T-T_o)}{C_2^o+(T-T_o)}, \qquad \text{Tg} < T < \text{Tg} + 100\ ^\circ\text{C} \qquad (2.\ 42)$$

where $C_1^o = 900 / C_2^o$ and $C_2^o = 51.6 + (T_o - T_g)$.

For temperatures greater than Tg + 100 °C, the Arrhenius-type equation (Mavridis et. al., 1992) is used:

$$a_T = \frac{\eta_o(T)}{\eta_o(T_o)} = exp\left[\frac{E_H}{R}\left(\frac{1}{T} - \frac{1}{T_o}\right)\right] \qquad T > Tg + 100\ °C \qquad (2.43)$$

where E_H is the horizontal activation energy for flow.

Similar equations to 2.39 can be obtained for other material functions (Dealy, 1990):

$$G_r'(a_T\omega) = a_T\omega\int_0^\infty G_r(t_r)sin[(a_T\omega)(t_r)]dt_r, \qquad (2.44)$$

$$G_r''(a_T\omega) = a_T\omega\int_0^\infty G_r(t_r)cos[(a_T\omega)(t_r)]dt_r \qquad (2.45)$$

where G_r' and G_r'' have the same relationship to the storage modulus G' and the loss modulus G'' as G_r has to G.

If the ratio $T_o\rho_o / T\rho$ varies little with temperature, superposition can often be accomplished by plotting: G(t) versus t / a_T, G'(ω) versus ωa_T, G''(ω) versus ωa_T, $\eta'(\omega)/a_T$ versus ωa_T, $\eta''(\omega)/a_T$ versus ωa_T, J(t) versus t / a_T.

5. Viscosity Models

Equations for modeling viscosity functions have been proposed by several authors, and are summarized in Darby (1976) and in Dealy and Winsburn (1990):

$$\eta = m|\dot{\gamma}|^{n-1}$$ Ostwald-de Waele (power law) model, (2. 46)

$$\frac{\eta_o}{\eta} = 1 + \left(\frac{\tau_{yx}}{\tau_{1/2}}\right)^{a-1}$$ Ellis model, (2. 47)

$$\eta = \eta_0\left[1 + (\lambda\dot{\gamma})^2\right]^{-p}$$ Carreau model, (2. 48)

$$\eta = \eta_0\left[1 + (\lambda\dot{\gamma})^a\right]^{\frac{n-1}{a}}$$ Yasuda model, (2. 49)

$$\eta = \eta_0\left[\left(1 + |\lambda\dot{\gamma}|^a\right)\right]^{-1}$$ Cross model, (2. 50)

$$\eta = \eta_o\left[1 + 0.6(\lambda\dot{\gamma})^{0.75}\right]^{-1}$$ Bueche-Harding model, (2. 51)

where: *n* describes the degree of deviation from Newtonian behavior; *m,* which has units of Pa.s^n, is called the *consistency*; η_o is the zero shear viscosity; $\tau_{1/2}$ is the value of τ_{yx} when $\eta = \eta_o / 2$; λ is the reciprocal of the shear rate at the onset of the shear thinning behavior, the parameter "a" indicates how fast the viscosity decreases with shear rate.

The power law model introduces an error in the very low shear rate region by not assuming that n = 1. Also the slope of the viscosity curve in the power law region is not exactly a constant, since the flow index *n* decreases with increasing shear rate. Thus the power law equation holds exactly only for limited ranges of shear rate, for a given value of *n.* On the other hand, the Ellis model predicts a Newtonian plateau at very low shear rate.

6. Zero-shear Viscosity

Until recent years η_o has been estimated by relations of the type $\eta_o = kM_w^a$. Such relation requires viscosity measurements at shear rates $\dot{\gamma} << 0.01$ 1/sec. Such long time measurements can promote chemical changes in the melted polymer. Another common way to estimate η_o was from experimental creep data. Since J(t) = $J_g + J_e(t) + t/\eta_o$ at very long times, $J(t) = t/\eta_o$, so $\eta_o = \Delta t / \Delta J(t)$.

Recently, Bonilla and Mier (2000) predicted the zero shear viscosity for polyproylene resins also from experimental creep data, but with the difference that only 0.1 seconds of creep data are enough to make the predictions for high MFI PP resins (20 < MFI < 40) applying a constant shear stress of 300 Pa. The estimation method is known as the McLaurin Series Method (MSM) since it is based on the McLaurin series expansion. The MSM was applied to the Jeffreys (1929) model:

$$\lambda_2 = -\frac{1}{3}\left(\frac{a_2}{a_3}\right), \tag{2. 52}$$

$$\lambda_1 = \frac{a_1\lambda_2}{a_1 + 2a_2\lambda_2}, \tag{2. 53}$$

$$\eta_o = \mu_1 = -\frac{1}{2}\left(\frac{\lambda_1 - \lambda_2}{a_2\lambda_2^2}\right), \tag{2. 54}$$

where the constants a_1, a_2 and a_3 known fitting parameters of a third order minimum square regression polynomial for experimental data of creep J(t) versus time (for at least 0.1 seconds).

C. Constitutive Equations

There is no usable constitutive equation that describes quantitatively *all* the flow phenomena of polymer melts. In the absence of it, scientists and engineers use equations that predict only the flow behavior that is important to the particular problem. All constitutive equations for polymer melts are special cases of a, still unknown, very general constitutive equation (Goddard, 1967):

$$\tau(x,t) = -\int_{-\infty}^{t} G_1(t-t')\dot{\Gamma}'dt' - \frac{1}{2}\int_{-\infty}^{t}\int_{-\infty}^{t} G_{11}(t-t',t-t')\left[\dot{\Gamma}'\bullet\dot{\Gamma}'' + \dot{\Gamma}''\bullet\dot{\Gamma}'\right]dt''dt' - \ldots \tag{2. 55}$$

where G_1, G_{11} are characteristic material functions; t', t'', t''' are integration variables, and t is the present time; ω is the vorticity tensor (which its components can be found in Bird, 1977); $\dot{\Gamma}$ is the corotating rate of strain tensor, which can be expanded in a Talylor series about t' = t (Bird, 1977):

$$\dot{\Gamma}(t,t') = \dot{\gamma}(t) - (t-t')\left[\frac{\partial \dot{\gamma}}{\partial t} + \{\upsilon \bullet \nabla\dot{\gamma}\} + \frac{1}{2}(\{\omega \bullet \dot{\gamma}\} - \{\dot{\gamma} \bullet \omega\})\right] + \ldots \qquad (2.56)$$

1. Criminale - Ericksen - Filbey Equation

Equation 2.55 is not a practical form to represent the stress tensor. However, by keeping only the first two terms of the Taylor series; for *steady shear flows*, the Criminale-Ericksen-Filbey (CEF) consitutive equation is obtained (Criminale, Ericksen, and Filbey, 1958; in Bird, 1987):

$$\tau = -\eta\dot{\gamma} - \left(\frac{1}{2}\Psi_1 + \Psi_2\right)\{\dot{\gamma} \bullet \dot{\gamma}\} + \frac{1}{2}\Psi_1\left[\frac{\partial \dot{\gamma}}{\partial t} + \{\upsilon \bullet \nabla\dot{\gamma}\} + \frac{1}{2}(\{\omega \bullet \dot{\gamma}\} - \{\dot{\gamma} \bullet \omega\})\right] \qquad (2.57)$$

where η, ψ_1, ψ_2 are the viscosity, first, and second normal stress difference coefficients, respectively. They are all functions of the magnitude of the rate of strain $\dot{\gamma} = \sqrt{1/2(\dot{\gamma} : \dot{\gamma})}$.

2. Doi – Edwards Model

Doi and Edwards proposed a constitutive equation based on the concept of entanglement (reptation) described by de Gennes (1971). They assumed that surrounding molecules form mesh of obstacles through which a polymer chain cannot pass. The chain is thus confined to a tube-like region. When the material is deformed, the mesh and the tube deform affinely, but the strand can slip or retract within the tube, and returns quickly to its equilibrium length: the orientation

of the strand, however, remains that of the deformed tube. From these assumptions, they derived a constitutive equation:

$$\tau = \int_{-\infty}^{t} m(t-t')Q(t,t')dt' \tag{2. 58}$$

where the memory function is given by:

$$m(t-t') = \sum_i \frac{G_i}{\lambda_i} \exp\left[\frac{t'-t}{\lambda_i}\right] \tag{2. 59}$$

and the relaxation moduli and times (G_i and λ_i) are determined by the reptational diffusion model:

$$G_i = \frac{8G}{\pi^2 i^2} \tag{2. 60}$$

$$G = \upsilon kT \tag{2. 61}$$

$$\lambda_i = \frac{\lambda_d}{i^2} \tag{2. 62}$$

λ_d is the longest relaxation time and ν is the number of entanglements per unit volume. The non-linear strain measure Q is a "universal tensor" dependent only upon the deformation history and not upon material properties.

3. Giesekus Model

The Giesekus model is based on a kinetic theory of closely packed polymer chains and on a series of simplifications leading to an equation for the extra stress that contains no explicit integrals over the configurations of individual molecules (Giesekus, 1982). The extra stress for the Giesekus model is given by

$$\tau_{(1)} + \frac{\alpha}{\lambda G}\tau^2 + \frac{1}{\lambda}\tau = G\dot{\gamma} \qquad (2.\ 63)$$

where α is an adjustable ("fitting") parameter.

4. Jeffreys Model

$$\tau + \lambda_1 \cdot \frac{\partial \tau}{\partial t} = -\eta_0 \cdot \left(\dot{\gamma} + \lambda_2 \cdot \frac{\partial \dot{\gamma}}{\partial t}\right), \qquad (2.\ 64)$$

This equation contains two time constants λ_1 and λ_2 (the "relaxation time" and "the retardation time", respectively). It was proposed for the study of wave propagation in the earth's mantle.

5. Johnson – Segalman Model

The Johnson-Segalman model is given by

$$\tau_{i(1)} + \alpha\left(\frac{\dot{\gamma}}{2} \cdot \tau_i + \tau_i \cdot \frac{\dot{\gamma}}{2}\right) + \frac{1}{\lambda_i}\tau_i = G_i\dot{\gamma} \qquad (2.\ 65)$$

The first two terms constitute the *Gordon-Schowalter nonaffine convected derivative* with α being a slip parameter. This parameter is a single nonlinear parameter of the model that is not obtained from the linear spectrum.

The model violates the experimentally observed Lodge-Meissner relation which relates the first normal stress difference to the shear stress after a step shear strain of magnitude γ, by the following equation

$$\gamma = \frac{\tau_{xx} - \tau_{yy}}{\tau_{xy}} \qquad (2.\ 66)$$

It is know that the J-S equation shows singularity in the steady state viscosity in uniaxial extension. These deficiencies limit the usefulness of this model. (Larson, 1987).

6. Kaye – BKZ Model

The K-BKZ equation was proposed by Bernstein, Kearsley, and Zapas (Bernstein et al., 1964). A. Kaye (1966) independently developed the same concept.

$$\tau(t) = \int_{-\infty}^{t} \left[\left[\frac{\partial V(t-t', I_1, I_2)}{\partial I_1} \right] \gamma_{[0]} + \left[\frac{\partial V(t-t', I_1, I_2)}{\partial I_2} \right] \gamma^{[0]} \right] dt', \qquad (2.67)$$

where V is an scalar function of the arguments indicated; I_1 , I_2 are the first and second scalar invariants of the Finger strain tensor, respectively. Very little work has been done on describing material functions or solving flow problems with the K-BKZ equation in its general form (equation 2.67). Instead, it is common to introduce a product of time-dependent and strain-dependent factors as follows:

$$\tau(t) = \int_{-\infty}^{t} M(t-t') \left[\frac{\partial W(I_1, I_2)}{\partial I_1} \gamma_{[0]} + \frac{\partial W(I_1, I_2)}{\partial I_2} \gamma^{[0]} \right] dt' \qquad (2.68)$$

where M(t-t') is the linear viscoelastic memory function and W is a potential function that must be determined experimentally by studying large and rapid deformations. Depending on the assumptions, this model can lead to the Rouse-Zimm model for dilute solutions, the Lodge network model, the Tanner-Simmons network rupture model, the Doi-Edwards model, the Wagner model or the Papanastasiou model.

7. Larson Model

The separable differential model proposed by Larson is given by

$$\tau_{(1)} + \frac{2}{3}\frac{\alpha}{G}\frac{\dot{\gamma}}{2} : \tau(\tau + GI) + \frac{1}{\lambda}\tau = G\dot{\gamma} \qquad (2.\ 69)$$

where I is the unit tensor.

The first two terms represent a nonaffine convected derivative. α describes the strain softening[1] character of the material, and causes equation 2.69 to vary between the upper-convected Maxwell model and an approximation to the Doi-Edwards model for α values of 0 and 0.6, respectively.

8. Marruci (Acierno) Model

The network model proposed by Acierno (1976), more commonly known as the Marruci model, takes the form

$$x^{1.4}\left(\frac{1}{x}\tau\right)_{(1)} + \frac{1}{x\lambda}\tau = x^{1.4}G\dot{\gamma} \qquad (2.\ 70)$$

where x satisfies the evolution equation

$$\frac{\partial x}{\partial t} = \frac{1}{\lambda}x^{-1.4}(1-x) - \frac{\alpha}{\lambda}x^{-0.4}\left(\frac{tr\tau}{2Gx}\right)^{1/2} \qquad (2.\ 71)$$

The scalar dimensionless quantity x can be considered as a structural parameter that represents the degree of connectivity of the macromolecular network with respect to that at equilibrium. x=1 corresponds to the equilibrium structure and x<1 describes the deviation of the existing structure from equilibrium. The 1.4

[1] The term strain-softening here refers to the behavior of the transient viscosities after the start-up of flow. It means that for strain rates in the nonlinear regime, the visocisty during the start-up falls below the linear viscoelastic (low strain rate) response. On the other hand, strain-hardening, means that the viscosity rises above the linear viscoelastic response (McLeish, 1998).

exponent in the above equations is empirical and originated from the dependence of shear viscosity on the 3.4 power of the polymer concentration in high molecular weight concentrated polymer solutions or melts (Larson, 1987).

9. Phan Thien – Tanner Model

The multi-mode Phan-Thien and Tanner (PTT) model arises from a molecular network theory. The PTT model is expressed by:

$$\boldsymbol{\tau} = \sum_{i=1}^{N} \boldsymbol{\tau}_i \tag{2.72}$$

$$Z(tr\boldsymbol{\tau}_i)\boldsymbol{\tau}_i + \lambda_i \boldsymbol{\tau}_{i(1)} + \frac{\xi}{2}\lambda_i (\dot{\boldsymbol{\gamma}} \cdot \boldsymbol{\tau}_i + \boldsymbol{\tau}_i \cdot \dot{\boldsymbol{\gamma}}) = -\eta_i \dot{\boldsymbol{\gamma}} \tag{2.73}$$

$$Z(tr\boldsymbol{\tau}_i) = \exp\left(-\frac{\alpha\lambda_i}{\eta_i} tr\tau_i\right) \tag{2.74}$$

where the shear-free parameter α is obtained from elongational viscosity data, the relaxation spectrum $G_i = \eta_i / \lambda_i$ is obtained from linear viscoelastic measurements, and the shear flow parameter ξ is obtained by fitting the viscosity curve with the equation $\eta(\dot{\gamma}) = \sum_{i=1}^{N} \frac{\eta_i}{1 + \xi(2-\xi)(\lambda_i \dot{\gamma})^2}$. $Z(tr\tau_i)$ is the rate of creation and destruction of junctions. Further explanations of the constitutive equation will be covered in chapters VIII and IX.

10. Pom – Pom Model

McLeish and Larson (1998) recently proposed the "pom-pom" model to describe the complex rheology of branched polymers. A refined model with a molecular drag-strain coupling has also been proposed (Blackwell, 2000) to smooth the sharp transitions in the extensional viscosity at the maximum stretch condition. Verbeeten (2001) proposed an extension to the model to improve the performance of the original model. The original model limitations were:

- Unbounded orientation for $\dot{\varepsilon}\lambda_{0b} > 1$.
- Non-smooth elongational viscosity due to maximum stretch condition.
- Second normal stress coefficient equal to zero.

According to Verbeeten (2001), the eXtended Pom – Pom (XPP) model solves these limitations, by eliminating the maximum stretch condition and modifying the orientation. The XPP model is written as:

$$\tau = G_0\left(3\Lambda^2 S - I\right) \tag{2. 75}$$

where S is the orientation tensor and it satisfies the evolution of orientation equation:

$$S_{(1)} + 2\left[\dot{\gamma} : S\right]S + \frac{1}{\lambda_{0b}\Lambda^2}\left[3\alpha\Lambda^4 S\cdot S + \left(1-\alpha-3\alpha\Lambda^4 tr\left(S\cdot S\right)\right)S - \frac{\left(1-\alpha\right)}{3}I\right] = 0 \tag{2. 76}$$

λ_{0b} is the relaxation time of the backbone tube orientation, α is a fitting parameter related to the amount of anisotropy of the material. Λ is the stretch and satisfies the evolution of stretch equation:

$$\dot{\Lambda} = \Lambda\left[\dot{\gamma} : S\right] - \frac{1}{\lambda_s}\left(\Lambda - 1\right) \tag{2. 77}$$

λ_s is the stretch relaxation time, and it is given by

$$\lambda_s = \lambda_{0s} e^{-\nu\left(\Lambda-1\right)} \tag{2. 78}$$

where ν is a measure of the influence of the surrounding polymer chains on the backbone tube stretch. It is approximated by

$$\nu = \frac{2}{q} \tag{2. 79}$$

where q is the number of dangling arms in the 'pom-pom" molecule. This is taken as a fitting parameter too.

Further explanation of this model will be covered in chapter X.

11. Wagner Model

Wagner (1976) is a special case of the K-BKZ constitutive equation (equation 2.58) with:

$$\frac{\partial W(I_1, I_2)}{I_1} = \exp(-\beta\sqrt{\alpha I_1 + (1-\alpha)I_2 - 3}), \tag{2. 80}$$

$$\frac{\partial W(I_1, I_2)}{I_2} = 0, \tag{2. 81}$$

However, the potential function W has been expressed in a variety of expressions, for *shear flow,* equation 2.80 turns into:

$$\frac{\partial W(I_1, I_2)}{I_1} = \exp(-\beta\sqrt{\gamma_{yx}^2}) \qquad \text{for } \sqrt{\gamma_{yx}^2} < 13 \tag{2. 82}$$

Wagner (1976) also used a two-exponential function to improve the predictions:

$$\frac{\partial W(I_1, I_2)}{I_1} = (c)\exp(-\beta_1\sqrt{\gamma_{yx}^2}) + (1-c)\exp(-\beta_2\sqrt{\gamma_{yx}^2}) \text{ for } \sqrt{\gamma_{yx}^2} > 13 \tag{2. 83}$$

And for *elongational flow,* the damping function is:

$$\frac{\partial W(I_1,I_2)}{I_1} = \exp(-\beta\sqrt{\alpha(2e^{-\dot{\varepsilon}s}+e^{2\dot{\varepsilon}s})+(1-\alpha)(2e^{\dot{\varepsilon}s}+e^{-2\dot{\varepsilon}s}-3)} \qquad (2.84)$$

The potential function is called the *damping function*, since it describes the diminishing of the fluid memory by the various kinematic events of the past.

Wagner model can be restated in terms of the Finger tensor as follows:

$$\tau(t) = \int_{-\infty}^{t} M(t-t')h(I_1,I_2)[B(t')-\delta]dt' \qquad (2.85)$$

where M(t-t') is the linear viscoelastic memory function, I_1 and I_2 are the first and second invariants of the Finger tensor B, δ is the unit tensor, and $h(I_1,I_2)$ is the damping function ($h(I_1,I_2) \leq 1$), and represents the probability of an entanglement surviving at a given strain. $h(I_1,I_2)$ tends to one for small deformations resulting in the Lodge rubber-like behavior. The critical point in the rubberlike-liquid theory is the assumption that the flow has no effect on the rate of formation and dissolution of network junctions (entanglements).

12. White – Metzner Model

The White-Metzner model has the advantage of being relatively simple and still giving reasonable shapes for the shear-rate dependent viscosity and first normal stress coefficient and can be used to describe fast time dependent motions. In steady shear free flows the model gives infinite elongational viscosities; the exact value of elongation rate at which these viscosities become infinite depends on the behavior of shear viscosity. The constitutive equation is given by

$$\tau_{(1)} + \frac{1}{\Lambda}\tau = G\dot{\gamma} \qquad (2.86)$$

where Λ is a relaxation time that depends on the deformation rate $\dot{\gamma}$. One suggested form of this dependence (Larson, 1987) is

$$\Lambda = \frac{\lambda}{1+\alpha\lambda(tr\dot{\gamma}:\dot{\gamma})^{\frac{1}{2}}} \qquad (2.87)$$

D. Introduction to Fractals Theory

Chaos science uses a different geometry called fractal geometry. It is providing us with a new perspective to view the world. Fractal geometry is a new language used to describe, model and analyze complex forms found in nature.

Fractal geometry is a mathematical tool for dealing with complex systems that have no characteristic length scale. A well know example is the shape of a coastline. When we see two pictures of a coastline on two different scales, with 1 cm corresponding for example to 0.1 km or 10 km, we cannot tell which scale belongs to which picture, both look the same. This means that the coastline is scale invariant or, equivalently, has no characteristic length scale (Armin, 1994). Other examples in nature are rivers, mountains, clouds, DNA, and, of course, polymers. Scale invariant (no characteristic length scale) systems are usually characterized by fractal (noninteger) dimensions.

A common way to measure the fractal dimension of an object is the Box Counting Method. This method consists in lay over the object to be measure a grid of lattice constant (box size) ε. The number of boxes, $N_B(\varepsilon)$, which cover any part of the object (the occupied or intersected boxes), are counted and each data couple $N_B(\varepsilon)$, ε is tabulated. The same procedure is repeated with a set of successively smaller ε. Log $[N_B(\varepsilon)]$ is plotted versus log $[1/\varepsilon]$ and the slope of the resulting

straight line (if such indeed exists) is taken as the fractal dimension of the object. If the resulting plot is not a straight line, or if the slope of the resulting straight line is an integer, then the object is not a fractal (Rothschild, 1998).

Fractals objects could be classified as deterministic and random fractals. Deterministic fractals are generated iteratively in a deterministic way, while random fractals are generated using a stochastic process. Although fractal structures in nature are random, it is useful to study deterministic fractals where the fractal properties can be determined exactly. By studying deterministic fractals one can gain also insight into the fractal properties of random fractals, which usually cannot be treated rigorously (Armin, 1994)

The simple fractal model is the random walk. Imagine a walker on a square lattice. In one unit of time, the walker advances one step of length *a* to a randomly chosen nearest neighbor site. The path that the walker follows after *N* number of steps is called a random walk. The random walk model is very useful in science; its most important use is to simulate the Brownian motion phenomena. Another important model is the self-avoiding walk. It is very similar to a random walk, but in this model, the walker can not return to a site in which he has already been.

In the past years, engineering empiricism has given way to obtain systematic analytic techniques in the study of the kinetics of transport in disordered media; however, these have been mainly based on different versions of the theory of random walks. Therefore, an understanding of the kinetics of transport in fractal and disordered media is almost necessarily phrased in terms of the random walk model (Armin, 1994).

This model is the simplest way to model a polymer chain, which could be considered as a fractal object. However, actual polymer chains have steric interaction that avoids monomers from placing on the top of each other. Random walk and self-avoiding walk models describe a polymer in a solvent. It is assumed

that polymer chains are made of *N* statistical units (some monomers units) which are randomly oriented with respect to each other. Random walk describes a linear chain where no interactions are present between monomers. Self-avoiding walk describes an interaction between monomers. Further information about fractals theory will be covered in chapter XII.

CHAPTER III. Experimental Techniques

This chapter presents the experimental techniques used for the characterization of eight polypropylene resins. The resins were tested for their rheological response under frequency sweeps, capillary and creep and recovery compliance. Standard well-documented and proven procedures (Bonilla, 1996; Aguirre, 2000; Mier, 2000) were followed in each rheological test.

A. Materials

Four pair of isotactic and syndiotactic polypropylene resins were used. Resins with the same melt flow index (MFI) were selected in order to observe differences in their rheological response. A small amount (approximately 0.1% wt) of 2-6 di-tert-butyl-p-cresol, BHT, (as stabilizer) was added to all samples. Table III.1 shows the description of the eight polypropylene resins.

Table III.1. Polypropylene resins used in the research.

Resin	ID	MFI	XS	Type	Lot
Finaplas 1251	A	2	4	Syndiotactic	HB-77239
Finaplas 1471	B	4	4	Syndiotactic	HB-77361
Finaplas 1571	C	12	5	Syndiotactic	HB-77141
Finaplas 1751	D	20	6	Syndiotactic	Lot 68459
Atofina 3276	E	2	2.5	Isotactic	Lot 77081
Atofina 3462	F	4	1.4	Isotactic	Lot 69342
Atofina 3652	G	12	2	Isotactic	HB-78128
Atofina 3761	H	18	2	Isotactic	Lot 71269

B. Standard Quality Control Techniques

The melt flow index (MFI), the molecular weight distribution (MWD), the percentage of xylene solubles (XS), the differential scanning calorimetry (DSC), and the synthesis' effectiveness by nuclear magnetic resonance (NMR) are the standard quality control attributes commonly used for PP resins.

1. Melt Flow Index

The melt flow index measurements (ASTM D1238) were carried out in a Tinius Olsen Model MP600 at 230°C. The equipment has a die diameter of 0.0825 inches, a die length of 0.315 inches, a barrel diameter of 0.375 inches, and a 180° die entrance angle. A constant load of 2.16 kg is applied to the plunger and the amount (in grams) of material flowing during a given time is recorded. The MFI is defined as the amount (in grams) of material flowing for 10 minutes.

The typical experimental error of a MFI study can be ± 10%; so duplicates samples are at least required and an average value is reported. A MFI measurement represents a single shear rate point (approximately 10 sec^{-1}) in the shear viscosity curve, if elastic and end effects are not present.

2. Percentage of Xylene Solubles

A Soxthlet extractor is used to extract material soluble in xylene. The xylene soluble portion of the resin is extracted and reported as a weight percentage in the sample. This portion is related to the low molecular weight and atactic species.

3. Molecular Weight Distribution

The molecular weight distribution (MWD) curves were determined using a Waters Model 150C Gel Permeation Chromatograph (GPC). The tests were performed at

135°C, with tricloro-benzene as the mobile phase. The system uses three columns in series: two Shodex 806 m/sec columns and a Waters Styragel HT column. The three columns used a styrene-divinyl benzene packing gel. A set of narrow molecular weight PS standards with Mw ranging from $8x10^6$ to $520x10^6$ were used for calibration.

4. Nuclear magnetic Resonance

NMR can be used to determine the isotactic or syndiotactic nature of polymers. The effectiveness of synthesis of an isotactic or syndiotactic polypropylene is attained by doing a NMR test on the xylene soluble fraction extracted from the polymer sample. Atactic chains and low molecular weight isotactic chains are soluble in some solvents and can be washed out of a polymer sample.

In an NMR study the soluble material is extracted from the samples in two steps.

1) Xylene soluble analysis: In this test the polymer is dissolved completely in boiling xylene. The solution is allowed to cool slowly overnight (in a normal xylene solubles procedure the solution is placed in an ice bath to speed up the crystallization). The solution is then filtered by gravity through a coarse filter paper and the filter cake is washed with cold xylene. The filter cake is the xylene insoluble fraction.
2) Heptane extraction: The xylene insoluble fraction is granulated, placed in an extraction thimble and extracted with heptane in a Soxtec apparatus. The procedure places the extraction thimble in boiling heptane for one hour, then it is raised and rinsed with refluxed heptane for one hour. After drying it in a vacuum oven the sample is ready for NMR analysis

To test the effectiveness of the xylene soluble extraction a second xylene soluble procedure can be performed on the sample before heptane extraction. This is

done because there could be some trapping of soluble material in the crystalline (insoluble) fraction during recrystallization.

5. Differential Scanning Calorimetry

A differential scanning calorimeter (DSC) has the ability to program a heating cycle and precisely control the cooling cycle to impose a thermal history upon a sample. A control of the thermal history is a requirement for the complete characterization of semi crystalline polymers. The melting profile of a polymer during heating can be different to the crystallization profile during cooling. Thermal history can have a major effect on the properties of a given polymer. Different thermal histories can produce a material with a different melting profile. To ensure an accurate DSC analysis (melting or crystallization points and latent heats) all samples received the same thermal history.

In the most popular DSC design, two pans sit on a pair of identically positioned platforms connected to a furnace by a common heat flow path. In one pan, the polymer sample is placed, while the other one (the reference pan) is left empty. The furnace is turn on at a specific heating rate, usually something like 10 °C per minute. The equipment is designed to assure that the heating rate stays exactly the same throughout the experiment and that the two separate pans heat at the same rate as each other. The polymer sample in one pan implies that there is extra material, so it will take more heat to keep the temperature of the sample pan increasing at the same rate as the reference pan. This difference is what is measured in a DSC experiment.

After a certain temperature the heat will be absorbed by the sample, which means a change (increase) in its heat capacity. This happens because the polymer has just gone through the glass transition. Above the glass transition, the polymers have a lot of mobility. They twist and struggle, and never stay in one position for very long. When they reach the right temperature, they will have gained enough

energy to move into very ordered arrangements, which are called crystals. When polymers fall into these crystalline arrangements, they give off heat. This could be seen as a big peak in the plot of heat flow versus temperature.

After the crystallization, if the heating continues, the polymer will reach another thermal transition, melting. When polymer's melting temperature, or T_m, is reached, those polymer crystals begin to fall apart, that is they melt. The chains come out of their ordered arrangements, and begin to move around freely. There is a latent heat of melting as well as a latent heat of crystallization. When the polymer crystals melt, they must absorb heat in order to do so. Remember melting is a first order transition, this means that when you reach the melting temperature, the polymer's temperature won't rise until all the crystals have melted. This also means that the furnace is going to have to put additional heat into the polymer in order to melt both the crystals and keep the temperature rising at the same rate as that of the reference pan. This extra heat flow during melting shows up as a large dip in the DSC plot as heat is absorbed by the polymer. The heat of melting is measured by calculating the area of this dip.

Reviewing the DSC process, we saw a step in the plot when the polymer was heated past its glass transition temperature. Then we saw a big peak when the polymer reached its crystallization temperature. Then finally we saw a big dip when the polymer reached its melting temperature. Putting all together, a whole plot will often look something like Figure III.1.

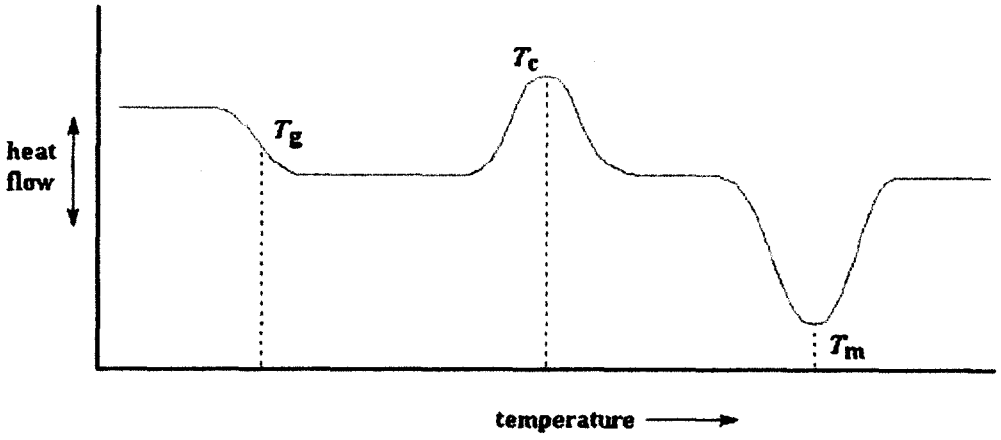

Figure III.1. Schematic DSC plot.

It is worth to mention that crystallization peak and the melting dip will only show up for polymers that can form crystals. Completely amorphous polymers won't show any crystallization, or any melting either. But polymers with both crystalline and amorphous domains, will present all the features shown in Figure III.1.

DSC can also tell us how much of a polymer is crystalline and how much is amorphous. The percentage of crystalline polymer is calculated by (Dealy, 1990):

$$\%crys = \frac{H_m - H_c}{H_m^*} x100 \qquad (3.\ 1)$$

where H_m, H_c are the heat absorbed during the melting and the heat give off in crystallization respectively. H^*_m is the latent heat of melting of the polymer.

C. Rheological Characterization

1. Sample Preparation

A specific sample preparation technique was used for two main purposes: to have homogeneous, bubble free and chemically stable samples; and to reduce variability in the results. Standard well-documented procedures (Aguirre, 2000; Mier, 2000) were followed in sample preparation. The samples were stabilized with 1000 ppm (0.1% weight) of 2-6 di-tert-butyl-p-cresol (BHT) and either used directly for testing in the capillary rheometer or formed into 1 mm thick, 25 mm diameter disks for oscillatory, and creep & recovery testing.

2. Testing Conditions

It is well known that the testing conditions are crucial in getting reliable linear viscoelastic information. If testing temperature is too low, the material can be very stiff and trimming of the sample to prepare the specimen for testing could be difficult. If the stress is too high, centrifugal forces might expel the material from between the plates. If strain is too high, stress overshoot can occur, and no measurement can be done. If the testing time is too long, thermal degradation might occur. Therefore, it was determined to use proven testing conditions (Mier, 2000).

3. Testing Equipment

The equipment used for rheological tests is presented in Table III.2. More specific information about the equipment as well as their procedures, can be found in Appendix C.

Table III.2. Equipment used for the rheological characterization.

Test	Type of Equipment	Make	Model
Frequency Sweeps	Strain Rheometer	Rheometrics	RAA
Shear and Elongational Viscosity	Capillary Rheometry	Rosand	RH7-2
Creep and Recovery	Controlled Stress Rheometer	Rheometrics	RS5000

4. Oscillatory Frequency Sweeps

In a small amplitude oscillatory shear experiment, a thin sample of material is subjected to a simple shearing deformation such that the imposed shear strain is:

$$\gamma(t) = \gamma_o \sin(\omega t) \qquad (3.2)$$

where γ_o is the strain amplitude and ω is the frequency (rad/sec), both defined by the experimenter. The imposed shear rate is then:

$$\dot{\gamma}(t) = \gamma_o \omega \cos(\omega t) = \dot{\gamma}_o \cos(\omega t), \qquad (3.3)$$

where $\dot{\gamma}_o$ is the shear rate amplitude. If γ_o is sufficiently small, the stress can be calculated substituting equation 3.1 into $\sigma(t) = G_d * \gamma(t)$, resulting in a sinusoidal stress:

$$\sigma(t) = \sigma_o \sin(\omega t + \delta), \qquad (3.4)$$

where $G_d = \sigma_o / \gamma_o$ is the amplitude ratio, σ_o is the stress amplitude, and δ is a phase shift, which is called the mechanical loss angle.

The amplitude ratio G_d and the loss angle (δ) are functions of the frequency, but are independent of the strain amplitude as long as γ_o is sufficiently small. A relation that has proven to be valid for a number of materials is (Booij and Thoone, 1982; in Dealy, 1992):

$$\delta(\omega) \approx \frac{\pi}{2}\left[\frac{d(\ln G_d)}{d(\ln \omega)}\right] \qquad (3.5)$$

Knowing that $\sigma_o = \gamma_o G_d$ and that $sin(\omega t + \delta) = sin(\omega t)cos(\delta) + cos(\omega t)sin(\delta)$, equation 3.3 can be restated as:

$$\sigma(t) = \gamma_o\left[G'(\omega)\sin(\omega t) + G''(\omega)\cos(\omega t)\right], \qquad (3.6)$$

where G'(ω) (the storage modulus) and G"(ω) (the loss modulus) are given by:

$$G'(\omega) = G_d \cos(\delta) \qquad (3.7)$$

$$G''(\omega) = G_d \sin(\delta) \qquad (3.8)$$

if $G_d = \sigma_o / \gamma_o$ then:

$$\sqrt{(G'(\omega))^2 + (G''(\omega))^2} = \sqrt{G_d^2 Cos^2\delta + G_d^2 Sin^2\delta} = G_d\sqrt{Cos^2\delta + Sin^2\delta} = G_d = \frac{\sigma_o}{\gamma_o} \qquad (3.9)$$

$$\tan(\delta(\omega)) = G''(\omega) / G'(\omega) \qquad (3.10)$$

if $\tan(\delta(\omega)) = G''(\omega) / G'(\omega)$ then G"(ω) and G'(ω) are the sides of a right triangle that can be thought as the real (G'(ω)) and imaginary (G"(ω)) components of a complex modulus:

$$G^*(\omega) \equiv G'(\omega) + iG''(\omega) \tag{3. 11}$$

Knowing that $\omega\sigma_o = \omega\gamma_o G_d = \dot{\gamma}_o G_d$, $\eta = \sigma_o / \dot{\gamma}_o = G_d / \omega$, and that $\sin(\omega t + \delta) = \sin(\omega t)\cos(\delta) + \cos(\omega t)\sin(\delta)$, equation 3.3 can be restated as:

$$\sigma(t) = \dot{\gamma}_o[\eta''(\omega)\sin(\omega t) + \eta'(\omega)\cos(\omega t)], \tag{3. 12}$$

where η'(ω) (the dynamic viscosity) and η"(ω) are given by:

$$\eta'(\omega) = (G_d / \omega)\sin(\delta), \tag{3. 13}$$

$$\eta''(\omega) = (G_d / \omega)\cos(\delta). \tag{3. 14}$$

From here, it can be obtained:

$$G_d \equiv \sigma_o / \gamma_o = \omega\sqrt{(\eta'(\omega))^2 + (\eta''(\omega))^2} \tag{3. 15}$$

$$\tan(\delta(\omega)) = \eta'(\omega)/\eta''(\omega) \tag{3. 16}$$

η'(ω) and η"(ω) can also be thought as the real and imaginary components of a complex viscosity, which according to the empirical Cox-Mertz rule is related to the steady shear viscosity:

$$\eta^*(\omega) \equiv \eta'(\omega) - i\eta''(\omega). \tag{3. 17}$$

Another important oscillatory parameter is the point at which the storage and loss modulus are equal, which is known as the cross-over point. The cross-over point G_c is related to the polydispersity index of the polymers.

In conclusion, the results of an oscillatory shear experiment can be presented as:

a) Plots of G'(ω) and G''(ω) versus frequency by means of equations 3.7 and 3.8.

b) Plots of η'(ω) and η''(ω) versus frequency by means of equations 3.13 and 3.14.

c) Plots of the phase shift δ versus frequency by means of equation 3.5.

5. Creep and Recovery Compliance

In a creep and recovery test, the polymer melt is subjected to a sudden shear stress of constant magnitude, which is held for a period of time, while the resulting deformation (called creep compliance J(t) when the deformation is divided by the imposed stress) is monitored as a function of time. After the steady state deformation is reached at a time t_o, the shear stress ceases ($\tau_o = 0$) and the material recoils in a direction opposite to that of the original applied force. This recoil, when divided by the initial stress is known as the elastic recovery or recovery compliance Jr(t). The amount of recovered shear strain is a function of time t_o and of time (t - t_o) that has elapsed since the cessation of the applied shear stress.

$$\gamma_r(t - t_o) \equiv \gamma(t_o) - \gamma(t); \qquad t > t_o \tag{3. 18}$$

If the stress is removed after the steady state has been achieved, then the recovery strain is no longer a function of t_o. If t_o is taken as t_o = 0; i.e. the beginning of the recovery test:

$$\gamma_r(t) \equiv \gamma(0) - \gamma(t) \tag{3. 19}$$

As mentioned above, the creep and the recovery strains are divided by the applied stress, the result is called creep and recovery compliance and is the result of several modes of deformation:

$$J(t) = \frac{\gamma(t)}{\tau_o} = J_g + J_e(t) + \frac{t}{\eta_o} \qquad \text{(creep compliance)} \qquad (3.20)$$

$$Jr(t) = \frac{\gamma_r(t)}{\tau_o} \qquad \text{(recovery compliance)} \qquad (3.21)$$

where J_g is the instantaneous or glassy compliance (or glassy deformation if multiplied by stress), $J_e(t)$ is the retarded elastic compliance [$J_e(t) = J_r(0) - J_r(t)$), where $J_r(0)$ is the compliance at the time the stress ceases t_o], $J_r(t)$ is the recoverable compliance at any time after the stress ceased, and $J_e°$ is the steady state recoverable compliance $J_e^o = J_r(t \to \infty)$.

6. Shear Viscosity by Capillary Rheometer

The capillary rheometer consists of a small tube (die) through which melt is forced to flow by means of a piston moving at a fixed speed. The instrument measures the pressure drop across the die (ΔP) (some capillary rheometers measures the load F_p and obtain the driving pressure (P_d) by $P_d = F_p / A$, where A is the transversal area of the barrel) over a range of piston velocities. Capillary rheometers are used to determine the viscosity in the shear rate range of 5 to 1000 1/s using dies with different L/D and with typical diameters between 0.5 mm and 1.5 mm, although very wide capillaries can be used.

To calculate the shear viscosity, it is necessary to know the wall shear stress and the wall shear rate. The wall shear stress is related to the pressure drop by:

$$\tau_w = \frac{\Delta P}{2(L/R + e)}. \qquad (3.22)$$

where L and R are the capillary die length and radius, respectively; and *e* is the Bagley (1957) correction factor. Bagley measured the pressure drop at various values of the flow rate:

$$Q = \upsilon \cdot \pi \cdot (R_b)^2, \tag{3. 23}$$

(where υ is the piston velocity) using a variety of capillaries having different lengths but the same diameter. For each value of the apparent wall shear rate:

$$\dot{\gamma}_a = \frac{4Q}{\pi R^3} = \frac{32 \cdot Q}{\pi \cdot D^3} \tag{3. 24}$$

Bagley plotted the driving pressure (P_d) versus L/R and drew a straight line through the points and by extrapolating the lines to the P_d = 0 axes, the *end correction* factor is obtained. The end correction factor "e" is defined as the negative of the value of L/R at the point of interception. It represents the L/R of the capillary for which fully developed flow would give a pressure drop equal to the excess pressure drop due to the entrance effect.

Finally, it remains to determine the shear rate at the wall:

$$\dot{\gamma}_w = \left(\frac{3 + b_R}{4}\right)\dot{\gamma}_a \tag{3. 25}$$

where b_R is the Rabinowitch correction factor given by:

$$b_R = \frac{d(\log \dot{\gamma}_a)}{d(\log \tau_w)} \tag{3. 26}$$

The principal sources of error in the use of a capillary rheometer are:

a) Nonuniform temperature due to viscous heating especially at large shear rates or capillary radius.

b) Effect of pressure on viscosity.

c) Wall slip or unsteady flow due to oscillating entry streamlines.

7. Elongational Viscosity by Capillary Rheometer

The Cogswell analysis (Cogswell 1972a and 1972b) was applied for the determination of the elongational viscosity. This estimation requires apparent shear viscosity data; corrected stress data and elastic pressure gradient information obtained from capillary measurements (see Appendix A). The equations proposed by Cogswell are:

$$\sigma_e = \frac{3\cdot(n+1)\cdot}{8}\cdot\Delta P_E \qquad (3.27)$$

$$\eta_e = \frac{\sigma_e}{\dot{\varepsilon}} = \frac{9\cdot(n+1)^2(\Delta P_E)^2}{32\cdot\eta_a\dot{\gamma}_a^2} \quad \text{(when using a die with flat (180°) entrance angle)} \qquad (3.28)$$

$$\eta_e = \frac{3(\Delta P_E)}{\mathrm{Tan}(\theta/2)\left[1-\left(\frac{D_b}{D}\right)^3\right]\dot{\gamma}_a} \quad \text{(when using a die with an entrance angle } \theta\text{)} \qquad (3.29)$$

$$\dot{\varepsilon} = \frac{\sigma_e}{\eta_e} \qquad (3.30)$$

where:

$\dot{\gamma}_a$ is the apparent shear rate,

η_a is the apparent viscosity $\eta_a = \tau_t / \dot{\gamma}_a$ (where τ_t is the true shear stress),

n is the power law parameter $n = d(\log\tau_t)/d(\log\dot{\gamma}_a)$,

ΔP_E is the pressure drop for a zero length die $\Delta P_E = \frac{\Delta P_S - \Delta P_L L_S/L_L}{1-L_S/L_L}$,

$\dot{\gamma}_t = \left[\frac{3n+1}{4n}\right]\dot{\gamma}_a$ is the corrected shear rate,

σ_e is the elongational stress,

η_e is elongational viscosity,

θ is the capillary die entrance angle (flat entrance θ = 180° = π radian, cone entrance θ = 90° = π /2 radian)

$\dot{\varepsilon}$ is elongational rate.

It is important to mention that Rosand software recalculates the power law index "n" using $n = d(\log \tau_t)/d(\log \dot{\gamma}_t)$ for equations 3.26 and 3.27 and uses the corrected shear rate instead of the apparent shear rate in equation 3.28. Such calculations differ from the original analysis done by Cogswell (1972a, 1972b). Figure III.2 shows a comparison between the elongational viscosity (using a die with 90° entrance angle) calculated from the original Cogswell's analysis and that obtained from Rosand software. The Rosand's approach changes the slope of η_e and predicts higher elongational rates (Mier, 2000). In this thesis, the original Cogswell approach will be used (see Appendix A).

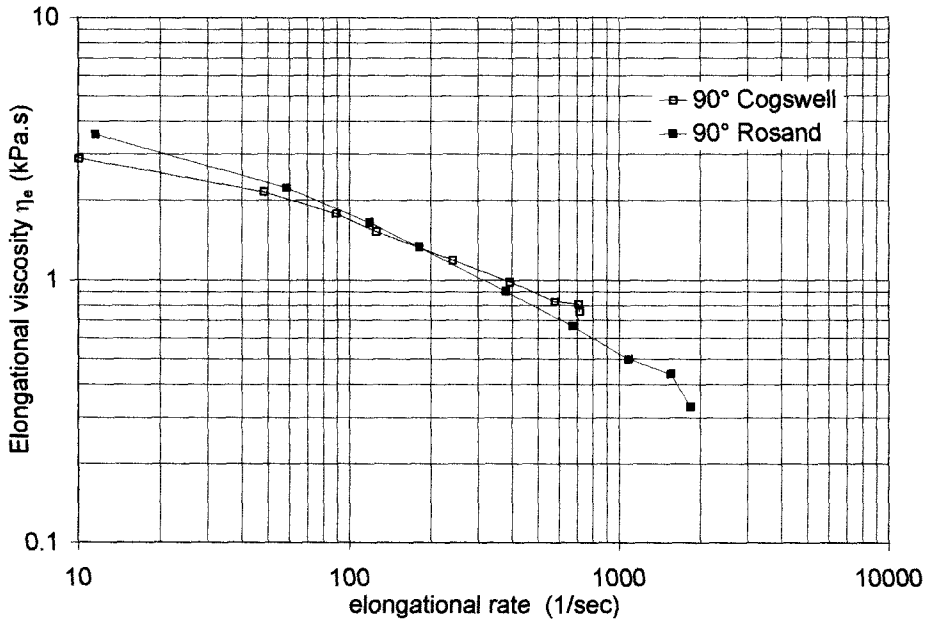

Figure III.2. Comparison between elongational viscosity at 200 °C calculated from the original Cogswell's analysis and that obtained from Rosand software. Mier (2000) developed this plot using a metallocene isotactic polypropylene resin.

CHAPTER IV. Standard Quality Properties

The basic standard quality properties (SQP) for polypropylene resins are the melt flow index (MFI) and the percentage of xylene solubles (XS). These properties (MFI and XS) for the resins used in this research are presented in Table III.1 in the previous chapter.

This chapter presents, as standard quality control properties, the Molecular Weigh Distribution (MWD), the Nuclear Magnetic Resonance (NMR) and the calorimetric properties for the resins.

A. Molecular Weight Distribution (MWD)

Table IV.1 presents the molecular weigh moments and polydispersity data as obtained from GPC measurements for all the resins. Mz/Mw is the polidispersity index related to the content of high molecular weight species. Figure IV.1 shows the molecular weight distributions for resins A and E (resins with melt flow 2, syndiotactic and isotactic respectively). These resins present some notable differences in their MWD. The MWD for resin A (syndiotactic) presents a bimodal behavior with a Mw lower than resin E (isotactic). Figure IV.2 shows the MWD for all the resins.

Table IV.1. Molecular weigh moments and polydispersity indices as obtained from GPC.

Resin	M_n	M_w	M_z	M_w/M_n	M_z/M_w	Peak M_w
A	42134	190554	518052	4.5	2.7	193756
B	37960	158366	421148	4.2	2.7	54742
C	33169	121042	318803	3.6	2.6	48785
D	27265	96422	247354	3.5	2.6	43963
E	64131	414092	1526508	6.5	3.7	191509
F	51229	345046	1411454	6.7	4.1	176522
G	36268	236114	855114	6.5	3.6	136878
H	35189	214871	736338	6.1	3.4	133754

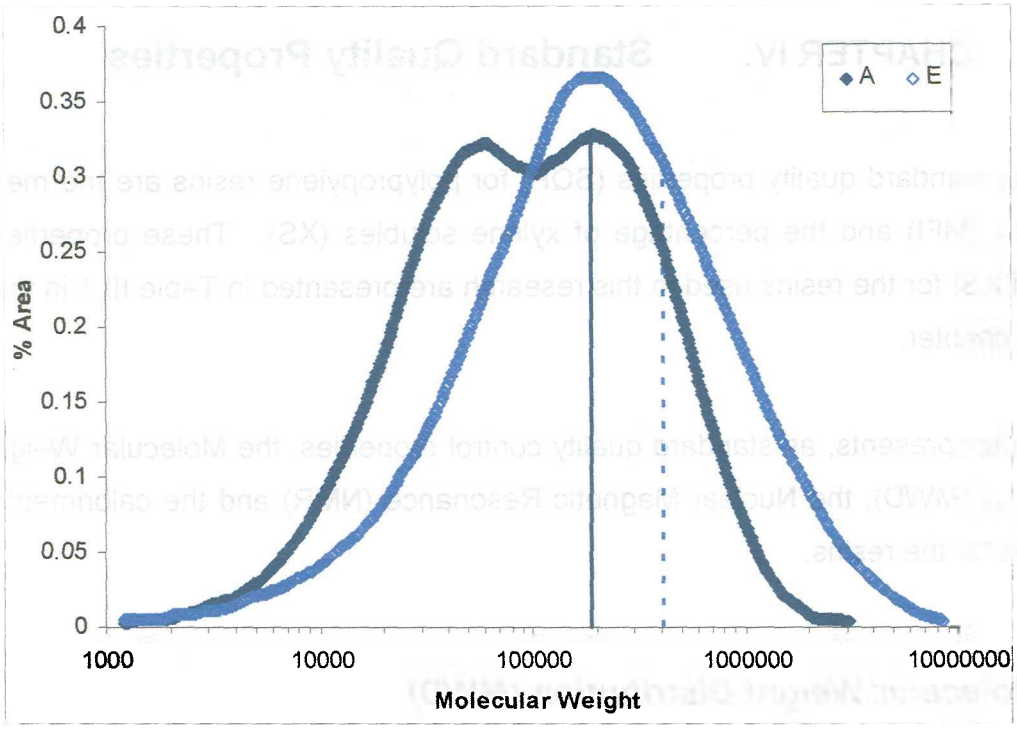

Figure IV.1. Molecular weight distributions as obtained from GPC for resin A and E.

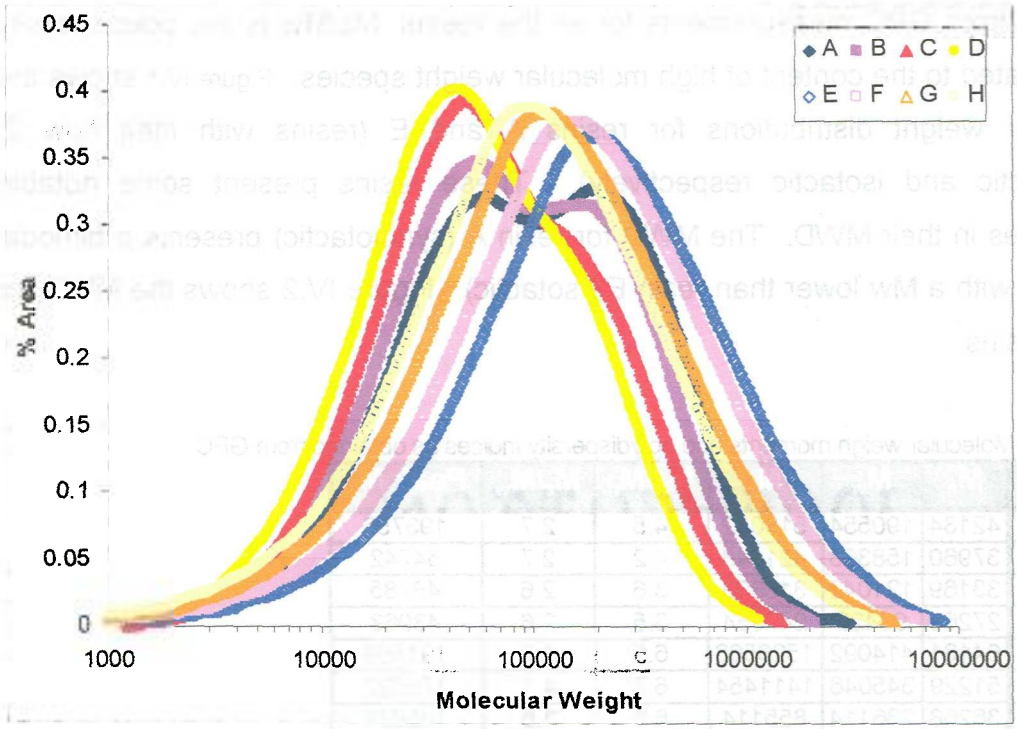

Figure IV.2. Molecular weight distributions as obtained from GPC for all the resins.

B. Nuclear Magnetic Resonance (NMR)

1. Principles (Odian, 1991)

To better understand the NMR results is important to review before some important concepts. Configurational (stereo) isomers differ in the spatial arrangements (*conformations*) of their atoms or substituents in a molecule in a manner such that they can be interconverted only by breaking and reforming chemical bonds.

The polymerization of a monosubstituted ethylene, CH_2=CHR (for propylene, R is a methyl group -CH_3), leads to polymers in which every tertiary carbon atom in the polymer chain is a *stereocenter*. A stereocenter is defined as an atom bearing several groups whose identities are such that an interchange of two of the groups produces a stereoisomer. Considering the main carbon-carbon chain of the polymer –(–CH_2–CHR–)$_n$– two different configurations are possible for each stereocenter since the R group may be situated on either side of the plane of the carbon-carbon polymer chain. The regularity in the configurations of successive stereocenters determines the overall order (*tacticity*) of the polymer chain. An *isotactic* structure occurs when the stereocenter in each repeating unit in the polymer chain has the same configuration. A *syndiotactic* polymer structure occurs when the configuration of the sterocenter alternates with the R groups located on the opposite sides of the plane of the polymer chain. If the R groups are randomly distributed on the two sides of the planar zigzag polymer chain, the polymer is termed *atactic*.

Dyad tacticity is defined as the fractions of pairs of adjacent repeating units that are isotactic or syndiotactic to one another. The isotactic (meso) and syndiotactic (racemic) dyads can be depicted as shown in Figure IV.3. where the horizontal line represent a segment of the polymer chain, the black circles represent the configuration of the R group at the stereocenter, and the vertical line represents the

two hidrogens at the carbon between adjacent stereocenters. The fractions of isotactic and syndiotactic dyads are referred to as (m) and (r), respectively.

Figure IV.3. Depicture of isotactic (meso) and syndiotactic (racemic) dyads.

Triad tacticity describes isotactic, syndiotactic, and heterotactic triads whose fractions are designated as (mm), (rr), and (mr), respectively (see Figure IV.4).

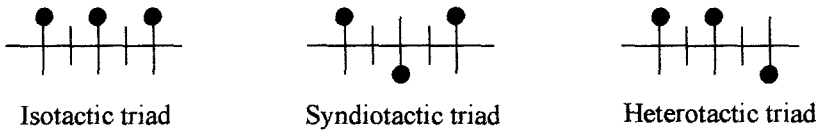

Figure IV.4. Depiction of isotactic (meso), syndiotactic (racemic), and heterotactic triads.

The above definitions can be clarified by considering an example portion of a polymer chain like the one shown in Figure IV.5. The chain segment has 8 dyads and 7 triads. There are 6 meso dyads (m = 6/8) and 2 racemic dyads (r = 2/8). There are 4 isotactic triads (mm = 4/7), 1 syndiotactic (rr = 1/7), and 2 heterotactic (mr = 2/7).

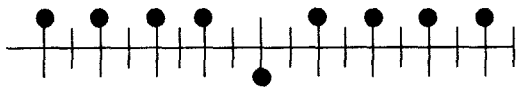

Figure IV.5. Depiction of isotactic (meso), syndiotactic (racemic), and heterotactic triads.

The determination of the triad fractions allows a complete definition of dyad structures using:

$$(m) = (mm) + 0.5(mr) \quad (4.1)$$

$$(r) = (rr) + 0.5(mr) \quad (4.2)$$

The advent of high-resolution NMR allow the determination of tetrad, pentad and even higher sequence distributions in many polymers. The tetrad distribution consists of the isotactic sequence (mmm), the syndiotactic sequence (rrr), and the heterotactic sequences (mmr), (rmr), (mrm), and (rrm). The following relationships exist between tetrad and triad fractions:

$$(mm) = (mmm) + 0.5(mmr) \quad (4.3)$$

$$(rr) = (rrr) + 0.5(mrr) \quad (4.4)$$

$$(mr) = (mmr) + 2(rmr) = (mrr) + 2(mrm) \quad (4.5)$$

The pentad distribution consists of the isotactic sequence (mmmm), the syndiotactic sequence (rrrr), and the heterotactic sequences (rmmr), (mmrm), (mmrr), (rmrm), (rmrr), (mrrm), and (rrmm). The following relationships exist between pentad and tetrad fractions:

$$(mmm) = (mmmm) + 0.5(mmmr) \quad (4.6)$$

$$(mmr) = (mmmr) + 2(rmmr) = (mmrm) + (mmrr) \quad (4.7)$$

$$(rmr) = 0.5(mrmr) + 0.5(rmrr) \quad (4.8)$$

$$(mrm) = 0.5(mrmr) + 0.5(mmrm) \quad (4.9)$$

$$(rrm) = 2(mrrm) + (mrrr) = (mmrr) + (rmrr) \quad (4.10)$$

$$(rrr) = (rrrr) + 0.5(mrrr) \quad (4.11)$$

2. Analysis of stereoregularity

As explained, NMR allows to obtain the sequence distribution of steroisomeric units within the polymer chain. The NMR data can be used to determine the effectiveness of the synthesis of an isotactic polypropylene by analyzing the

soluble fraction of each resin. A typical commercial polypropylene resin is a mixture of isotactic, syndiotactic and atactic chains.

Table IV.2 presents the NMR spectrum (mol percentages) for the resins under study. In Table IV.2 xmrx is the sum of mmrm and rmrr pentads since by NMR such two sequences are indistinguishable.

Table IV.2. NMR Spectrum (% mol) for all the resins.

PENTAD	A	B	C	D	E	F	G	H
mmmm	0	0	0	0	87.8	93.9	93.5	93.5
mmmr	0.2	0.2	0.3	0.2	3.4	2.3	2.4	2.4
rmmr	2.3	2.3	2.4	2.8	0.6	0.6	0.4	0.4
mmrr	4.5	4.7	4.6	5	3.1	1.5	1.5	1.5
xmrx	3.3	3.7	3.6	3.9	1.3	0.5	0.5	0.5
mrmr	0.5	0.6	0.7	0.8	0	0	0.2	0.2
rrr	76.6	75.8	76.7	75.2	1.5	0.5	0.5	0.4
rrm	10.5	70.5	10.3	10.7	0.8	0	0.3	0.4
mrrm	2	2.1	1.5	1.4	1.5	0.7	0.8	0.7
% meso	6.7	7.1	7.1	7.8	94	97.8	97.4	97.4
% racemic	93.3	92.9	92.9	92.2	6	2.2	2.6	2.6
% error	4	4.2	4.2	4.7	1.2	0.9	0.6	0.7
Defects per 1000 carbons	33.6	35.4	35.5	39.2	30	11.2	13.2	12.8

C. Calorimetric Data

Table IV.3 shows the DSC calorimetric properties of all the polypropylene resins under study. In general, higher latent heats correspond to higher recrystallization and second melt temperatures. When polypropylene crystallizes from the melt, different crystalline formations may develop; Table IV.4 presents the unit cell parameters for syndiotactic and isotactic polypropylene as well as the theoretical melting temperature (Tm). It can be seen that for syndiotactic resins, resin D with the highest melt flow present the most similar melting temperature to the theoretical melting temperature presented in Table IV.4. However, for isotactic resins, the melting temperature closer to the theoretical melting temperature is the

melting temperature of resin E, the isotactic resin with lowest melt flow. Finally Table IV.5 presents the percentage of crystals in the samples according to equation 3.1.

Table IV.3. DSC analysis results for all the resins.

RESIN	Recrystallization Peak (°C)	Recrystallization ΔH (Joules/gram)	Second Melt Peak (°C)	Second Melt ΔH (Joules/gram)
A	66.63	-31.06	127.0	28.31
B	64.30	-30.23	127.4	28.09
C	71.63	-39.07	128.0	24.87
D	67.96	-38.96	131.7	30.46
E	107.3	-105.4	162.0	71.58
F	110.6	-114.4	160.7	86.19
G	110.3	-113.2	160.7	87.16
H	110.3	-121.8	159.0	89.48

Table IV.4. Polypropylene unit cell parameters.

	Isotactic	Syndiotactic
Unit Cell	α monoclinic	Orthorhombic
a (nm)	0.664	1.45
b (nm)	2.096	0.58
c (nm)	0.650	0.74
β	99° 20'	90°
Density (gr/cm^3)	0.936	0.91
Tm °C	165	135
Heat of Fusion (J/gr)	209	50.2

Table IV.5. Percentage of crystallinity for all the resins.

RESIN	% Crystallinity
A	5.48
B	4.26
C	28.29
D	16.93
E	16.18
F	13.50
G	12.46
H	15.46

CHAPTER V. Oscillatory Data

For each resin, the oscillatory data was obtained from frequency sweep tests at 200 °C by means of a RAA (see Table III.2) with a 25 mm parallel plates configuration and 1 mm gap. The frequency range used was from 500 to 0.01 rad/s and 10 % of the strain was utilized. In addition, frequency sweeps at 190 °C and 210 °C were done and together with the 200 °C data, were brought into a single master curve according to Mavridis (1992).

A. Storage and Loss Moduli

Figure V.1 through Figure V.8 show the storage (G') and loss (G") moduli for each resin. The cross-over point is presented in the plots by a cross (x). The cross-over point will be analyzed in the section B and C of this chapter. It is worth to mention that data with a torque lower than 0.8 gr-cm were eliminated because of equipment resolution.

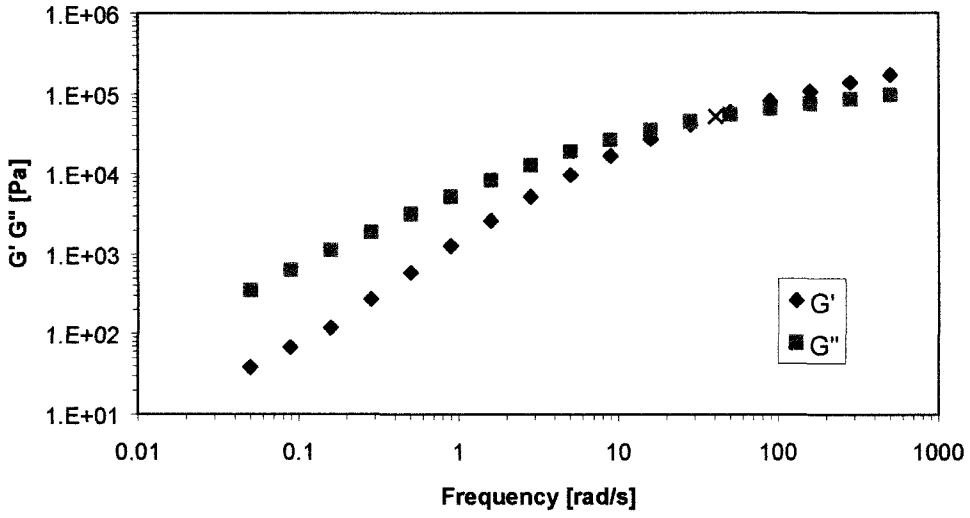

Figure V.1. Storage and loss moduli at 200 °C for resin A.

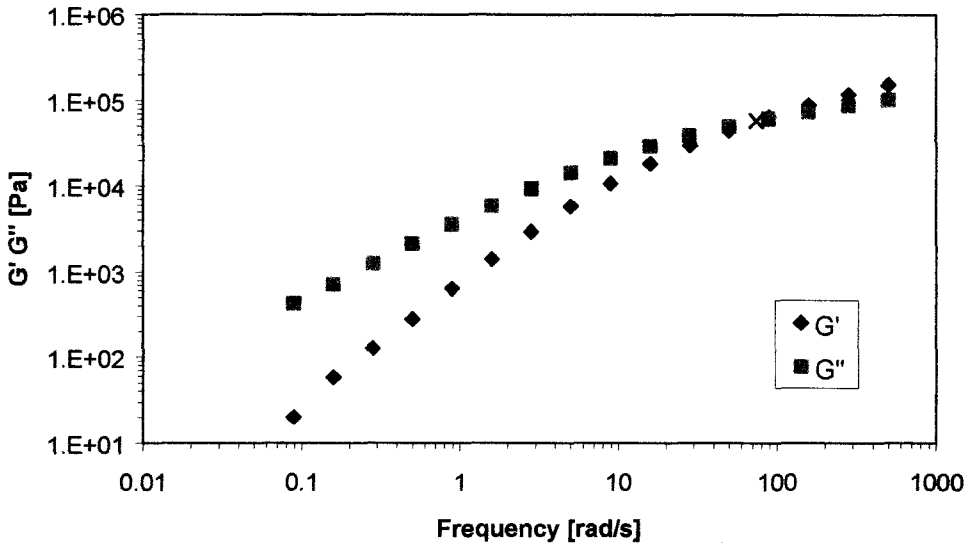

Figure V.2. Storage and loss moduli at 200 °C for resin B.

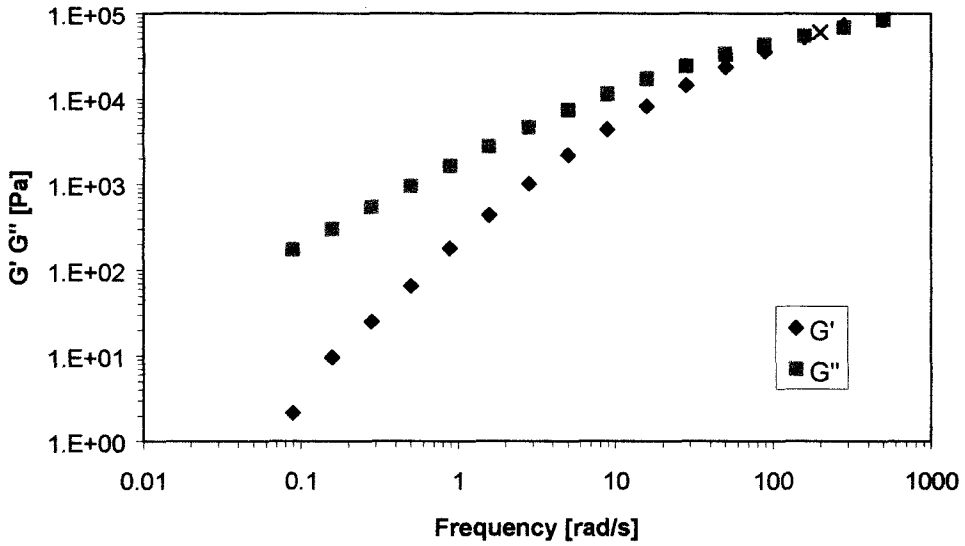

Figure V.3. Storage and loss moduli at 200 °C for resin C.

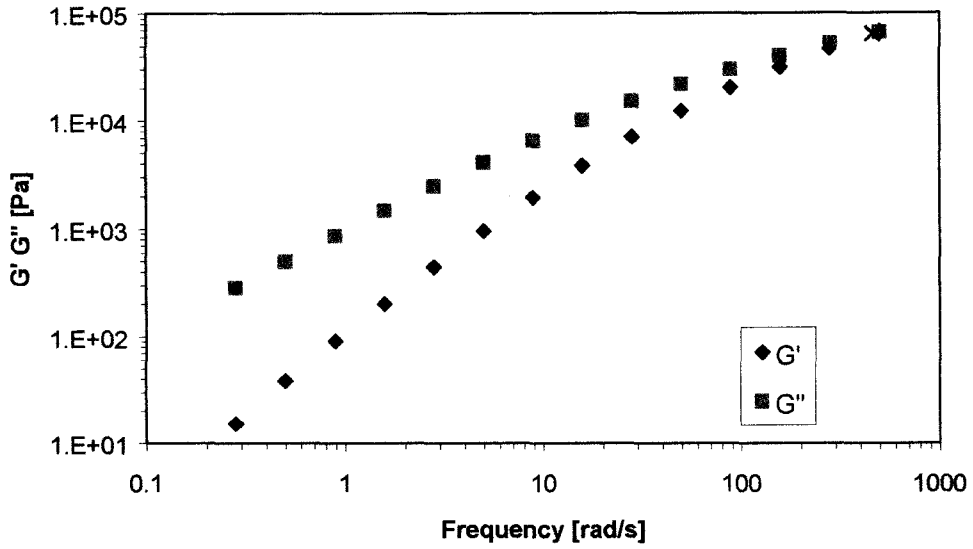

Figure V.4. Storage and loss moduli at 200 °C for resin D.

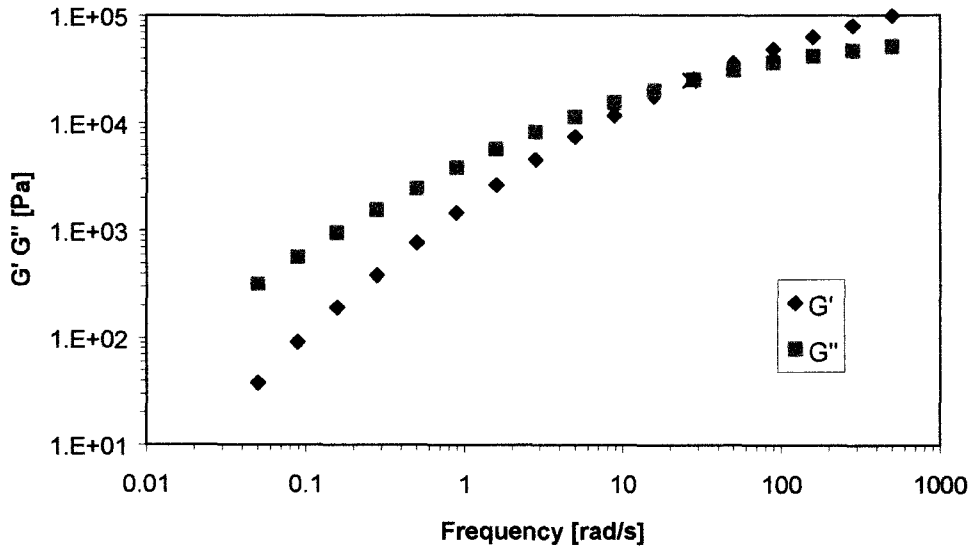

Figure V.5. Storage and loss moduli at 200 °C for resin E.

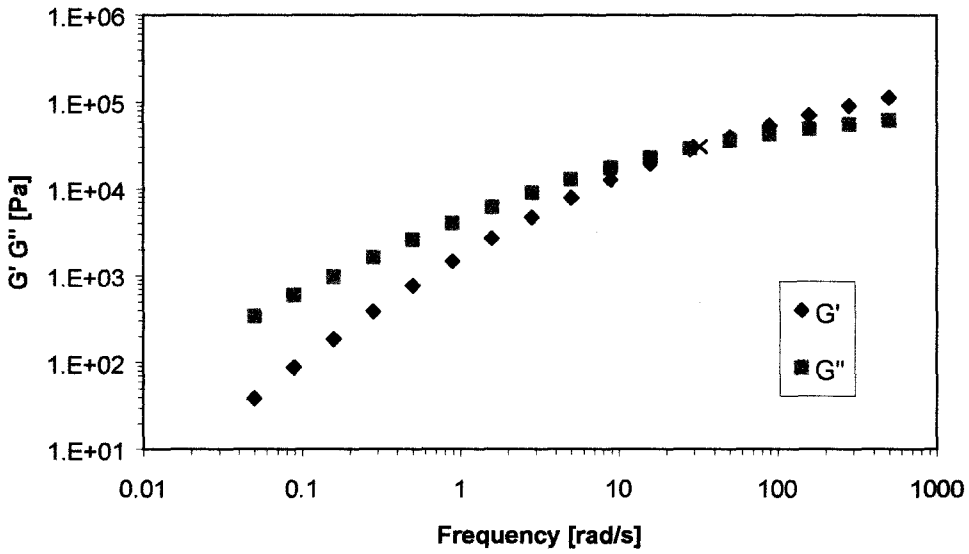

Figure V.6. Storage and loss moduli at 200 °C for resin F.

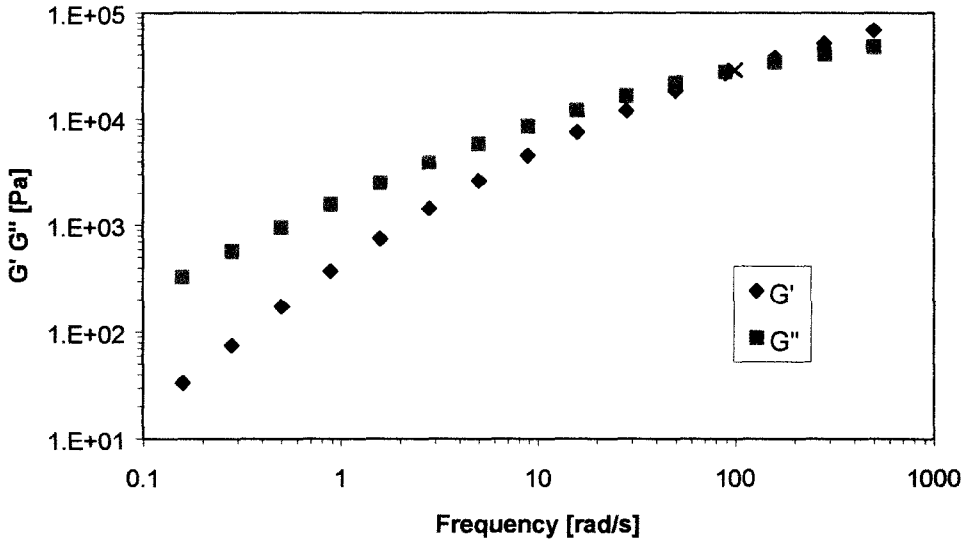

Figure V.7. Storage and loss moduli at 200 °C for resin G.

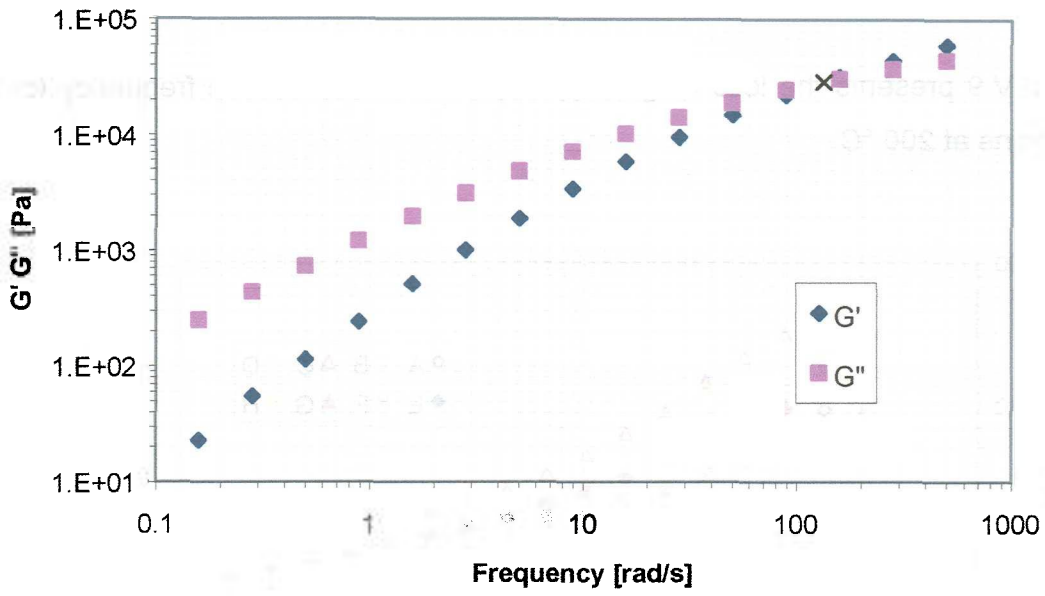

Figure V.8. Storage and loss moduli at 200 °C for resin H.

B. Cross-over point

The cross-over point rheological parameter is obtained from direct reading from the combined plots of G'(ω) and G"(ω). The cross-over points (ω_x, G_x) for each resin are listed in Table V.1.

Table V.1. Cross-over frequency and modulus for all resins at 200 °C.

Resin	ω_x [rad/s]	G_x [Pa]	Resin	ω_x [rad/s]	G_x [Pa]
A	40.44	52250	E	26.508	24850
B	74.286	58110	F	32.286	30760
C	199.53	60440	G	99.14	28670
D	459.17	64180	H	133.58	29050

C. Loss Tangent

Figure V.9 presents the loss tangent (tan δ) as a function of the frequency for all the resins at 200 °C.

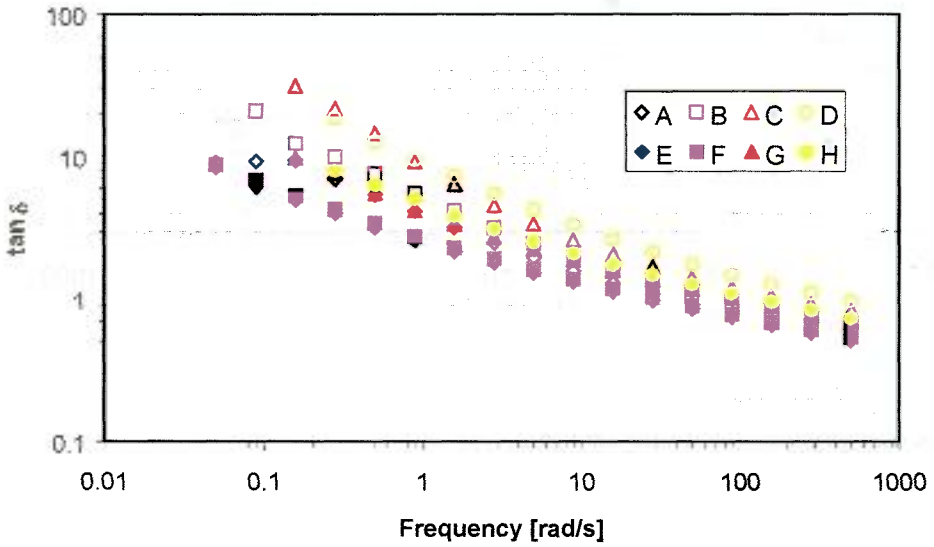

Figure V.9. Loss tangent vs. frequency for all resins at 200 °C. The open symbols were used for syndiotactic PP. Same type of symbols are used for similar MF. Diamonds are for MF=2, squares for MF=4, triangles for MF=12 and circles for MF=19.

D. Complex Viscosity

The loss and storage moduli are used to estimate are used to estimate the complex viscosity by:

$$\eta^*(\omega) = \frac{\sqrt{G'(\omega)^2 + G''(\omega)^2}}{\omega} \qquad (5.\ 1)$$

Figure V.10 shows the complex viscosity for all the resins. By means of the Cox-Mertz rule, such complex viscosity curves will be used to determine the shear

viscosity at intermediate shear rates. Such shear viscosity points will be presented in the next chapter together with the capillary shear viscosity.

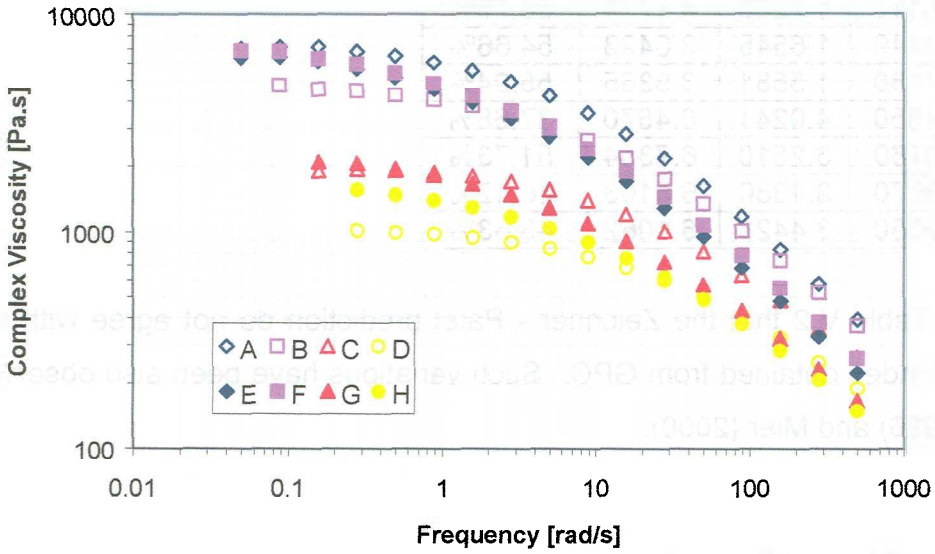

Figure V.10. Complex Viscosity for all the resins at 200 °C. The open symbols were used for syndiotactic PP. Same type of symbols are used for similar MF. Diamonds are for MF=2, squares for MF=4, triangles for MF=12 and circles for MF=19.

E. Polidispersity Index

The polidispersity index (PDI = Mw/Mn) can be estimated from the cross-over modulus using the equation below proposed by Zeichner and Patel (1981). Table V.2 shows the estimated PDI and the PDI obtained from GPC.

$$\frac{Mn}{Mw} = \frac{10^5}{G_x(Pa)} \qquad (5.\ 2)$$

Table V.2. Comparison between PDI estimated as suggested by Zeichner and Patel (1981) and PDI obtained from GPC measurements.

Resin	G_x [Pa]	PDI $10^5/G_x$	PDI GPC	% Error
A	52250	1.9139	4.5226	57.68%
B	58110	1.7209	4.1719	58.75%
C	60440	1.6545	3.6493	54.66%
D	64180	1.5581	3.5365	55.94%
E	24850	4.0241	6.4570	37.68%
F	30760	3.2510	6.7354	51.73%
G	28670	3.4880	6.5103	46.42%
H	29050	3.4423	6.1062	43.63%

It is clear in Table V.2 that the Zeichner - Patel prediction do not agree with the polidispersity index obtained from GPC. Such variations have been also observed by Bonilla (1996) and Mier (2000).

F. Zero - Shear Viscosity

The zero shear viscosity (η_0) could be determined from the loss modulus by:

$$\eta_0 = \lim_{\omega \to 0}\left[\frac{G''(\omega)}{\omega}\right] \qquad (5.\ 3)$$

In Table V.3 are presented the values for all the resins of the zero shear viscosity obtained using the lowest frequency point of the loss modulus curve. The complex viscosity at this is also shown just as a point of reference.

Table V.3. Zero shear viscosity calculated with the lowest frequency point of the loss modulus.

Resin	ω [rad/s]	G"(ω) [Pa]	η* [Pa.s]	η_0 [Pa.s]
A	0.05	348	7006	6964
B	0.09	423	4764	4759
C	0.16	301	1906	1905
D	0.28	286	1017	1015
E	0.05	317	6379	6334
F	0.05	341	6864	6819
G	0.16	329	2092	2081
H	0.28	435	1560	1548

G. Discrete Relaxation Spectrum

The discrete relaxation spectrum (η_i, λ_i) for each resin can be obtained by fitting its storage and loss moduli with equations:

$$G'(\omega) = \sum_{i=1}^{N} \frac{\eta_i \lambda_i \omega^2}{1 + (\lambda_i \omega)^2} \tag{5.4}$$

$$G''(\omega) = \sum_{i=1}^{N} \frac{\eta_i \omega}{1 + (\lambda_i \omega)^2} \tag{5.5}$$

where $\eta_i = G_i \lambda_i$.

Mier (2000) developed a C language program for the determination of the discrete relaxation spectrum from the loss modulus. This software is well-documented in the cited reference. Mier (2000) used the relaxation spectrum of a LDPE at 150 °C reported by Phan-Thien (1978) and Papanastasiou (1987) to validate his software, and he used the software to obtain the discrete relaxation spectrum of eight polypropylene resins with excellent results using 4 elements.

Therefore, the discrete relaxation spectrum for the resin under study was obtained using the software developed by Mier (2000). Since Mier (2000) proved that the best results are given by using 4 relaxation elements, such elements were used in

this thesis. The discrete relaxation spectrum obtained from Mier's software for all the resins is presented in Table V.4.

Table V.4. Disrete relaxation spectrum obtained from Mier's (2000) software for all the resins.

Resin	A	B	C	D	E	F	G	H
λ_i [s]	η_i [Pa.s]	η_i [Pa.s]	η_i [Pa.s]	η_i [Pa.s]	η_i [Pa.s]	η_i [Pa.s]	η_i [Pa.s]	η_i [Pa.s]
0.001	199.6	216.8	187.3	151.4	104.2	127.1	102.8	97.4
0.01	938.6	859.2	548.9	350.6	536.5	625.5	375.1	330.1
0.1	3631.9	2517.5	1115.8	439.9	2110.9	2300.8	938.1	729.6
1	1551.9	284.4	0	0	2706.6	2673.5	541.7	292.4

The discrete relaxation presented in Table V.4 fits very well equations 5.4 and 5.5. The fittings produced residuals lowers than 5 % in most cases, just a few points were higher than 5 %, but they were less than 10 %.

H. Time – Temperature Superposition (TTS)

According to Mavridis (1992) methodology, the dynamic data measure at different temperatures must be screened by plotting tan δ vs $G^*(\omega)$:

1) If the data from different temperatures superimpose (within experimental error) then a vertical shift factor (b_T) is not required (b_T=1) and the vertical energy of activation (E_V) is zero.
2) If the data from different temperatures do not superimpose but fall onto parallel curves, then a vertical shift factor is required.

Figure V.11 shows the plot of tan δ vs $G^*(\omega)$ at different temperatures for all the resins. Since the data superimpose (case 1 above), therefore E_V=0 and b_T=1.

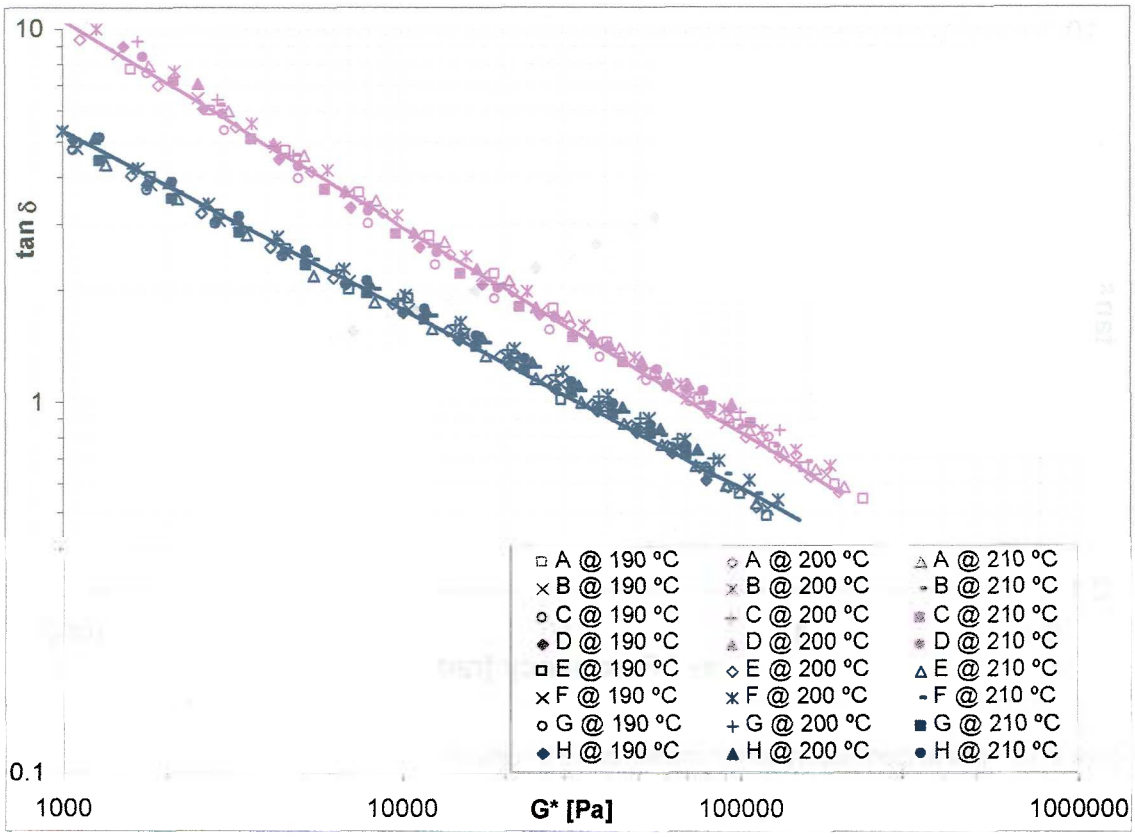

Figure V.11. Loss tangent vs. complex modulus data at different temperatures for all the resins.

Once proven that no vertical shift factor is needed, the horizontal shift factor can be determined. Following the Mavridis (1992) methodology, the horizontal shift factor was obtained by superimposing the loss tangent vs frequency data at different temperatures. Plotting data from different temperatures as loss tangent vs frequency gives parallel curves separated by a certain distance determined by the horizontal shift factor a_T. Figure V.12 shows for resin A the loss tangent superposition master curve after the horizontal shift factor has been applied to the data. From the shift factors at each temperature, the horizontal shift activation energy (EH) is obtained, according to Mavridis (1992), using the WLF equation. This procedure was done for the eight resins; the computed activation energies are show in Table V.5.

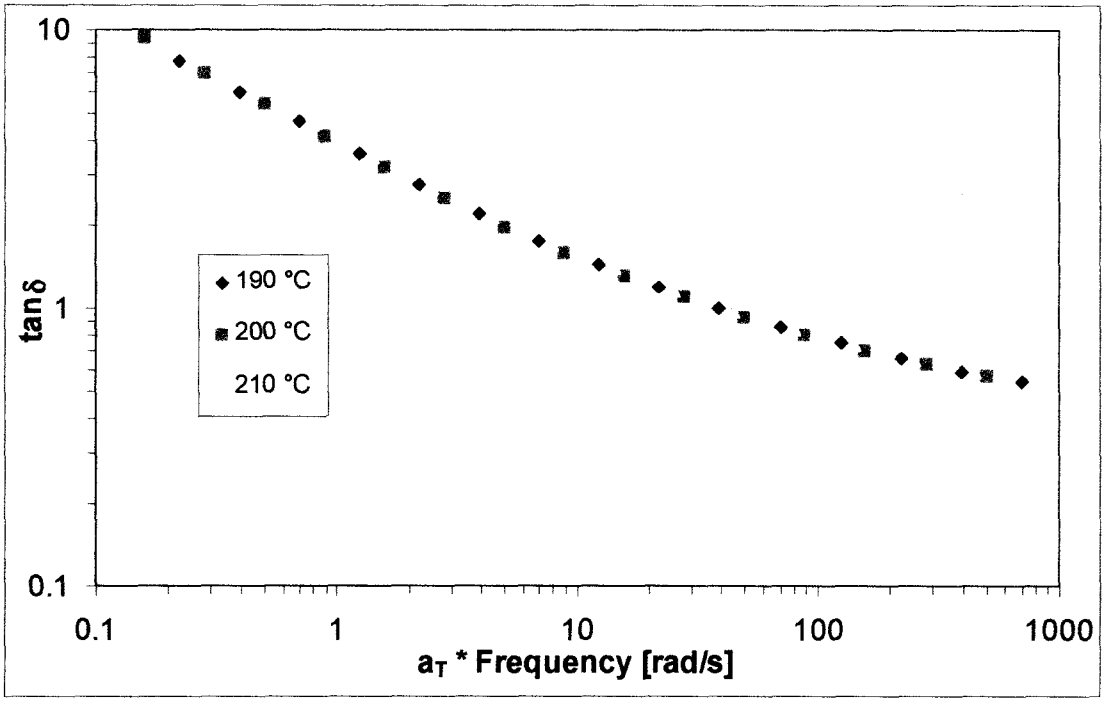

Figure V.12. Loss tangent superposition master curve for resin A.

Table V.5. Horizontal activation energies for all the resins.

Resin	E_H [cal/mol]	Resin	E_H [cal/mol]
A	9712	E	8094
B	10218	F	8544
C	9398	G	8610
D	10497	H	9719

CHAPTER VI. Capillary Data

Chapter VI is divided in four sections. Section A shows the shear and extensional viscosity at steady state. Shear and extensional viscosity were calculated from experimental data according to the procedure shown in Appendix A. Capillary steady-state tests were done using three dies with different diameters (see Appendix A). Section B presents the shear and extensional viscosity at transient state. Transient state data was obtained with the 0.5 mm diameter die.

Section C presents the steady shear viscosity data fitted using the Cross, Carreau and Yasuda models. Finally, section D presents a capillary analysis done to the eight resins in order to obtain the compressibility effect in the capillary flow. All the capillary data presented in this chapter was obtained with the Rosand double bore capillary rheometer (see Table III.2) at 200 °C.

A. Steady State

Figure VI.1 shows the shear viscosity curves calculated for resin B. It can be seen that all three dies generate the same shear viscosity curve. Similar results are observed for the rest of the resins.

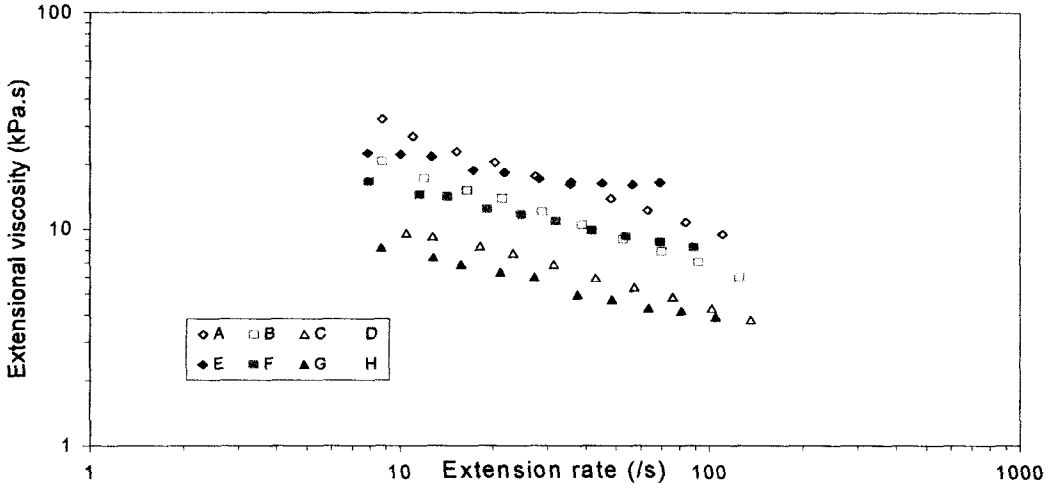

Figure VI.1. Shear viscosity curves for resin B obtained with three different dies.

On the other hand, Figure VI.2 presents the extensional viscosity curves for the same resin (resin B). This figure shows that each die generate a different extensional viscosity curve. The curve obtained from using the 0.5 mm die presents the highest extensional viscosity. Similar results are observed for the rest of the resins.

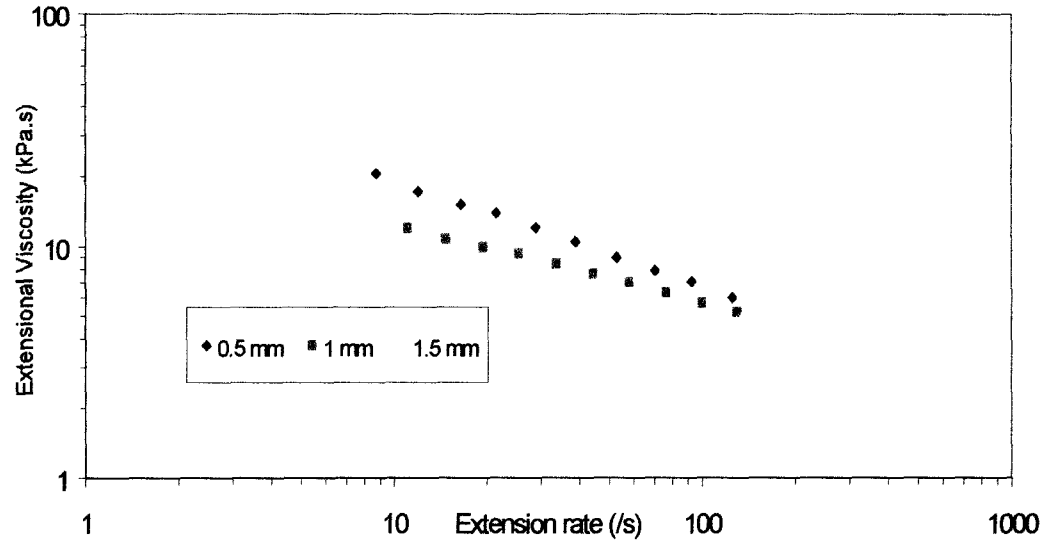

Figure VI.2. Elongational viscosity curves for resin B using three different dies.

Since, the data obtained from using the 0.5 mm die gives the highest values, and then only the results obtained with such diameter are presented. Figure VI.3 and Figure VI.4 show the shear viscosity and extensional viscosity for all resins.

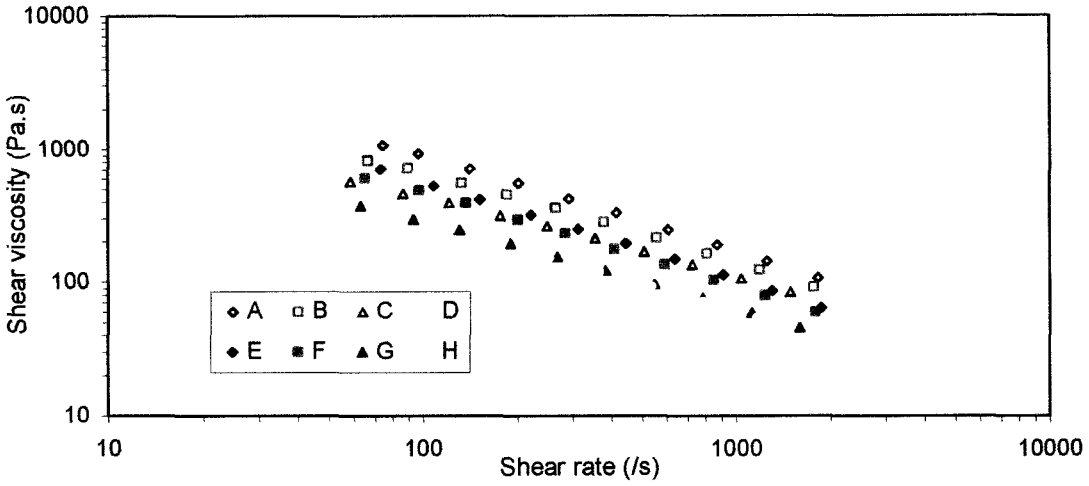

Figure VI.3. Shear viscosity for all the resins (@ D=0.5 mm). The open symbols were used for syndiotactic PP. Same type of symbols are used for similar MF. Diamonds are for MF=2, squares for MF=4, triangles for MF=12 and circles for MF=19.

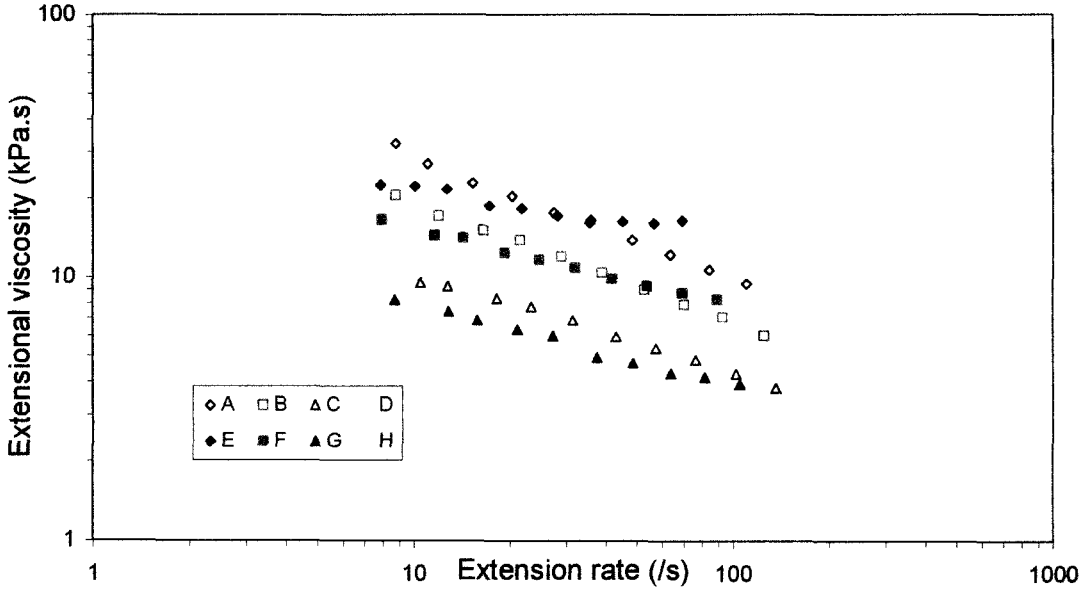

Figure VI.4. Extensional viscosity for all the resin (@ D=0.5 mm). The open symbols were used for syndiotactic PP. Same type of symbols are used for similar MF. Diamonds are for MF=2, squares for MF=4, triangles for MF=12 and circles for MF=19.

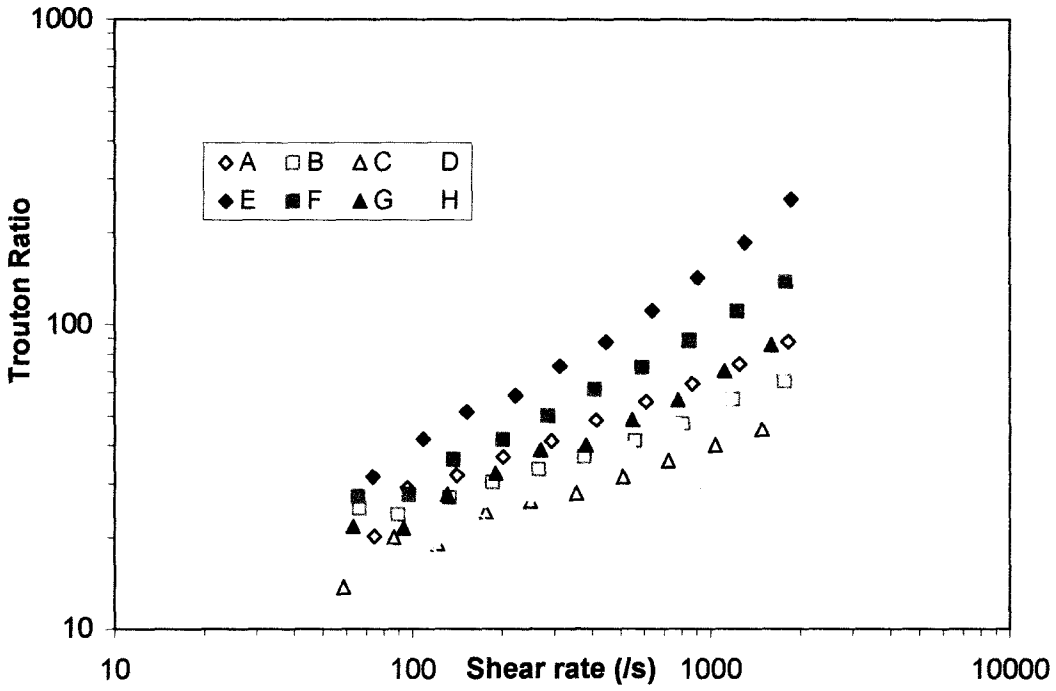

Figure VI.5. Trouton ratio for all the resin (@ D=0.5 mm). The open symbols were used for syndiotactic PP. Same type of symbols are used for similar MF. Diamonds are for MF=2, squares for MF=4, triangles for MF=12 and circles for MF=19.

B. Transient State

Using the procedure shown in Appendix A, the transient shear and elongational viscosity were obtained from capillary data. Figure VI.6 and Figure VI.7 present the transient shear viscosity for all the resins at apparent shear rate of 500 /s and 1000 /s respectively. Similarly, in Figure VI.8 and Figure VI.9 are shown the transient elongational viscosity for all the resins at the same apparent shear rates.

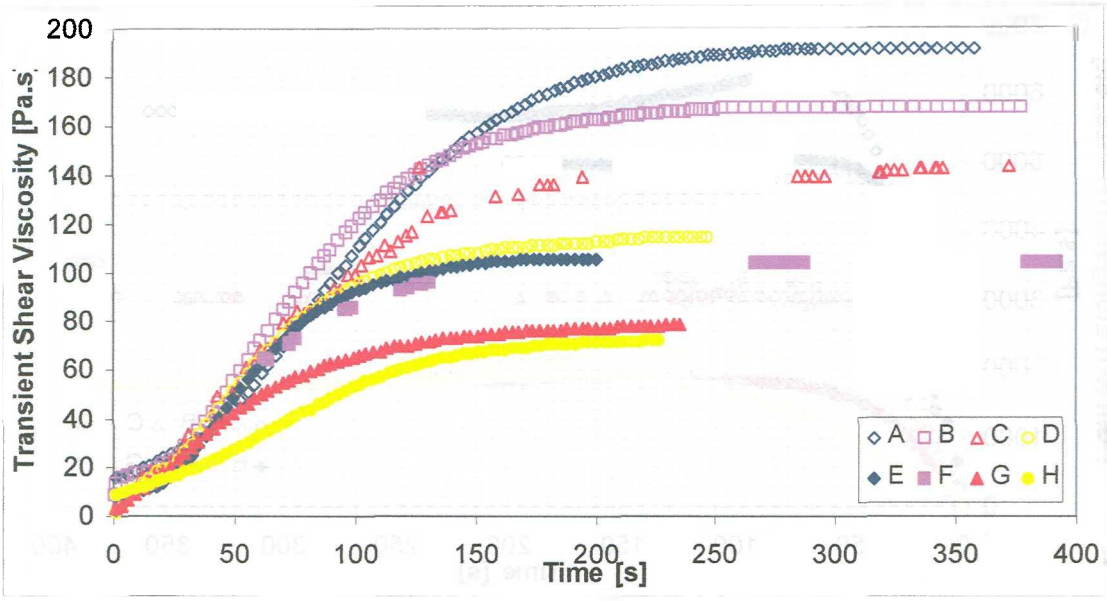

Figure VI.6. Transient shear viscosity at apparent shear rate of 500 /s at 200 °C. The open symbols were used for syndiotactic PP. Same type of symbols are used for similar MF. Diamonds are for MF=2, squares for MF=4, triangles for MF=12 and circles for MF=19.

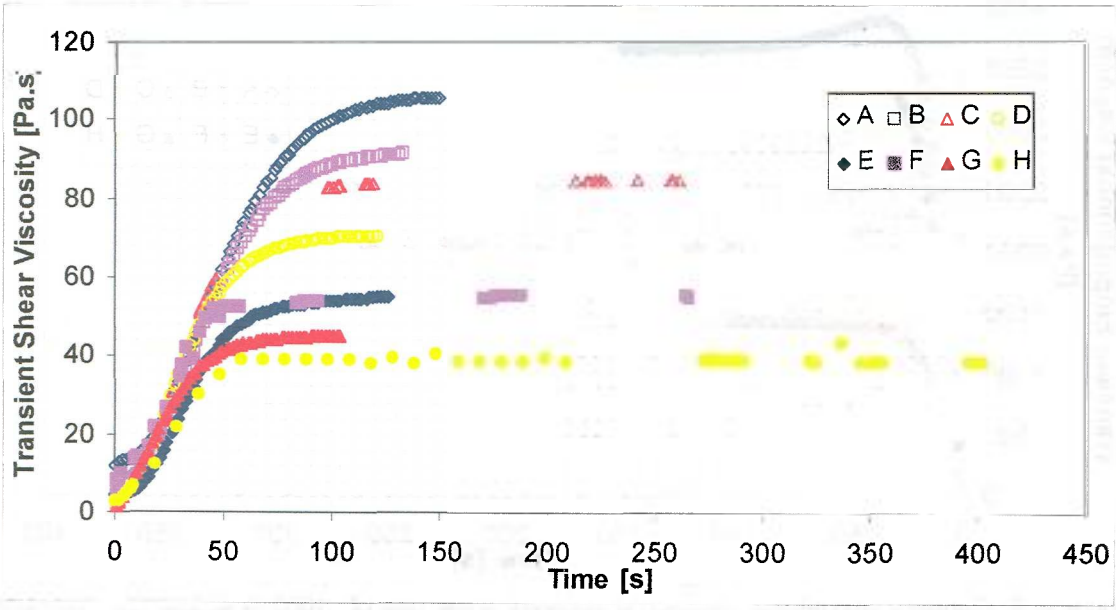

Figure VI.7.Transient shear viscosity at apparent shear rate of 1000 /s at 200 °C. The open symbols were used for syndiotactic PP. Same type of symbols are used for similar MF. Diamonds are for MF=2, squares for MF=4, triangles for MF=12 and circles for MF=19.

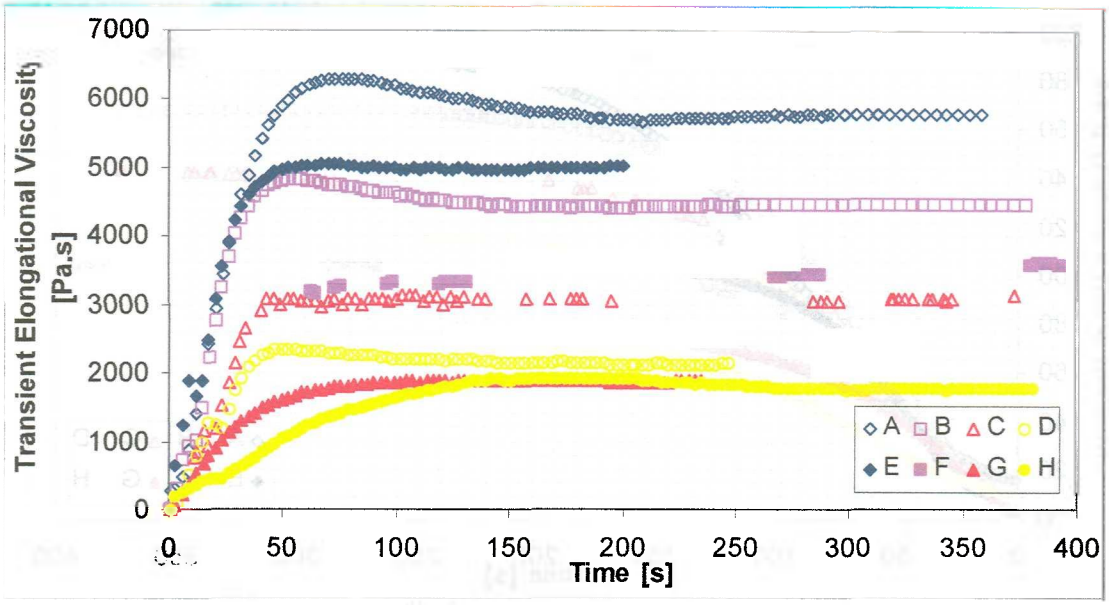

Figure VI.8. Transient elongational viscosity at apparent shear rate of 500 /s at 200 °C. The open symbols were used for syndiotactic PP. Same type of symbols are used for similar MF. Diamonds are for MF=2, squares for MF=4, triangles for MF=12 and circles for MF=19.

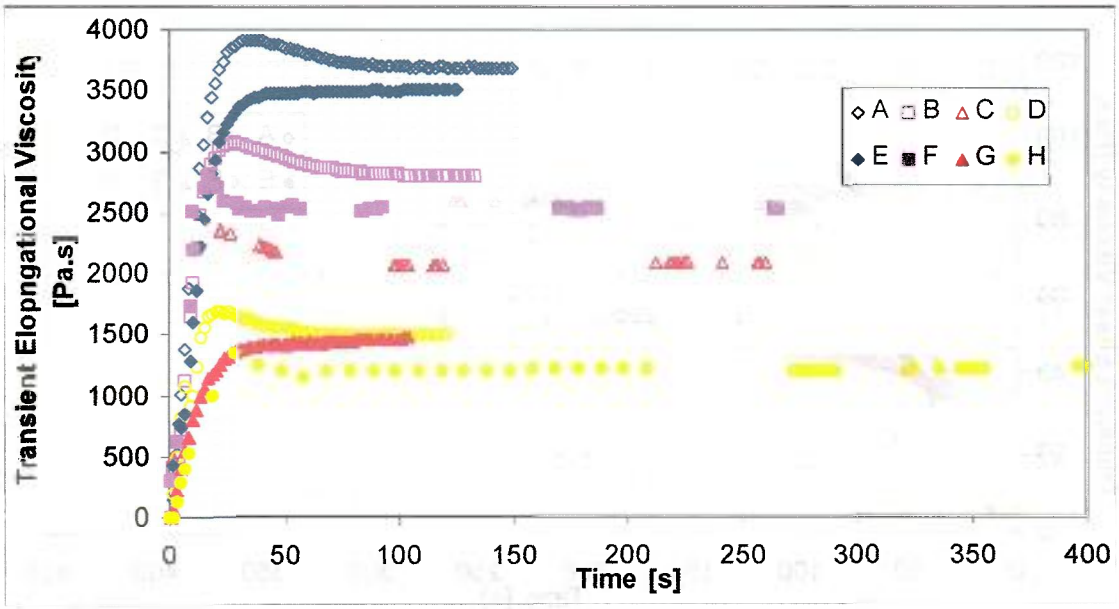

Figure VI.9. Transient elongational viscosity at apparent shear rate of 1000 /s at 200 °C. The open symbols were used for syndiotactic PP. Same type of symbols are used for similar MF. Diamonds are for MF=2, squares for MF=4, triangles for MF=12 and circles for MF=19.

C. Fitting Viscosity Curves

The shear viscosity curves were fitted by the Carreau, Yasuda and Cross models. The modification to the Cross model proposed by Dealy and Wissburn (1990) was considered. This modification requires that $|\lambda\dot{\gamma}|^a$ be multiplied by 0.6 and the parameter "a" to be equal to 0.75. However, it was decided to use the unmodified Cross model, because the exponent 0.75 produced poor fittings.

$$\eta = \eta_0\left[\left(1+|\lambda\dot{\gamma}|^2\right)\right]^{-p} \qquad \text{Carreau Model}$$

$$\eta = \eta_0\left[\left(1+|\lambda\dot{\gamma}|^a\right)\right]^{\frac{n-1}{a}} \qquad \text{Yasuda Model}$$

$$\eta = \eta_0\left[\left(1+|\lambda\dot{\gamma}|^a\right)\right]^{-1} \qquad \text{Cross Model}$$

The three models used fit very well the viscosity curve for the eight resins, they all produced fittings with an error lower than 5 % and correlation coefficients (R^2) higher than 0.99. From Table VI.1 to Table VI.3 are presented the models' parameters.

Table VI.1. Cross model parameters for fitting the shear viscosity curves.

Resin	η_0 Pa.s	λ s	m	R^2
A	6635	0.11	0.76	0.9998
B	2252	0.03	0.80	0.9996
C	2096	0.07	0.67	0.9998
D	1476	0.10	0.59	0.9990
E	7098	0.25	0.76	0.9997
F	6061	0.32	0.71	0.9986
G	2037	0.13	0.70	0.9999
H	779	0.03	0.77	0.9996

Table VI.2. Yasuda model parameters for fitting the shear viscosity curves.

Resin	η_0 Pa.s	λ s	a	n	R^2
A	8300	0.25	3.53	0.31	0.9991
B	5121	0.03	0.44	0.08	0.9994
C	1967	0.05	0.64	0.30	0.9998
D	1014	0.07	0.80	0.43	0.9988
E	7975	0.39	1.55	0.28	0.9998
F	6848	0.15	0.46	0.17	0.9991
G	2095	0.03	0.47	0.10	0.9997
H	1634	0.03	0.44	0.15	0.9996

Table VI.3. Carreau model parameters for fitting the shear viscosity curves.

Resin	η_0 Pa.s	λ s	p	R^2
A	4285	0.09	0.35	0.9992
B	4125	0.19	0.31	0.9971
C	1775	0.12	0.28	0.9986
D	600	0.04	0.26	0.9985
E	8744	0.44	0.36	0.9998
F	6811	0.52	0.34	0.9975
G	2027	0.22	0.31	0.9990
H	1512	0.23	0.29	0.9957

Since these models are empirical, even though they were created to fit shear viscosity curves, it was decided to fit elongational viscosity curves with these models too. It was observed that these empirical models produce good fittings (R^2 higher than 0.9) of the elongational viscosity; however they are not as good as those for shear viscosity. Table VI.4 through Table VI.6 presents the parameters of the model as well as the correlation coefficient (R^2).

Table VI.4. Cross model parameter for fitting the elongational viscosity

Resin	η_0 Pa.s	λ s	m	R^2
A	42817	0.06	0.74	0.9848
B	119677	2.75	0.50	0.9973
C	10171	0.01	0.88	0.9368
D	26148	1.23	0.44	0.9352
E	96657	2.33	0.43	0.9896
F	84703	9.52	0.34	0.9794
G	29183	1.68	0.37	0.9545
H	23858	1.45	0.40	0.9023

Table VI.5. Yasuda model parameters for fitting the elongational viscosity curves.

Resin	η_0 Pa.s	λ s	a	n	R^2
A	389357	6.80	0.29	0.47	0.9776
B	54736	1.05	3.89	0.55	0.9976
C	8458	0.05	4.94	0.60	0.9461
D	21290	1.20	5.18	0.57	0.9537
E	28926	0.19	1.45	0.59	0.9904
F	81810	0.23	0.23	0.52	0.9776
G	377431	2.58	0.11	0.52	0.9552
H	39554	22.78	1.95	0.66	0.9141

Table VI.6. Carreau model parameters for fitting the elongational viscosity curves.

Resin	η_0 Pa.s	λ s	p	R^2
A	29394	0.09	0.28	0.9881
B	36822	0.41	0.23	0.9974
C	8937	0.05	0.24	0.9424
D	23149	1.45	0.22	0.9534
E	26339	0.17	0.20	0.9912
F	33757	1.61	0.14	0.9809
G	17764	1.75	0.15	0.9557
H	21044	3.54	0.17	0.9141

D. Capillary Analysis

Hatzikiriakos (1992, 1994) & Dealy (1995) concluded that the melt viscosity and compressibility are the dominant factor in capillary flow and that the contribution of melt elasticity is too small. Mier (2001a) develop software based on the Hatzikiriakos and Dealy (1994) previous work, but the results were not conclusive. However, we believe that the entrance pressure is a combination of both, the compressibility and the elasticity of the polymer and that a procedure to determine each value should be established. A capillary analysis using different diameters of die is proposed to evaluate these effects.

The purpose of the capillary analysis with three different diameter dies was to evaluate the compressibility of the resins. It was expected to obtain for each shear rate the relationship between the pressure drop and the diameter of die.

It is assumed that the total pressure is the sum of the pressure drop due to the melt compressibility, the pressure drop due to the melt viscosity and the pressure drop due to melt elasticity. In addition, it has been accepted that the pressure drop due to the entrance effect (change in the diameter) is a measure of the melt elasticity of the polymer and that the pressure drop due to the resistance against the wall of the die is a measure of the polymer's viscosity (see Figure VI.10). For an ideal situation where the die is not present, the pressure drop is due to a compressibility of the material while flowing against a wall. Therefore, when there is no die the total pressure drop will be equal to the pressure drop due to the melt compressibility; that is, there is neither an elastic effect nor a viscous effect. It is worth to mention that the viscous dissipation or pressure "resistance" of the shaft against the barrel is not an issue in this study because the pressure transducer is in the barrel wall and not at the top of the shaft as it happens in other capillary rheometers.

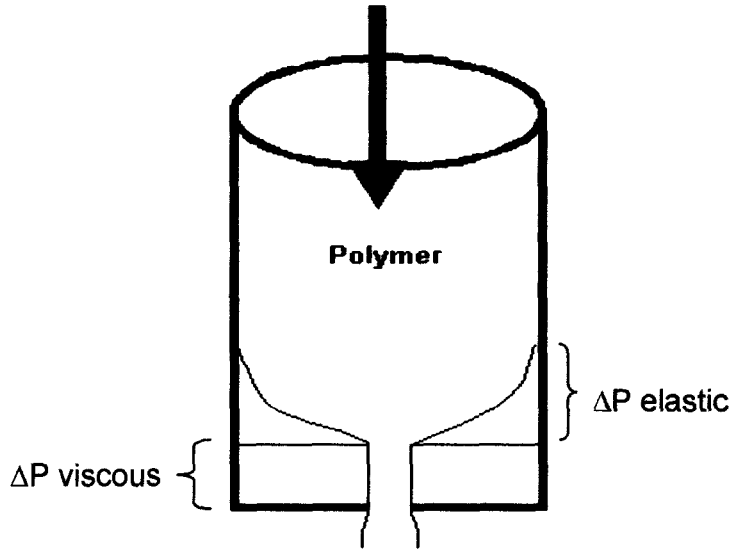

Figure VI.10. Pressure drop in a capillary flow.

Therefore, plotting entrance pressure drop (pressure drop at L/D=0 according to Bagley correction) vs. 1/D we can obtain the pressure drop due to the melt compressibility. An extrapolation to 1/D zero (when the die diameter tends to infinite, therefore there is no change of diameter between the barrel and the die)

might be done (see Figure VI.11) to obtain the pressure drop due to compressibility, when no contraction occurs.

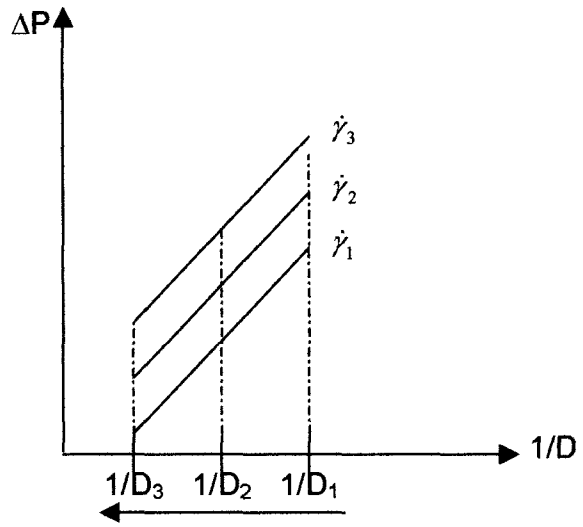

Figure VI.11. Capillary analysis in order to look at the compressibility effects.

Figure VI.12 shows the capillary analysis in order to obtain the compressibility effect for resin B. The equations on the left were obtained from linear regression with Microsoft Excel in order to make the extrapolation. Similar results are observed for the rest of the resins.

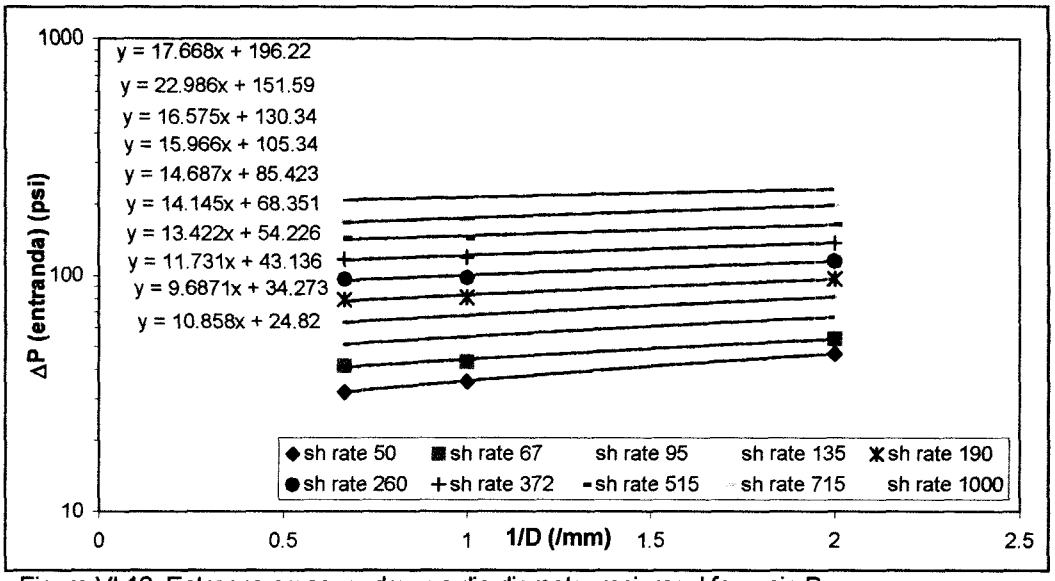

Figure VI.12. Entrance pressure drop vs die diameter reciprocal for resin B.

On Table VI.7 are presented for all resins the pressure drop values due to the melt compressibility obtained from the capillary analysis described.

Table VI.7. Pressure drop due to the melt compressibility for all the resins.

	ΔP @ 1/D =0 (psi)							
shear rate (/s)	**A**	**B**	**C**	**D**	**E**	**F**	**G**	**H**
50	45	25	14	0	45	20	8	7
67	52	34	15	7	54	33	12	12
95	68	43	22	10	68	41	16	15
135	86	54	26	13	91	52	21	19
190	107	68	34	17	113	65	26	24
260	130	85	45	25	143	81	37	33
372	160	105	55	31	178	104	46	42
515	196	130	69	40	229	131	60	54
715	236	152	86	51	281	165	76	69
1000	288	196	120	66	326	212	100	95

Since, the Cogswell's extensional viscosity is obtained from the entrance pressure drop, it was decided to make a correction by subtracting the pressure drop due to the melt compressibility to the entrance pressure.

$$\Delta P_{elas} = \Delta P_{ent} - \Delta P_{com} \qquad (6.1)$$

Now, on Table VI.8 are presented the pressure drop due to elasticity, for all resins, obtained from equation 6.1 using the 0.5 mm die diameter data. Figure VI.13 shows the corrected extensional viscosity for resin B.

Table VI.8. Pressure drop due to the melt elasticity for all the resins.

	ΔP_{elas} (psi)							
shear rate (/s)	**A**	**B**	**C**	**D**	**E**	**F**	**G**	**H**
50	17	22	7	17	7	16	11	8
67	33	20	16	12	12	11	10	5
95	32	24	13	13	13	16	13	6
135	34	27	22	18	6	16	16	10
190	35	29	24	20	8	19	19	11
260	41	30	25	19	4	21	16	11
372	41	32	30	24	4	19	19	13
515	40	34	35	28	0	20	20	14
715	43	46	39	32	4	22	24	14
1000	41	37	30	36	34	17	23	9

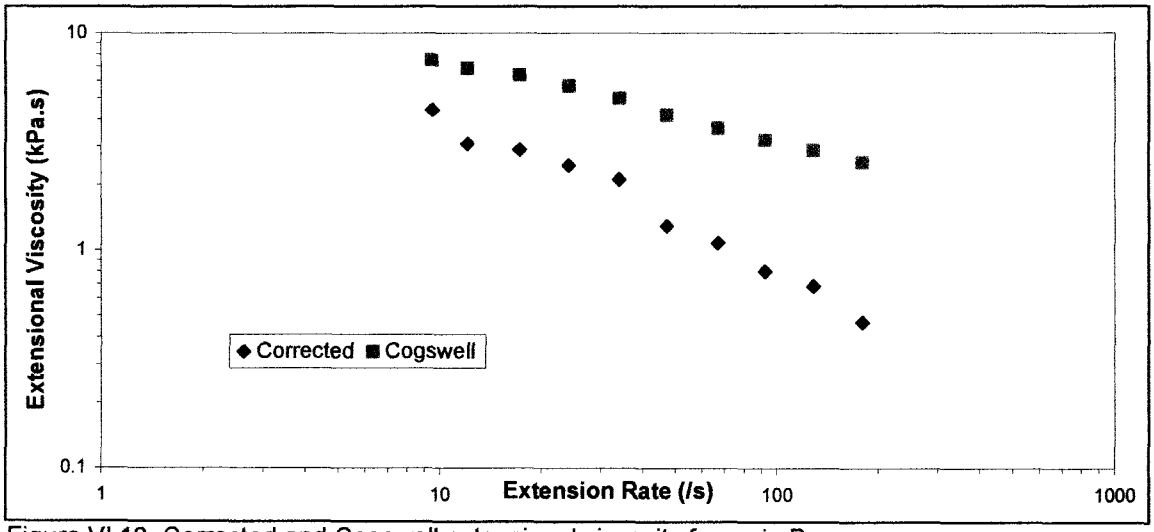

Figure VI.13. Corrected and Cogswell extensional viscosity for resin B.

It is thought that this corrected extensional viscosity is a better way to measure the melt elasticity because Cogswell's extensional viscosity considers the pressure drop due to the melt compressibility too. However, for some resins the corrected extensional viscosity shows an irregular behavior even with some negative values. It is thought that this irregular behavior is due to the regression technique used, so it is proposed to make measurements with larger diameter of dies (1/D closer to

zero) in order to have more points and then have a better regression and extrapolation.

CHAPTER VII. Creep and Recovery Compliance

This chapter is divided in three sections. Section A presents the creep and recovery measurements using standard tests. Sections B and C present an analysis of creep and recovery data using different creep times and different shear stress respectively. All the data presented was obtained from SR5000 (see Table III.2) at 200 °C.

A. Creep and Recovery Standard Test

Standard well-documented tests (Bonilla, 1996; Aguirre, 1999; Mier, 2000) indicate that the testing stress should be 600 Pa, the creep time 400 s and the recovery time 800 s. Figure VII.1 shows the strain for all the resins during the creep and recovery test, and Figure VII.2 shows the recovery compliance for all the resins.

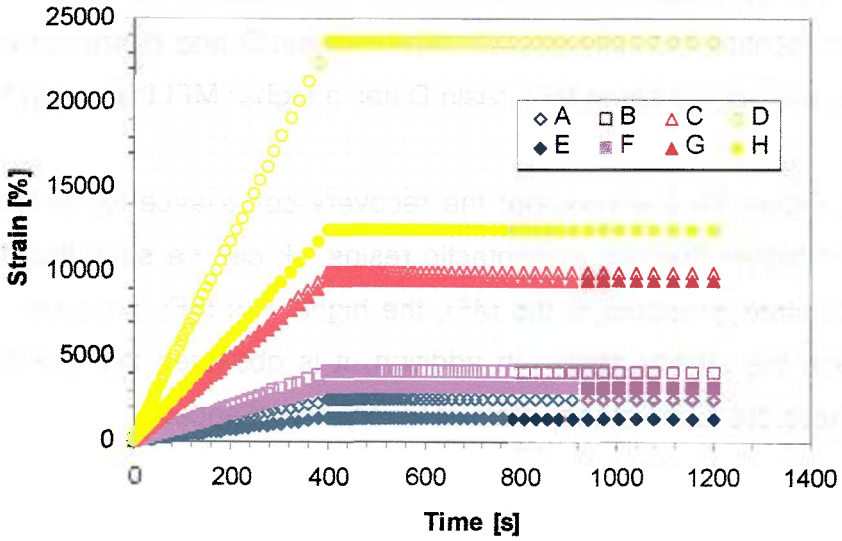

Figure VII.1. Strain response vs time applying a stress of 600 Pa for 400 s for all the resins. The open symbols were used for syndiotactic PP. Same type of symbols are used for similar MF. Diamonds are for MF=2, squares for MF=4, triangles for MF=12 and circles for MF=19.

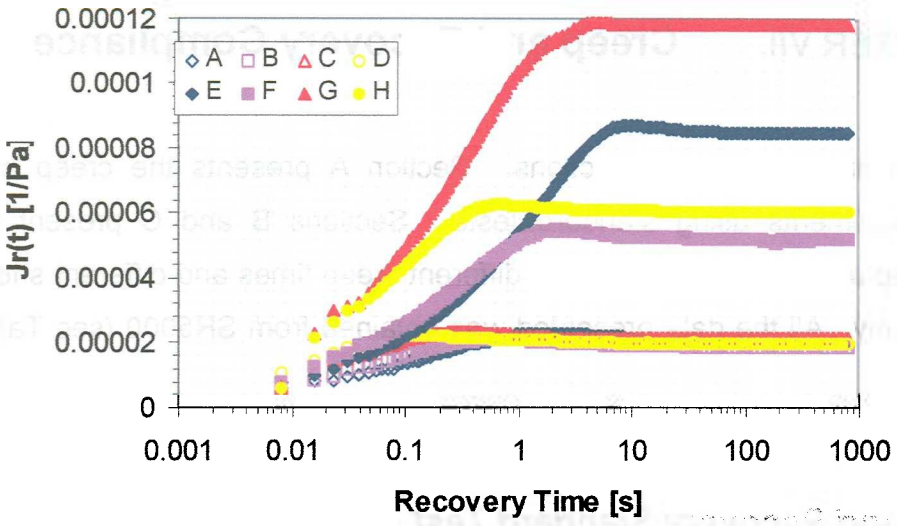

Figure VII.2. Recovery compliance vs recovery time after applying a stress of 600 Pa for 400 s for all the resins. The open symbols were used for syndiotactic PP. Same type of symbols are used for similar MF. Diamonds are for MF=2, squares for MF=4, triangles for MF=12 and circles for MF=19.

Figure VII.1 shows that the strain response for resins with similar MFI is similar too, besides, it can be seen that the higher the MFI the higher the strain. It can also be seen in Figure VII.1 that syndiotactic resins presents a strain just a little higher than isotactic. It worth to mention that strain responses for resin D and H are not that similar because they are not the same MFI, resin D has a higher MFI than resin H.

On the other hand, Figure VII.2 shows that the recovery compliance for isotactic resins is significantly higher than for syndiotactic resins. It can be seen that the time to reach steady state is related to the MFI, the higher the MFI the lower the time it takes to reach the steady state. In addition, it is observed that the four syndiotactic resins have the same steady state recovery compliance.

B. Creep Time Analysis

Using the same shear stress (600 Pa), the creep time was varied in order to observe differences between the resins. Figure VII.3 and Figure VII.4 present the

strain while Figure VII.5 and Figure VII.6 show the recovery compliance for all the resins for creep times of 1 s and 60 s respectively.

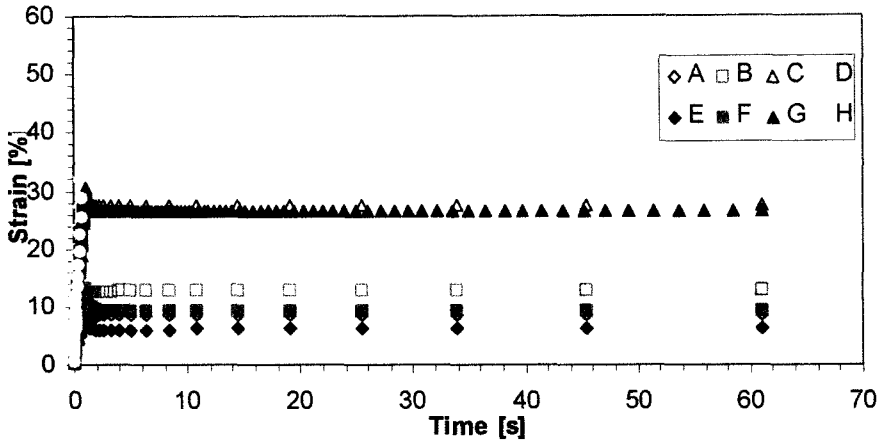

Figure VII.3. Strain response vs time applying a stress of 600 Pa for 1 s for all the resins. The open symbols were used for syndiotactic PP. Same type of symbols are used for similar MF. Diamonds are for MF=2, squares for MF=4, triangles for MF=12 and circles for MF=19.

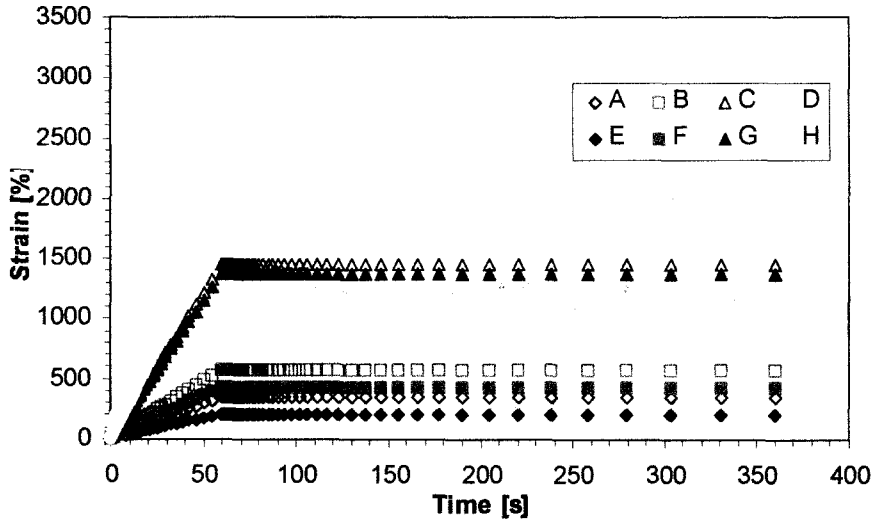

Figure VII.4. Strain response vs time applying a stress of 600 Pa for 60 s for all the resins. The open symbols were used for syndiotactic PP. Same type of symbols are used for similar MF. Diamonds are for MF=2, squares for MF=4, triangles for MF=12 and circles for MF=19.

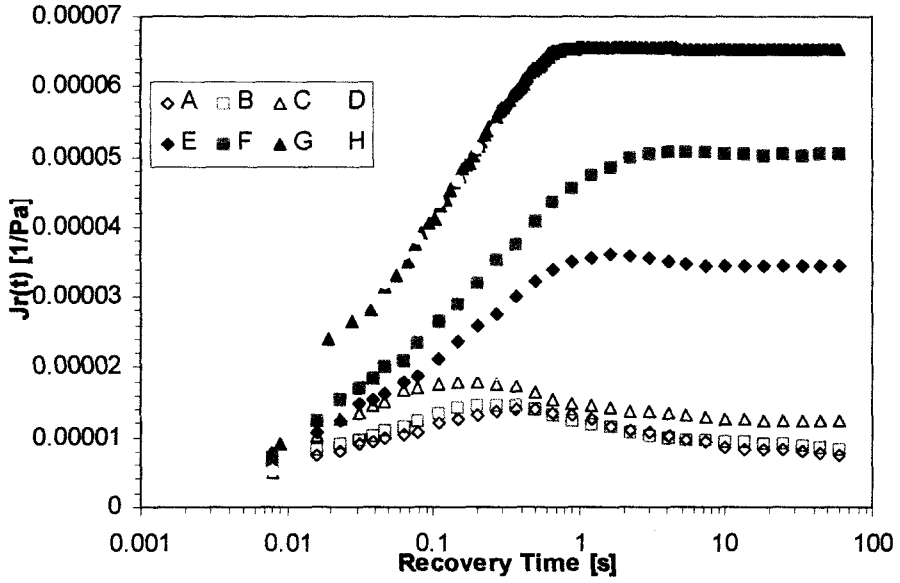

Figure VII.5. Recovery compliance vs recovery time after applying a stress of 600 Pa for 1 s for all the resins. The open symbols were used for syndiotactic PP. Same type of symbols are used for similar MF. Diamonds are for MF=2, squares for MF=4, triangles for MF=12 and circles for MF=19.

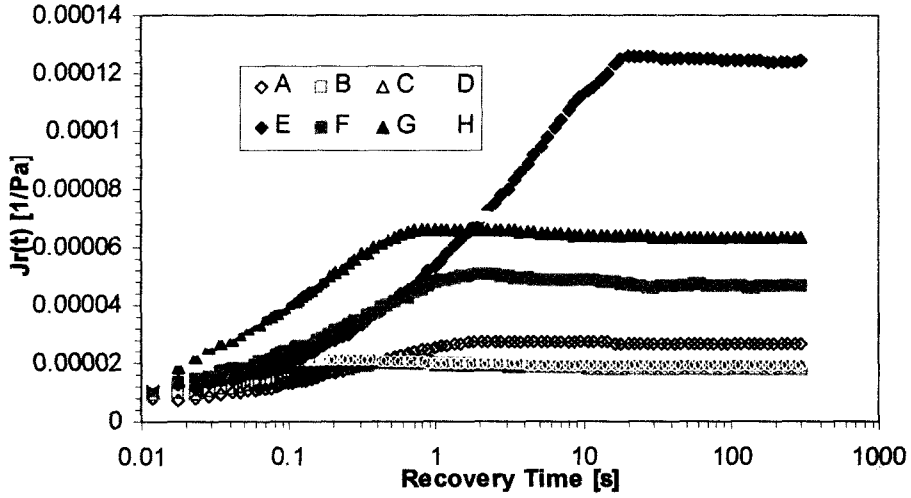

Figure VII.6. Recovery compliance vs recovery time after applying a stress of 600 Pa for 60 s for all the resins. The open symbols were used for syndiotactic PP. Same type of symbols are used for similar MF. Diamonds are for MF=2, squares for MF=4, triangles for MF=12 and circles for MF=19.

Figure VII.3 and Figure VII.4 show that the strain responses present the same behavior observed when using 400 seconds of creep time. However, in Figure VII.5 and Figure VII.6 it can be seen that the recovery compliance behavior is similar using 60 seconds of creep time, but for 1 second, there are some differences. The same relation found when using 400 seconds between the MFI and the time to reach steady state is present using 60 seconds of creep time too, but it is not when using 1 second. It can also be seen that for 60 seconds only three of the syndiotactic resins presents the same steady state recovery compliance, and for 1 second only two of them.

C. Shear Stress Analysis

From previous section, it can be seen that the steady state recovery compliance for the syndiotactic resins is the same when the creep time is 400 s and very similar at the others creep times. It was decided to vary the shear stress to 300 Pa, 1200 Pa and 2400 Pa to observe the recovery compliance behavior. The results for syndiotactic resins are presented next in Figure VII.7 to Figure VII.9.

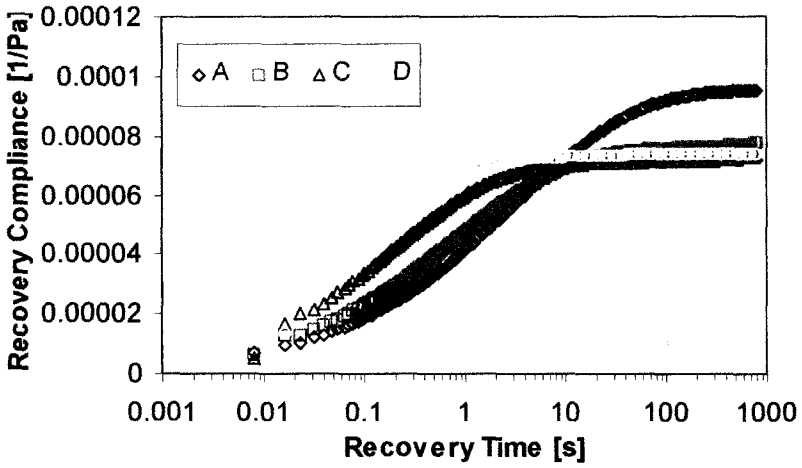

Figure VII.7. Recovery compliance vs recovery time after applying a stress of 2400 Pa for 400 s for all the resins.

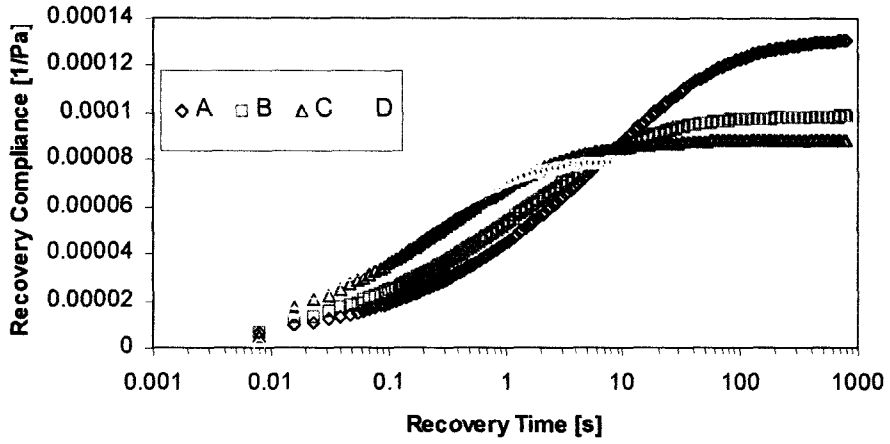

Figure VII.8. Recovery compliance vs recovery time after applying a stress of 1200 Pa for 400 s for all the resins.

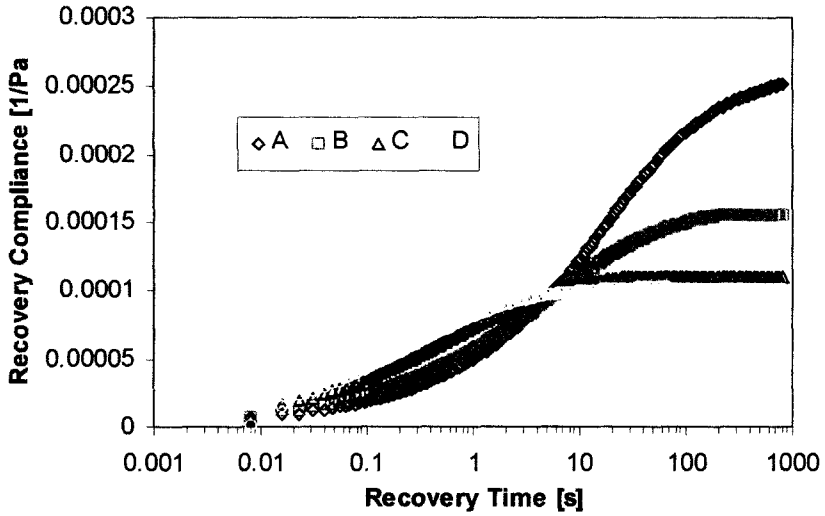

Figure VII.9. Recovery compliance vs recovery time after applying a stress of 300 Pa for 400 s for all the resins.

These results confirm the relation observed in previous sections between the MFI and the time to reach the steady state. Besides, it can be seen for the three shear stresses applied that even thought the steady state recovery compliance is similar, a relation with the MFI could be observed; the higher the MFI, the lower the steady state recovery compliance.

CHAPTER VIII. PTT Model

This chapter presents the prediction of rheological properties using the Multi-mode Phan-Thien-Tanner (PTT) model. Section A presents the PTT model. Section B shows the expressions obtained and predictions of the shear viscosity. Section C shows the expressions obtained and predictions of the elongational viscosity for the resins under study. Software (C-language codes) created and validated by Mier (2000) was used to accomplish the purposes of this chapter.

A. The Multi Mode Phan Thien – Tanner (PTT) Model

The PTT model has already been introduced in Chapter II under the constitutive equations section. In tensorial notation, the multi-mode PTT model is expressed by:

$$\tau = \sum_{i=1}^{N} \tau_i \tag{8. 1}$$

$$Z(tr(\tau_i))\tau_i + \lambda_i \, \boldsymbol{\tau}_{i(1)} + \frac{\xi}{2} \lambda_i \, (\dot{\boldsymbol{\gamma}} \cdot \boldsymbol{\tau}_i + \boldsymbol{\tau}_i \cdot \dot{\boldsymbol{\gamma}}) = -\eta_i \, \dot{\boldsymbol{\gamma}} \tag{8. 2}$$

For shear flow:

$$Z(tr(\boldsymbol{\tau}_i)) \begin{pmatrix} \tau_{xx}^i & \tau_{xy}^i & 0 \\ \tau_{yx}^i & \tau_{yy}^i & 0 \\ 0 & 0 & \tau_{zz}^i \end{pmatrix} + \lambda_i \left[\frac{\partial}{\partial t} \begin{pmatrix} \tau_{xx}^i & \tau_{xy}^i & 0 \\ \tau_{yx}^i & \tau_{yy}^i & 0 \\ 0 & 0 & \tau_{zz}^i \end{pmatrix} - \dot{\gamma} \begin{pmatrix} 2\tau_{yx}^i & \tau_{yy}^i & 0 \\ \tau_{yy}^i & 0 & 0 \\ 0 & 0 & 0 \end{pmatrix} \right]$$

$$+ \frac{\xi}{2} \lambda_i \begin{pmatrix} 2\tau_{yx}^i & \tau_{yy}^i + \tau_{xx}^i & 0 \\ \tau_{xx}^i + \tau_{yy}^i & 2\tau_{xy}^i & 0 \\ 0 & 0 & 0 \end{pmatrix} \dot{\gamma} = -\eta_i \begin{pmatrix} 0 & \dot{\gamma} & 0 \\ \dot{\gamma} & 0 & 0 \\ 0 & 0 & 0 \end{pmatrix} \tag{8. 3}$$

For shear-free flow:

$$Z(tr(\boldsymbol{\tau}_i))\begin{pmatrix}\tau^i_{xx} & 0 & 0\\ 0 & \tau^i_{yy} & 0\\ 0 & 0 & \tau^i_{zz}\end{pmatrix}+\lambda_i\left[\frac{\partial}{\partial t}\begin{pmatrix}\tau^i_{xx} & 0 & 0\\ 0 & \tau^i_{yy} & 0\\ 0 & 0 & \tau^i_{zz}\end{pmatrix}-\dot{\varepsilon}\begin{pmatrix}-(1+b)\tau^i_{xx} & 0 & 0\\ 0 & -(1-b)\tau^i_{yy} & 0\\ 0 & 0 & 2\tau^i_{zz}\end{pmatrix}\right]$$

$$+\frac{\xi}{2}\lambda_i\,2\dot{\varepsilon}\begin{pmatrix}-(1+b)\tau^i_{xx} & 0 & 0\\ 0 & -(1-b)\tau^i_{yy} & 0\\ 0 & 0 & 2\tau^i_{zz}\end{pmatrix}=-\eta_i\begin{pmatrix}-(1+b) & 0 & 0\\ 0 & -(1-b) & 0\\ 0 & 0 & 2\end{pmatrix}\dot{\varepsilon} \qquad (8.4)$$

where $Z(tr(\tau_i))=\exp\left(-\frac{\alpha\lambda_i}{\eta_i}tr(\tau_i)\right)$ (8.5)

The rationale of the notation used is as follows: "i" as a subscript refers to the stress tensor for the i-th relaxation element or i-th relaxation element of the relaxation spectrum; "i" as a superscript refers to the component of the stress tensor for the i-th relaxation element. $\tau_{i(1)}$ is the contravariant (upper) convected time derivative[2] of the stress tensor given by equation 2.22.

B. Predictions of PTT Model in Simple Shear

In simple shear the tensors of the multi-mode PTT model are given by:

$$Z(tr\boldsymbol{\tau}_i)=\exp\left(-\frac{\alpha\lambda_i}{\eta_i}(\tau^i_{xx}+\tau^i_{yy}+\tau^i_{zz})\right) \qquad (8.6)$$

---

[2] The convected time derivative in the material may be described by using a material frame of reference that is deformed and convected with the material. This can be understood to be the time derivative calculated in a coordinate system that is translating and deforming with the fluid. This then ensures frame invariance. There are a number of frame invariant choices for defining the material frame of reference and thus the overall rate of change. The most common choices are: contravariant base (upper convected derivative), covariant base (lower convected derivative) and corotating base (Jauman derivative). Since the upper convected time derivative emphasizes the stretching of materials planes, it is used in most constitutive equations. Usually, contravariant (upper) is implied in the phrase "convected time derivative" if nothing else is specified. (Bird, 1987)

$$\tau_i = \begin{pmatrix} \tau^i_{xx} & \tau^i_{xy} & 0 \\ \tau^i_{yx} & \tau^i_{yy} & 0 \\ 0 & 0 & \tau^i_{zz} \end{pmatrix} \tag{8. 7}$$

$$\dot{\gamma} = \begin{pmatrix} 0 & \dot{\gamma} & 0 \\ \dot{\gamma} & 0 & 0 \\ 0 & 0 & 0 \end{pmatrix} \tag{8. 8}$$

$$(\dot{\gamma} \cdot \tau_i + \tau_i \cdot \dot{\gamma}) = \begin{pmatrix} 2\tau^i_{yx} & \tau^i_{yy} + \tau^i_{xx} & 0 \\ \tau^i_{xx} + \tau^i_{yy} & 2\tau^i_{xy} & 0 \\ 0 & 0 & 0 \end{pmatrix} \dot{\gamma} \tag{8. 9}$$

$$\tau_{i(1)} = \frac{\partial}{\partial t} \begin{pmatrix} \tau^i_{xx} & \tau^i_{xy} & 0 \\ \tau^i_{yx} & \tau^i_{yy} & 0 \\ 0 & 0 & \tau^i_{zz} \end{pmatrix} - \dot{\gamma} \begin{pmatrix} 2\tau^i_{yx} & \tau^i_{yy} & 0 \\ \tau^i_{yy} & 0 & 0 \\ 0 & 0 & 0 \end{pmatrix} \tag{8. 10}$$

Therefore, a set of coupled nonlinear algebraic equations result:

$$\tau^i_{xx}) \qquad \lambda_i \frac{d\tau^i_{xx}}{dt} + \exp\left(-\frac{\alpha\lambda_i}{\eta_i}(\tau^i_{xx} + \tau^i_{yy} + \tau^i_{zz})\right)\tau^i_{xx} - 2\lambda_i\dot{\gamma}\tau^i_{yx} + \xi\lambda_i\dot{\gamma}\tau^i_{yx} = 0 \tag{8. 11}$$

$$\tau^i_{yy}) \qquad \lambda_i \frac{d\tau^i_{yy}}{dt} + \exp\left(-\frac{\alpha\lambda_i}{\eta_i}(\tau^i_{xx} + \tau^i_{yy} + \tau^i_{zz})\right)\tau^i_{yy} + \xi\lambda_i\dot{\gamma}\tau^i_{xy} = 0 \tag{8. 12}$$

$$\tau^i_{zz}) \qquad \lambda_i \frac{d\tau^i_{zz}}{dt} + \exp\left(-\frac{\alpha\lambda_i}{\eta_i}(\tau^i_{xx} + \tau^i_{yy} + \tau^i_{zz})\right)\tau^i_{zz} = 0 \tag{8. 13}$$

$$\tau^i_{xy}) \qquad \lambda_i \frac{d\tau^i_{xy}}{dt} + \exp\left(-\frac{\alpha\lambda_i}{\eta_i}(\tau^i_{xx} + \tau^i_{yy} + \tau^i_{zz})\right)\tau^i_{xy} - \lambda_i\dot{\gamma}\tau^i_{yy} + \frac{\xi\lambda_i\dot{\gamma}}{2}(\tau^i_{yy} + \tau^i_{xx}) = -\eta_i\dot{\gamma} \tag{8. 14}$$

$$\tau^i_{yx}) \qquad \lambda_i \frac{d\tau^i_{yx}}{dt} + \exp\left(-\frac{\alpha\lambda_i}{\eta_i}(\tau^i_{xx} + \tau^i_{yy} + \tau^i_{zz})\right)\tau^i_{yx} - \lambda_i\dot{\gamma}\tau^i_{yy} + \frac{\xi\lambda_i\dot{\gamma}}{2}(\tau^i_{yy} + \tau^i_{xx}) = -\eta_i\dot{\gamma} \tag{8. 15}$$

Since the stress tensor is symmetric, $\tau^i_{yx} = \tau^i_{xy}$; equation 8.15 is trivial and it is only included for sake of completeness. Equations 8.11 to 8.14 form a system of ordinary differential equations which must be solved numerically to determine the transient expressions for the shear viscosity.

The shear viscosity is given by:

$$\eta(\dot{\gamma},t)=\frac{\tau_{xy}}{\dot{\gamma}}=\frac{\sum_{i=1}^{N}\tau_{xy}^{i}}{\dot{\gamma}} \qquad (8.16)$$

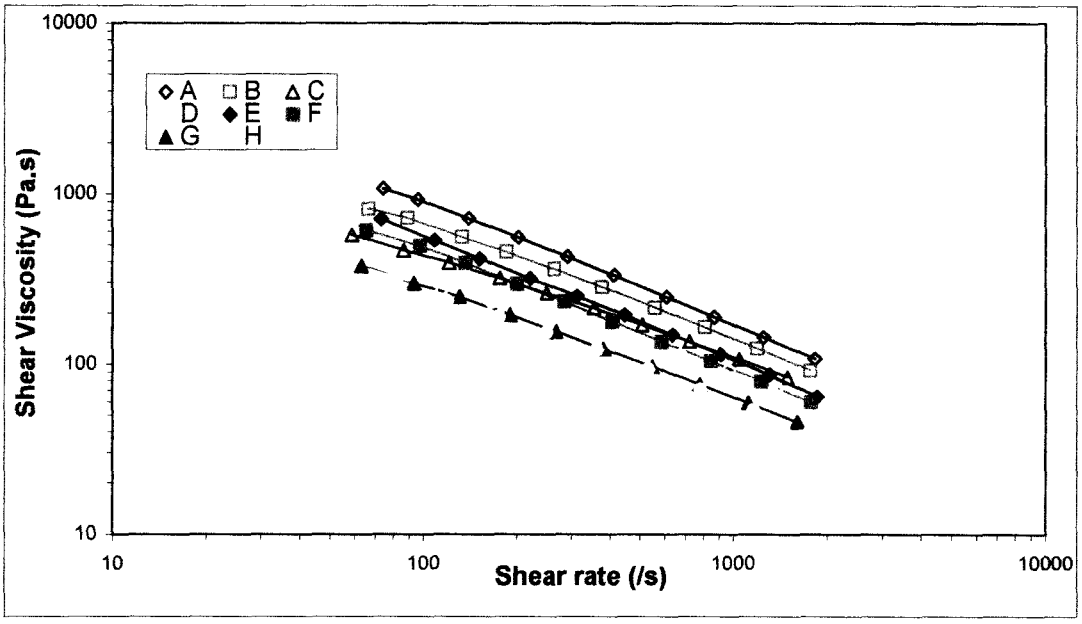

Figure VIII.1. Experimental (symbols) and predicted (solid lines) steady shear viscosity.

Figure VIII.1 presents the experimental and predicted steady-state shear viscosity. This figures shows that shear viscosity predictions (solid lines) are very accurate with respect to the experimental data (symbols). PTT model parameters are shown in Table VIII.1.

Table VIII.1. PTT Model parameters

	Fitting Parameters	
	Elongational	Shear
Resin	α	ξ
A	0.22	0.24
B	0.24	0.15
C	0.17	0.33
D	0.12	0.31
E	0.15	0.24
F	0.22	0.24
G	0.17	0.25
H	0.2	0.25

C. Predictions of PTT Model in Shear-Free Flow

In shear-free flow the tensors of the multi-mode PTT model are given by:

$$Z(tr\boldsymbol{\tau}_i) = \exp\left(-\frac{\alpha\lambda_i}{\eta_i}(\tau^i_{xx}+\tau^i_{yy}+\tau^i_{zz})\right) \tag{8. 17}$$

$$\tau_i = \begin{pmatrix} \tau^i_{xx} & 0 & 0 \\ 0 & \tau^i_{yy} & 0 \\ 0 & 0 & \tau^i_{zz} \end{pmatrix} \tag{8. 18}$$

$$\dot{\boldsymbol{\gamma}} = \begin{pmatrix} -(1+b) & 0 & 0 \\ 0 & -(1-b) & 0 \\ 0 & 0 & 2 \end{pmatrix}\dot{\varepsilon} \tag{8. 19}$$

$$(\dot{\boldsymbol{\gamma}}\cdot\boldsymbol{\tau}_i + \boldsymbol{\tau}_i\cdot\dot{\boldsymbol{\gamma}}) = 2\dot{\varepsilon}\begin{pmatrix} -(1+b)\tau^i_{xx} & 0 & 0 \\ 0 & -(1-b)\tau^i_{yy} & 0 \\ 0 & 0 & 2\tau^i_{zz} \end{pmatrix} \tag{8. 20}$$

$$\tau_{i(1)} = \frac{\partial}{\partial t}\begin{pmatrix} \tau^i_{xx} & 0 & 0 \\ 0 & \tau^i_{yy} & 0 \\ 0 & 0 & \tau^i_{zz} \end{pmatrix} - \dot{\varepsilon}\begin{pmatrix} -(1+b)\tau^i_{xx} & 0 & 0 \\ 0 & -(1-b)\tau^i_{yy} & 0 \\ 0 & 0 & 2\tau^i_{zz} \end{pmatrix} \tag{8. 21}$$

Therefore, a set of coupled nonlinear algebraic equations result:

$$\tau^i_{xx}) \qquad \lambda_i\frac{d\tau^i_{xx}}{dt} + \exp\left(-\frac{\alpha\lambda_i}{\eta_i}(\tau^i_{xx}+\tau^i_{yy}+\tau^i_{zz})\right)\tau^i_{xx} + (1-\xi)\lambda_i\dot{\varepsilon}(1+b)\tau^i_{xx} = \eta_i\dot{\varepsilon}(1+b) \tag{8. 22}$$

$$\tau^i_{yy}) \qquad \lambda_i\frac{d\tau^i_{yy}}{dt} + \exp\left(-\frac{\alpha\lambda_i}{\eta_i}(\tau^i_{xx}+\tau^i_{yy}+\tau^i_{zz})\right)\tau^i_{yy} + (1-\xi)\lambda_i\dot{\varepsilon}(1-b)\tau^i_{yy} = \eta_i\dot{\varepsilon}(1-b) \tag{8. 23}$$

$$\tau^i_{zz}) \qquad \lambda_i\frac{d\tau^i_{zz}}{dt} + \exp\left(-\frac{\alpha\lambda_i}{\eta_i}(\tau^i_{xx}+\tau^i_{yy}+\tau^i_{zz})\right)\tau^i_{zz} - 2(1-\xi)\lambda_i\dot{\varepsilon}\tau^i_{zz} = -2\eta_i\dot{\varepsilon} \tag{8. 24}$$

Equations 8.22 to 8.24 form a system of ordinary differential equations which must be solved numerically to determine the transient values of the stress tensor components, which will be used to calculate the elongational stress ($\tau_e = \tau_{zz} - \tau_{xx}$) and then calculate the elongational viscosity, $\eta_e(\dot{\varepsilon},t)$, at a given elongational rate. Therefore elongational viscosity is given by:

$$\eta_e(\dot{\varepsilon},t) = \frac{\tau_e}{\dot{\varepsilon}} = \frac{\tau_{zz} - \tau_{xx}}{\dot{\varepsilon}} = \frac{\sum_{i=1}^{N}(\tau_{zz}^i - \tau_{xx}^i)}{\dot{\varepsilon}} \qquad (8.25)$$

The α value must be of a magnitude that can fit the experimental transient elongational viscosity. A C-language code, created and validated by Mier (2000) was used for this purpose.

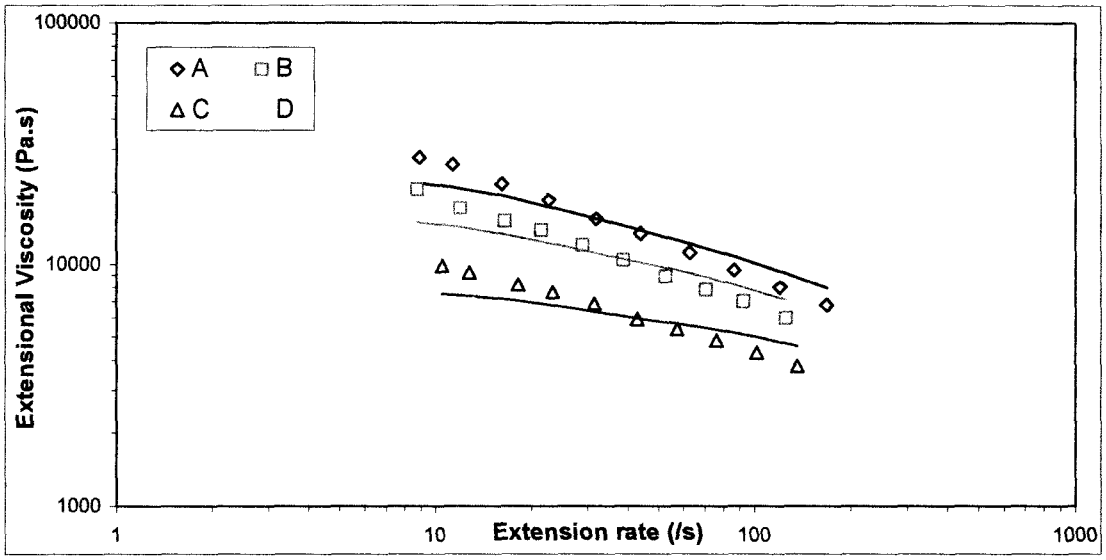

Figure VIII.2. Experimental (Symbols) and predicted (solid lines) elongational viscosity for syndiotactic resins.

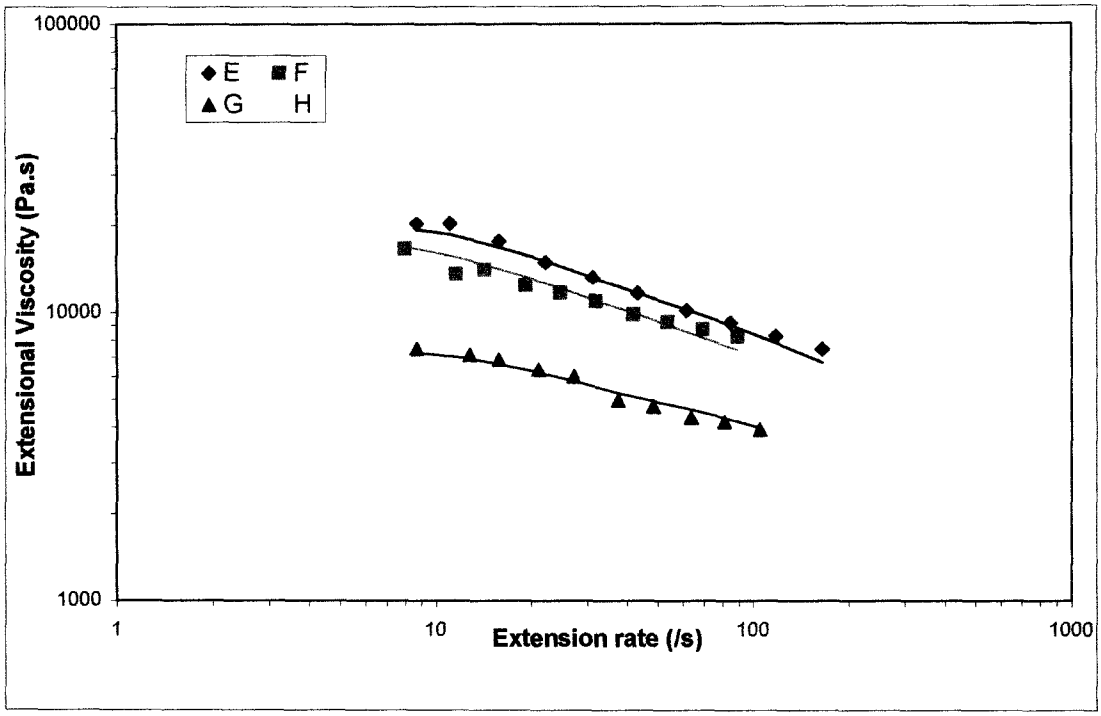

Figure VIII.3. Experimental (symbols) and predicted (solid lines) elongational viscosity for isotactic resins.

Figure VIII.2 and Figure VIII.3 present experimental and predicted elongational viscosity for the syndiotactic and isotactic resins under study respectively. The PTT model parameters used in the fitting for each resin are shown in Table VIII.1.

These figures show that the PTT model predicts accurately elongational viscosity for isotactic resins (see Figure VIII.3). However, for syndiotactic resins (see Figure VIII.2) PTT model predictions are not that accurate, actually the fitting is very poor.

CHAPTER IX. PTT Model Modification

Since PTT model gives poor predictions for elongational viscosity of the syndiotactic resins, it was decided to do an analysis to the elongational parameter (α) to look for possible explanations to the poor fittings and to propose a modification to the model. In this chapter is presented this analysis and the modification proposed as well as the predictions of the shear and elongational viscosity of the new model.

A. Elongational Parameter Analysis

It was decided to analyze the elongational parameter because it is in the rate of creation and destruction of junctions, which is related to the elastic energy. This analysis consisted of two parts, first the elongational parameter was obtained as a function of the extension rate and on the other hand, the PTT model was evaluated when there was no elongational parameter (α = 1) in order to observe its effect in the model output.

Figure IX.1 shows the analysis for one isotactic resin. Similar results were obtained for the other isotactic resins. This figure shows that the original PTT model fittings is very similar to the one obtained with an elongational parameter as a function of the extensional rate ($\dot{\varepsilon}$). This suggests that for isotactic resins the elongational parameter is a constant with respect to the extensional rate (see Figure IX.4). Furthermore, the predictions of the elongational viscosity using α = 1 are very similar to the actual elongational viscosity, but shifted to a lower value. This shows that the elongational parameter (α) is just a damping function in the model; actually, it is equivalent to a vertical shift factor.

On the other hand, Figure IX.2 shows the elongational parameter analysis for one syndiotactic resins. Similar results were obtained for the rest of the syndiotactic resins. This figure confirms that the elongational parameters is just a damping function in the model, because the predictions of the elongational viscosity using α = 1 are again very similar to the actual elongational viscosity, but shifted to a lower value.

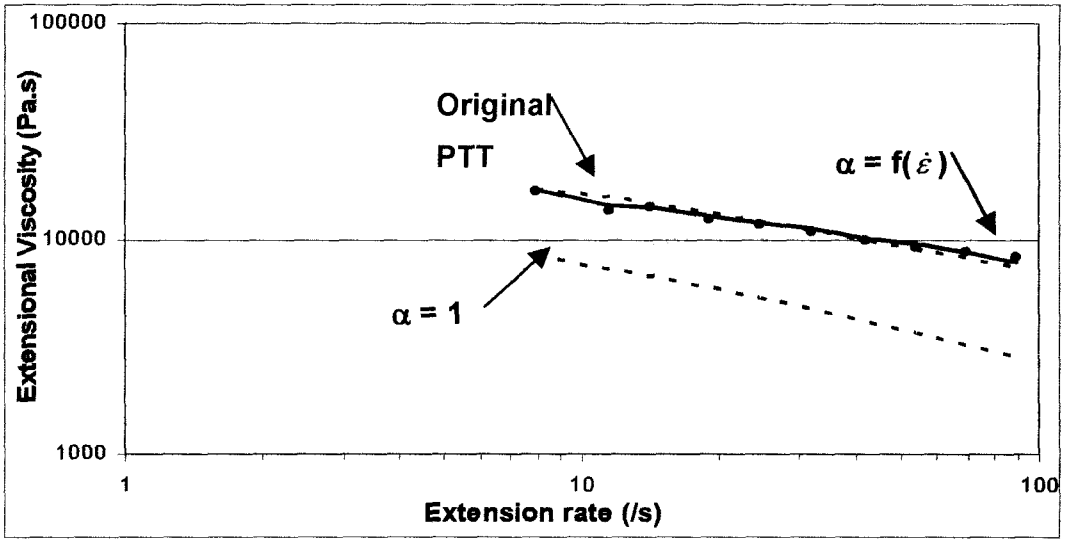

Figure IX.1. Elongational parameter analysis for isotactic resin F.

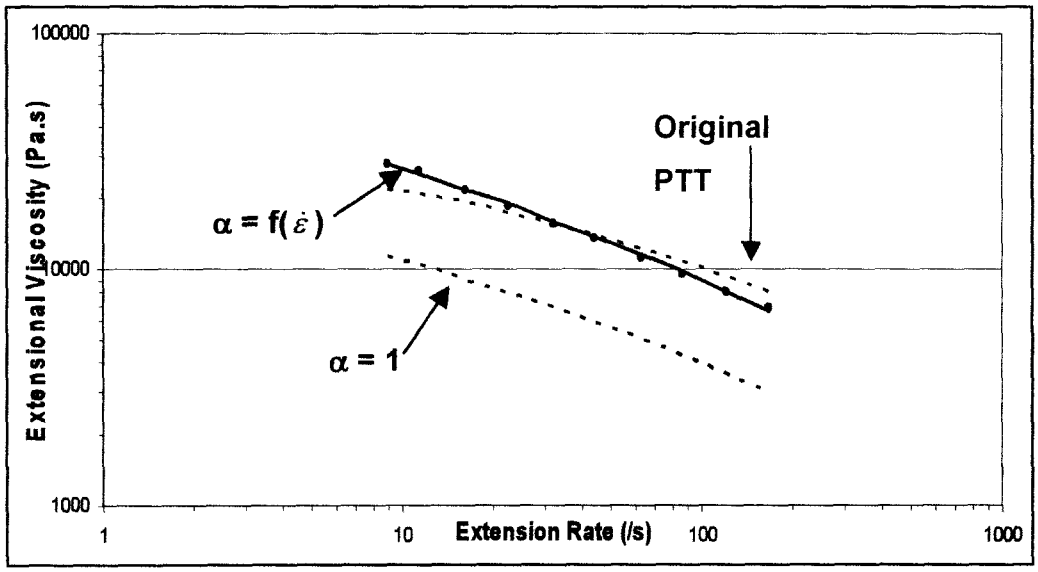

Figure IX.2. Elongational parameter analysis for syndiotactic resin A.

Figure IX.2 also shows that the PTT model using an elongational parameter as a function of the extension rate gives better fittings of the experimental data. It was observed that the functionality of the elongational parameter (α) with respect of the extension rate is a logarithmic function for syndiotactic resins, while isotactic resins do not present any functionality and the elongational parameter (α) could be considered as a constant value. Figure IX.3 presents the elongational parameter as a function of the extension rate for syndiotactic resins and their fitting to a logarithmic function. The functions for each resin as well as their correlation coefficient (R^2) are also presented in this figure. Figure IX.4 presents the behavior of the elongational parameter for isotactic resins. The straight lines in this figure show the average value of the elongational parameter. The deviation of the points from the average value is between ± 5 %.

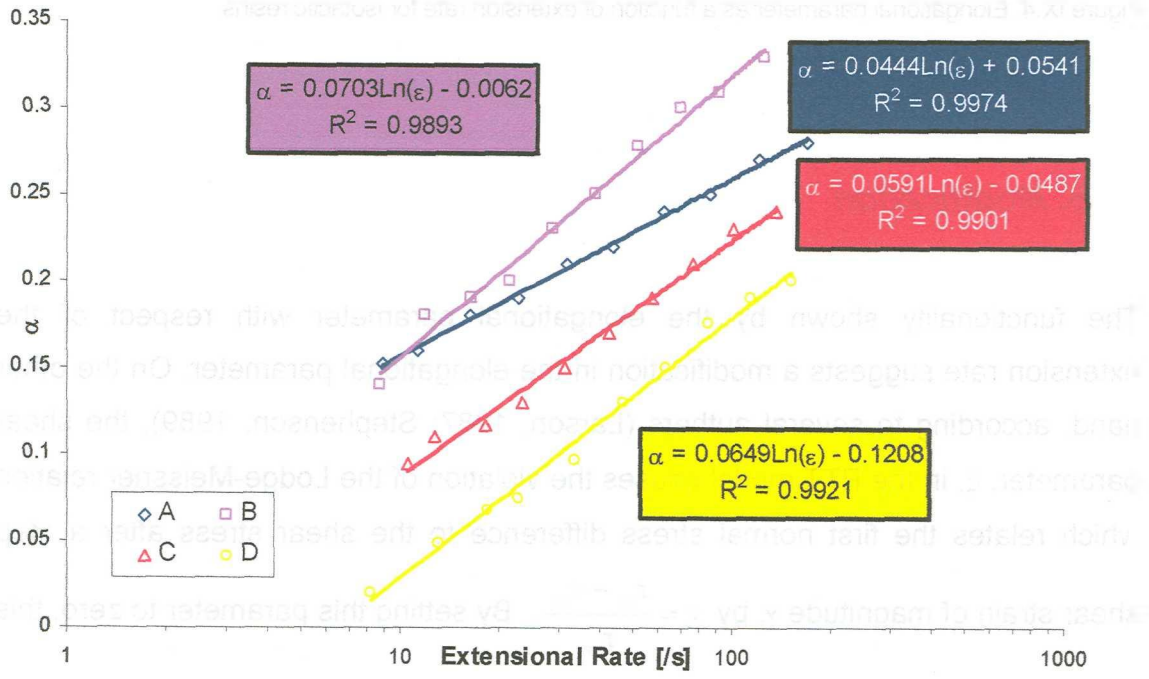

Figure IX.3. Elongational parameter as a function of the extension rate for syndiotactic resins.

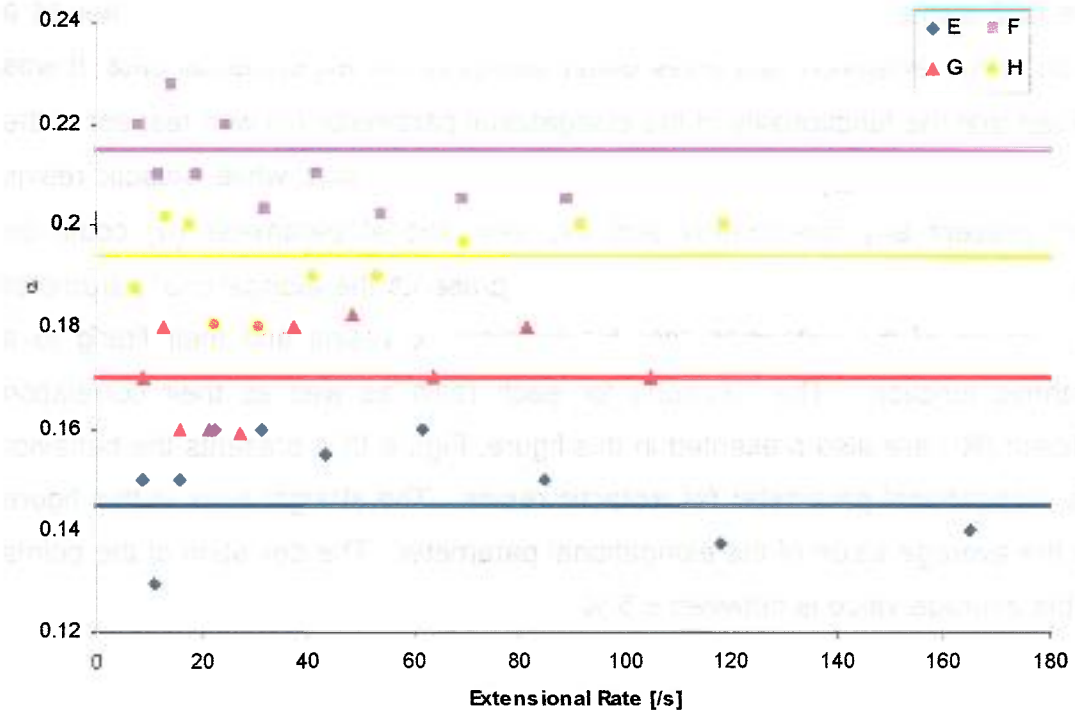

Figure IX.4. Elongational parameter as a function of extension rate for isotactic resins.

B. Modification

The functionality shown by the elongational parameter with respect of the extension rate suggests a modification in the elongational parameter. On the other hand, according to several authors (Larson, 1987; Stephenson, 1989), the shear parameter, ξ, in the PTT model causes the violation of the Lodge-Meissner relation which relates the first normal stress difference to the shear stress after a step shear strain of magnitude γ, by $\gamma = \frac{\tau_{xx} - \tau_{yy}}{\tau_{xy}}$. By setting this parameter to zero, this violation is avoided (Larson, 1987; Verbeeten, 2001; Tanner, 2002). Then, using these findings, a modification of the model is proposed as follows:

$$\boldsymbol{\tau} = \sum_{i=1}^{N} \boldsymbol{\tau}_i \tag{9. 1}$$

$$Z(tr\boldsymbol{\tau}_i)\boldsymbol{\tau}_i + \lambda_i\, \tau_{i(1)} = -\eta_i\, \dot{\boldsymbol{\gamma}} \tag{9. 2}$$

$$Z(tr\boldsymbol{\tau}_i) = \exp\left(-\frac{\alpha\lambda_i}{\eta_i} tr\tau_i\right) \tag{9. 3}$$

where α is a constant (C) for simple shear, and for shear-free flow is given by

$$\alpha = A\ln(\dot{\varepsilon}) + B \tag{9. 4}$$

C. Predictions in Simple Shear

In simple shear the tensors of the modify PTT model are given by:

$$\tau_i = \begin{pmatrix} \tau^i_{xx} & \tau^i_{xy} & 0 \\ \tau^i_{yx} & \tau^i_{yy} & 0 \\ 0 & 0 & \tau^i_{zz} \end{pmatrix} \tag{9. 5}$$

$$\dot{\boldsymbol{\gamma}} = \begin{pmatrix} 0 & \dot{\gamma} & 0 \\ \dot{\gamma} & 0 & 0 \\ 0 & 0 & 0 \end{pmatrix} \tag{9. 6}$$

$$\tau_{i(1)} = \frac{\partial}{\partial t}\begin{pmatrix} \tau^i_{xx} & \tau^i_{xy} & 0 \\ \tau^i_{yx} & \tau^i_{yy} & 0 \\ 0 & 0 & \tau^i_{zz} \end{pmatrix} - \dot{\gamma}\begin{pmatrix} 2\tau^i_{yx} & \tau^i_{yy} & 0 \\ \tau^i_{yy} & 0 & 0 \\ 0 & 0 & 0 \end{pmatrix} \tag{9. 7}$$

Besides the fitting parameter α is just a constant C

$$\alpha = C \tag{9. 8}$$

Introducing these definitions in the modified PTT model, a set of coupled nonlinear algebraic equations result:

$$\tau^i_{xx}) \qquad \lambda_i \frac{d\tau^i_{xx}}{dt} + \exp\left(-\frac{C\lambda_i}{\eta_i}(\tau^i_{xx} + \tau^i_{yy} + \tau^i_{zz})\right)\tau^i_{xx} - 2\lambda_i \dot{\gamma}\tau^i_{yx} = 0 \qquad (9.\ 9)$$

$$\tau^i_{yy}) \qquad \lambda_i \frac{d\tau^i_{yy}}{dt} + \exp\left(-\frac{C\lambda_i}{\eta_i}(\tau^i_{xx} + \tau^i_{yy} + \tau^i_{zz})\right)\tau^i_{yy} = 0 \qquad (9.\ 10)$$

$$\tau^i_{zz}) \qquad \lambda_i \frac{d\tau^i_{zz}}{dt} + \exp\left(-\frac{C\lambda_i}{\eta_i}(\tau^i_{xx} + \tau^i_{yy} + \tau^i_{zz})\right)\tau^i_{zz} = 0 \qquad (9.\ 11)$$

$$\tau^i_{xy}) \qquad \lambda_i \frac{d\tau^i_{xy}}{dt} + \exp\left(-\frac{C\lambda_i}{\eta_i}(\tau^i_{xx} + \tau^i_{yy} + \tau^i_{zz})\right)\tau^i_{xy} - \lambda_i \dot{\gamma}\tau^i_{yy} = -\eta_i \dot{\gamma} \qquad (9.\ 12)$$

$$\tau^i_{yx}) \qquad \lambda_i \frac{d\tau^i_{yx}}{dt} + \exp\left(-\frac{C\lambda_i}{\eta_i}(\tau^i_{xx} + \tau^i_{yy} + \tau^i_{zz})\right)\tau^i_{yx} - \lambda_i \dot{\gamma}\tau^i_{yy} = -\eta_i \dot{\gamma} \qquad (9.\ 13)$$

Just like the in the original PTT model, the stress tensor is symmetric, $\tau^i_{yx} = \tau^i_{xy}$; therefore equation 9.13 is trivial. Equations 9.9 to 9.12 form a system of ordinary differential equations which must be solved numerically to determine the transient expressions for the shear viscosity.

The shear viscosity is given by:

$$\eta(\dot{\gamma}, t) = \frac{\tau_{xy}}{\dot{\gamma}} = \frac{\sum_{i=1}^{N} \tau^i_{xy}}{\dot{\gamma}} \qquad (9.\ 14)$$

A Fortran-language code was developed to solve this model (see Appendix B) with satisfactory results. Figure IX.5 shows the modified PTT model predictions in shear flow for one isotactic (Resin E) and one syndiotactic (resin A) resin. Similar results are obtained for the rest of the resins. Table IX.1 present the shear parameters (C) used in the fitting of the experimental data for all the resins. The transient response of the model for resin A and resin E could be seen in Figure IX.6 and Figure IX.7 respectively. Similar results were observed for the rest of the resins.

Table IX.1. Shear parameter (C) for the Modified PTT Model for all resins.

Resin	C	Resin	C
A	2.8	**E**	2.33
B	4.91	**F**	5.1
C	3.92	**G**	4.24
D	3.21	**H**	3.67

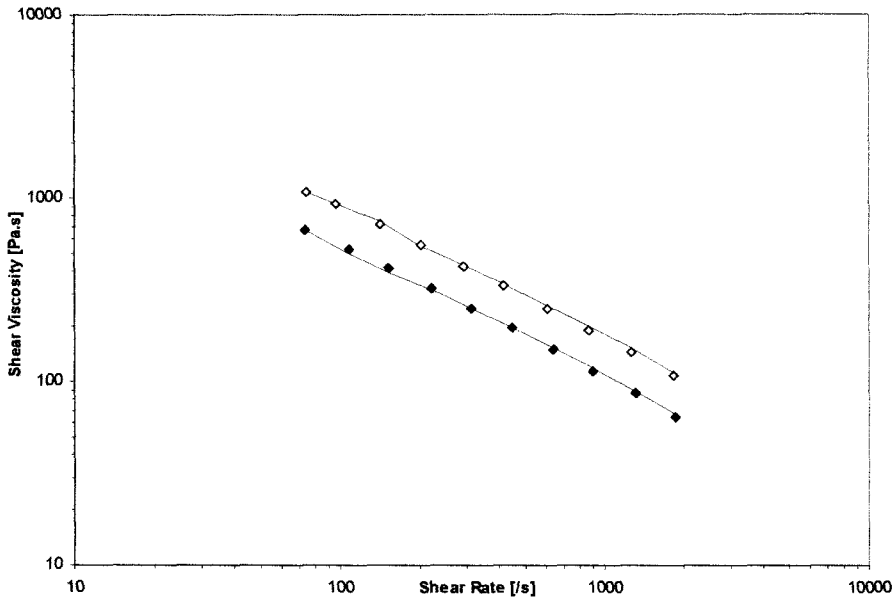

Figure IX.5. Modified PTT model's predictions and experimental shear viscosity for syndiotactic resin A (open symbols) and isotactic resin E (filled symbols).

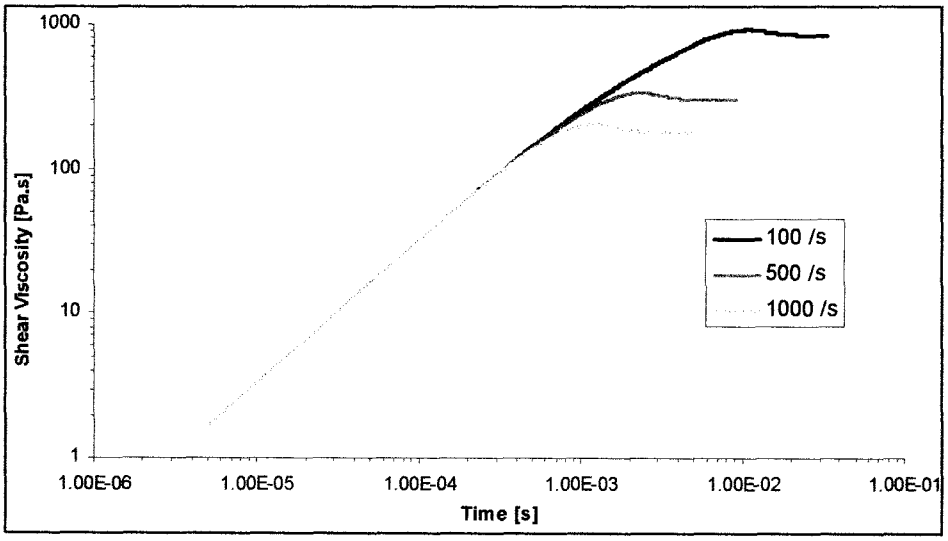

Figure IX.6. Prediction of the modified PTT model for the transient shear viscosity of synditactic resin A at different shear rates.

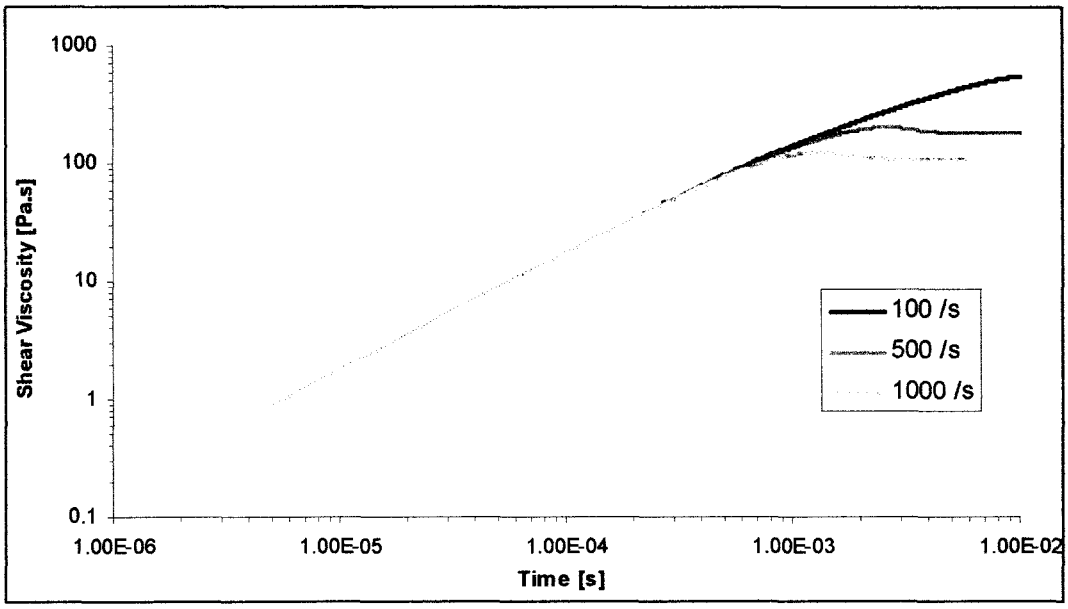

Figure IX.7. Prediction of the modified PTT model for the transient shear viscosity of isotactic resin E at different shear rates.

D. Predictions in Shear – Free Flow

In shear-free flow the tensors of the modified PTT model are given by:

$$Z(tr\boldsymbol{\tau}_i) = \exp\left(-\frac{\alpha\lambda_i}{\eta_i}(\tau^i_{xx} + \tau^i_{yy} + \tau^i_{zz})\right) \tag{9. 15}$$

$$\tau_i = \begin{pmatrix} \tau^i_{xx} & 0 & 0 \\ 0 & \tau^i_{yy} & 0 \\ 0 & 0 & \tau^i_{zz} \end{pmatrix} \tag{9. 16}$$

$$\dot{\boldsymbol{\gamma}} = \begin{pmatrix} -(1+b) & 0 & 0 \\ 0 & -(1-b) & 0 \\ 0 & 0 & 2 \end{pmatrix} \dot{\varepsilon} \tag{9 .17}$$

$$\tau_{i(1)} = \frac{\partial}{\partial t}\begin{pmatrix} \tau^i_{xx} & 0 & 0 \\ 0 & \tau^i_{yy} & 0 \\ 0 & 0 & \tau^i_{zz} \end{pmatrix} - \dot{\varepsilon}\begin{pmatrix} -(1+b)\tau^i_{xx} & 0 & 0 \\ 0 & -(1-b)\tau^i_{yy} & 0 \\ 0 & 0 & 2\tau^i_{zz} \end{pmatrix} \qquad (9.\ 18)$$

Therefore, a set of coupled nonlinear algebraic equations result:

$$\tau^i_{xx}) \qquad \lambda_i \frac{d\tau^i_{xx}}{dt} + \exp\left(-\frac{\alpha\lambda_i}{\eta_i}(\tau^i_{xx}+\tau^i_{yy}+\tau^i_{zz})\right)\tau^i_{xx} + \lambda_i\dot{\varepsilon}(1+b)\tau^i_{xx} = \eta_i\dot{\varepsilon}(1+b) \qquad (9.\ 19)$$

$$\tau^i_{yy}) \qquad \lambda_i \frac{d\tau^i_{yy}}{dt} + \exp\left(-\frac{\alpha\lambda_i}{\eta_i}(\tau^i_{xx}+\tau^i_{yy}+\tau^i_{zz})\right)\tau^i_{yy} + \lambda_i\dot{\varepsilon}(1-b)\tau^i_{yy} = \eta_i\dot{\varepsilon}(1-b) \qquad (9.\ 20)$$

$$\tau^i_{zz}) \qquad \lambda_i \frac{d\tau^i_{zz}}{dt} + \exp\left(-\frac{\alpha\lambda_i}{\eta_i}(\tau^i_{xx}+\tau^i_{yy}+\tau^i_{zz})\right)\tau^i_{zz} - 2\lambda_i\dot{\varepsilon}\tau^i_{zz} = -2\eta_i\dot{\varepsilon} \qquad (9.\ 21)$$

Equations 9.19 to 9.21 form a system of ordinary differential equations which must be solved numerically to determine the transient values of the stress tensor components, which will be used to calculate the elongational stress ($\tau_e = \tau_{zz} - \tau_{xx}$) and then calculate the elongational viscosity, $\eta_e(\dot{\varepsilon},t)$, at a given elongational rate. Therefore elongational viscosity is given by:

$$\eta_e(\dot{\varepsilon},t) = \frac{\tau_e}{\dot{\varepsilon}} = \frac{\tau_{zz}-\tau_{xx}}{\dot{\varepsilon}} = \frac{\sum_{i=1}^{N}(\tau^i_{zz}-\tau^i_{xx})}{\dot{\varepsilon}} \qquad (8.\ 26)$$

The parameter α is given by equation 9.4, where the A and B values must be of magnitude that can fit experimental elongational viscosity. A Fortran-language code was developed to solve this model (see Appendix B). Figure IX.8 shows the predictions of elongational viscosity for resins A and E. Figure IX.11 and Figure IX.12 present the modified PTT model's predictions and experimental elongational viscosity for all syndiotactic and isotactic resins respectively. The parameters used in the fitting could be seen in Table IX.2. Finally, the transient response of resins A

and E at different extension rates can be seen in Figure IX.11 and Figure IX.12. Similar results are obtained for the rest of the resins.

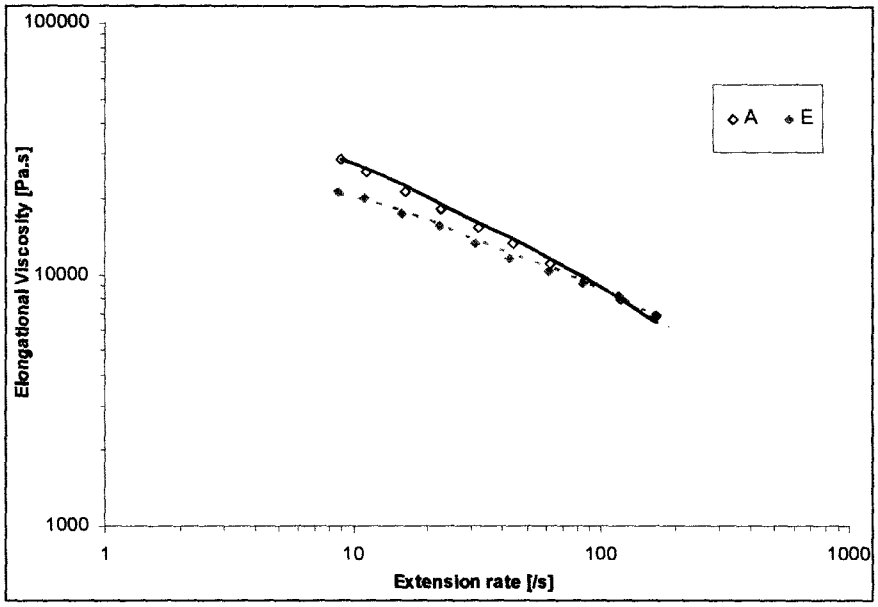

Figure IX.8. Modified PTT model's predictions and experimental elongational viscosity for syndiotactic resin A (open symbols) and isotactic resin H (filled symbols).

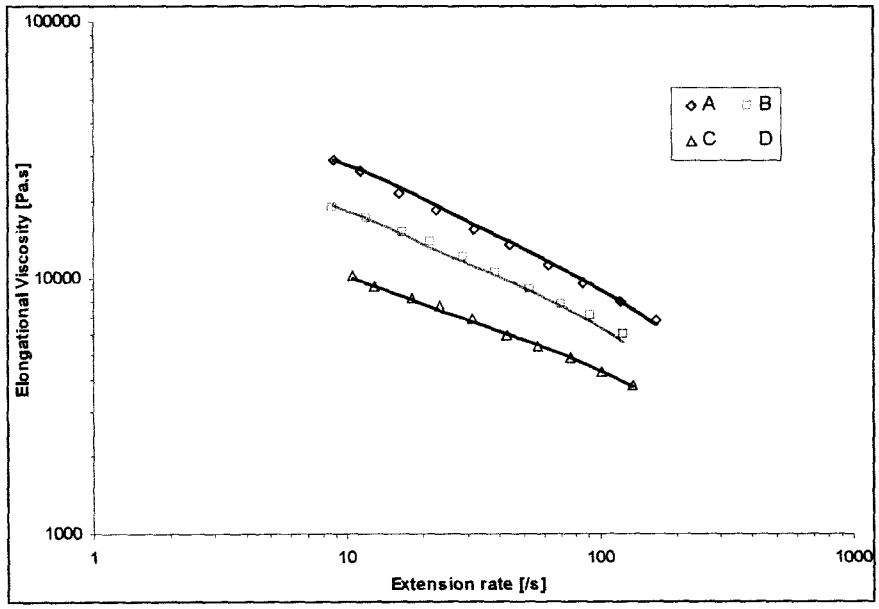

Figure IX.9. Modified PTT model's predictions and experimental elongational viscosity for syndiotactic resins.

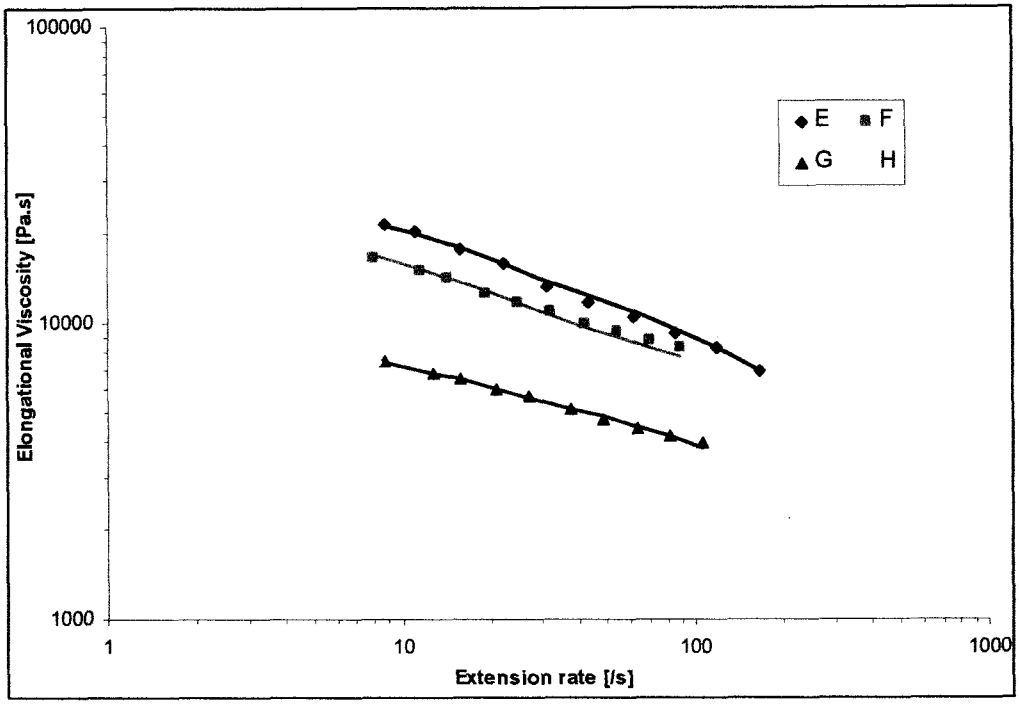

Figure IX.10. Modified PTT model's predictions and experimental elongational viscosity for isotactic resins.

Table IX.2. Elongational fitting parameters for the Modified PTT Model for all resins.

	Fitting Parameters	
	Elongational	
Resin	*A*	*B*
A	0.05	0.06
B	0.07	0.02
C	0.057	0.009
D	0.0714	-0.106
E	0	0.16
F	0	0.26
G	0	0.21
H	0	0.2

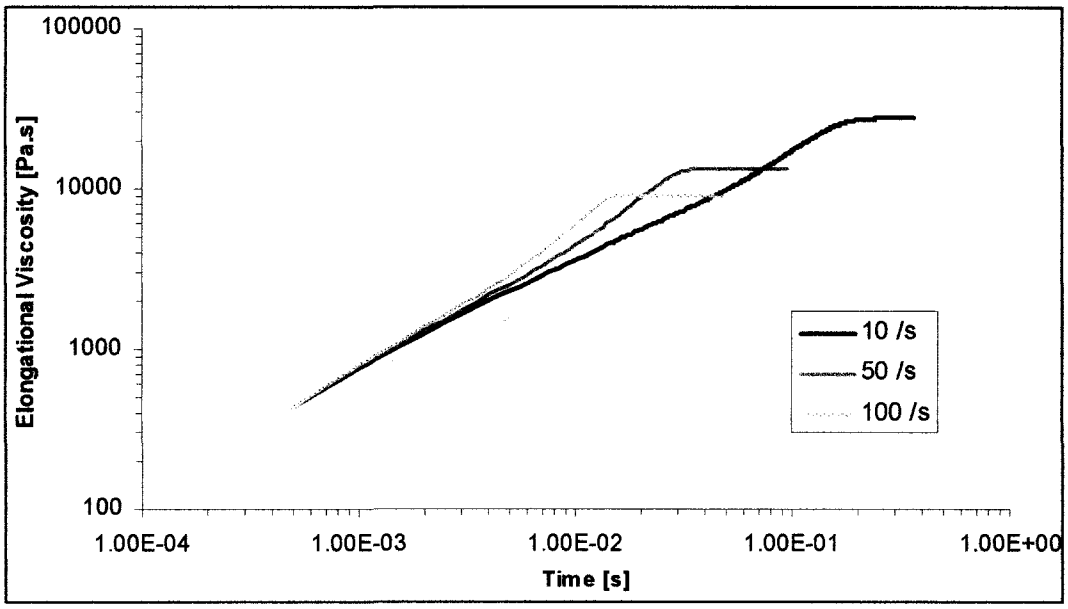

Figure IX.11. Prediction of the modified PTT model for the transient elongational viscosity of syndiotactic resin A at different extension rates.

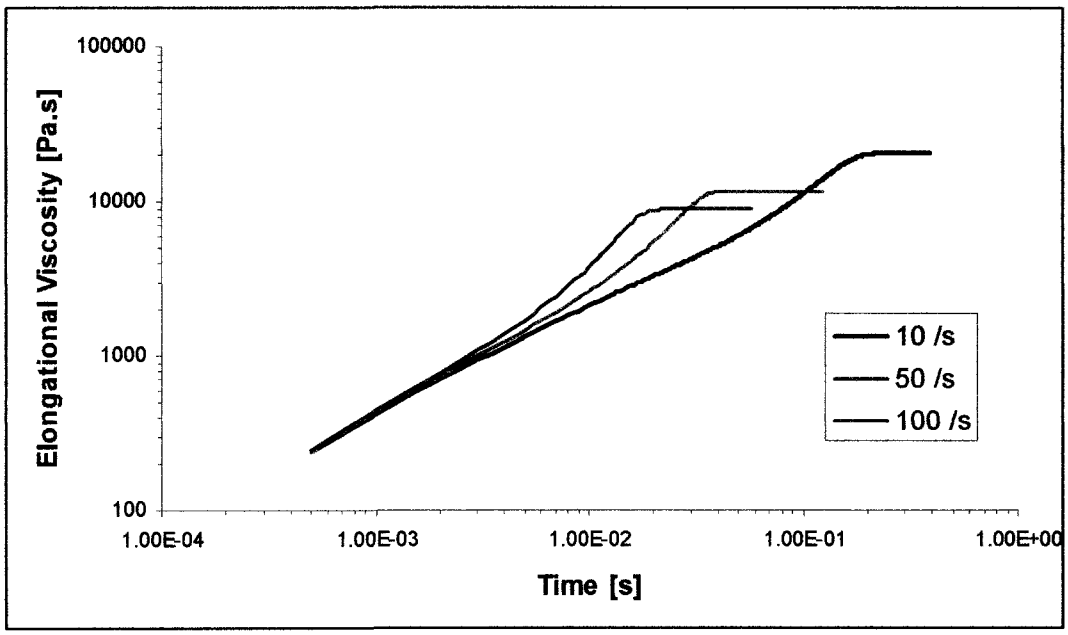

Figure IX.12. Prediction of the modified PTT model for the transient elongational viscosity of isotactic resin E at different extension rates.

CHAPTER X. POM – POM Model

This chapter presents the prediction of rheological properties using the extended pom-pom model (XPP) introduced in Chapter II. Section A presents the pom-pom and XPP model. Section B shows the deduced expressions and predictions of the shear viscosity. Section C shows the deduced expression for the elongational viscosity predicted by the XPP model, as well as the prediction of such elongational material function for the resins under study.

A. The POM – POM and XPP Model

Polymer melts with long chain branching have rheological properties that differ distinctly from those of the linear polymers or polymer with side braches too short to entangle with surrounding polymers. The POM-POM model is based on the idea that the strain hardening behavior in extensional flow of multiply branched polymer molecules is due to the trapped polymer chain segments in between branch points. The simplest molecular structure that would have this property is an idealized "pom-pom" molecule (see Figure X.1).

An idealized molecule called pom-pom, has a single backbone with multiples branches emerging from each end. Because these branches are entangled with the surrounding molecules, the backbone can readily be stretched in an extensional flow, producing strain hardening. In start-up of shear, however, the backbone stretches only temporarily, and eventually collapses as the molecule is aligned, producing strain softening.

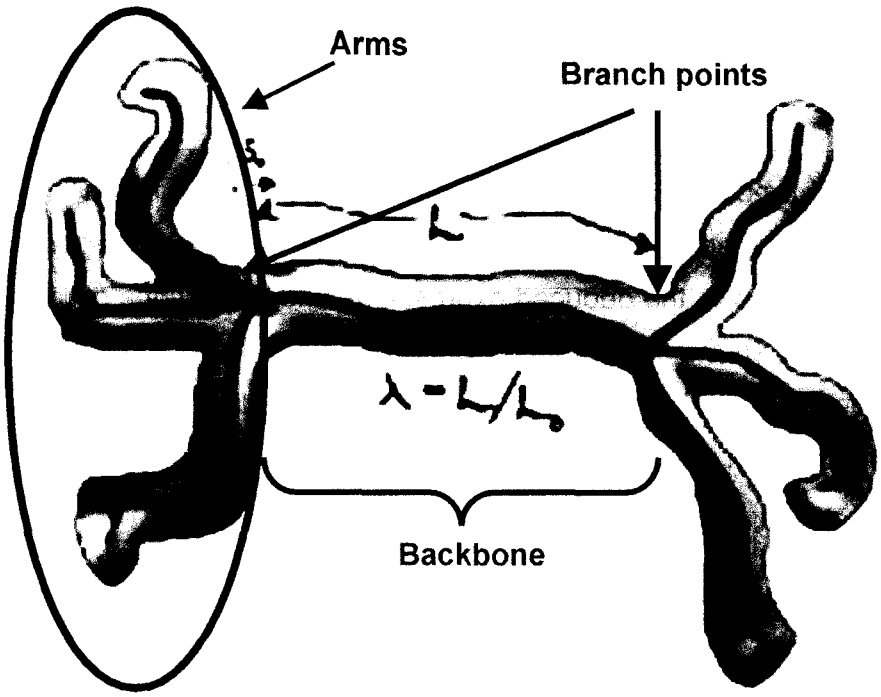

Figure X.1. Description of the Pom - Pom molecule.

After a strain (deformation), the orientation of the chains is remembered (fluid memory). At short times the polymer chains are trapped in tubes. At longer times the arms can relax from the free ends by fluctuation. At still longer times the arms have totally relaxed and the backbones can move and relax (by reptation).

The POM-POM model consists of an equation set that describes the orientation and stretch of the pom-pom backbones as they flow. The number of arms of each mode is used as the parameter to fit extensional viscosity measurements. As it was mentioned on Chapter II, there are several versions of this model. The extended Pom – Pom model (Verbeeten, 2001), XPP model, overcome the drawbacks of the original version, besides it presents some mathematical advantages when solving the model.

The XPP model is written as:

$$\tau = G_0\left(3\Lambda^2 S - I\right) \tag{10.1}$$

where S is the orientation tensor and it satisfies the evolution of orientation equation:

$$S_{(1)} + 2[\dot{\gamma} : S]S + \frac{1}{\lambda_{0b}\Lambda^2}\left[3\alpha\Lambda^4 S \cdot S + (1-\alpha-3\alpha\Lambda^4 tr(S \cdot S))S - \frac{(1-\alpha)}{3}I\right] = 0 \quad (10.2)$$

λ_{0b} is the relaxation time of the backbone tube orientation, α is a fitting parameter related to the amount of anisotropy of the material. Λ is the stretch and satisfies the evolution of stretch equation:

$$\dot{\Lambda} = \Lambda[\dot{\gamma} : S] - \frac{1}{\lambda_s}(\Lambda - 1) \quad (10.3)$$

λ_s is the stretch relaxation time, and it is given by

$$\lambda_s = \lambda_{0s} e^{-\nu(\Lambda-1)} \quad (10.4)$$

where ν is a measure of the influence of the surrounding polymer chains on the backbone tube stretch. It is approximated by

$$\nu = \frac{2}{q} \quad (10.5)$$

where q is the number of dangling arms in the 'pom-pom" molecule (see Figure X.1). This is taken as a fitting parameter too.

B. Predictions of XPP Model in Shear – Free Flow

In shear-free flow the tensor of the XPP model are given by:

$$\dot{\gamma} = \begin{bmatrix} -\dot{\varepsilon} & 0 & 0 \\ 0 & -\dot{\varepsilon} & 0 \\ 0 & 0 & 2\dot{\varepsilon} \end{bmatrix} \tag{10.6}$$

$$\tau = \begin{bmatrix} \tau_{xx} & 0 & 0 \\ 0 & \tau_{yy} & 0 \\ 0 & 0 & \tau_{zz} \end{bmatrix} \tag{10.7}$$

$$S = \begin{bmatrix} S_{xx} & 0 & 0 \\ 0 & S_{yy} & 0 \\ 0 & 0 & S_{zz} \end{bmatrix} \tag{10.8}$$

$$S_{(1)} = \frac{\partial}{\partial t}\begin{pmatrix} S_{xx} & 0 & 0 \\ 0 & S_{yy} & 0 \\ 0 & 0 & S_{zz} \end{pmatrix} - \dot{\varepsilon}\begin{pmatrix} -S_{xx} & 0 & 0 \\ 0 & -S_{yy} & 0 \\ 0 & 0 & 2S_{zz} \end{pmatrix} \tag{10.9}$$

$$[\dot{\gamma} : S] = -\dot{\varepsilon}S_{xx} - \dot{\varepsilon}S_{yy} + 2\dot{\varepsilon}S_{zz} \tag{10.10}$$

$$tr(S \cdot S) = S_{xx}^2 + S_{yy}^2 + S_{zz}^2 \tag{10.11}$$

It is worth to mention that, since τ_{xx} and τ_{yy} components of the stress tensor are the same, S_{xx} and S_{yy} components of the orientation tensor S, are the same too. Now, introducing these definitions in the model, we obtain a system of three ordinary differential equations.

$$\frac{dS_{xx}}{dt} + \dot{\varepsilon}S_{xx} - 4\dot{\varepsilon}(S_{xx} - S_{zz})S_{xx} + \frac{3\alpha\Lambda^2}{\lambda_{0b}}S_{xx}^2 + \frac{1-\alpha-3\alpha\Lambda^4(2S_{xx}^2 + S_{zz}^2)}{\lambda_{0b}\Lambda^2}S_{xx} - \frac{1-\alpha}{3\lambda_{0b}\Lambda^2} = 0 \tag{10.12}$$

$$\frac{dS_{zz}}{dt} - 2\dot{\varepsilon}S_{zz} - 4\dot{\varepsilon}(S_{xx} - S_{zz})S_{zz} + \frac{3\alpha\Lambda^2}{\lambda_{0b}}S_{zz}^2 + \frac{1-\alpha-3\alpha\Lambda^4(2S_{xx}^2 + S_{zz}^2)}{\lambda_{0b}\Lambda^2}S_{zz} - \frac{1-\alpha}{3\lambda_{0b}\Lambda^2} = 0 \tag{10.13}$$

$$\frac{d\Lambda}{dt} = -2\dot{\varepsilon}(S_{xx} - S_{zz})\Lambda - \frac{1}{\lambda_s}(\Lambda - 1) \tag{10.14}$$

Solving simultaneously these differential equations, we obtain S_{xx}, S_{zz} and Λ as a function of time. Now, we obtain the transient stress components using the equations:

$$\tau_{xx} = 3G_0\Lambda^2 S_{xx} - G_0 \tag{10.15}$$

$$\tau_{zz} = 3G_0\Lambda^2 S_{zz} - G_0 \tag{10.16}$$

Finally we obtain elongational viscosity using

$$\eta_e(\dot{\varepsilon},t) = \frac{\tau_{zz} - \tau_{xx}}{\dot{\varepsilon}} \tag{10.17}$$

A FORTRAN – language code was developed in order to make the XPP model predictions. This code was validated using the experimental data presented by Verbeeten *et. al.* (2001). For further information about the code see Appendix B.

Figure X.2 and Figure X.3 show the predictions of the XPP model for syndiotactic and isotactic resins respectively. It can be seen that the fitting is good for most resins; however, the fitting process is very complicated because the fitting parameters must be fitted for each relaxation element. This means that there are twelve fitting parameters[3] for most resins. These are too many parameters, which mean that the model is not that robust. In addition, because of the number of fitting parameters, more than one combination could be obtained. In any case, Table X.1 shows the parameters used in the fitting of all the resins. It is worth to mention that these parameters where found by fitting the experimental elongational viscosity, and these same parameter, according to Verbeeten *et. al.* (2001), must fit accurately the shear viscosity curve. Figure X.4 and Figure X.5 show the transient response of resin A and E respectively. Similar results were obtained for the rest of the resins.

---

[3] All the resins present four relaxation elements, except for resins C and D, which present three relaxation elements as shown in Table V.4. Therefore, for resins C and D, there are nine fitting parameters.

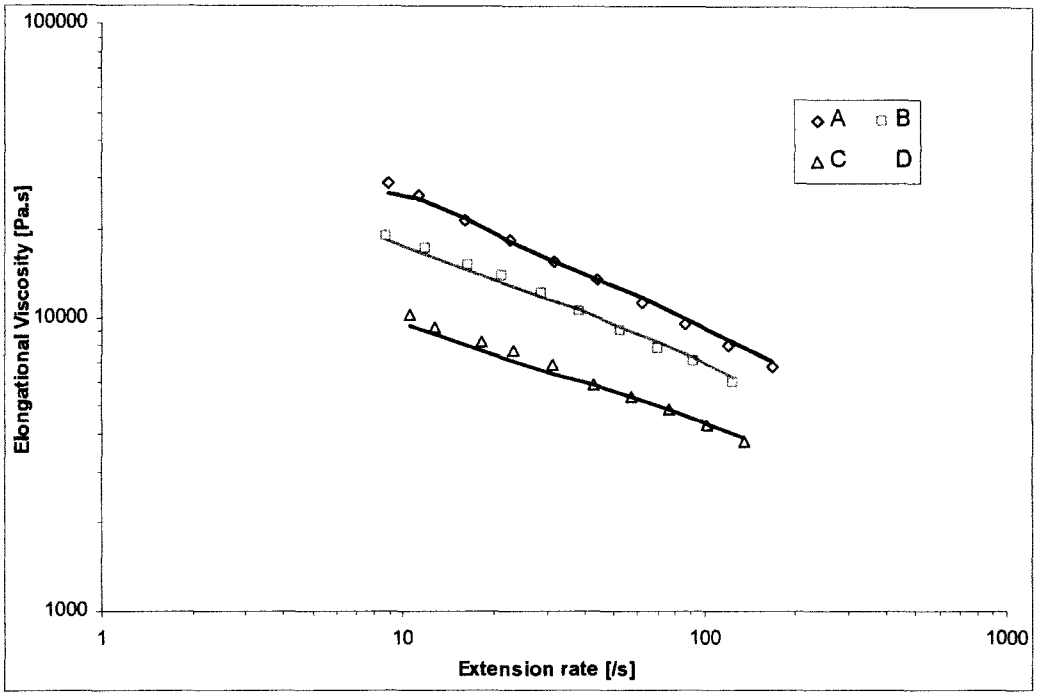

Figure X.2. XPP model's predictions and experimental elongational viscosity for syndiotactic resins.

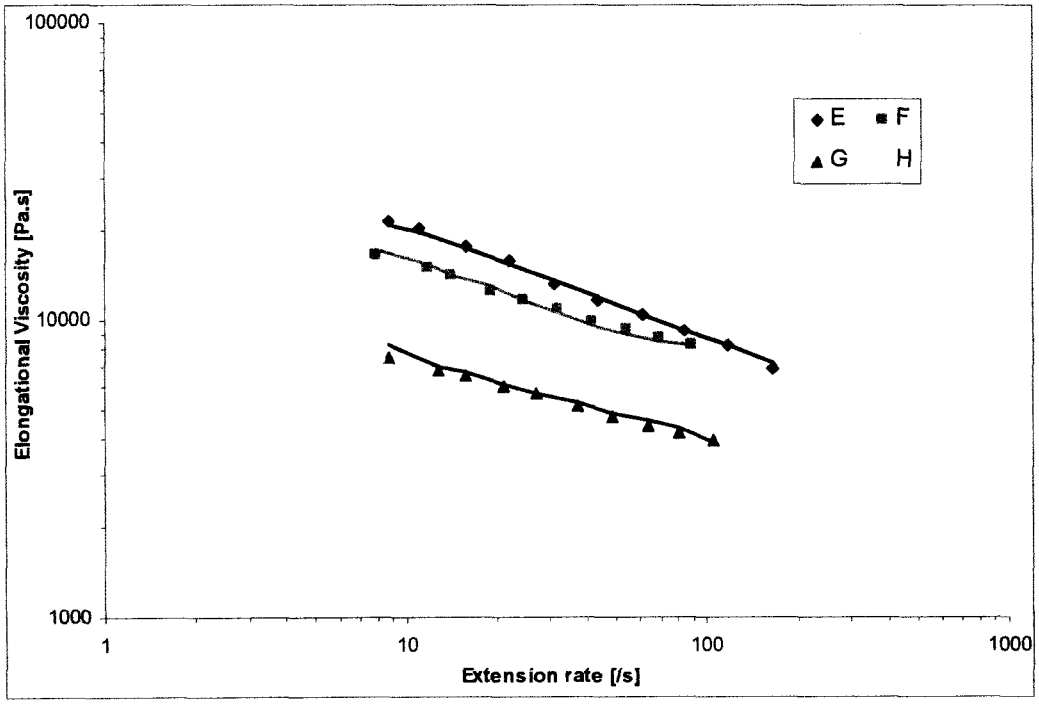

Figure X.3. XPP model's predictions and experimental elongational viscosity for isotactic resins.

Table X.1. XPP model parameters for fitting the elongational viscosity for all the resins.

Resin A				Resin B			
i	q_i	$\lambda_{0b,i}$ / $\lambda_{0s,i}$	α_i	i	q_i	$\lambda_{0b,i}$ / $\lambda_{0s,i}$	α_i
1	1	17	0.1	1	1	15	0.05
2	1	9	0.1	2	1	11	0.05
3	1	0.2	0.1	3	1	0.75	0.1
4	2	0.2	0.1	4	2	0.3	0.1
Resin C				**Resin D**			
i	q_i	$\lambda_{0b,i}$ / $\lambda_{0s,i}$	α_i	i	q_i	$\lambda_{0b,i}$ / $\lambda_{0s,i}$	α_i
1	1	15	0	1	1	14	0.15
2	1	9	1	2	1	8	0.01
3	2	0.4	1	3	1	0.3	0.01
Resin E				**Resin F**			
i	q_i	$\lambda_{0b,i}$ / $\lambda_{0s,i}$	α_i	i	q_i	$\lambda_{0b,i}$ / $\lambda_{0s,i}$	α_i
1	1	3.5	0.3	1	1	3.5	0.2
2	1	3.5	0.3	2	1	2	0.2
3	1	2.9	0.2	3	2	2	0.2
4	3	2.9	0.2	4	2	2	0.2
Resin G				**Resin H**			
i	q_i	$\lambda_{0b,i}$ / $\lambda_{0s,i}$	α_i	i	q_i	$\lambda_{0b,i}$ / $\lambda_{0s,i}$	α_i
1	1	3.3	0.2	1	1	3	0.2
2	1	2.8	0.2	2	1	3	0.1
3	2	2.5	0.1	3	1	2.6	0.1
4	3	2.5	0.3	4	2	1.8	0.1

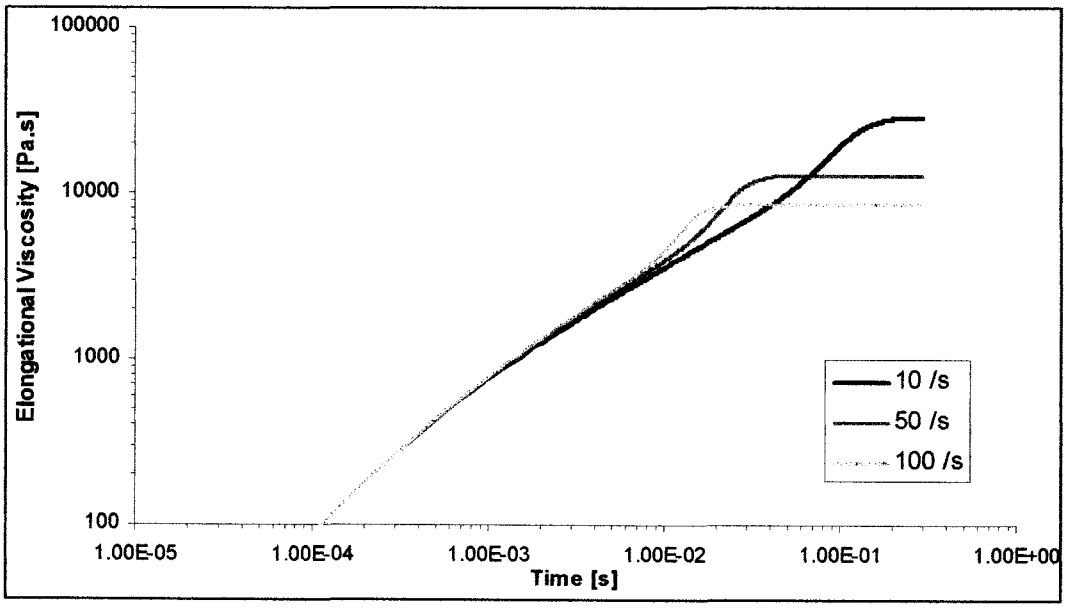

Figure X.4. XPP model's predictions of transient elongational viscosity for syndiotactic resin A at different extension rates.

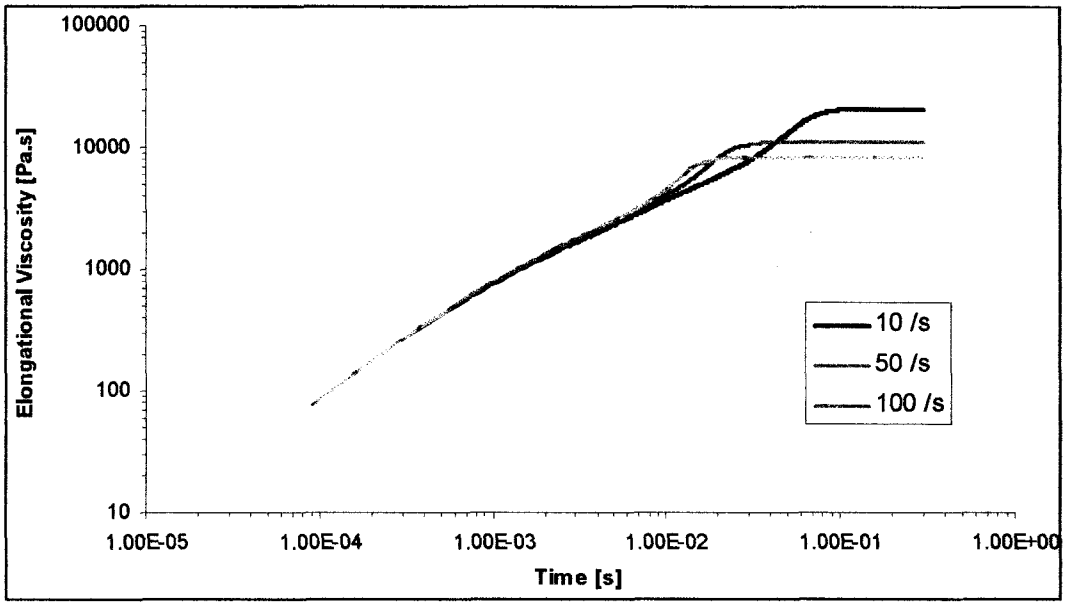

Figure X.5. XPP model's predictions of transient elongational viscosity for isotactic resin E at different extension rates.

C. Predictions of XPP Model in Simple Shear

In shear-free flow the tensor of the XPP model are given by:

$$\tau_i = \begin{pmatrix} \tau^i_{xx} & \tau^i_{xy} & 0 \\ \tau^i_{yx} & \tau^i_{yy} & 0 \\ 0 & 0 & \tau^i_{zz} \end{pmatrix} \tag{10.18}$$

$$\dot{\gamma} = \begin{pmatrix} 0 & \dot{\gamma} & 0 \\ \dot{\gamma} & 0 & 0 \\ 0 & 0 & 0 \end{pmatrix} \tag{10. 19}$$

$$S_i = \begin{pmatrix} S^i_{xx} & S^i_{xy} & 0 \\ S^i_{yx} & S^i_{yy} & 0 \\ 0 & 0 & S^i_{zz} \end{pmatrix} \tag{10. 20}$$

$$S_{i(1)} = \frac{\partial}{\partial t}\begin{pmatrix} S^i_{xx} & S^i_{xy} & 0 \\ S^i_{yx} & S^i_{yy} & 0 \\ 0 & 0 & S^i_{zz} \end{pmatrix} - \dot{\gamma}\begin{pmatrix} 2S^i_{yx} & S^i_{yy} & 0 \\ S^i_{yy} & 0 & 0 \\ 0 & 0 & 0 \end{pmatrix} \tag{10.21}$$

$$\left[\dot{\gamma} : S\right] = \dot{\gamma}\left(S^i_{xy} + S^i_{yx}\right) \tag{10.22}$$

$$tr\left(S \cdot S\right) = S^2_{xx} + S^2_{yy} + S^2_{zz} + 2S^i_{xy}S^i_{yx} \tag{10.23}$$

It is worth to mention that, since τ_{xy} and τ_{yx} components of the stress tensor are the same, S_{xy} and S_{yx} components of the orientation tensor S, are the same too. Now, introducing these definitions in the model, we obtain a system of five ordinary differential equations.

$$\frac{dS_{xx}}{dt} - 2\dot{\gamma}S_{xy} + 4\dot{\gamma}S_{xy}S_{xx} + \frac{3\alpha\Lambda^2}{\lambda_{0b}}\left(S^2_{xx} + S^2_{xy}\right) + \frac{1-\alpha-3\alpha\Lambda^4\left(S^2_{xx} + S^2_{yy} + S^2_{zz} + 2S^2_{xy}\right)}{\lambda_{0b}\Lambda^2}S_{xx} - \frac{1-\alpha}{3\lambda_{0b}\Lambda^2} = 0 \tag{10.24}$$

$$\frac{dS_{yy}}{dt} + 4\dot{\gamma}S_{xy}S_{yy} + \frac{3\alpha\Lambda^2}{\lambda_{0b}}\left(S^2_{yy} + S^2_{xy}\right) + \frac{1-\alpha-3\alpha\Lambda^4\left(S^2_{xx} + S^2_{yy} + S^2_{zz} + 2S^2_{xy}\right)}{\lambda_{0b}\Lambda^2}S_{yy} - \frac{1-\alpha}{3\lambda_{0b}\Lambda^2} = 0 \tag{10.25}$$

$$\frac{dS_{xy}}{dt} - \dot{\gamma}S_{yy} + 4\dot{\gamma}S^2_{xy} + \frac{3\alpha\Lambda^2}{\lambda_{0b}}\left(S_{xx} + S_{xy}\right)S_{xy} + \frac{1-\alpha-3\alpha\Lambda^4\left(S^2_{xx} + S^2_{yy} + S^2_{zz} + 2S^2_{xy}\right)}{\lambda_{0b}\Lambda^2}S_{xy} = 0 \tag{10.26}$$

$$\frac{dS_{zz}}{dt} + 4\dot{\gamma}S_{xy}S_{zz} + \frac{3\alpha\Lambda^2}{\lambda_{0b}}S^2_{zz} + \frac{1-\alpha-3\alpha\Lambda^4\left(S^2_{xx} + S^2_{yy} + S^2_{zz} + 2S^2_{xy}\right)}{\lambda_{0b}\Lambda^2}S_{zz} - \frac{1-\alpha}{3\lambda_{0b}\Lambda^2} = 0 \tag{10.27}$$

$$\frac{d\Lambda}{dt} = 2\dot{\gamma}S_{xy}\Lambda - \frac{1}{\lambda_s}(\Lambda - 1) \tag{10.28}$$

Solving simultaneously these differential equations, we obtain S_{xx}, S_{xy}, S_{yy}, S_{zz} and Λ as a function of time. Now, we introduce them to the components of the viscoelastic stress equations, given by:

$$\tau_{xx} = 3G_0\Lambda^2 S_{xx} - G_0 \tag{10.29}$$

$$\tau_{xy} = 3G_0\Lambda^2 S_{xy} - G_0 \tag{10.30}$$

$$\tau_{yy} = 3G_0\Lambda^2 S_{yy} - G_0 \tag{10.31}$$

$$\tau_{zz} = 3G_0\Lambda^2 S_{zz} - G_0 \tag{10.32}$$

Finally we obtain the transient shear viscosity using

$$\eta(\dot{\gamma},t) = \frac{\tau_{xy}}{\dot{\gamma}} \tag{10.33}$$

A FORTRAN – language code was developed in order to make the XPP model predictions. This code was validated using the experimental data presented by Verbeeten *et. al.* (2001). For further information about the code see Appendix B.

As mentioned in previous section, the same parameters used to fit the elongational viscosity are used to fit the shear viscosity. These parameters are presented in Table X.1. Figure X.6 show the XPP model's predictions in comparison to the experimental values for all the resins. It can be seen that the model predicts satisfactorily the shear viscosity too.

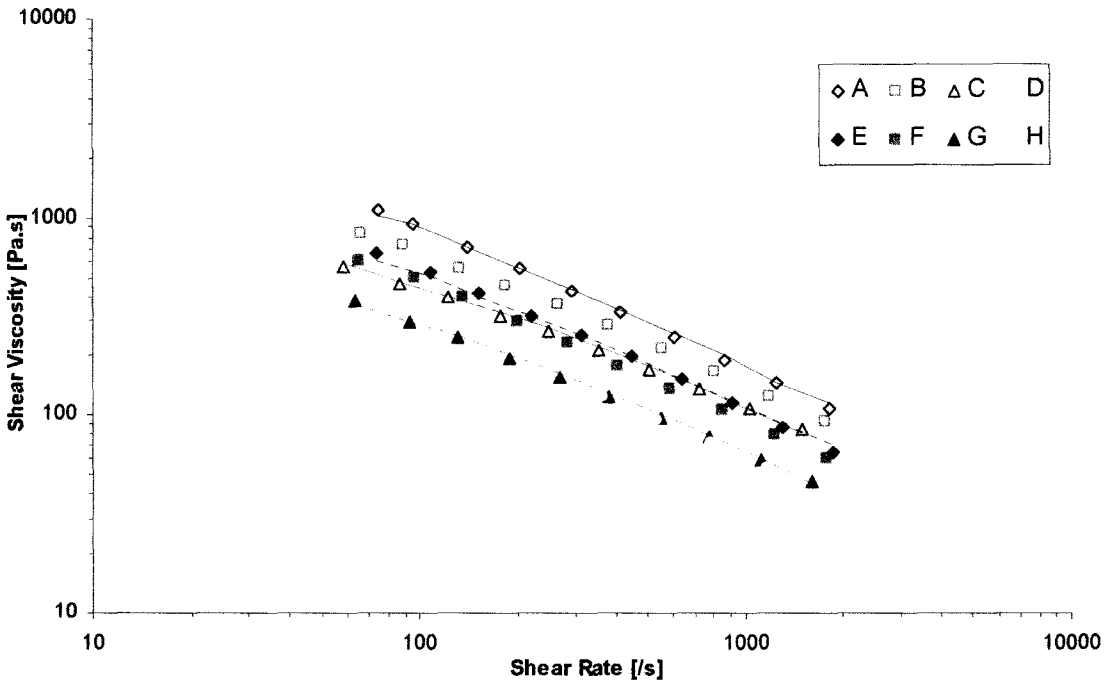

Figure X.6. XPP model's predictions and experimental shear viscosity for all the resins.

CHAPTER XI. Discussion of Results

A. Comparison of viscoelastic properties of syndio- and isotactic polypropylenes.

It is known that polypropylene is a polyolefin which monomer (propylene) consists of a methyl group attached to a vinyl group. The existence of this methyl group allows different stereochemical configurations of polypropylene (see Figure XI.1). Figure XI.1 (a) shows the atactic polypropylene. It contains the methyl groups placed randomly on both sides of the chain. On the other hand, Figure XI.1 (b) presents the isotactic polypropylene, which has all the methyl groups on one side of the chain. Finally, syndiotactic polypropylene, in which methyl groups come on alternating sides of the chain, is shown on Figure XI.1 (c).

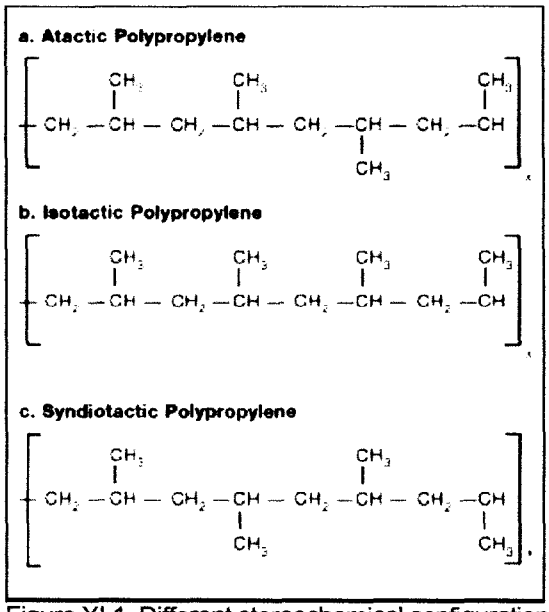

Figure XI.1. Different stereochemical configurations of polypropylene.

Recently, with the developing of the metallocene based catalysts, the syndiotactic polypropylene has become a very important material in plastic industry. Nevertheless, the research that has been carried out on this material is limited. In addition, the information with respect to the relation of the rheological properties and the esterochemical configuration of polypropylene is limited. However, from the experimental data obtained for this thesis, some interesting observations about the role of stereoregularity on the rheological behavior could be made.

Figure V.1 through Figure V.8 show the storage and loss moduli, including the crossover point, for all the resins. Even though the storage and loss moduli do not present any trend or significant difference between isotactic and syndiotactic resins; the crossover points do present some trends (see Table V.1).

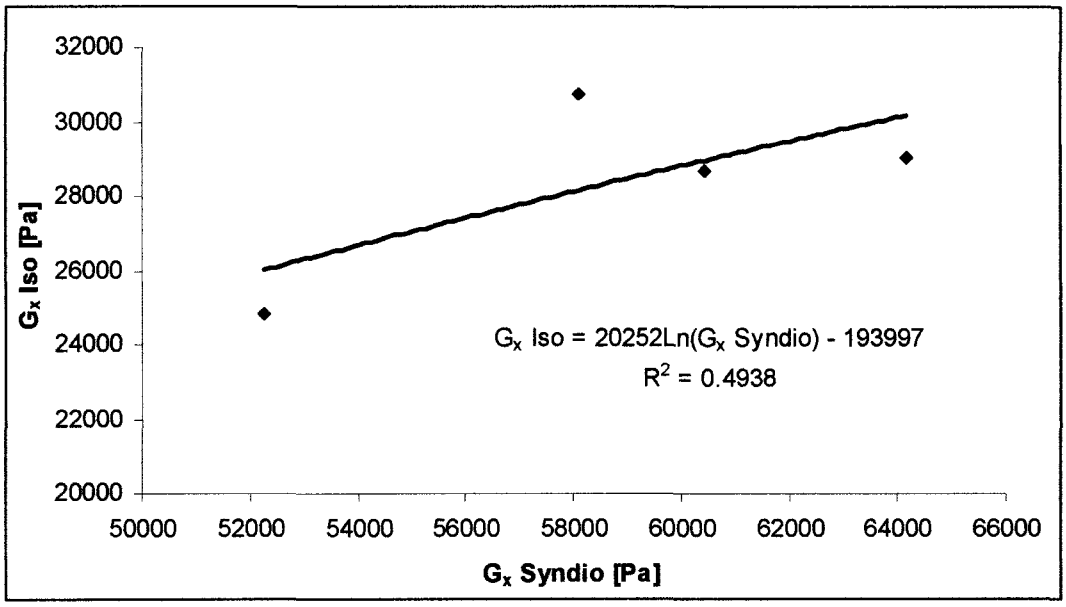

Figure XI.2. Relationship between isotactic and syndiotactic resins' crossover modulus.

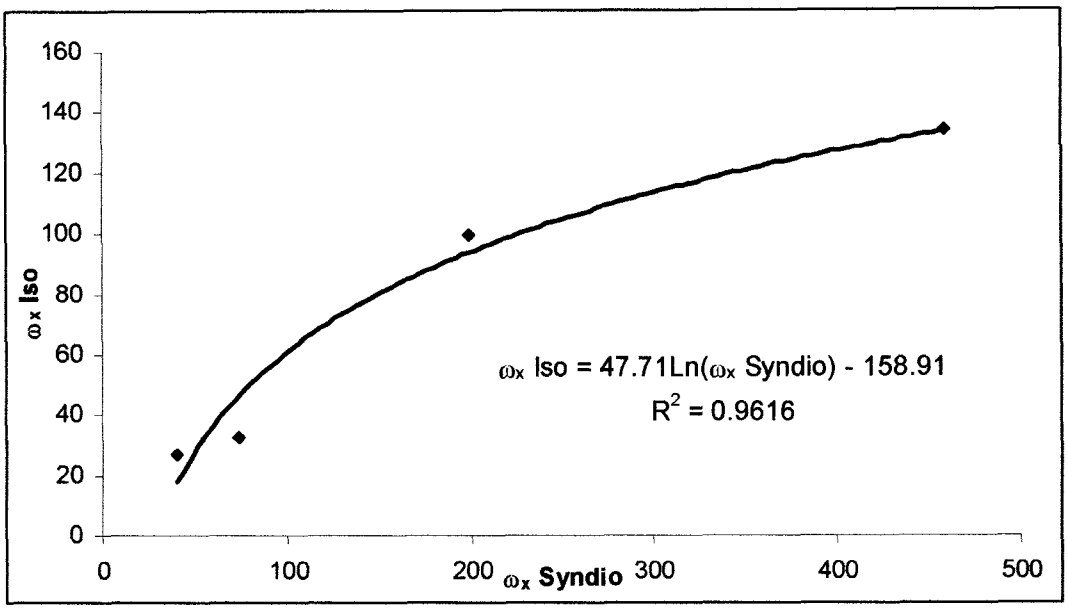

Figure XI.3. Relationship between isotactic and syndiotactic resins' crossover frequency.

Figure XI.2 and Figure XI.3 show the relationship between isotactic and syndiotactic resins' crossover modulus and frequency respectuvely. It is observed in these figures that there is a logarithmic functionality in both cases. In Figure XI.2 there is a poor fitting (R^2=0.4938); however, it can be seen that it is only one point (resin) out of trend (Resin F, approximatily +10%) . This suggests that there is a slight experimental error in this point. This is opinion is reinforce by Figure XI.3, because again Resin F point is slightly out of trend, although in this case the fitting is a lot better (R^2=0.9616).

On the hand, it was also found that there is a relationship between the crossover point and the MFI. Figure XI.4 and Figure XI.5 present the relationship between MFI and the crossover modulus and frequency respectively. It can be seen in these figures that isotactic and syndiotactic resins have a different behavior, but both present the same power law functionality. Figure XI.4 shows a poor fitting for isotactic resins because of a point out of trend. This point is again corresponding to Resin F, which confirms that it might be an experimental error in this point.

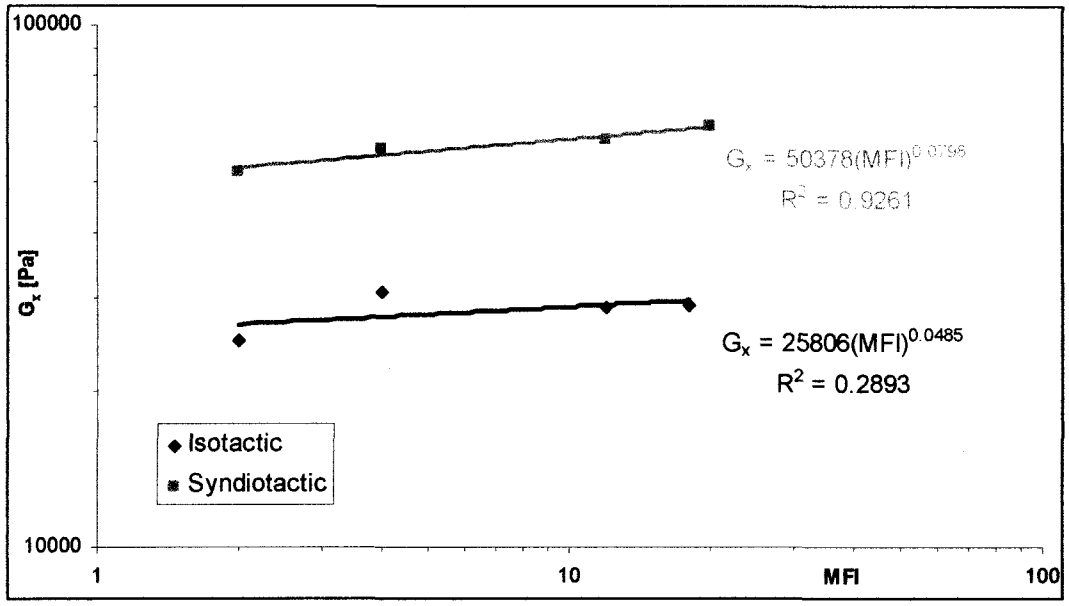

Figure XI.4. Relationship between crossover modulus and MFI.

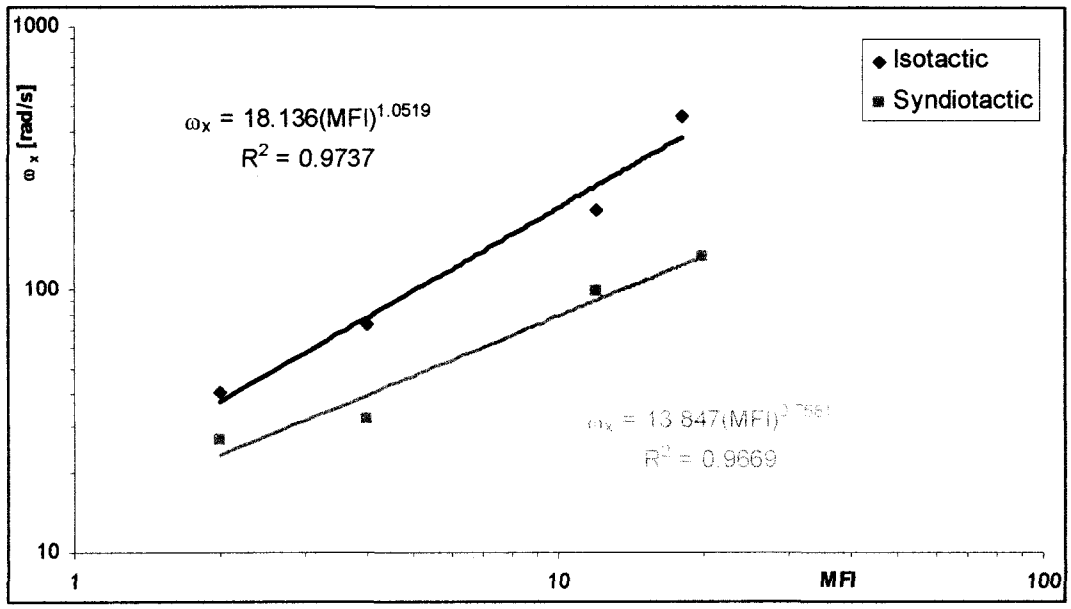

Figure XI.5. Relationship between crossover frequency and MFI.

On the other hand, it was also observed a trend in the horizontal activation energies, E_H (see Table V.5). It can be seen that the horizontal activation energies for syndiotactic resins are about 15 to 20% larger than those for isotactic resins. This difference was also observed by Eckstein *et. al.* (1997).

Another important observation is shown in Figure XI.6. It was observed that plotting the loss tangent (tan δ) versus the complex modulus (G*) at different temperatures, data of all isotactic resins superimpose in the same curve. The same happens with syndiotactic resins. These curves present power law functionalities, as it is presented in Figure XI.6.

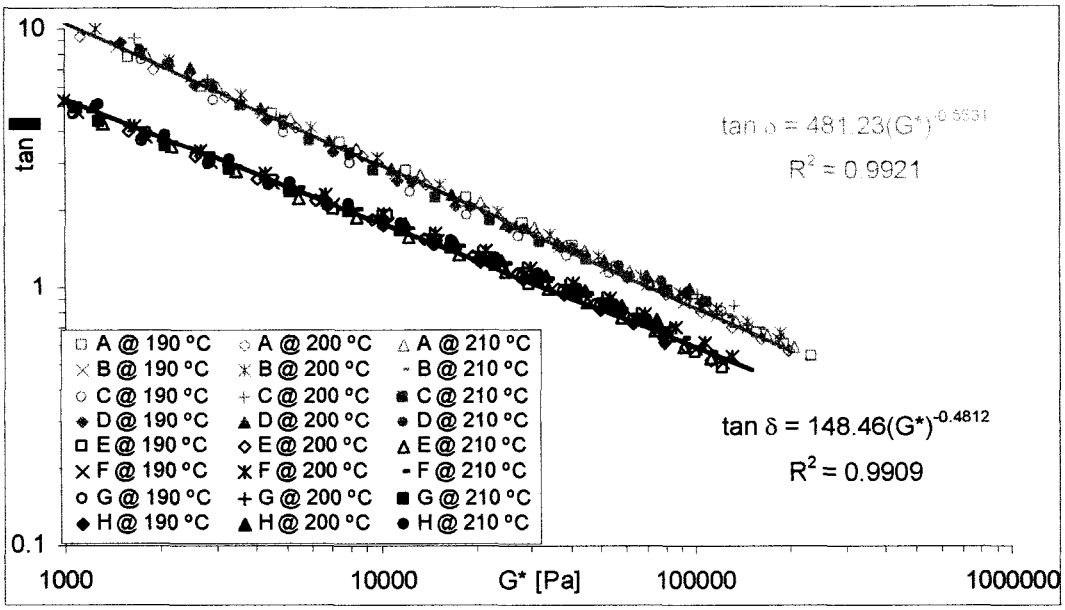

Figure XI.6. Loss tangent vs. complex modulus data at different temperatures for all resins.

Now then, capillary data shows similarities (in both, shear and elongational viscosity) between isotactic and syndiotactic resins with similar MFI (see Figure VI.3 and Figure VI.4). However, it is worth to mention that Trotoun ratio[4] (Figure VI.5) shows significantly differences, especially for high shear (extension) rates. Trouton ratio for isotactic resins is considerably higher than syndiotactic resin's ratio. Therefore, Trouton ratio seems like a good alternative to discriminate isotactic and syndiotactoc resins with the same MFI. However, it is recommended more experimental data to have more conclusive results.

[4] Ratio between elongational and shear vicosity.

In addition, creep and recovery data (Chapter VII) show that the strain under the same stress is very similar for both types of resins. Syndiotactic resins present a slightly higher strain. It can also be seen that there is a relationship between the MFI and the strain (creep compliance) as well as to the time that the applied stress lasts (creep time). Figure XI.7 shows that there is an exponential functionality between the maximum compliance (Jmax) and the MFI in spite of the type of resin. This figure also shows that the longer the creep time, the higher the maximum compliance.

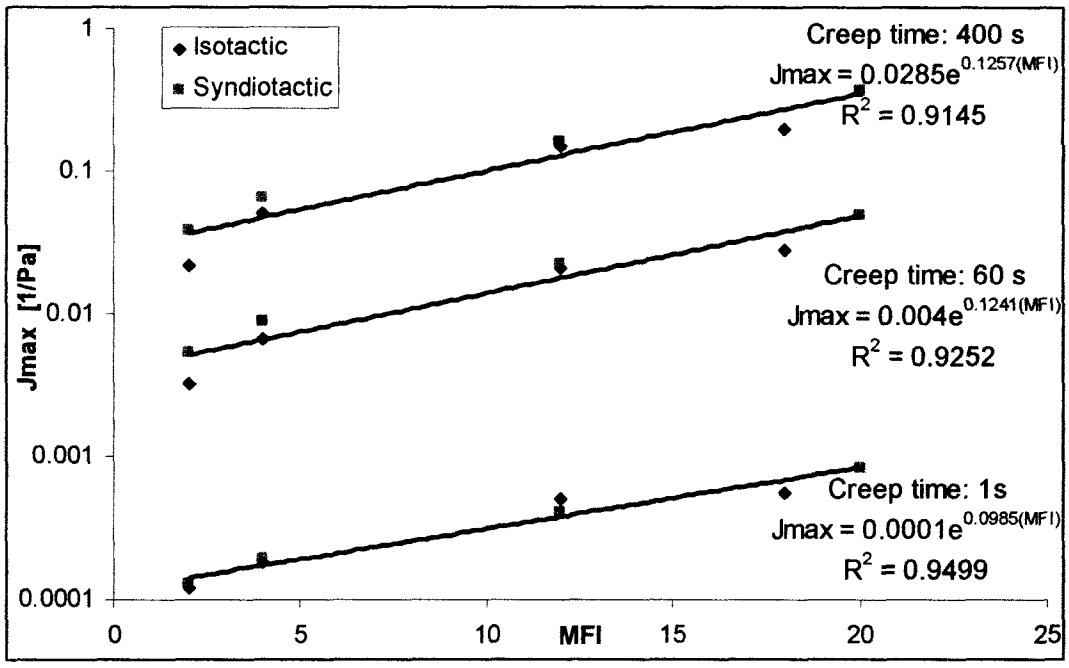

Figure XI.7. Creep compliance relation to MFI and creep time.

Now then, all the differences and similarities found in the rheological behavior must be related to molecular aspects related to the stereochemical configuration, because all the experimental conditions were the same for all the resins. It is thought that a syndiotactic molecule, because of the configuration of the methyl groups, might behave as a branched molecule. And then, it would produce more entanglements with its surrounding molecules, creating a more complex network than isotactic molecules.

In any case, experimental data show significant viscoelastic differences between these types of resins. However, it is recommended further analysis to evaluate these differences and relate them to fundamental aspects of the molecular conformation in the melt.

B. PTT Model

Since its publication (1977), PTT model has been used by many researchers to model viscoelastic properties. It is considered like one of the best costitutive equations. Besides, it has been used to model processing behavior in processes such as fiber spinning. (Phan Thien and Tanner, 1977; Phan Thien, 1978; Stephenson, 1986; Larson, 1987; Tanner, 1998; Tanner, 2003).

A sensibility analysis on the fitting parameters (elongational α and shear ξ) was done in order to observe the effect of the fitting parameters in the model output. The model output features evaluated were the zero-shear viscosity, η_0; the slope of the viscosity curve; the elongational viscosity at low extension rate, η_{e0}; and the slope of the elongational viscosity curve. Table XI.1 shows the results of this analysis. The arrow pointing upwards means that the model output increases, if pointing downwards the model output decreases and both means no change in the model output.

Table XI.1. PTT model parameters effects on the model output.

If the parameter increases	then η_0	then Slope η vs $\dot{\gamma}$	then η_{e0}	then Slope η_e vs $\dot{\varepsilon}$
α	↑↓	↑↓	↓	↑
ξ	↓	↑	↓	↓

It can be seen in Table XI.1 that the elongational parameter (α) does not have any effect on the steady state shear viscosity curve. Nevertheless, this parameter has a huge effect in the transient behavior of the shear viscosity. If this parameter is

equal to zero, the transient response of the model will be an oscillatory curve that will reach the same steady state value. On the other hand, it is shown in this table that the shear parameter (ξ) has a significant effect on the elongational viscosity curve, which is contradictory with its name.

In any case, in Chapter VIII the PTT model was used to fit experimental data of the isotactic and syndiotactic polypropylene resins. In Table VIII.1 are presented the fitting parameters for all the resins. Mier (2000) found an empirical relationship between the shear and the elongational parameter using metallocene-based isotactic polypropylene resins. This relationship was a power law function; however, this function do not applied for the resins under study as it is shown in Figure XI.8.

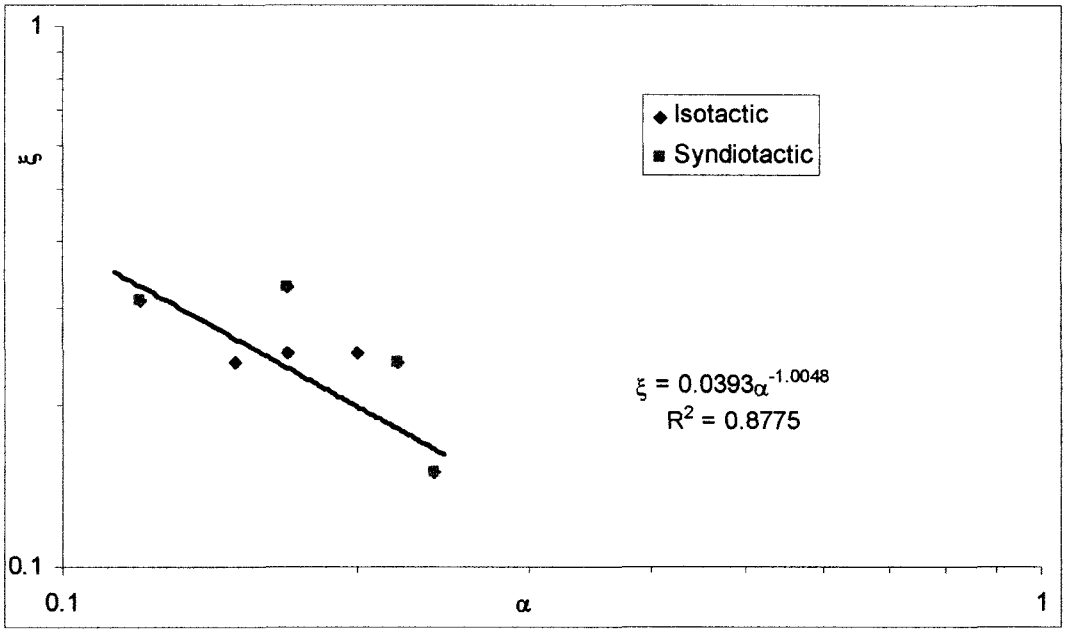

Figure XI.8. Relationship between PTT model's shear and elongational parameters.

Nevertheless, practical empirical relationships were found for the fitting parameters. The elongational parameter (α) was found to be related to percentage of xylene soluble (XS) as shown in Figure XI.9. It worth to mention that

syndiotactic and isotactic resins present the same negative exponential functionality, but with different function parameters.

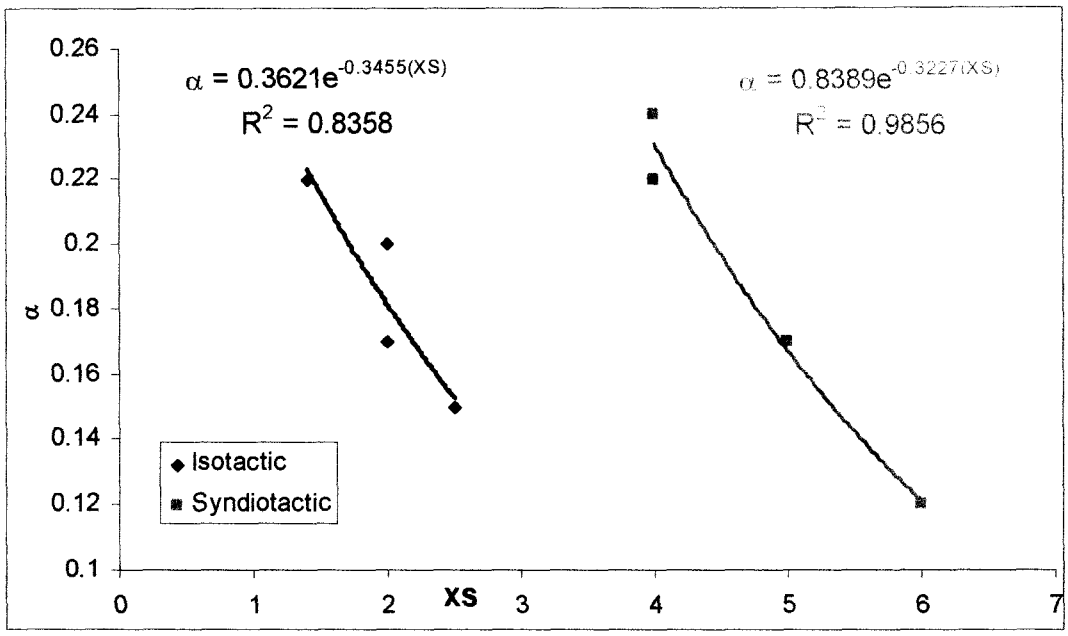

Figure XI.9. Relationship between elongational parameter and the percentage of xylene solubles.

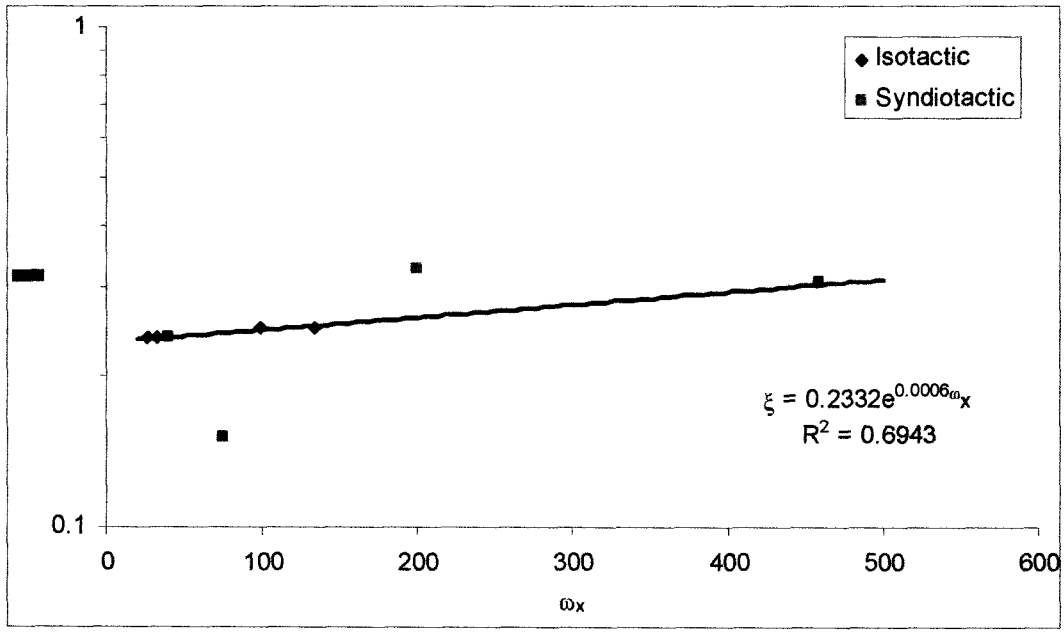

Figure XI.10. Relationship between shear parameter and the crossover frequency.

Now then, the shear parameter (ξ) presents an exponential functionality with respect to the crossover frequency (ω_x). In this case, both resins present the exact same functionality, but two points corresponding to syndiotactic resins are out of trend. This deviation from the trend might be related to the poor fitting of the model for the syndiotactic resins. It worth to remember that the model fits excellently the isotactic resins' data; however, it fails to predict accurately the syndiotactic resins' experimental data as shown in Chapter VIII.

Since the PTT model fails to predict accurately the elongational viscosity of the syndiotactic resins, a modification was proposed in Chapter IX. The same parametric analysis done to the PTT model (see Table XI.1) was done to the modified PTT model. Table XI.2 shows the results of this analysis.

Table XI.2. Modified PTT model parameter effects on the model output.

If the parameter increases	then η_0	then Slope η vs $\dot{\gamma}$	then η_{e0}	then Slope η_e vs $\dot{\varepsilon}$
A	-	-	↑↓	↑
B	-	-	↑	↓
C	↓	↑	-	-

The modification proposed to the model gives a better fitting of the experimental data for both, isotactic and syndiotactic resins, as shown in Chapter IX. With the modification, now there are three parameters. There are two elongational parameter (A, B) and one shear parameter (C). Even though it seems like a more complex constitutive equation because of the number of parameters, it is not. The elongational parameters are only used in predictions of the elongational flow, while the shear parameter is only used to fit shear flow experimental data.

Now then, since A, B and C parameters control the model predictions; it was thought that these adjustable parameters should be related to molecular aspects and that there is a procedure to determine these parameters other than the empiric fitting process.

It was found that these parameters are related with standard properties and molecular aspects. It was observed that the shear parameter (C) is related to MFI as shown in Figure XI.11. This figure shows that for resin with similar MFI, the shear parameter C is very similar too. The slight differences could be due to the experimental error in the MFI determination. However, no quantitative relationship was found.

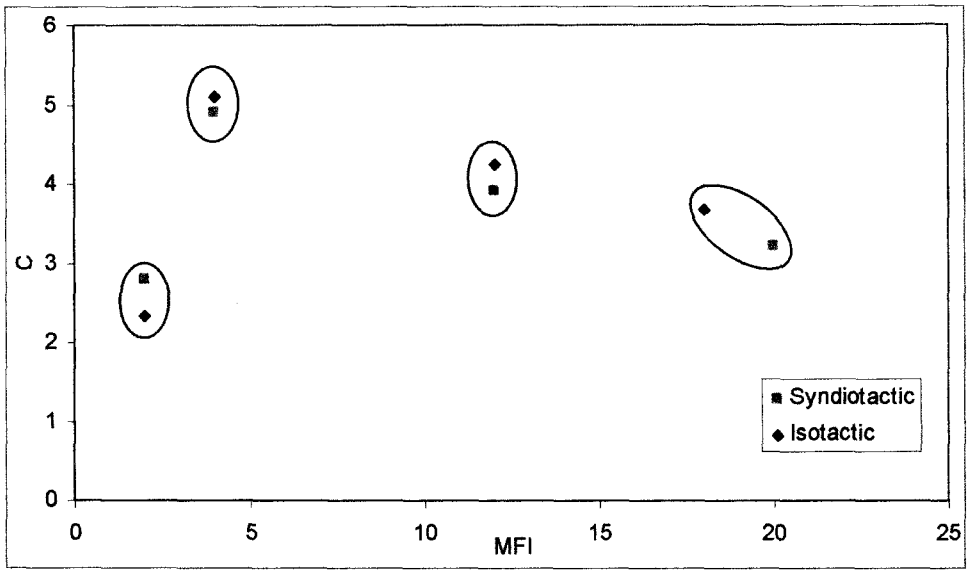

Figure XI.11. Relationship between modified PTT model shear parameter C and the MFI.

Nonetheless, it was found that this parameter is related to the average number of entanglements (Mw/Me)[5]. Figure XI.12 shows a logarithmic functionality between shear parameter C and the average number of junctions Mw/Me. Then, this might imply that the number of junctions in the melt network is the determinant issue in shear flow for both, isotactic and syndiotactic resins. Anyway, it is recommended further study to have more conclusive results.

---

[5] Me refers to the average molecular weight between entanglements, then Mw/Me is the average number of entanglements. Me is obtain using the plateau modulus definition, $G_N^0 = \frac{\rho RT}{Me}$. The plateau modulus can be obtained from the frequency where the minimum of the loss tangent (tan δ) is located, $G_N^0 = G'(\varpi)_{\tan\delta \min}$ (Eckstein, 1998). The theoretical density of polypropylene at 200 °C was found to be 0.7617 gr/cm^3 (Bicerano, 1993).

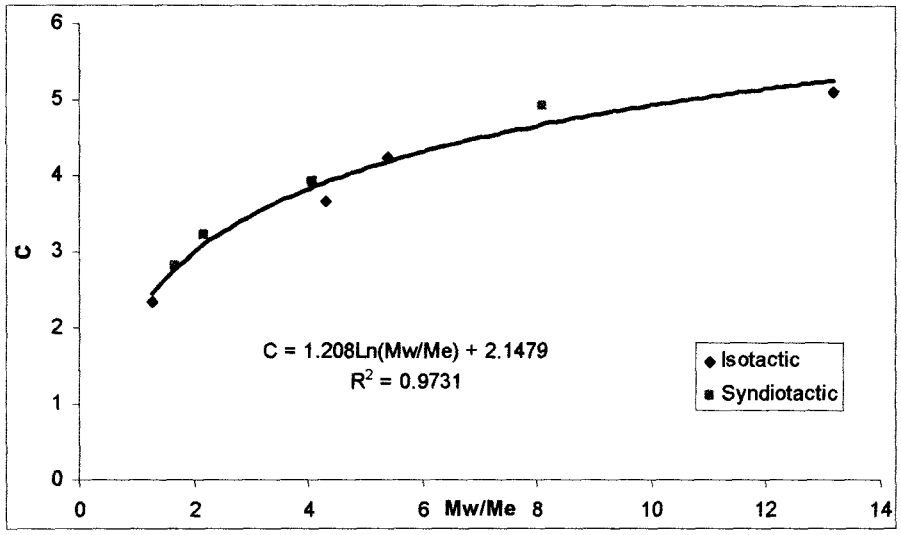

Figure XI.12. Relationship between modified PTT model shear parameter C and Mw/Me ratio.

On the other hand, the elongational parameter B was found to be related with the percentage of xylene soluble (XS) and to the third moment of the molecular weight distribution, Mz. Even though the relationship with the percentage of xylene solubles (XS) gives a better correlation coefficient (R^2), both could be useful for further analysis of the model. The relationship between B and XS is linear, while B presents a logarithmic functionality with respect to Mz as it is shown in Figure XI.13 and Figure XI.14 respectively.

Regarding the relationship to XS, it can be seen that a higher value of XS gives a lower value of B (which means that a higher value of XS gives a lower value of elongational viscosity). This behavior can be explained considering the low molecular weight species. It is thought that shorter chains (low molecular weight) might act like a "lubricator" between the longer chains (high molecular weight) and help them flow, which means a lower stress and consequently a lower viscosity.

On the other hand, the relationship found between B and Mz indicates that a higher value of Mz gives a higher value of B (which means a higher value of elongational viscosity). It is known that Mz is related to the longest chains in the melt and it is

thought that these chains, because of their size, present more entanglements and impediments to flow, and then a higher elongational viscosity.

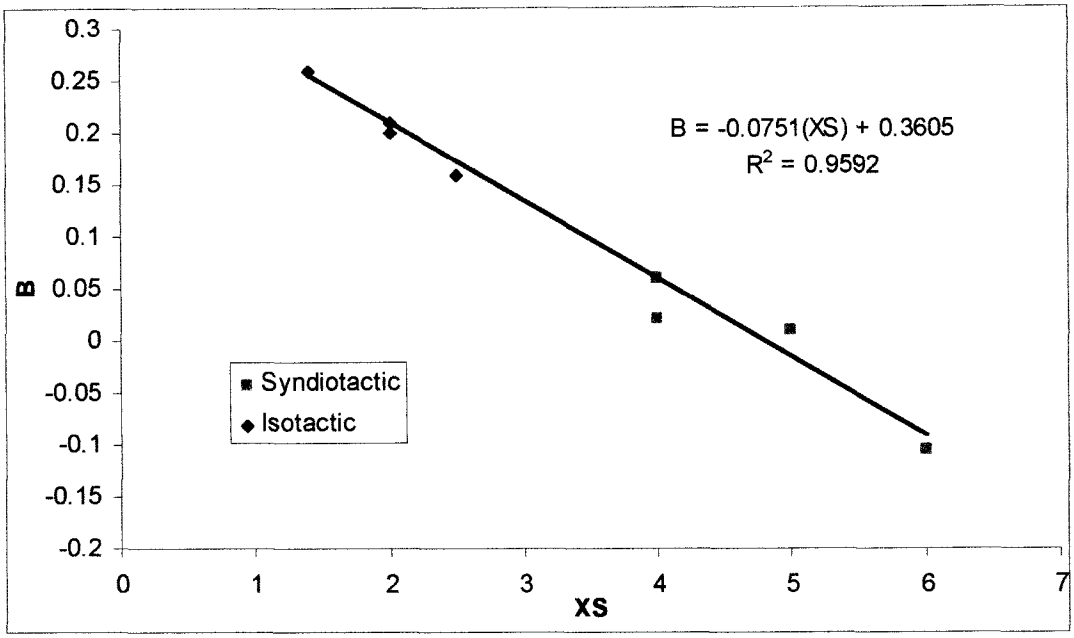

Figure XI.13. Relationship between modified PTT model elongational parameter B and the percentage of xylene soluble.

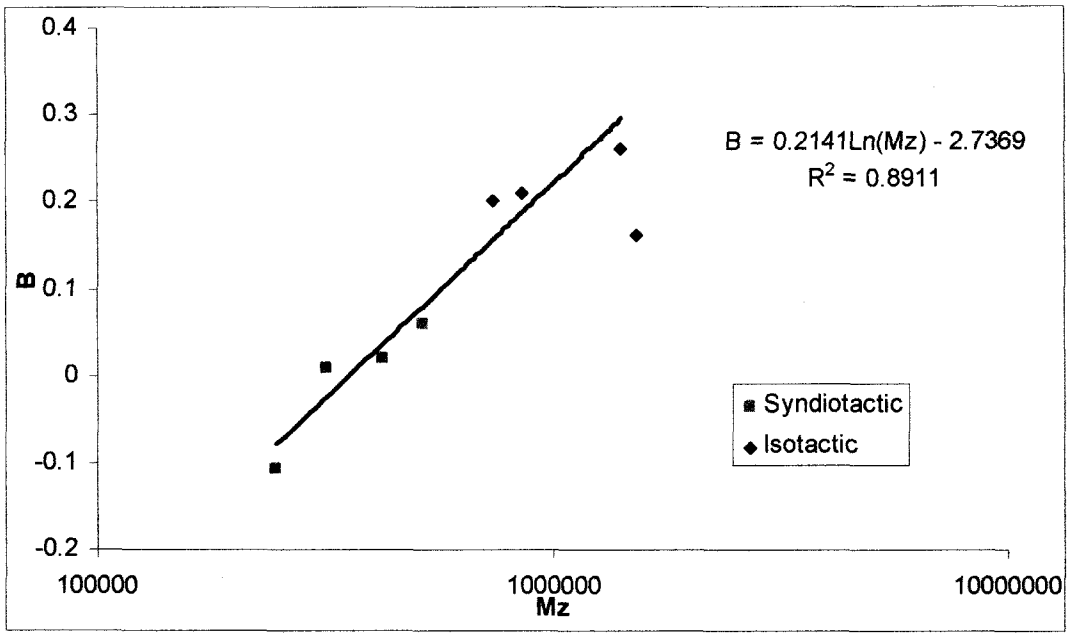

Figure XI.14. Relationship between modified PTT model elongational parameter B and molecular weight average Mz.

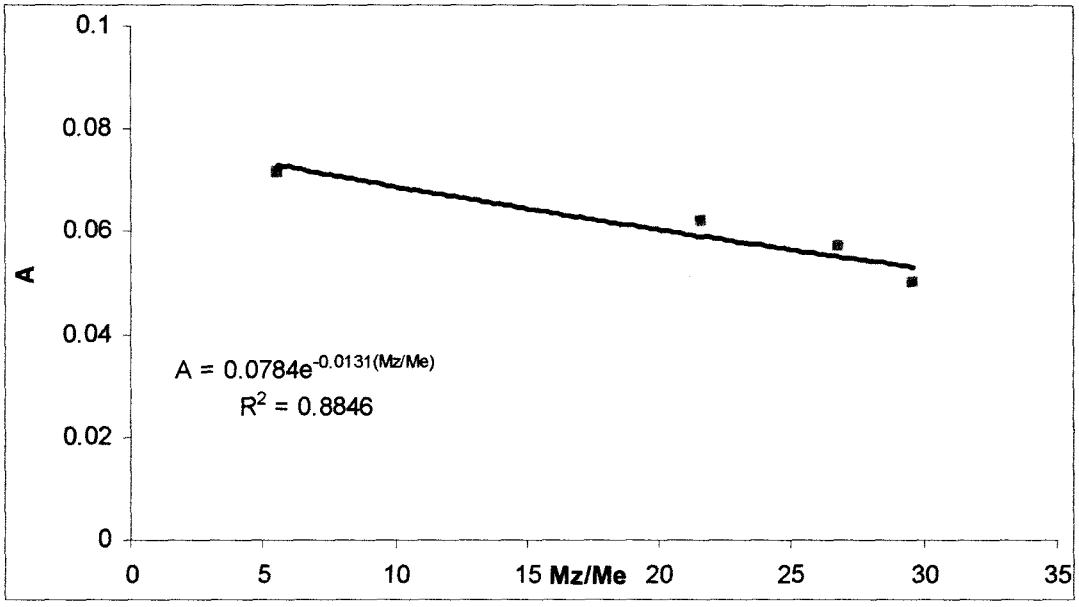

Figure XI.15. Relationship between modified PTT model elongational parameter A and Mz/Me ratio.

Finally, the elongational parameter A was found to be related, with an exponential functionality to the Mz/Me ratio as it is presented in Figure XI.15. The Mz/Me ratio is related to the average number of junctions of the longest chains in the polymer melts. Then, it can be conclude that the elongational rheological properties are related to the longest chains in the melt.

It can be seen that Mz, Me and Mw result to be the important issues in the determination of the fitting parameters of the modified PTT model. This suggests that with an accurate determination of these molecular aspects, the shear and elongational viscosity could be determined easily using this new model.

On the other hand, since these molecular weight distribution features are the most important factors in the determination of the m-PTT model parameters, it is thought that the viscoelastic response of a material is determined by the average number of entanglements (Mw/Me) and the number of entanglements in the longest chains (Mz/Me).

Therefore, it is thought that an accurate determination of the number of entanglements in a polymer melt could give a lot of information about the rheological response of the material.

In addition, it can be seen that the relationships presented between the parameters and the molecular features are logarithmic and exponential functions. It is thought that these functions could be related between them and that a new function could be obtained.

All this could be explained with the findings obtained during the simulation of the random growth of polymers chains using random and self-avoiding walks (see Chapter XII). It was found that the number of junctions between two chains presents an exponential functionality with respect to the distance between them at their origin (this distance was taken to be the active sites in the catalysis system).

It worth to mention that this function is very similar to the PTT model's rate of creation and destruction of junctions, which suggest that there is a relationship between the catalysis system and the rheological behavior. Such relationship might be implied in the relationships presented before, but further study is needed to make conclusions.

C. XPP Model

In Chapter X, the XPP model was used to predict shear and elongational viscosity of the resins under study. The XPP model, based on the Pom-Pom model introduce by McLeish and Larson (1998), is considered a breakthrough in the field of viscoelastic constitutive equations. The XPP model was created to predict the viscoelastic behavior of highly entangled polymer melts. It is based on the tube model (Doi-Edwards) and a simplified topology of branched molecules (pom-pom molecule).

According to several authors (Blackwell, 2000; Chodankar, 2001; Graham, 2001; Verbeeten, 2002) the Pom-Pom and XPP models accomplish a correct nonlinear behavior in both elongation and shear flow. It gives excellent results in HDPE and LDPE resins; however, it hadn't been used in polypropylene resins before.

The application of this model to the polypropylene resins gives a good fitting of the viscoelastic behavior. Nonetheless, it is worth to mention that the fitting process is complicated because the fitting parameters must be fit for each relaxation element. Then, there are too many fitting parameters, which means that the model is not that robust.

On the other hand, the shear viscosity is predicted (using the same parameters) after fitting the elongational viscosity first. This is not what we are looking for. It is needed a way to found elongational viscosity, but this model needs the experimental data to make the fitting, and then the shear viscosity is calculated. The shear viscosity is easy to obtain, then it would be better to fit the experimental data of the shear viscosity and then predict the elongational viscosity, but this can't be done with this model.

The fitting parameters are related to molecular aspects according to the model creator (Verbeeten, 2001). The q parameter is the number of dangling arms in a pom-pom molecule and α is a measure of anisotropy in the material; however, no relationship between the parameters and the standard properties or molecular aspects was found.

In any case, a sensibility analysis on the fitting parameters, similar to the one done to the PTT and modified PTT models, was done. Table XI.3 shows the results of this analysis. It worth to remember that the parameters must be fitted for each relaxation element, and then the information in this table is the general effect of the parameter in the model output.

Table XI.3. XPP model parameter effects on the model output.

If the parameter increases	then η_0	then Slope η vs $\dot{\gamma}$	then η_{e0}	then Slope η_e vs $\dot{\varepsilon}$
q	↑	↑↓	↑↓	↓
α	↑↓	↑	↓	↑↓

It would be really helpful to develop a practical method to make the fitting of the XPP model, because it is very complicated to fit that many parameters. Actually, it is thought that there could be some relationships between the parameters, which would reduce the number of fitting parameters and make easier and more useful this model.

D. Constitutive Equations Comparison

In this section a comparative analysis of the constitutive equations used in this thesis is presented. PTT and XPP model were used in Chapters VIII and X respectively. In addition, a modified PTT was proposed and evaluated in Chapter IX. Table XI.4 shows a summary of each constitutive equation. On the other hand, Table XI.5 presents the most important advantages and disadvantages of the models under study.

Figure XI.16 shows the three models' predictions of elongational viscosity for syndiotactic resin A. It can be seen, that PTT model fails to predict accurately this propertie, while mPTT and XPP models give good predictions. Since XPP model's fitting process and mathematical computations were found to be more complicated, the modified PTT model (mPTT) seems to be an excellent alternative in constitutive modeling. This new model predicts accurately shear and elongational properties and its application is very easy. Even though, it has to be fitted twice, one for shear and another for elongational; it does not represent any difficulty, because the fitting process is very easy. In addition, the fitting parameters are related to molecular aspects, which could help in the fitting process.

Table XI.4. Comparison of the constitutive equations used in this thesis.

	PTT	m-PTT	XPP
Constitutive equation	**Equations 8.1, 8.2 and 8.5**	**Equations 9.1, 9.2, 9.3 and 9.4**	**Equations 10.1, 10.2, 10.3, 10.4 and 10.5**
Development	Molecular network theory which considers that the number of subunits between two junctions has a distribution giving multiple relaxation times. (Phan Thien and Tanner, 1977)	Semiempirical modification of the PTT model.	Tube model theory and a simplified topology of branched molecules. (Verbeeten, 2001)
Parameters	**Shear parameter (ξ)** **Elongational parameter (α)**	**Shear parameter (C)** **Elongational parameters (A and B)**	**Number of dangling arms (q)** **Stretch relaxation time (λ_{0s})** **Measurement of anisotropy (α)**
Fitting process	The shear paramters is obtained from steady state shear viscosity data. Afterwards, the α is used to fit the elongational viscosity.	Different fitting processes are made for shear and elongational flow. On one hand, C is used to fit shear viscosity and on the other hand, A and B fit the elongational viscosity.	First, the elongational viscosity must be fitted, and then, using the parameters found in the fitting, the shear viscosity is fitted. The parameters must be fitted for each relaxation elements, then the actual number of fitting parameters is 3 x N, where N is the number of relaxation elements.
Major differences	**1. Based on the idea that the elastic energy of the network strand is important (Phan Thien and Tanner, 1977).** **2. The shear parameter (ξ) has a significant effect on the elongational viscosity.** **3. Poor fitting in syndiotactic resins' data.**	**1. The shear parameter is set to zero and the elonation parameter is a function of the extension rate.** **2. Complete different parameters for each type of flow. A and B are not used in shear flow, while C is not used in elongation.** **3. Excellent fitting of the syndiotactic resins.**	**1. Developed for high branched polymers such as LDPE melts.** **2. Modification of the orientation and stretch in the original Pom-Pom model (McLeish, 1998).** **3. Good fitting in syndiotactic resins' experimental dat.**
Remarks	1. Predictions are in good agreement for isotactic resins. 2. It had been used by other researchers to predict processing characteristics with statisfactory results. (Mier, 2000) 3. The shear parameter was found to cause some problems such as the violation of the Lodge-Meissner relation (Larson, 1987)	1. Predictions are in excellent agreement to experimental data. 2. Fitting parameters are related to standard quality properties and molecular weight distribution aspects. 3. Further study is recommended.	1. Predictions are in good agreement for both types of resins. 2. There are too many fitting parameters, which implies that the model is not robust. 3. Since it is a relatively new model (2001), further study is recommended.

Table XI.5. Advantages and disadvantages of the constitutive equations used in this thesis.

Model	Advantages	Disadvantages
PTT	⇨ The mathematical computations needed in the solving of the model are fairly simple. ⇨ The fitting process is simple. ⇨ Predictions are in good agreement to experimental data.	⇨ Poor fitting for syndiotactic resins. ⇨ Poor fitting for high branched polymers (Larson, 1987; McLeish, 1998, Verbeeten, 2001) ⇨ Violation of the Lodge-Meissner relationship (Larson, 1987; Stephenson, 1989).
m-PTT	⇨ Excellent predictions in shear and shear-free flow for syndio- and isotactic resins. ⇨ Easy mathematical computations. ⇨ The fitting process is very simple. ⇨ Fitting parameters are related to molecular aspects like Mz and Me.	⇨ Different fittings must be done for elongation and shear flow. ⇨ Further study is needed
XPP	⇨ A correct viscoelastic prediction of high branched polymers without the drawbacks of the original Pom-Pom model (Verbeeten, 2001). ⇨ The same fitting parameters are used for elongation and shear flow.	⇨ There are too many parameters to fit, which makes this model not that robust. ⇨ The fitting process is very complicated. ⇨ The elongational viscosity has to be fitted first. ⇨ The mathematical computations are not that simple.

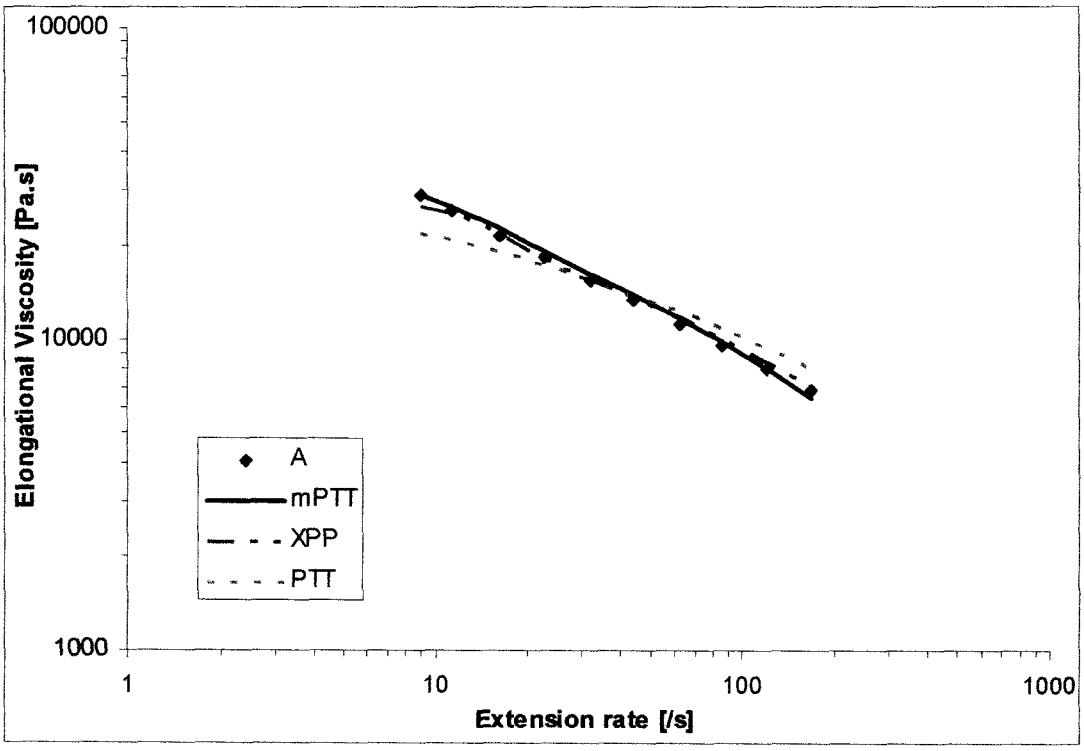

Figure XI.16. Experimental elongational viscosity and mPTT, XPP and PTT models' predictions for syndiotactic resins A.

E. Other Practical Relationships

The purpose of this section is to present several empirical relationships that might be useful in further studies. Such relationships can be used as an alternative practical tool to determine properties from other know data. However, all the relationships presented still need to be tested using more resins in order to verify the relation. These relationships hold for 200 °C, which is the temperature at which rheological tests were done.

Figure XI.17 and Figure XI.18 present relationships of the MFI. As it was expected, the MFI was found to be related to the zero shear viscosity and the molecular weight average Mw. In both cases, it can be seen a power law functionality with good correlation coefficients ($R^2 > 0.9$). It is worth to mention that in both cases, syndiotactic and isotactic resins present different function parameters.

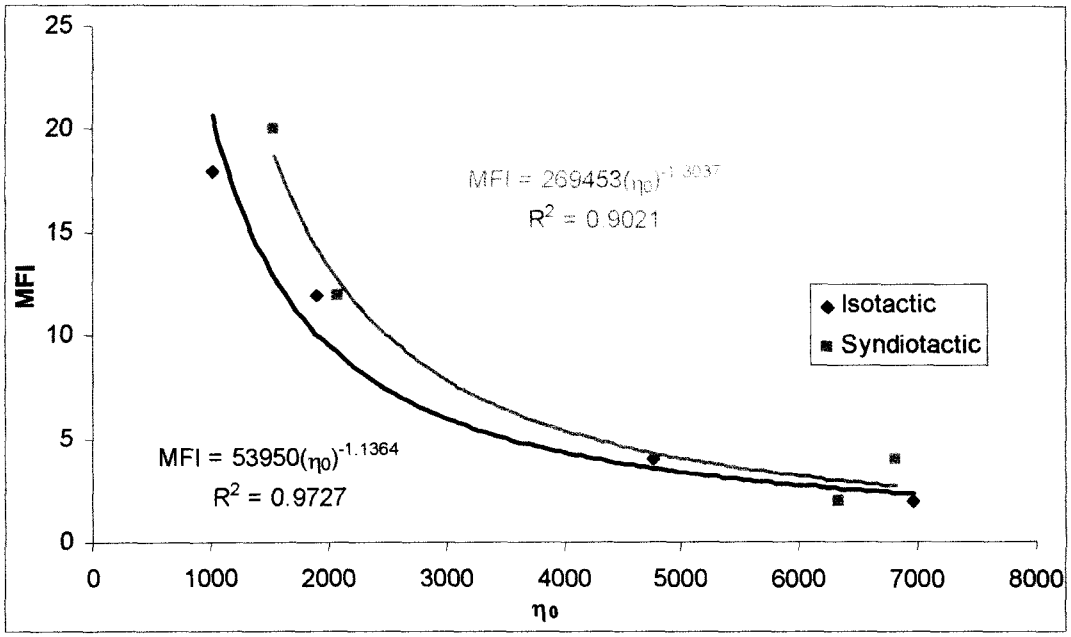

Figure XI.17. Relationship between MFI and Zero-shear viscosity.

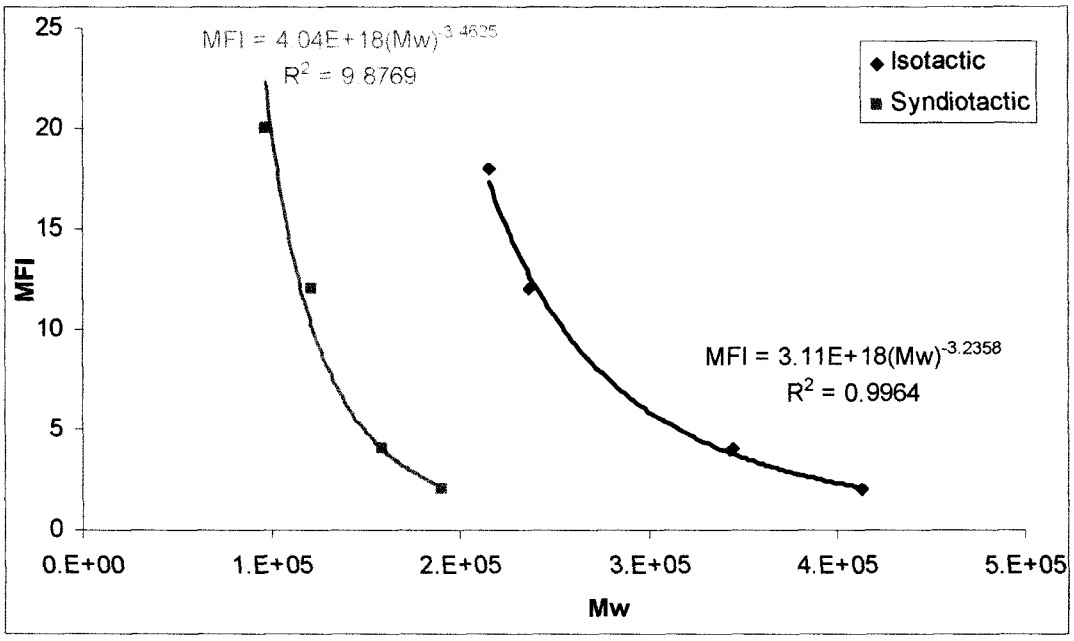

Figure XI.18. Relationship between MFI and the molecular weight average Mw.

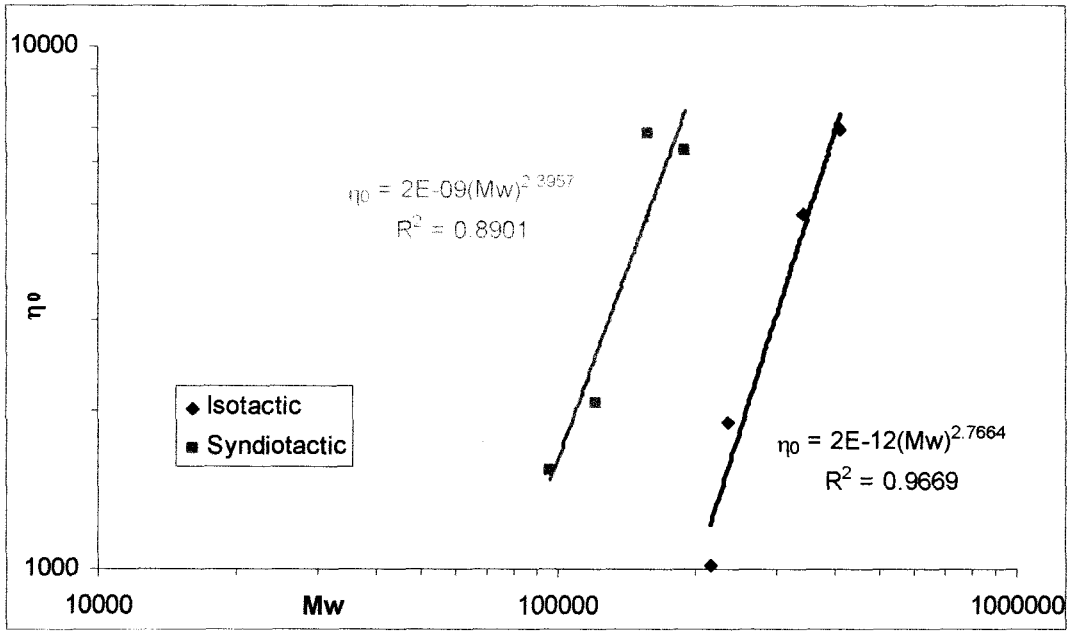

Figure XI.19. Relationship between the zero-shear viscosity (@ 200 °C) and the molecular weight average Mw.

Now then, Figure XI.19 presents the relationship between the zero shear viscosity and the molecular weight average Mw. As it was expected, the zero shear viscosity depends on power law function with respect to the molecular weight

average Mw. It can be seen that the power law index is lower than 3.4, which is mentioned in the literature (Bird, 1987; Dealy, 1990) as the power law index of this relationship. However, Figure XI.20 shows the same relationship, but with the zero shear viscosity shifted[6] to 230 °C. In this case, the power law index is very similar to 3.4 which is in agreement with the theory.

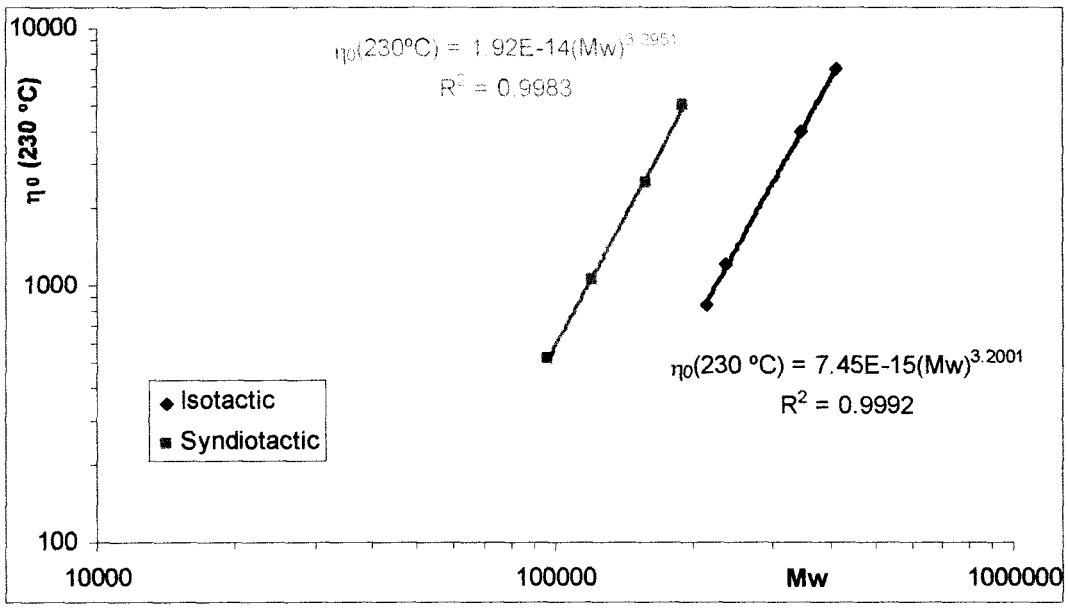

Figure XI.20. Relationship between the zero-shear viscosity shifted to 230 °C and the molecular weight average Mw.

On the other hand, the zero shear viscosity was found to be related to the crossover frequency (ω_x). As well as the zero shear viscosity, the molecular weigh average Mw and Mz were also found to be related to the crossover frequency. Figure XI.21, Figure XI.22 and Figure XI.23 present these relationships.

[6] $\eta_0(200°C) = \eta_0(230°C) \cdot a_T$

a_T is found using the Arhenius type equation (Mavridis, 1992) and the E_H found in the TTS (see Table V.5).

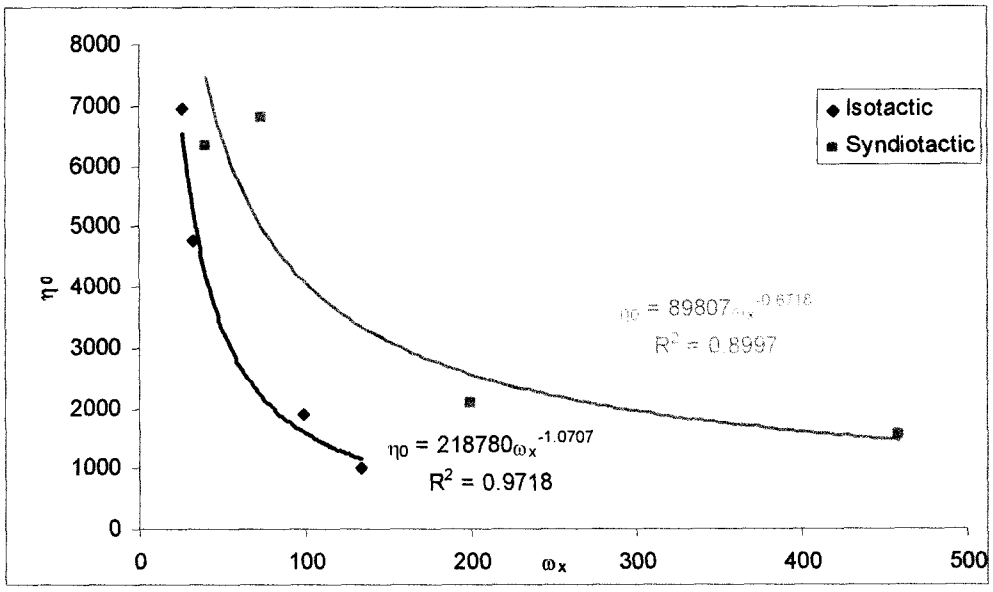

Figure XI.21. Relationship between the zero-shear viscosity and the crossover frequency.

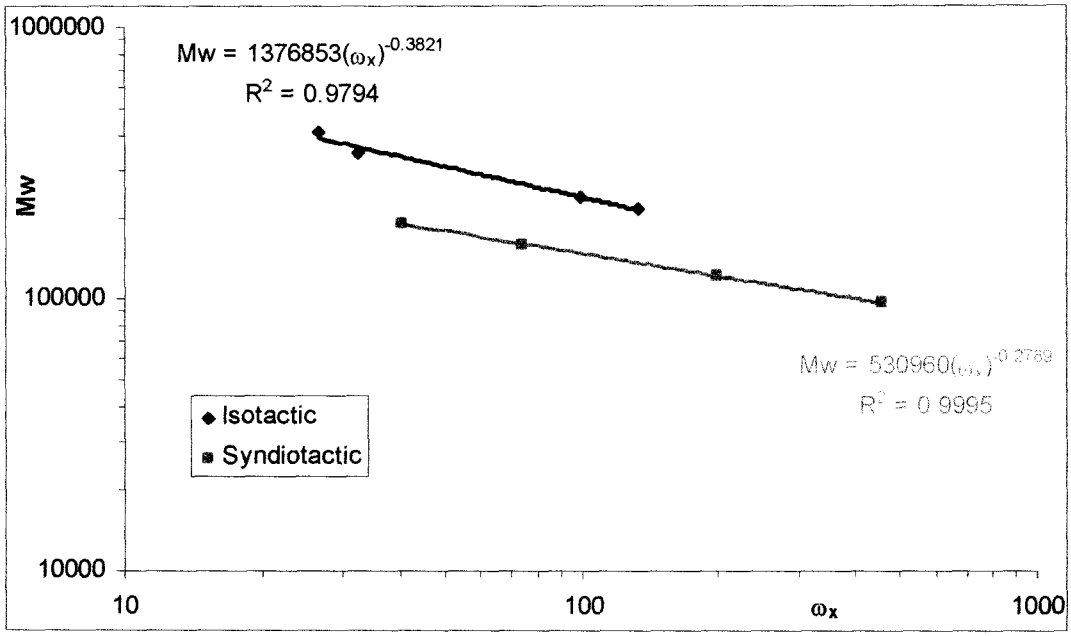

Figure XI.22. Relationship between the molecular weight average Mw and the crossover frequency.

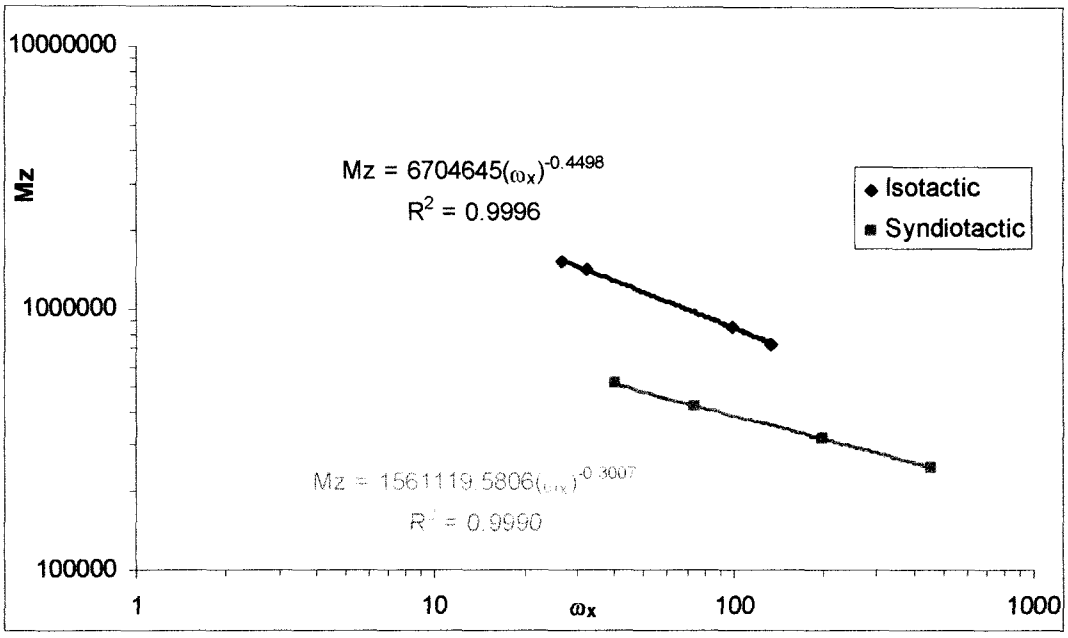

Figure XI.23. Relationship between the molecular weight average Mz and the crossover frequency.

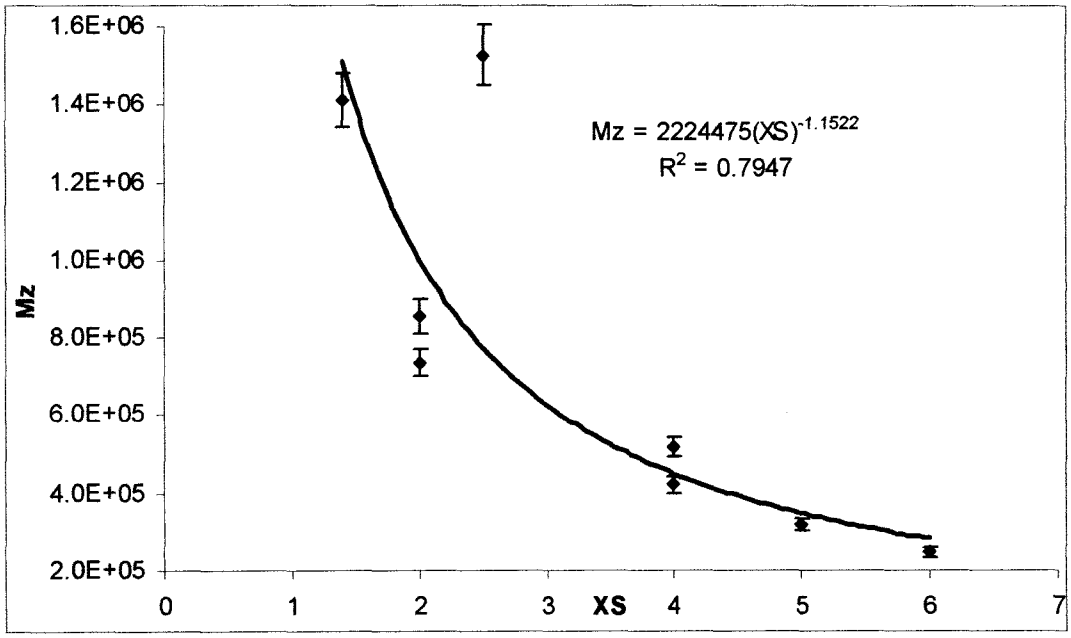

Figure XI.24. Relationship between the molecular weight average Mz and the percentage of soluble XS.

Otherwise, the percentage of xylene soluble (XS) was found to be related some molecular aspects, such as Mz and Mw/Mn, Mz/Mw and Mz/Mn ratios. These relationships are presented in Figure XI.24 through Figure XI.27.

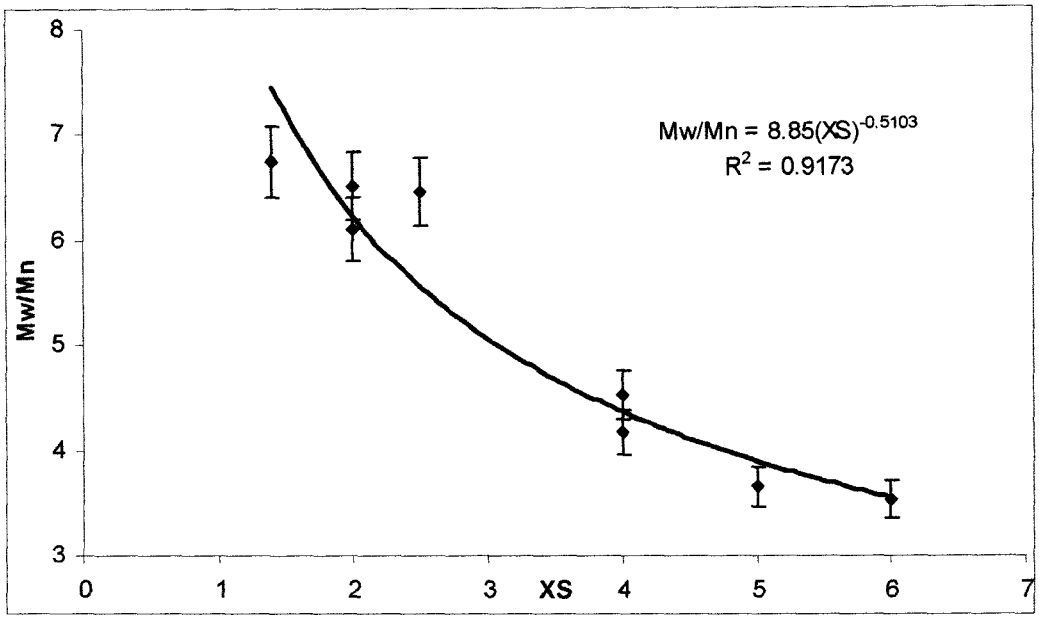

Figure XI.25. Relationship between the polidispersity Mw/Mn and the percentage of soluble XS

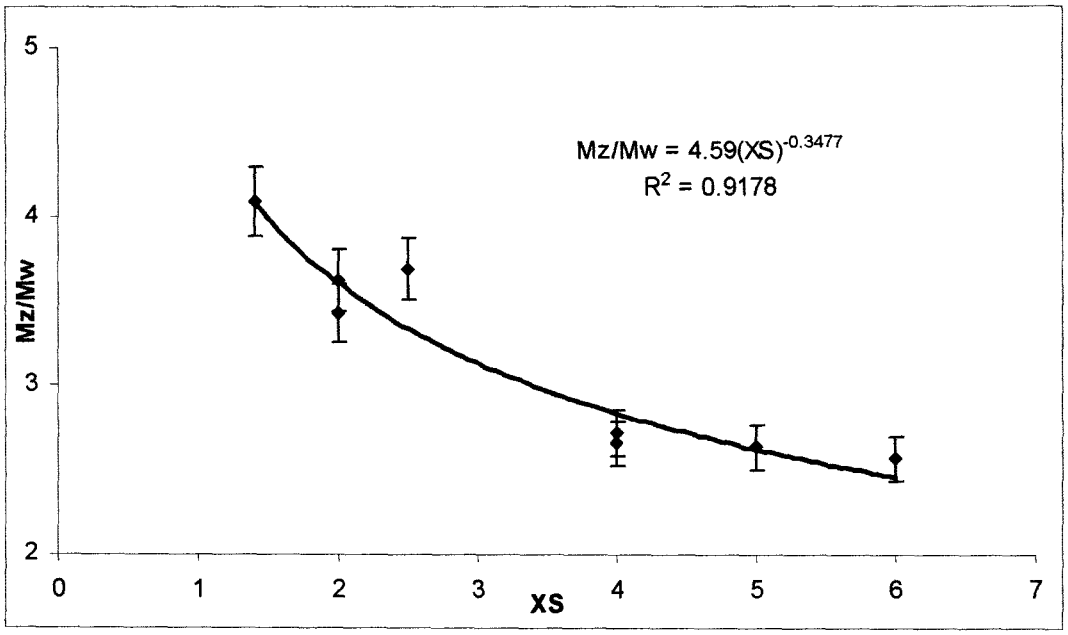

Figure XI.26. Relationship between Mz/Mw ratio and the percentage of soluble XS

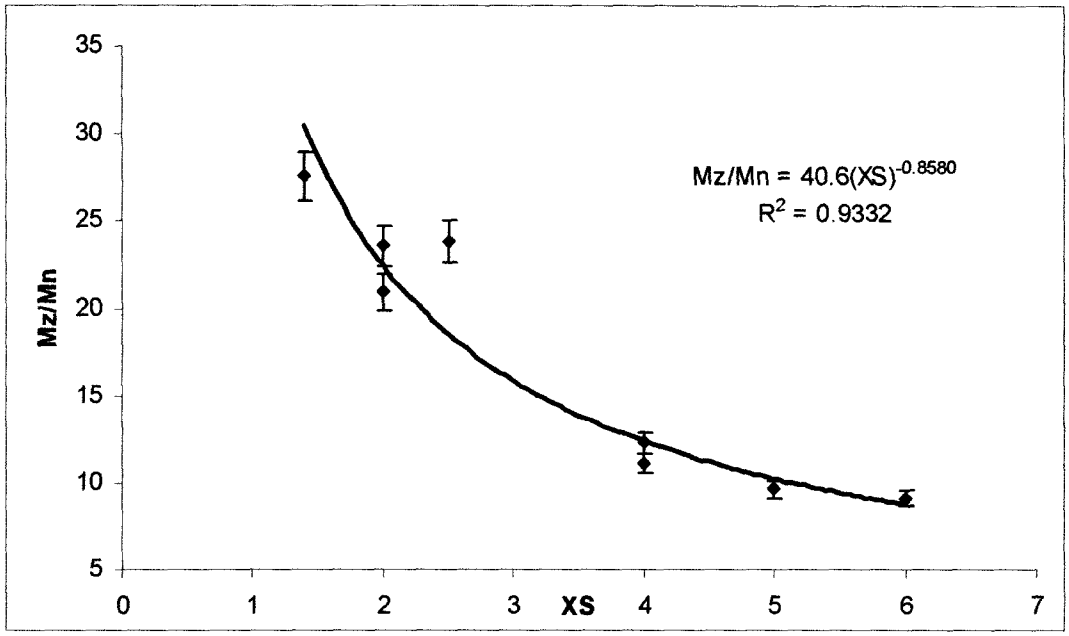

Figure XI.27. Relationship between Mz/Mn ratio and the percentage of soluble XS

In addition, XS is also related to the percentage of isotacticity (%meso) as shown in Figure XI.28.

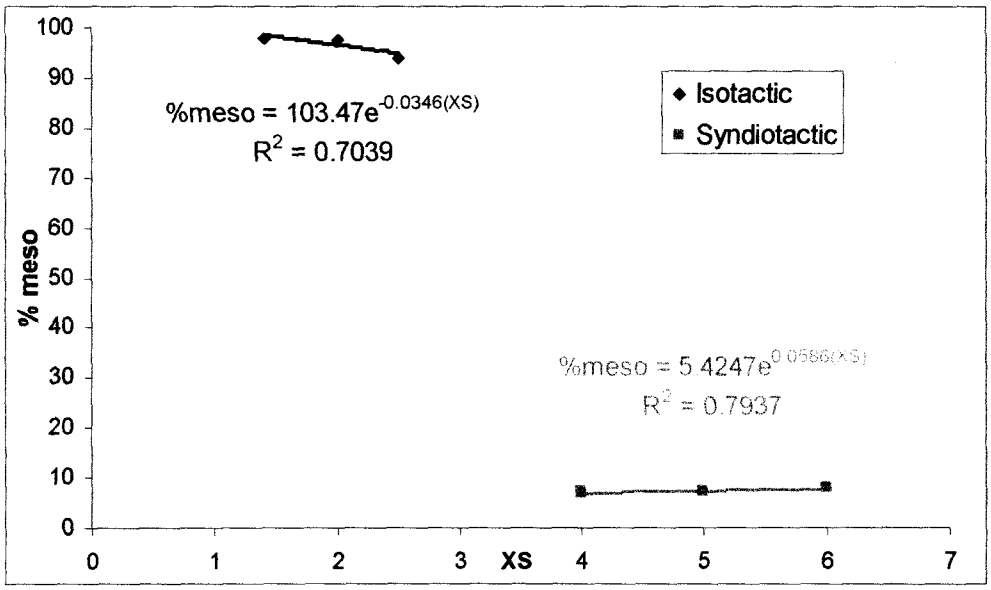

Figure XI.28. Relationship between percentage of isotacticity (%meso) and the percentage of soluble XS

Calorimetric data was found to be related to the percentage of isotacticity as shown in Figure XI.29 and Figure XI.30.

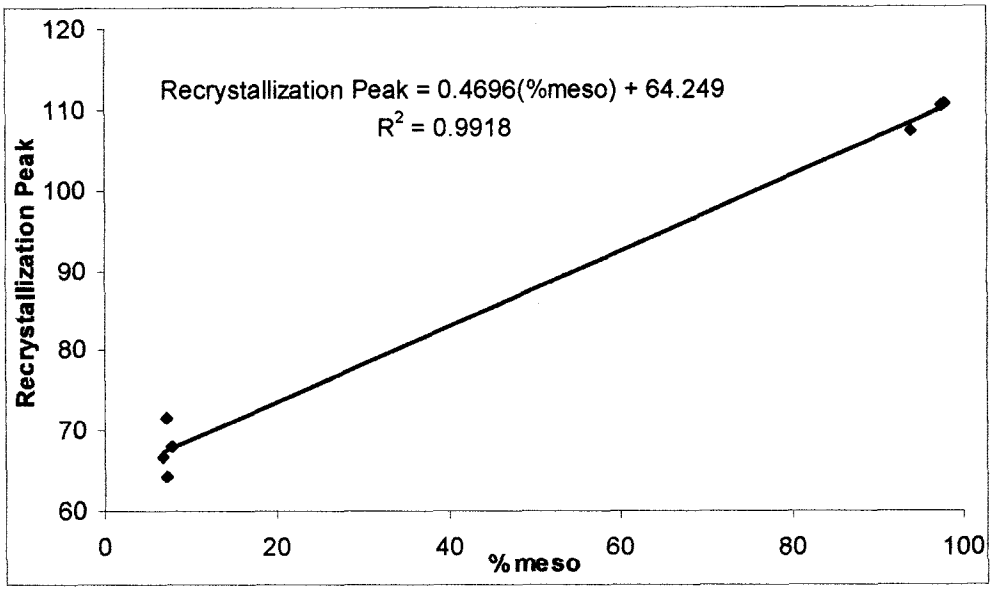

Figure XI.29. Relationship between the recrystallization peak and the percentage of isotacticity (%meso).

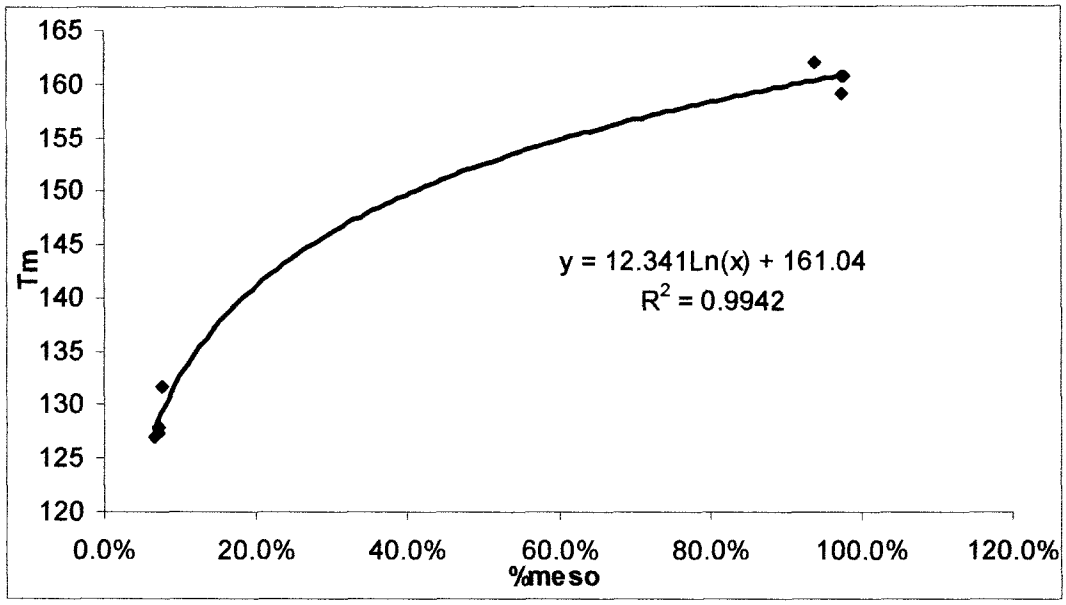

Figure XI.30. Relationship between the melting temperature and the percentage of isotacticity (% meso).

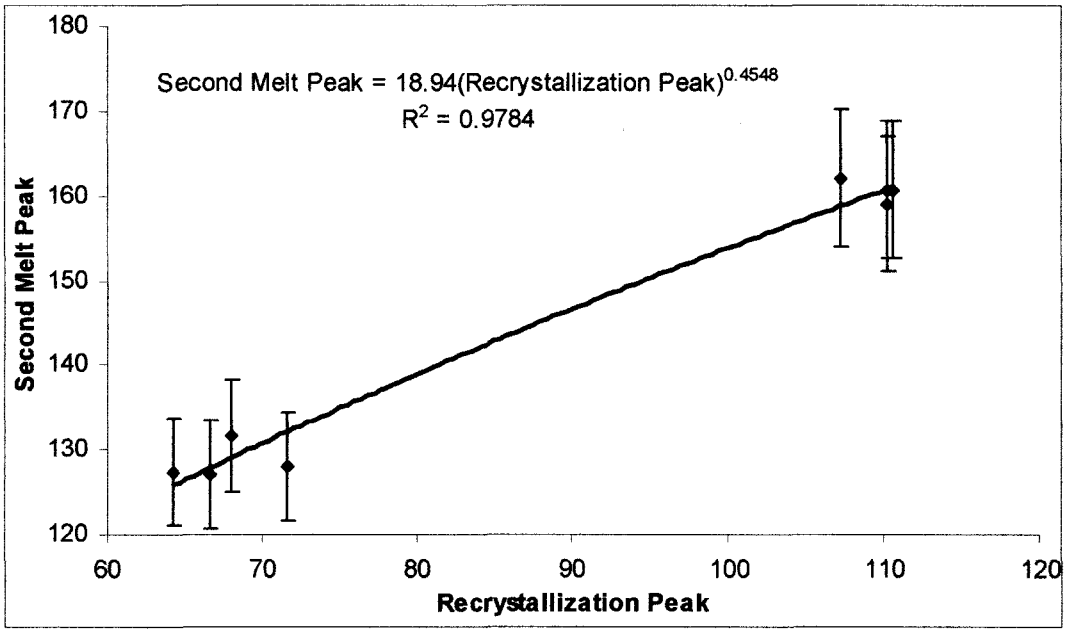

Figure XI.31. Relationship between the second melt peak and the recrystallization peak in the DSC.

Finally, a practical relationship between the second melt peak and the recrystallization peak in the DSC experiment was found. This relationship presents a power law functionality and it is presented in Figure XI.31.

CHAPTER XII. Fractals Approach

There is no usable constitutive equation that describes quantitatively all the flow phenomena of polymer melts. In the absence of it, scientists and engineers use equations that predict only the flow behavior that is important to the particular problem (Mier, 2000). Flows that consist primarily of shearing deformations, with no strong convergence or divergence, have been succesufully modeled using purely viscous models. But when elasticity plays an important role, traditional numerical techniques fail to yield useful results. This suggests that a new approach is needed if useful models are to be developed. In any case, it is thought that a fundamental constitutive equation, which could describe all the flow phenomena of polymer melts, could arise from understanding the polymers nature since the polymerization. It is believed that fractals theory could help in understanding this nature and therefore, a new and better constitutive equation could be developed.

A. Background

Chaos science uses a different geometry called fractal geometry. It is providing us with a new perspective to view the world. Fractal geometry is a new language used to describe, model and analyze complex forms found in nature.

Polymers chains could be considered as fractals, and then fractal geometry could be applied to explain polymers behavior. The simplest way to model a polymer is to assume that it is a random walk.

However, actual polymer chains have steric interaction that avoids monomers from placing on the top of each other. Random walk and self-avoiding walk models describe a polymer in a solvent. It is assumed that polymer chains are made of *N*

statistical units (some monomers units) which are randomly oriented with respect to each other. Random walk describes a linear chain where no interactions are present between monomers. Self-avoiding walk describes an interaction between monomers.

In a polymer melt, two regimes may be found, depending on the mass of the chains. For short chains, the viscosity is proportional to the mass of the polymers (Rouse model). For large chains, it becomes proportional to $N^{3.4}$ (Reptation theory).

Fractals theory is not exclusive to polymers chains. A lot of things could be describe by fractals; for example, the abstract painter Jackson Pollock (1912-1956) is widely known for his spectacular, wall-sized paintings, which typically feature a combination of swirling drips, bright splotches, and bold, rhythmic streaks. Figure XII.1 and Figure XII.2 present examples of Pollock's work.

Figure XII.1. Pollock's *Convergence: Number 10*, 1952 (Albright - Know Gallery, USA).

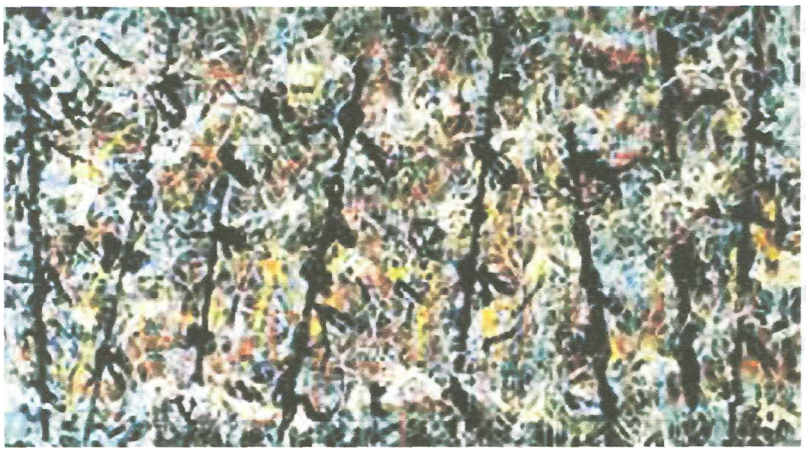

Figure XII.2. Pollock's *Blue Poles*, 1952 (Australian National Gallery).

Physicist Richard P. Taylor of the University of New South Wales in Sydney, Australia, who is also trained as an artist, has taken a mathematical look at Pollock's splatter paintings to try to uncover the secret of their appeal to many viewers. He discovered that Pollock's patterns could be characterized as fractals.[7] A description of fractals dimension is shown in Figure XII.3 and it could be observed that there is a huge similarity between fractals dimensions and Pollock's paintings.

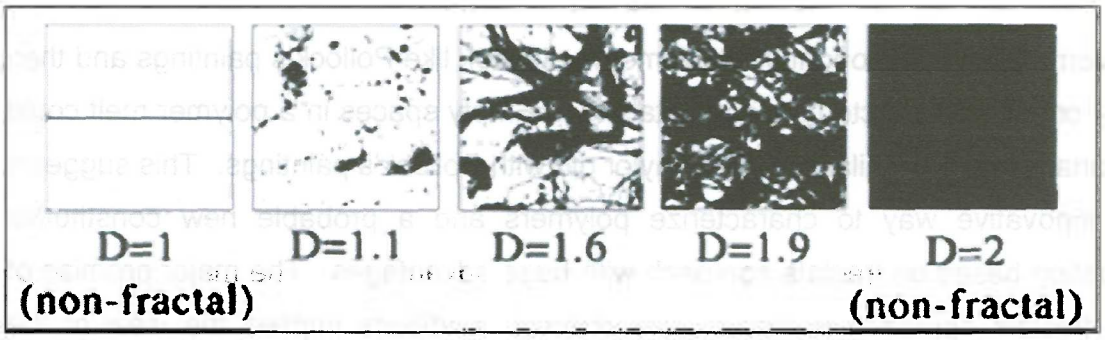

Figure XII.3. Description of fractals dimensions.

[7] The technique that Taylor used to characterize Pollock's paintings was the Box Counting Method. This method consists in lay over the object to be measure a grid of lattice constant (box size) ε. The number of boxes, $N_B(\varepsilon)$, which cover any part of the object (the occupied or intersected boxes), are counted and each data couple $N_B(\varepsilon)$, ε is tabulated. The same procedure is repeated with a set of successively smaller ε. Log $[N_B(\varepsilon)]$ is plotted versus log $[1/\varepsilon]$ and the slope of the resulting straight line (if such indeed exists) is taken as the fractal dimension of the object. If the resulting plot is not a straight line, or if the slope of the resulting straight line is an integer, then the object is not a fractal (Rothschild, 1998).

According to Taylor's analysis (2003), Pollock perfected his technique over ten years. Art theorists categorize the evolution of Pollock's drip technique into three phases. In the 'preliminary' phase of 1943-45, his initial efforts were characterized by low fractal dimension (D) values. During his 'transitional phase' from 1945-1947, he started to experiment with the drip technique and his D values rose sharply (as indicated by the first dashed gradient in Figure XII.4). In his 'classic' period of 1948-52, he perfected his technique and D rose more gradually to the value of D = 1.7-1.9 (see Figure XII.4).

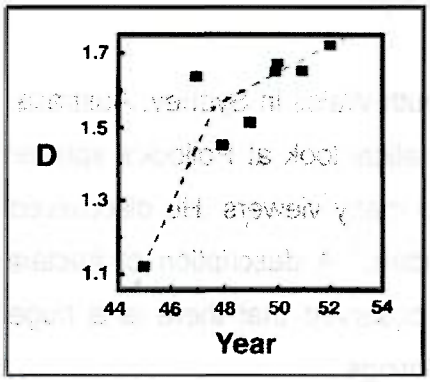

Figure XII.4. Fractal dimension evolution in Pollock's paintings

Nevertheless, it is thought that polymer melts look like Pollock's paintings and then they could be characterized as fractals too. Empty spaces in a polymer melt could be analyzed in a similar way that Taylor did with Pollock's paintings. This suggests an innovative way to characterize polymers and a probable new constitutive equation based on fractals approach with huge advantages. The major promise of the fractals approach is that a view of local conditions implied the view of the whole.

B. Random Walks

One dimension (1-D) random walk theory was applied to simulate the random growth of polymer chains, where the starting points were considered as the active sites in a catalyst surface. Different distances between the starting points and different number of steps were used. By using two and three "chains" (random walks), it was observed that the number of times that the chains crossed over (junctions) was related to the distance between the starting points and the number of steps in the random grow. Similar analysis was done using 2-D random grow.

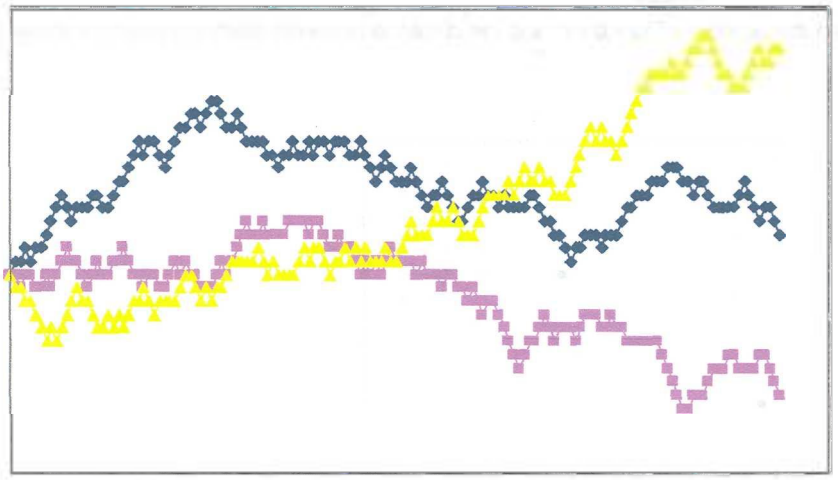

Figure XII.5. Three1-D random walks starting at the same point (distance = 0).

Figure XII.5 shows an example of three "chains" (random walks) starting at the same point. On the other hand, Figure XII.6 presents the relation between the number of junctions and the distance between the starting points. The number of junctions is taken as the average of 1000 iterations. Finally,

Figure XII.7 shows an example of 2-D random walks. It is worth to mention that the relationship between the number of junctions and the distance between starting points for 2-D random walks, was also a negative exponential function.

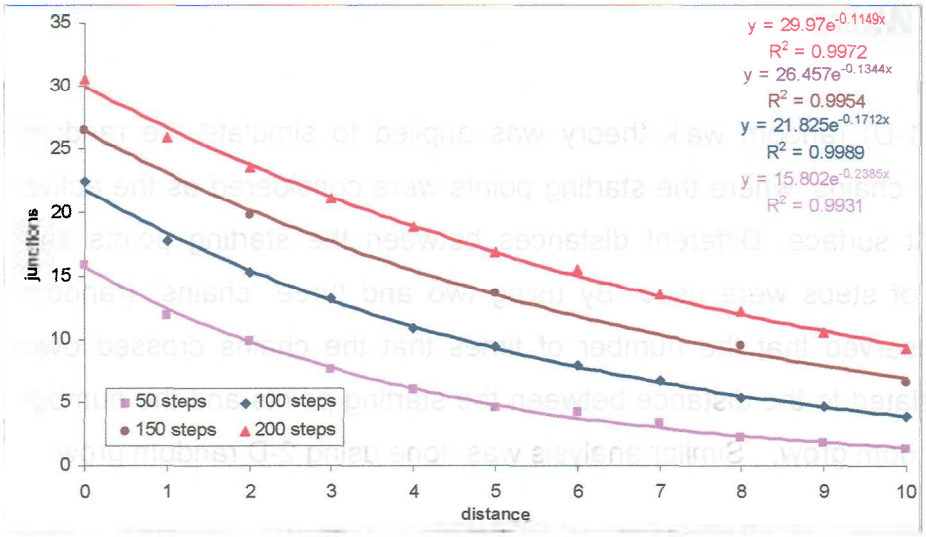

Figure XII.6. Relation between the number of junctions and the distance between starting points for three 1-D random walks.

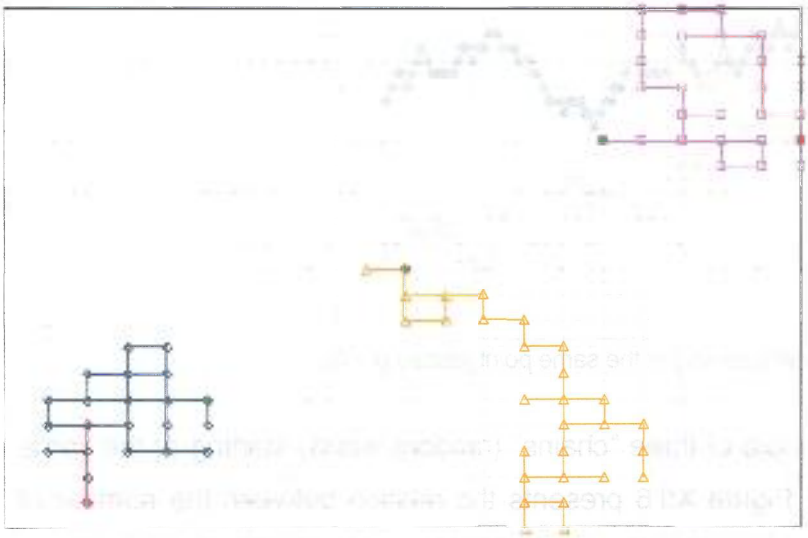

Figure XII.7. 2-D random walks starting at different points (distance = 5).

C. Self-avoiding Walks

In order to make the simulation of random growth of polymer chains more realistic, self-avoiding walk theory was applied. Polymer chains have steric interaction that avoids monomers from placing on the top of each other. Then, if it is assumed that polymer chains are made of *N* statistical units (some monomers units) which are

randomly oriented with respect to each other, random walk describes a linear chain where no interactions are present between monomers and self-avoiding walk describes an interaction between monomers.

The same analysis done with random walks was applied as well to 2-D and 3-D self avoiding walks (SAW). In these cases, it was also found a negative exponential function for the number of junctions with respect of distance between the starting points.

Figure XII.8 shows examples of 2-D self-avoiding walks, and Figure XII.9 and Figure XII.10 present examples of 3-D self-avoiding walks.

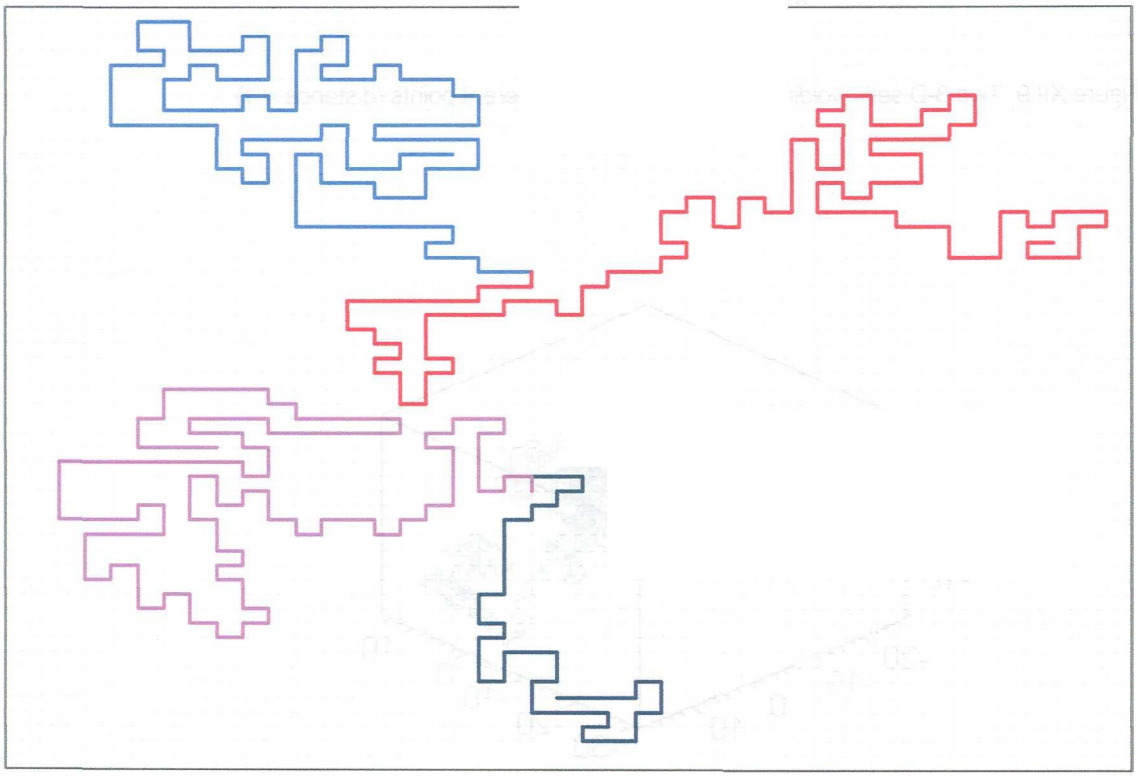

Figure XII.8. Examples of 2-D self -avoiding walks.

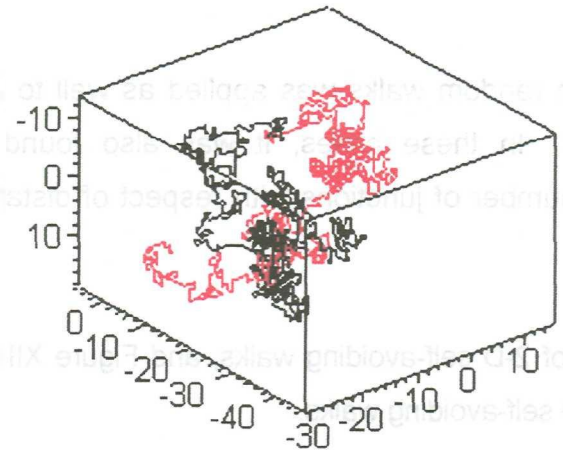

Figure XII.9. Two 3-D self-avoiding walks starting from different points (distance = 1).

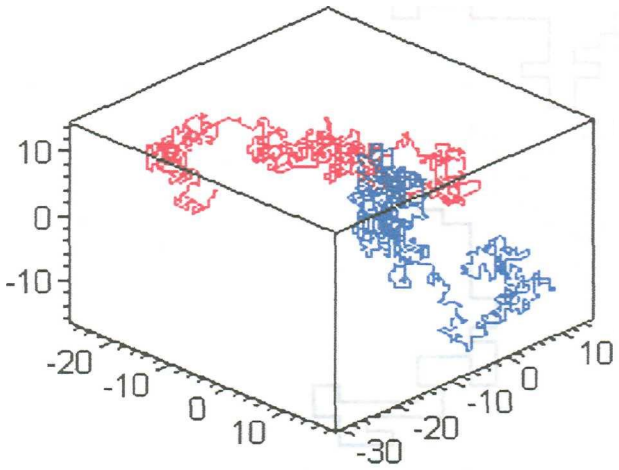

Figure XII.10. Two 3-D self-avoiding walks starting from the same point (distance = 0).

It worth to mention that since self-avoiding walks model do not allow the walker to return to a site already visited, sometimes the chain must be terminated because it can not grow farther.

D. Discussion

The results from random growth analysis are very promising, because of the similarity of the function found for the number of junctions and the function in the PTT model for the rate of creation and destruction of junctions ($Z(tr\tau)$); they are both negative exponential functions. This could suggest a new approach for a constitutive equation, which could relate the rheological properties with the catalyst site distribution in the polymerization.

Figure XII.11 to Figure XII.13 present ten 3-D self avoiding walks starting form different points. All three figures are the same picture. Figure XII.12 is the exact same view of Figure XII.11 but without the dimension axes (xyz). It could be seen that the picture without the frame of the axes, is a two dimensional picture and looks very similar to Pollock's paintings. This suggests that an analysis similar to the one done with Pollock's paintings is suitable to polymer chains. On the other hand, Figure XII.13 shows the same picture, but with different view. This picture shows a view of the xy plane. This picture looks very similar to Figure XII.12 and confirms the similarity with Pollock's paintings.

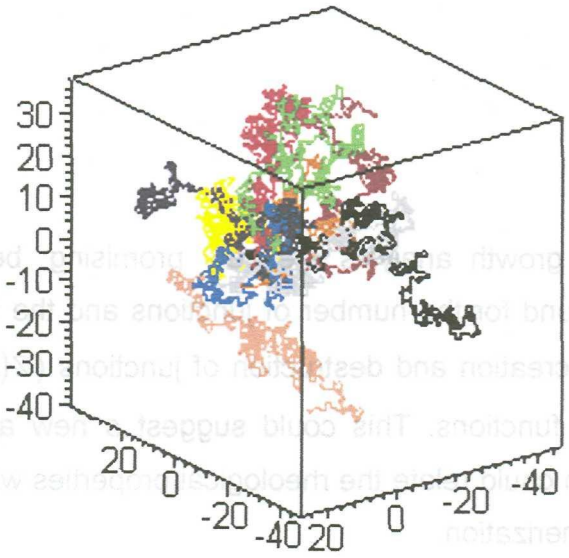

Figure XII.11. Ten3-D self-avoiding walks starting from different points.

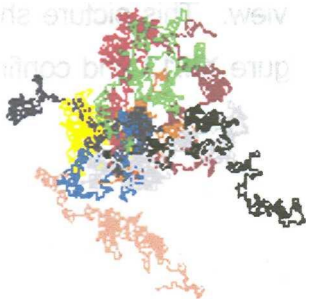

Figure XII.12. Same picture that previous picture, but with out the dimension axes.

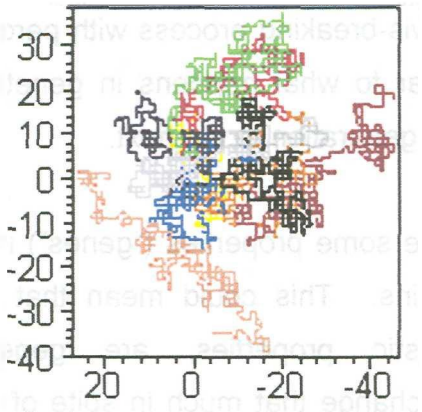

Figure XII.13. View of xy plane of previous picture.

Then, if actual polymer melts network looks something similar to Pollock's paintings (or to figures above), they could be characterized as fractals. Empty spaces in a polymer melt could be analyzed in a similar way that Taylor did with Pollock's paintings. This suggests an innovative way to characterize polymers and a probable new constitutive equation based on fractals approach with huge advantages. In spite of this, a huge problem appears: how to get the actual picture of a polymer melt network? Even though we can get it from an electronic microscope, it won't be enough, because during the processing of the material, this network will be changing through time.

However, the idea of a model based on fractals theory is still very promising. The major promise of the fractals approach is that a view of local conditions implied the view of the whole. In addition, this model would be based on more fundamental aspects of the polymer chains (such as the catalysis and the polymerization itself) and therefore it would be able to describe a wider range of polymers.

On the other hand, Bonilla (1996) found that viscoelastic properties of CRPP (controlled-rheology polypropylene) are related with the properties of their "mother" resins. This suggests that there are intrinsic properties that are not modified with modifications (in this case, the vis-breaking process with peroxide radicals) of the resins. This is something similar to what happens in genetics, there are some genes that are passed from one generation to the next.

Then, it is thought that there are some properties ("genes") in the resins that are inherited from its "mother" resins. This could mean that some properties of polymers, including viscoelastic properties, are generated during the polymerization, and they won't change that much in spite of some modifications. These properties are their "genes". This reinforces the possibility of a general constitutive equation based on fundamental aspects of the polymerization capable of predicting viscoelastic properties. Fractals theory seems like the best alternative to attain such model.

The idea of constitutive equations based on fractals theory is not that new. Some constitutive equations are based indirectly on fractals theory. The Doi – Edwards (DE) model, mentioned under the constitutive equations section in Chapter II (page 19), is based in the concept of reptation (the tube model), and this concept uses fractals to explain the polymer chain behavior. The DE model is very successful in describing the rheological behavior of linear polymers with narrow molecular weight distribution. However, other polymers, such as those with long side branches like LDPE, are not well described by the DE model. (Larson, 1984; Dealy, 1990). Nevertheless, there are several models based on the DE model (therefore, in a certain way based on fractals theory), such as the Pom-Pom (Mcleish and Larson, 1998) and XPP (Verbeeten, 2000) that are very accurate.

Alternatively, the Marruci Model (1976) considers a scalar dimensionless quantity, x, related to the degree of connectivity of the macromolecular network with respect

to that at equilibrium (see Chapter II, page 23). This degree of connectivity is related to the number of junctions, and as it is mentioned before, the number of junctions is in some way related to fractals. The same happens with the PTT model and other constitutive equations based on molecular network theory. However, these models consider empirical fitting parameters that are not based on fundamentals aspects of the polymerization, and then they still have some drawbacks in the predictions of viscoelastic properties.

A rheological model completely based on fractals theory and fundamentals aspect of the polymerization would be a huge innovation to constitutive modeling and to plastic engineering. It is thought that this is the best, and maybe the only, solution for solving the drawbacks in constitutive modeling of polymer melts.

Now then, a lot of work is left to do. The simulation of the random growth of polymer chains using 3-D self-avoiding walks (SAW's) looks like a good way to model a polymer network. However, some issues have to be improved in order to make the model more realistic.

First of all, a better program is needed to generate the chains since FORTRAN presented some limitations. It can't generate chains greater than 2000 steps, which makes the simulation unrealistic because actual polymer chains consist of much more than 2000 monomeric units.

On the other hand, the simulations using 3-D SAW's presented before, are not considering the mass and volume of actual polymer chains. They only represent the path of a probable growth of the chain. However, in order to have a better model of the polymer chain's growth, the mass and volume of the chain must be considered. In addition, stereochemical conformation must be considered too. The angles between the chemical bonds, the stereochemical configuration (*cis-, trans-,* isotactic or syndiotactic), and all the chemical and physical interactions have to be taken into account in the simulation. Important issues to consider are that:

- ➔ Monomeric units are no connected by 90° angles like it is shown in the SAW's presented before.
- ➔ Van de Waals forces could play an important role in the elongational flow; therefore special attention must be put to these forces.
- ➔ Molecualr weigh distribution moments (Mw, Mn and Mz) must be properly replicate by the model.
- ➔ The model should be able to describe all kinds of polymerization and catalysis systems.

All these considerations will make possible the modeling of the growth of different kinds of polymers, and then a proper constitutive equation could arise from these simulations.

The fundamental idea for this new constitutive equation would be that a certain strain will produce the destruction of some junctions and the viscoelastic stress would be proportional the total force needed to destroy these junctions. However, is important to consider that the force required to break a junction consist of two parts. The process of destruction of junctions is described in Figure XII.14. First, Figure XII.14 (a) represents a polymer network, which could be view, in an ideal way, like a circle made of two chains, such as it is shown in Figure XII.14 (b). Figure XII.14 (c) and (d) present these chains undergoing a certain deformation. To reach this point (just before the break of junctions) a certain force was required. Then, it comes the rupture of the junctions, represented in Figure XII.14 (e). Another force was needed here to actually break the entanglement. After this rupture, it comes the relaxation of the polymer chains represented by Figure XII.14 (f) and (g).

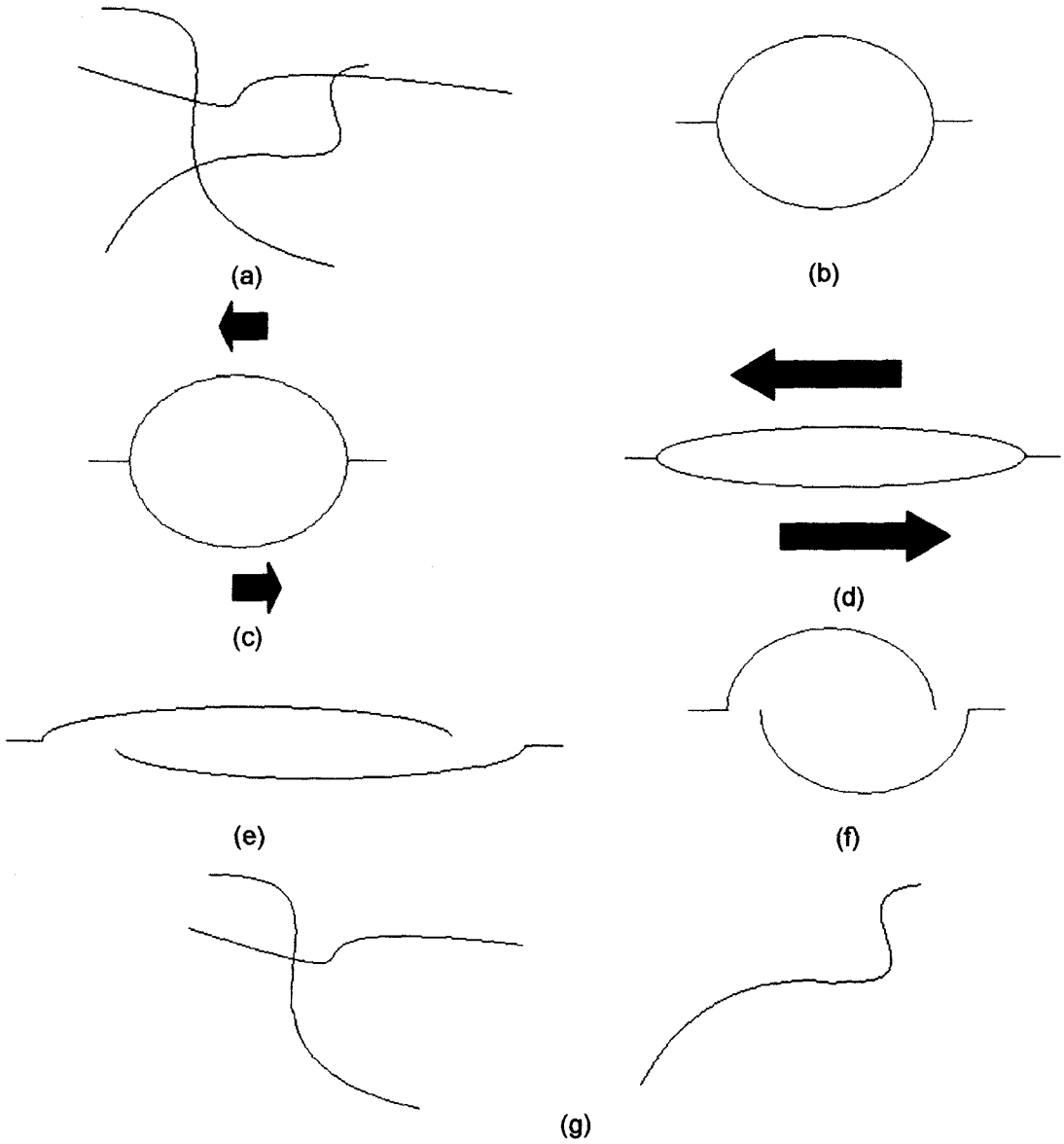

Figure XII.14. Ilustration of the process of destruction of junctions.

Therefore, the viscoelastic stress is related with the force required to reach the point of break and the force needed to actually break the junction. It is thought that the forces required to break the junctions are the determinant issue in the viscoelastic stress. It is also thought that to break a junction, is needed to beat van der Waals forces (interaction between the chains). Consequently, the viscoelastic stress must be related to the van der Waals forces.

Now then, the number of junctions becomes very important in the development of this new constitutive equation. Actually, the important feature is the change in the number of junctions. However, the junctions can be inderectly related to the empty spaces in the network, and it is thought that a quantitave relation could be found between this two features. In addition, according to the box counting method, described in section D of Chapter II, the empty spaces in the network give the fractal dimension of the object. Then, the number of junctions is actually related to the fractal dimension of the network. Therefore, the determinant element in this new model would be the fractal dimension of the polymer network.

Even though the fractal dimension is silent on the detailed structure and absolute size of the object (Rothschild, 1998), it is a characteristic feature and it seems to be a good way to describe the polymer melt. It is important to mention, that this fractal dimension is not a constant. Since the number of junctions changes through time, the fractal dimension is also a function of time.

Another important thing to mention is that fundamental aspects must be involved in the model in order to make this equation more useful. It was found that Me and Mz are closely related to the parameters in mPTT model. This suggests that this molecular features influence significantly the viscoselastic response of the material; then, it is thought that this features could be involved in the new model too.

In any case, a lot of work has to be done in this subject. Further study of polymerization mechanisms and catalysis systems as well as of fractals theory is required. However, a general procedure, shown in Figure XII.15, to develop the new constitutive equation based on fractals theory is proposed.

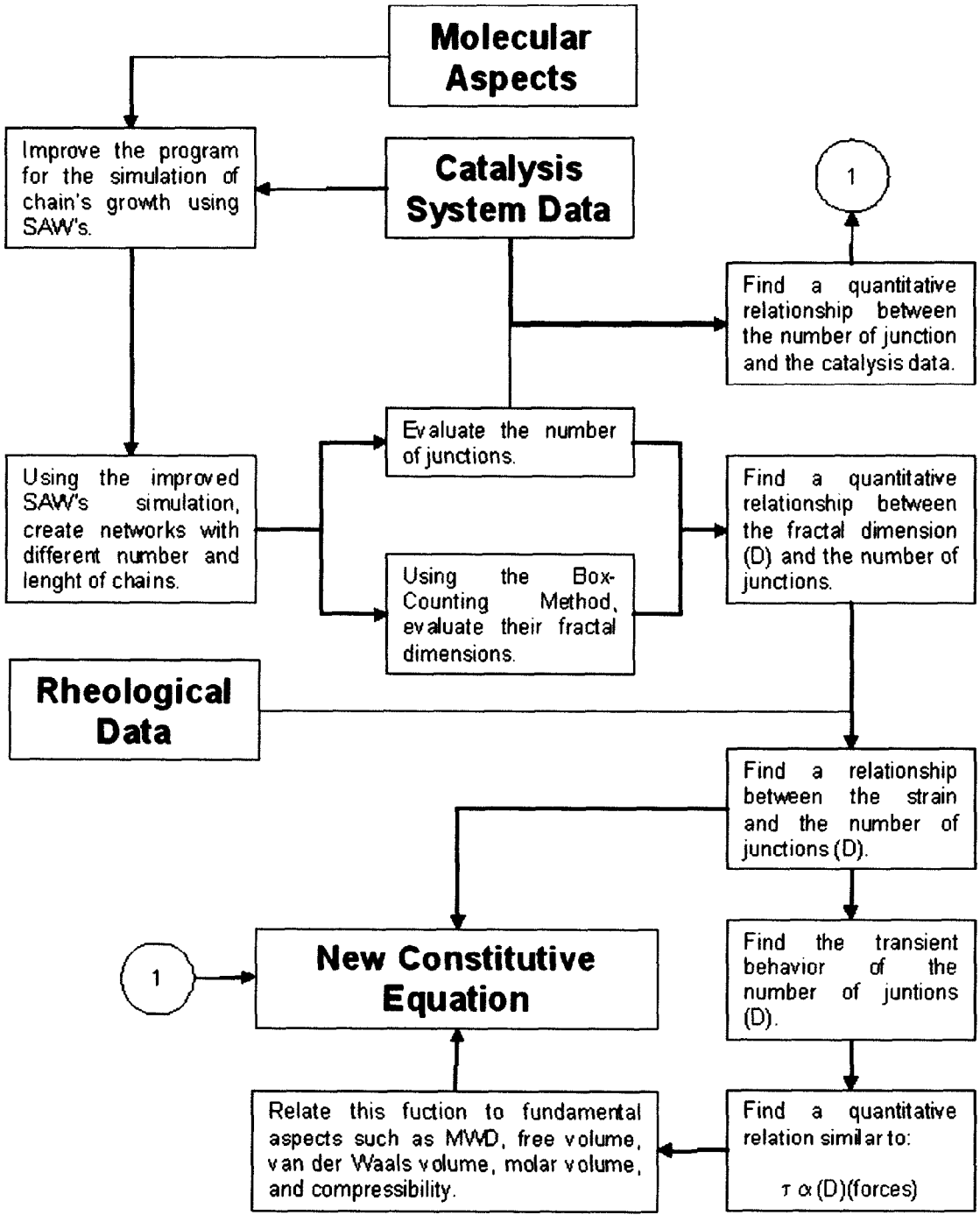

Figure XII.15. Procedure proposed to attain a new constitutive equation.

References

Aguirre, Juan José, *Blow Molding Modeling: Pressure Rise and Die Swell Predictions*, Thesis ITESM campus Monterrey, May 2000

Aris, Rutherford, *Vectors, Tensors and the Basic Equations of Fluid Mechanics*, Dover Publications, New York, 1989

Armin, Bunde, *Fractals in Science*, Springer-Vergal, Germany 1994

Baird D.G., Collias D. I., *"Polymer Processing, Principles and Design"*, John Wiley & Sons, Inc., New York, 9-31, (1998).

Bicerano, Jozef, *Prediction of Polymer Properties*, Marcel Dekker, Inc., USA 1993

Benkoski, J.J., Fredrickson, G.H., Kramer, E.J.; "Model for the fracture energy of glassy polymer-polymer interfaces"; Journal of Polymer Science, Part B, Volume 40, Issue 20, 2377-2386 (2002)

Bird, R. B., R.C. Amstrong, and O. Hassanger, *Dynamics of Polymeric Liquids, 2nd Edition,* Volumes I & II, (John Wiley, New York, 1987).

Bird R. B., Stewart W. E., Lightfoot E. N., *Transport Phenomena* (John Wiley & Sons, New York, 1960).

Bonilla J., *Efects of Peroxide on Molecular Weight and Rheological Properties of Polypropylene Resins*, (Dissertation, Texas A&M University, 1996).

Bonilla, Jaime & Mier, Rodolfo, *Balance de Materia para la Predicción de la Presión Transitoria Observada en un Reometro Capilar*, XXXII Congreso de Investigación y Extensión del Sistema Tecnológico de Monterrey, Enero 2002

Braun, Eliezer, *Caos, Fractales y Cosas Raras*, SEP la ciencia para todos, México D.F. 1996.

Chodankar, C.D., Schieber, J.D. and Venerus, D.C., "Evaluation of rheological constitutive equations for branched polymers in step shear strain flows", *Rheol. Acta*, 42, 123-131 (2003)

Concise Encyclopedia of Polymer Science and Engineering (John Wiley & Sons, Inc., New York, 1990).

Cogswell F.N., "Converging flow of polymer melts in extrusion dies," Polym. Eng. Sci., **12**, No. 1, 64-73, (1972a).

Cogswell F.N., "Measuring the extensional rheology of polymer melts," Transactions of the Society of Rheology, **16**, No. 3, 383-403, (1972b).

Cogswell, F. N., "Converging flow and stretching flow: a compilation," *J. Non-Newt. Fluid Mech.,* 4, 23, (1978).

Cox, W. P., and E. H. Merz, "Correlation of the complex viscosity with steady shear viscosity," *J. Polym. Sci.,* 28, 619-622, (1958).

Darby, R., *Viscoelastic Fluids: An Introduction to Their Properties and Behavior* (Marcel Dekker, Inc.; New York, 1976).

Dealy J.M., Wissbrun K. F., *Melt Rheology and Its Role in Plastics Processing. Theory and Applications* (Van Nostrand Reinhold, New York, 1990).

Dealy, John, "On the Significance of Pressure Relaxations in Capillary or Slit Flow", Rheologica Acta, 34(1), 115 - 116, (1995).

Eckstein, A., Friedrich, C., Lobbrecht, A., Spitz, R., Mülhaupt, R.; "Comparison of the viscoelastic properties of syndio- and isotactic polypropylenes"; Acta Polymerica, 48, 41-46 (1997)

Eckstein, A, Suhm, J., Friedrich, C., Maier, R.D., Sassmannshausen, J., Bochmann, M., Müljaupt, R.; "Determination of Plateau Moduli and Entanglement Molecular Weights of Isotactic, Syndiotactic, and Atactic Polypropylenes Synthesized with Metallocene Catalysts", Macromolecules, 31, 1335-1340 (1998)

Encyclopedia of Polymer Science and Engineering (John Wiley & Sons, Inc., New York, 1985).

Encyclopedia of Polymer Science and Technology: plastics, resins, rubbers, fibers (Interscience Publishers, New York, 1964).

Ferry, J., "*Viscoelastic Properties of Polymers,*" (John Wiley & Sons, 3rd. Edition, New York, 1980).

Fulchiron R., Verney V., Marin G., "Determination of the elongational behavior of polypropylene melts from transient shear experiments using Wagner's Model," J. Non-Newt. Fluid Mech., **48**, 49-61, (1993).

Fuller, G. G., L. G. Leal, *Rheol. Acta.,* 19, 580, (1980).

Giesekus, H., "A simple constitutive equation for polymer fluids based on the concept of deformation-dependent tensorial mobility," *J. of Non-Newt. Fluid Mech,* 11, 69-109, (1982).

Goddard, J. D., "A modified functional expansion for viscoelastic fluids," *Trans. Soc. Rheol.,* 11, 381 (1967).

Goddard, J. D., *Rheol. Acta,* 5, 177 (1966).

Han C. D., Yu T. C., Kim U., "Rheological properties of molten polymers.I. Homopolymer systems," Journal of Applied Polymer Science, **15**, 1149-, (1971).

Han, C.D., *Rheology in Polymer Processing (*Academic Poress, New York, 1976).

Han, C. D., "Studies on melt spinning. I. Effect of molecular weight distribution on elongational viscosity," *Trans. Soc. Rheol.,* 16(3), 447-472, (1972).

Hatzikiriakos, Savvas & Dealy, John, "Role of Slip and Fracture in the Oscillatory Flow of HDPE in a Capillary", Journal of Rheology, 36 (5) 845 - 884 (1992a).

Hatzikiriakos, Savvas & Dealy, John, "Start-Up Pressure Transients in a Capillary Rheometer", Polymer Engineering and Science, **34,** No. 6, 493-499 (1994).

Hatzikiriakos S. G., Dealy J. M., "Wall slip of molten high density polyethylene. I. Sliding plate rheometer studies," Journal of Rheology, **35**, No. 4, 497-523, (1991).

Hatzikiriakos S. G., Dealy J. M., "Wall slip of molten high density polyethylene. II. Capillary rheometer studies," Journal of Rheology, **36**, No. 4, 703-741, (1992b).

Khan, S. A., Larson, R. G., "Comparison of Simple Constitutive Equations for Polymer Melts in Shear and Biaxial and Uniaxial Extensions", Journal of Rheology, 31(3), 207-234, (1987).

Kim, S., Dealy, J. M.; "Design of an orifice die to measure entrance pressure drop"; J. Rheol. 45 (6), (2001).

Lacaze J. M., Marin, G., Monge Ph., "Elongational rheology of polyethylene melts-temporary network constitutive laws," Rheol. Acta, **27**, No. 5, 540-545, (1988).

Lanfray, Y., and G. Marin, "The effect of molecular weight distribution on the elongational properties of linear polymers," *Rheol. Acta,* 29(5), 390-399, (1990).

Larson, R. G., "A Constitutive Equation for Polymer Melts Based on Partially Extending Strand Convection", Journal of Rheology, 28(5), 545-571, (1984).

Larson, R. G., "Analysis of isothermal fiber spinning with the Doi-Edwards constitutive equation," *J. Rheol.,* 27, 475, (1983).

Larson, R. G., Valesano, V. A., "Are Polymer Melts Visco-Anelastic?", Journal of Rheology, 30 (6), 1093-1108, (1986).

Larson, R. G., Sridhar, T., Leal, L. G., McKinley, G. H., "Definitions of entanglement spacing and time constants in the tube model", Journal of Rheology, 47(3), 809-818, (2003).

Laun H.M., " Description of the non linear shear behavior of a low density polyethylene melt by means of an experimentally determined strain dependent memory function," Rheol. Acta, **17**, No. 1, 1-15, (1978).

Laun H. M., "Prediction of elastic strains of polymer melts in shear and elongation," Journal of Rheology, **30**, No. 3, 459-501, (1986).

Laun, H.M., "Transient elongational viscosities and drawability of polymer melts," *J. Rheol.,* 33, 119-175, (1989).

Laun, H. M., H. Munstedt, "Comparison of the elongational behavior of a polyethylene melt at constant stress and constant strain rate," 15, 517-524, (1976).

Lodge, A. S., "Constitutive equations from molecular network theories for polymer solutions," *Rheol. Acta*, 7, No. 4, (1968).

Mavridis H., and Shroff R. N., "Temperature dependence of polyolefin melt rheology," Polymer Engineering and Science, **32**, No.23, 1778-1791, (1992).

McLeish, T. C., Larson, R. G., "Molecular constitutive equations for a class of branched polymers: The pom-pom polymer", Journal of Rheology, 42(1), 81-110, (1998).

Mier, R. & Bonilla, J.; *A Mass Balance for the Reproduction of the Pressure Transients Observed in a Capillary Rheometer*, Project Report AtoFina Research and Technology Center; June 4th , 2001a

Mier, R. & Bonilla, J.; *Effect of Pressure Transducer Accuracy in the Elongational Viscosity of Polyolefins Resins*, Project Report AtoFina Research and Technology Center; May 21st , 2001b

Mier, Rodolfo, *A Rhelogical Study of Isotactic Metallocene Based Polypropylene Resins and Mathematical Modeling of the Fiber Spinning Process*, Thesis ITESM campus Monterrey, December 2002

Morrison, R.T., Boyd, R.N.; *Quimica Organica*, Addison-Wesley Iberoamericana, USA (1990)

Nakagawa, M., *Chaos and Fractals in Engineering*, World Scientific USA (1999)

Odian G., *Principles of Polymerization*, Third Edition, John Wiley & Sons Inc., New York 1991

Papanastasiou A. C., Scriven L. E., Macosko C. W., "An integral constitutive equation for mixed flows: viscoelastic characterization," Journal of Rheology, **27**, No. 4, 387-410, (1983).

Papanastasiou, A. C., L. E. Scriven, C. W. Macosko, and Z. Chen, "Fiber spinning of viscoelastic liquid," *AIChE J.*, 33, 834, (1987).

Phan-Thien, N., and R. I. Tanner, "A new constitutive equation derived from network theory," *J. Non-Newt. Fluid Mech.*, 2, 353, (1977).

Phan-Thien, N., "A nonlinear network viscoelastic Model," *J. Rheol.*, 22(3), 259-283, (1978).

Polymer Handbook, John Wiley & Sons, New York, 4th Edition, 1999

Revenu P., Guillet J., Carrot C., Arsac A., "Validation of Cogswell's convergent flow analysis," Journal of Applied Polymer Science, **26**, 1783-1792, (1996).

Rothschild, Walter, *Fractals in Chemistry,* John Wiley & Sons INC, Canada (1998)

Samurkas, T., Larson, R. G., Dealy, J. M., "Strong Extensional and Shearing Flows of a Branched Polyethylene", Journal of Rheology, 33(4), 559-578, (1989).

Stephenson, S. E., "Limitations of the Phan-Thien non-linear viscoelastic model," *Rheol. Acta*, 25, 66, (1986)

Tadmor Z., Gogos C. G., *Principles of Polymer Processing*. (John Wiley & Sons, New York, 1979).

Tanner, R. I., "From A to (BK)Z in constitutive relations", Journal of Rheology, **32**, No. 7, 673-702, (1988).

Tanner R.I., "Some useful consititutive models with a kinematic slip hypothesis," *J. Non-Newtonian Fluid Mech.,* 5, 103-112, (1979).

Taylor, Richard, "El orden en el caos de Pollock", *Scientific American México*, Año I Núm. 8, 56-61, (2003)

Veerbeeten, W, Peters, G. & Baaijens, F.; *Differential constitutive equations for polymers melts: The extended Pom – Pom model*, J. Rheol. 45 (4) July/August 2001.

Wagner M.H., "Analysis of time-dependent non-linear stress-growth data for shear and elongational flow of a low-density branched polyethylene melt," Rheol. Acta, **15**, 136-142, (1976 a).

Wagner, M. H., "Analysis of stress-growth data for simple extension of a low-density branched polyethylene melt, *Rheol. Acta,* 15, 133-135, (1976 b).

Wagner M.H., Laun H.M., "Non-linear shear creep and constrained elastic recovery of a LDPE melt," Rheol. Acta, **17**, 138-148, (1978 a).

Wagner, M. H., J. Non-Newt. Fluid Mech., 4, 39, (1978 b).

Wagner M. H., Stephenson S. E., "The irreversibility assumption of network disentanglement in flowing polymer melts and its effects on elastic recoil predictions," Journal of Rheolgy, **23**, No. 4, 489-504, (1979 a).

Wagner, M. H., J. Non-Newt. Fluid Mech., 4, 681, (1979 b).

Wagner, M. H., *Rheol. Acta.,* 18, 33-50, (1979 c).

Wagner, M. H., A. Demarmels, "A constitutive analysis of extensional flows of polyisobutylene," *J. Rheol.,* 34(6), 943-958, (1990).

Wagner, M. H., and J. Schaeffer, "Nonlinear strain measures for general biaxial extension of polymer melts," *J. Rheol.,* 36, 1, (1992)

Wagner, M. H., P. Ehrecke, P. Hachmann, J. Meissner, "A constitutive analysis of uniaxial, equibiaxial and planar extension of a commercial linear high density polyethylene melt," *J. Rheol.,* 42(3), 621-638, (1998).

Wientjes, R.H., Jongschaap, R.J., Duits, M.H. and Mellena, J., "A new transient network model for associative polymer networks", *J. Rheol., 43(2), 375-391, (1999).*

Appendix A. Calculations to Transform Capillary Rheometer Raw Data into Shear and Elongational Viscosity

A. Equipment Description

- Rosand Double Bore Capillary Rheometer
  Model RH7-2
  Barrel Diameter (D_b): 15 mm

Table A.1. Long dies used in the capillary analysis

Diameter	Lenght	L/D	Entrance
0.5 mm	8 mm	16	90°
1 mm	16 mm	16	90°
1.5 mm	24 mm	16	90°

Table A.2. Short dies used in the capillary analysis

Diameter	Lenght	L/D	Entrance
0.5 mm	0.25 mm	0.5	90°
1 mm	0.25 mm	0.25	90°
1.5 mm	0.25 mm	0.1667	90°

B. Raw Data

Rosand software calculates the shear and extensional viscosity, but as explained in chapter III, it gives different results to the Bagley and Rabinowitch correction and the Cogswell (1972a, 1972b) analysis for shear and elongational viscosity respectably. Therefore, the piston velocity (v) and the pressure drop in the short (ΔP_S) and long die (ΔP_L) are the only data needed as raw data, in addition to the barrel and die dimensions, to calculate the shear and elongational viscosity.

C. Steady Shear Viscosity

1. Calculate the volumetric flow Q (mm^3/s) for each piston velocity.

$$Q = \upsilon\pi\left(\frac{D_b}{2}\right)^2 \tag{A.1}$$

2. Calculate the apparent shear rate $\dot{\gamma}_a$.

$$\dot{\gamma}_a = \frac{32Q}{\pi D^3} \tag{A.2}$$

3. The apparent shear stress τ_a, is determined by:

$$\tau_a = \frac{D}{4}\cdot\frac{\Delta P_L}{L_L} \tag{A.3}$$

4. Then the apparent shear viscosity η_a is obtained by:

$$\eta_a = \frac{\tau_a}{\dot{\gamma}_a} \tag{A.4}$$

5. The pressure drop for a polymer melt flowing through a die is due to viscous deformation and elastic deformation. The elastic deformation occurs due to the contraction of the flow in going from the bigger diameter of the reservoir (barrel) into the smaller diameter of the die. Therefore, it is important to subtract the elastic pressure drop from the total pressure drop. The pressure drop due to the elongation of the melt ΔP_E, can be taken as the total pressure registered in the transducer above the short die (ΔP_S) minus the pressure due to viscous resistance in the small length of the short die.

$$\Delta P_E = \Delta P_S - \frac{\Delta P_L - \Delta P_S}{L_L - L_S}L_S \tag{A.5}$$

6. Determine the viscous pressure drop ΔP_{vis} (Pa) for each apparent shear rate.

$$\Delta P_{vis} = \Delta P_T - \Delta P_E \tag{A.6}$$

7. For every apparent shear rate, the true shear stress τ_t is determined by:

$$\tau_t = \left(\frac{D}{4}\right)\left(\frac{\Delta P_L - \Delta P_E}{L_L}\right) \tag{A.7}$$

8. The true shear rate is determined by using the Rabinowitch technique, in which the parameter "n" is obtained from the point slope of the curve of the log τ_t versus log $\dot{\gamma}_A$, Tadmor et al. (1979) noticed that "n" is constant if the polymer melt is a power law fluid. For other non-Newtonian fluids, "n" will vary with the apparent shear rate or true shear stress.

$$n = \frac{d(log\,\tau_t)}{d(log\,\dot{\gamma}_a)} \qquad (A.8)$$

$$\dot{\gamma}_t = \left[\frac{3n+1}{4n}\right]\dot{\gamma}_a \qquad (A.9)$$

9. Determine the true shear viscosity η_t.

$$\eta_t = \frac{\tau_t}{\dot{\gamma}_t} \qquad (A.10)$$

D. Transient Shear Viscosity

1. Calculate the volumetric flow, the apparent shear rate, the power law index and the corrected shear rate from steady state values (see section C).
2. Calculate the elastic pressure drop ΔP_E (equation A.5) using the transient pressure data.
3. Similarly, calculate the true shear stress τ_t (equation A.7) for each recorded time.
4. Then, calculate the transient true shear viscosity η_t (equation A.10) for each time.

E. Steady Elongational Viscosity

The steady elongational viscosity can be determined from steady shear viscosity capillary data by means of the Cogswell analysis as an extension of the procedure follow in section C to calculate the steady shear viscosity.

10. Calculate the elongational stress σ_E by:

$$\sigma_e = \frac{3(n+1)}{8} \cdot \Delta P_E \qquad \text{(A.11)}$$

11. Determine the elongational viscosity η_e using the corresponding equation.

$$\eta_e = \frac{3(\Delta P_E)}{Tan(\theta/2)\left[1-\left(\frac{D}{D_b}\right)^3\right]\dot{\gamma}_a} \qquad \text{(for die with entrance angle θ)} \qquad \text{(A.12)}$$

$$\eta_e = \frac{9(n+1)^2(\Delta P_E)^2}{32\eta_a\dot{\gamma}_a^2} \qquad \text{(for 180° entrance angle die)} \qquad \text{(A.13)}$$

12. Calculate the elongational rate $\dot{\varepsilon}$.

$$\dot{\varepsilon} = \frac{\sigma_e}{\eta_e}$$

F. Transient Elongational Viscosity

The procedure to obtain the transient elongational viscosity from transient capillary test is a continuation of the procedure followed in section D to calculate the transient shear viscosity.

5. Calculate the transient elongational stress σ_E at each recorded time by equation A.11.
6. Similarly, calculate the transient elongational viscosity η_e using equation A.12 or A.13 at each time.
7. Determine the elongational rate $\dot{\varepsilon}$ (equation A.14).

Appendix B. Software Developed

It was needed to develop some programs (coded in Fortran-language) in order to make easier and faster some calculations along this research. There were developed programs to solve the modified PTT model and XPP model in shear flow, as well as in elongational flow. In addition, there were created other programs to generate random walks and self-avoiding walks as well as to obtain the number of junctions. It worth to mention that programs (coded in C-languege) created by Mier (2000) were also used in this thesis.

A. Modified PTT Model

Chapter IX presents the modified PTT model as well as its rheological functions predictions. The shear flow behavior is described by equations 9.9 to 9.12, which form a system of ordinary differential equations that must be solved numerically. In the same way, equations 9.19 to 9.21 describe the shear free flow. The fouth order Runge Kutta method was applied to solve these systems of ordinary differential equations. This method states that for a system of ordinary differential equations of the form

$$\frac{dy}{dx} = f(x,y) \tag{B.1}$$

the next step

$$x_{n+1} = x_n + h \tag{B.2}$$

has for solution

$$y_{n+1} = y_n + \frac{1}{6}(k_1 + 2k_2 + 2k_3 + k_4) \tag{B.3}$$

where

$$k_1 = h \cdot f(x_n, y_n) \tag{B.4}$$

$$k_2 = h \cdot f\left(x_n + \frac{h}{2}, y_n + \frac{k_1}{2}\right) \tag{B.5}$$

$$k_3 = h \cdot f\left(x_n + \frac{h}{2}, y_n + \frac{k_2}{2}\right) \tag{B.6}$$

$$k_4 = h \cdot f(x_n + h, y_n + k_3) \tag{B.7}$$

Next are presented the Fortran-language code developed to solve these systems easier and faster.

1. Shear Flow

```
! MPTT_SHEAR.f90
!
! FUNCTIONS:
!       This program finds the shear viscosity using the modified PTT model.
!
!*****************************************************************************
!
! INPUT:        Relaxation spectrum, fitting parameter C, shear rate, step (h)
!                       and tolerance.
!
! OUTPUT: Transient shear viscosity.  The data is printed in an ASCI file
!                       called svisc.dat
!
!*****************************************************************************

      PROGRAM mPTT_shear

      IMPLICIT NONE

      !*****VARIABLES*****
      REAL              C, srate, lamda(4), eta(4), svis, svisn, erate
      REAL              txx(4), tzz(4), tyy(4), txy(4)
      REAL              txxn(4), tzzn(4), tyyn(4), txyn(4)
      REAL              k1xx(4), k2xx(4), k3xx(4), k4xx(4)
      REAL              k1yy(4), k2yy(4), k3yy(4), k4yy(4)
      REAL              k1zz(4), k2zz(4), k3zz(4), k4zz(4)
      REAL              k1xy(4), k2xy(4), k3xy(4), k4xy(4)
      REAL              t, h, tn
      REAL              tol, error
      INTEGER           i, j, no
```

```
CHARACTER*20        out1

!*****OPENING OUPUT FILE*****
out1 = 'svisc.dat'
OPEN (1, FILE=out1)

!*****INPUT*****
! Fitting Parameter
WRITE(*,*) 'Fitting parameter C'
READ(*,*) C

! Shear rate
WRITE(*,*) 'Shear rate'
READ(*,*) srate

!Relaxation Spectrum
WRITE(*,*) 'Number of elements of de relaxation spectrum'
READ(*,*) no

DO i=1, no
        WRITE(*,*) 'Relaxation time', i
        READ(*,*) lamda(i)
        WRITE(*,*) 'Relaxation spectrum viscosty', i
        READ(*,*) eta(i)
END DO

! Step
WRITE(*,*) 'Step size h'
READ(*,*) h

! Tolerance
tol=0.000000000001

!*****SOLVING SIMULTANEOUS DIFF EQNS SYSTEM*****
! Runge-Kutta Method (Fourth Order)
DO i=1, no
        txxn(i)=0
        tyyn(i)=0
        tzzn(i)=0
        txyn(i)=0
END DO
svisn=0
tn=0
error=tol+1

DO WHILE (error>tol)                                    !(1)
        t=tn
        DO j=1, no
                txx(j)=txxn(j)
                tyy(j)=tyyn(j)
                tzz(j)=tzzn(j)
                txy(j)=txyn(j)
        END DO
        svis=svisn
        WRITE(1,*) t, svis, error
        tn=t+h
```

```
            DO i=1, no                                                    !(2)
                ! txx
                k1xx(i)=h*(1/lamda(i))*((2*lamda(i)*srate*txy(i))-(EXP(-
(C)*lamda(i)*(txx(i)+tyy(i)+tzz(i))/eta(i))*txx(i)))
                k2xx(i)=h*(1/lamda(i))*((2*lamda(i)*srate*txy(i))-(EXP(-
(C)*lamda(i)*((txx(i)+(k1xx(i)/2))+tyy(i)+tzz(i))/eta(i))*(txx(i)+(k1xx(i)/2))))
                k3xx(i)=h*(1/lamda(i))*((2*lamda(i)*srate*txy(i))-(EXP(-
(C)*lamda(i)*((txx(i)+(k2xx(i)/2))+tyy(i)+tzz(i))/eta(i))*(txx(i)+(k2xx(i)/2))))
                k4xx(i)=h*(1/lamda(i))*((2*lamda(i)*srate*txy(i))-(EXP(-
(C)*lamda(i)*((txx(i)+(k3xx(i)))+tyy(i)+tzz(i))/eta(i))*(txx(i)+(k3xx(i)))))
                txxn(i)=txx(i)+(k1xx(i)+2*k2xx(i)+2*k3xx(i)+k4xx(i))/6
                ! tyy
                k1yy(i)=h*(1/lamda(i))*(-(EXP(-
(C)*lamda(i)*(txx(i)+tyy(i)+tzz(i))/eta(i))*tyy(i)))
                k2yy(i)=h*(1/lamda(i))*(-(EXP(-
(C)*lamda(i)*((tyy(i)+(k1yy(i)/2))+txx(i)+tzz(i))/eta(i))*(tyy(i)+(k1yy(i)/2))))
                k3yy(i)=h*(1/lamda(i))*(-(EXP(-
(C)*lamda(i)*((tyy(i)+(k2yy(i)/2))+txx(i)+tzz(i))/eta(i))*(tyy(i)+(k2yy(i)/2))))
                k4yy(i)=h*(1/lamda(i))*(-(EXP(-
(C)*lamda(i)*((tyy(i)+(k3yy(i)))+txx(i)+tzz(i))/eta(i))*(tyy(i)+(k3yy(i)))))
                tyyn(i)=tyy(i)+(k1yy(i)+2*k2yy(i)+2*k3yy(i)+k4yy(i))/6
                ! tzz
                k1zz(i)=h*(1/lamda(i))*(-(EXP(-
(C)*lamda(i)*(txx(i)+tyy(i)+tzz(i))/eta(i))*tzz(i)))
                k2zz(i)=h*(1/lamda(i))*(-(EXP(-
(C)*lamda(i)*((tzz(i)+(k1zz(i)/2))+txx(i)+tyy(i))/eta(i))*(tzz(i)+(k1zz(i)/2))))
                k3zz(i)=h*(1/lamda(i))*(-(EXP(-
(C)*lamda(i)*((tzz(i)+(k2zz(i)/2))+txx(i)+tyy(i))/eta(i))*(tzz(i)+(k2zz(i)/2))))
                k4zz(i)=h*(1/lamda(i))*(-(EXP(-
(C)*lamda(i)*((tzz(i)+(k3zz(i)))+txx(i)+tyy(i))/eta(i))*(tzz(i)+(k3zz(i)))))
                tzzn(i)=tzz(i)+(k1zz(i)+2*k2zz(i)+2*k3zz(i)+k4zz(i))/6
                ! txy
                k1xy(i)=h*(1/lamda(i))*((-eta(i)*srate)+(lamda(i)*srate*tyy(i))-(EXP(-
(C)*lamda(i)*(txx(i)+tyy(i)+tzz(i))/eta(i))*txy(i)))
                k2xy(i)=h*(1/lamda(i))*((-eta(i)*srate)+(lamda(i)*srate*tyy(i))-(EXP(-
(C)*lamda(i)*(tyy(i)+txx(i)+tzz(i))/eta(i))*(txy(i)+(k1xy(i)/2))))
                k3xy(i)=h*(1/lamda(i))*((-eta(i)*srate)+(lamda(i)*srate*tyy(i))-(EXP(-
(C)*lamda(i)*(tyy(i)+txx(i)+tzz(i))/eta(i))*(txy(i)+(k2xy(i)/2))))
                k4xy(i)=h*(1/lamda(i))*((-eta(i)*srate)+(lamda(i)*srate*tyy(i))-(EXP(-
(C)*lamda(i)*(tyy(i)+txx(i)+tzz(i))/eta(i))*(txy(i)+(k3xy(i)))))
                txyn(i)=txy(i)+(k1xy(i)+2*k2xy(i)+2*k3xy(i)+k4xy(i))/6
            END DO                                                        !(2)
            svisn=-(txyn(1)+txyn(2)+txyn(3)+txyn(4))/srate
            error=ABS(svisn-svis)
            WRITE(*,*) tn, svisn, error
        END DO                                                            !(1)

        !*****CLOSING OUTPUT FILE*****
        CLOSE (1, STATUS='KEEP')

        END PROGRAM mPTT_shear
```

2. Shear Free Flow

```
! MPTT_ELONGATION.f90
!
! FUNCTIONS:
!               This program finds the elongational viscosity using the modified PTT model.
!
!**************************************************************************
!
! INPUT:        Relaxation spectrum, fitting parameters A and B, extension rate,
!                       step (h) and tolerance.
!
! OUTPUT:  Transient elongational viscosity.  The data is printed in an ASCI
!                       file called evisc.dat
!
!**************************************************************************

        PROGRAM mPTT_ELONGATION

        IMPLICIT NONE

        !*****VARIABLES*****
        REAL                    A, B, erate, lamda(4), eta(4), evis, evisn
        REAL                    txx(4), tzz(4), t, h, tn, txxn(4), tzzn(4)
        REAL                    k1xx(4), k2xx(4), k3xx(4), k4xx(4)
        REAL                    k1zz(4), k2zz(4), k3zz(4), k4zz(4)
        REAL                    tol, error
        INTEGER                 i, j, no
        CHARACTER               out1


        !*****OPENING OUTPUT FILE*****

        out1 = 'evisc.dat'
        OPEN (1, FILE=out1)


        !*****INPUT*****
        ! Fitting Parameters
        WRITE(*,*) 'Fitting parameter A'
        READ(*,*) A
        WRITE(*,*) 'Fitting parameter B'
        READ(*,*) B

        ! Extension rate
        WRITE(*,*) 'Extension rate'
        READ(*,*) erate

        !Relaxation Spectrum
        WRITE(*,*) 'Number of elements of de relaxation spectrum'
        READ(*,*) no

        DO i=1, no
                WRITE(*,*) 'Relaxation time', i
                READ(*,*) lamda(i)
                WRITE(*,*) 'Relaxation spectrum viscosty', i
```

```
            READ(*,*) eta(i)
        END DO

        ! Step
        WRITE(*,*) 'Step size h'
        READ(*,*) h

        ! Tolerance
        tol=0.000000001

        !*****SOLVING DIFF EQNS SYSTEM*****
        ! Runge-Kutta Method (Fourth Order)
        error=tol+1
        tn=0
        txxn(1)=0
        txxn(2)=0
        txxn(3)=0
        txxn(4)=0
        tzzn(1)=0
        tzzn(2)=0
        tzzn(3)=0
        tzzn(4)=0
        evisn=0
        DO WHILE (error>tol)                                          !(1)
                t=tn
                txx(1)=txxn(1)
                txx(2)=txxn(2)
                txx(3)=txxn(3)
                txx(4)=txxn(4)
                tzz(1)=tzzn(1)
                tzz(2)=tzzn(2)
                tzz(3)=tzzn(3)
                tzz(4)=tzzn(4)
                evis=evisn
                WRITE(1,*) t, evis, error
                tn=t+h
                DO i=1, no                                            !(2)
                        ! txx
                        k1xx(i)=h*(1/lamda(i))*((eta(i)*erate)-(exp(-
(A*LOG(erate)+B)*lamda(i)*(2*txx(i)+tzz(i))/eta(i))*txx(i))-(lamda(i)*erate*txx(i)))
                        k2xx(i)=h*(1/lamda(i))*((eta(i)*erate)-(exp(-
(A*LOG(erate)+B)*lamda(i)*(2*(txx(i)+(k1xx(i)/2))+tzz(i))/eta(i))*(txx(i)+(k1xx(i)/2)))-
(lamda(i)*erate*(txx(i)+(k1xx(i)/2))))
                        k3xx(i)=h*(1/lamda(i))*((eta(i)*erate)-(exp(-
(A*LOG(erate)+B)*lamda(i)*(2*(txx(i)+(k2xx(i)/2))+tzz(i))/eta(i))*(txx(i)+(k2xx(i)/2)))-
(lamda(i)*erate*(txx(i)+(k2xx(i)/2))))
                        k4xx(i)=h*(1/lamda(i))*((eta(i)*erate)-(exp(-
(A*LOG(erate)+B)*lamda(i)*(2*(txx(i)+(k3xx(i)))+tzz(i))/eta(i))*(txx(i)+(k3xx(i))))-
(lamda(i)*erate*(txx(i)+(k3xx(i)))))
                        txxn(i)=txx(i)+(k1xx(i)+2*k2xx(i)+2*k3xx(i)+k4xx(i))/6
                        ! tzz
                        k1zz(i)=h*(1/lamda(i))*((-2*eta(i)*erate)-(exp(-
(A*LOG(erate)+B)*lamda(i)*(2*txx(i)+tzz(i))/eta(i))*tzz(i))+(2*lamda(i)*erate*tzz(i)))
                        k2zz(i)=h*(1/lamda(i))*((-2*eta(i)*erate)-(exp(-
(A*LOG(erate)+B)*lamda(i)*(2*txx(i)+(tzz(i)+(k1zz(i)/2)))/eta(i))*(tzz(i)+(k1zz(i)/2)))+(2*lamda(i)*erat
e*(tzz(i)+(k1zz(i)/2))))
```

```
                    k3zz(i)=h*(1/lamda(i))*((-2*eta(i)*erate)-(exp(-
(A*LOG(erate)+B)*lamda(i)*(2*txx(i)+(tzz(i)+(k2zz(i)/2)))/eta(i))*(tzz(i)+(k2zz(i)/2)))+(2*lamda(i)*erat
e*(tzz(i)+(k2zz(i)/2))))
                    k4zz(i)=h*(1/lamda(i))*((-2*eta(i)*erate)-(exp(-
(A*LOG(erate)+B)*lamda(i)*(2*txx(i)+(tzz(i)+(k3zz(i))))/eta(i))*(tzz(i)+(k3zz(i))))+(2*lamda(i)*erate*(tz
z(i)+(k3zz(i)))))
                    tzzn(i)=tzz(i)+(k1zz(i)+2*k2zz(i)+2*k3zz(i)+k4zz(i))/6
            END DO                                                    !(2)
            evisn=(txxn(1)+txxn(2)+txxn(3)+txxn(4)-tzzn(1)-tzzn(2)-tzzn(3)-tzzn(4))/erate
            error=ABS(evisn-evis)
            WRITE(*,*) tn, evisn, error
        END DO                                                        !(1)

        !*****CLOSING OUPUT FILE*****

        CLOSE (1, STATUS='KEEP')

        END PROGRAM mPTT_ELONGATION
```

B. XPP Model

On the other hand, Chapter X presents the XPP model. The shear flow behavior using this model is described by equations 10.24 to 10.28, while the shear-free flow is governed by equation 10.12 to 10.14. Each of these two sets of equations form a system of ordinary differential equations that must be solved numerically. As well as with the modified PTT model, the fouth order Runge Kutta method was applied. This method is presented in section A.

Next are presented the Fortran-language code developed to solve these systems of equations.

1. Shear Flow

```
! XPPSHEAR.f90
!
!*****************************************************************************
!
! PROGRAM: XPPSHEAR
!
! PURPOSE:  To obtain shear viscosity using XPP model.
!
!*****************************************************************************
```

```
PROGRAM XPPSHEAR

IMPLICIT NONE

!*****VARIABLES*****
REAL        t, tn     !time
REAL        Sxx(8), Syy(8), Sxy(8), Szz(8)   !S tensor components
REAL        Sxxn(8), Syyn(8), Sxyn(8), Szzn(8)
REAL        txx(8), tyy(8), txy(8), tzz(8)       !Stress tensor components
REAL        txxn(8), tyyn(8), txyn(8), tzzn(8)
REAL        SRB(8), SRBn(8)                  !Strech ratio of the backbone
REAL        ls        !lamdas: stretch relaxation time
REAL        l0s(8)    !lamda0s: stretch relaxation time 0
REAL        v(8)      !measure of the influence of the surroundings polymer chains
REAL        a(8)      !alpha: Material parameter defining the amount of anisotropy
REAL        lamda(8), eta(8)          !discrite relaxation spectrum
INTEGER     no        !Number of elements in the discrete relaxation spectrum
INTEGER     q(8)      !Number of dangling arms in the pom-pom molecule
REAL        h, tol, error, srate, svis, svisn, sumxy
REAL        k1xx(8), k2xx(8), k3xx(8), k4xx(8)
REAL        k1yy(8), k2yy(8), k3yy(8), k4yy(8)
REAL        k1xy(8), k2xy(8), k3xy(8), k4xy(8)
REAL        k1zz(8), k2zz(8), k3zz(8), k4zz(8)
REAL        k1SRB(8), k2SRB(8), k3SRB(8), k4SRB(8)
REAL        svisc(8), sviscn(8), r(8)
INTEGER     i, j, k, l, m, n
CHARACTER*20        out1

!*****OPENING OUTPUT FILE*****
out1 = 'svisc.dat'
OPEN (1, FILE=out1)

!*****INPUT*****
! Relaxation Spectrum and fitting parameters
WRITE(*,*) 'Number of relaxation elements:  '
READ(*,*)  no

DO k=1, no
        WRITE(*,*) 'Relaxation time'
        READ(*,*) lamda(k)
        WRITE(*,*) 'Relaxation spectrum viscosity'
        READ(*,*) eta(i)
        WRITE(*,*) 'Number of dangling arms in the pom-pom molecule  q', k
        READ(*,*) q(k)
        WRITE(*,*) 'Ratio between relaxation time and stretch relaxation time 0', k
        READ(*,*) r(k)
        WRITE(*,*) 'Material parameter defining the amount of anisotropy   a', k
        READ(*,*) a(k)
!measure of the influence of the surroundings polymer chains on thebackbone tube stretch
        v(k)=2/q(k)
!stretch relaxation time 0
        l0s(k)=lamda(k)/r(k)
END DO

! Shear rate
WRITE(*,*) 'Shear rate'
```

```
READ(*,*) srate

! Step
WRITE(*,*) 'Step size'
READ(*,*) h

! Tolerance
tol=1E-12

!*****SOLVING DIFFERENTIAL EQUATIONS*****
! Runge-Kutta Method (Fourth Order)
error=tol+1
tn=0
svisn=0
SRBn(1)=1.12998
SRBn(2)=1.53499
SRBn(3)=2.63701
SRBn(4)=7.41824
SRBn(5)=15.24720
SRBn(6)=72.01033
DO i=1, no                                          !(a)
        Sxxn(i)=1/(3*SRBn(i)*SRBn(i))
        Syyn(i)=1/(3*SRBn(i)*SRBn(i))
        Sxyn(i)=1/(3*SRBn(i)*SRBn(i))
        Szzn(i)=1/(3*SRBn(i)*SRBn(i))
END DO                                              !(a)
DO WHILE (error>tol)                                !(2)
        t=tn
        svis=svisn
        DO j=1, no                                  !(b)
                Sxx(j)=Sxxn(j)
                Syy(j)=Syyn(j)
                Sxy(j)=Sxyn(j)
                Szz(j)=Szzn(j)
                SRB(j)=SRBn(j)
                txx(j)=txxn(j)
                tyy(j)=tyyn(j)
                txy(j)=txyn(j)
                tzz(j)=tzzn(j)
                svisc(j)=sviscn(j)
        END DO                                      !(b)
        tn=t+h
        DO i=1, no                                  !(c)
                k1xx(i)=h*((2*srate*Sxy(i))-(4*srate*Sxx(i)*Sxy(i))-
((3*a(i)*SRB(i)*SRB(i)*(Sxx(i)*Sxx(i)+Sxy(i)*Sxy(i)))/(lamda(i)))-(((1-a(i))-
((3*a(i)*(SRB(i))**4)*((Sxx(i)*Sxx(i))+(Syy(i)*Syy(i))+(2*Sxy(i)*Sxy(i))+(Szz(i)*Szz(i)))))*(Sxx(i)))/(lam
da(i)*SRB(i)*SRB(i)))+((1-a(i))/(3*lamda(i)*SRB(i)*SRB(i))))
                k2xx(i)=h*((2*srate*Sxy(i))-(4*srate*(Sxx(i)+(k1xx(i)/2))*Sxy(i))-
((3*a(i)*SRB(i)*SRB(i)*(Sxx(i)+(k1xx(i)/2))*(Sxx(i)+(k1xx(i)/2))+Sxy(i)*Sxy(i))/(lamda(i)))-(((1-a(i))-
((3*a(i)*(SRB(i))**4)*(((Sxx(i)+(k1xx(i)/2))*(Sxx(i)+(k1xx(i)/2)))+(Syy(i)*Syy(i))+(2*Sxy(i)*Sxy(i))+(Szz
(i)*Szz(i)))))*((Sxx(i)+(k1xx(i)/2))))/(lamda(i)*SRB(i)*SRB(i)))+((1-a(i))/(3*lamda(i)*SRB(i)*SRB(i))))
                k3xx(i)=h*((2*srate*Sxy(i))-(4*srate*(Sxx(i)+(k2xx(i)/2))*Sxy(i))-
((3*a(i)*SRB(i)*SRB(i)*(Sxx(i)+(k2xx(i)/2))*(Sxx(i)+(k2xx(i)/2))+Sxy(i)*Sxy(i))/(lamda(i)))-(((1-a(i))-
((3*a(i)*(SRB(i))**4)*(((Sxx(i)+(k2xx(i)/2))*(Sxx(i)+(k2xx(i)/2)))+(Syy(i)*Syy(i))+(2*Sxy(i)*Sxy(i))+(Szz
(i)*Szz(i)))))*((Sxx(i)+(k2xx(i)/2))))/(lamda(i)*SRB(i)*SRB(i)))+((1-a(i))/(3*lamda(i)*SRB(i)*SRB(i))))
```

```
                    k4xx(i)=h*((2*srate*Sxy(i))-(4*srate*(Sxx(i)+(k3xx(i)/1))*Sxy(i))-
((3*a(i)*SRB(i)*SRB(i)*(Sxx(i)+(k3xx(i)/1))*(Sxx(i)+(k3xx(i)/1))+Sxy(i)*Sxy(i))/(lamda(i)))-(((1-a(i)-
((3*a(i)*(SRB(i))**4)*(((Sxx(i)+(k3xx(i)/1))*(Sxx(i)+(k3xx(i)/1)))+(Syy(i)*Syy(i))+(2*Sxy(i)*Sxy(i))+(Szz
(i)*Szz(i)))))*((Sxx(i)+(k3xx(i)/1))))/(lamda(i)*SRB(i)*SRB(i)))+((1-a(i))/(3*lamda(i)*SRB(i)*SRB(i))))
                    Sxxn(i)=Sxx(i)+(k1xx(i)+2*k2xx(i)+2*k3xx(i)+k4xx(i))/6

                    k1yy(i)=h*(-(4*srate*Sxy(i)*Syy(i))-
((3*a(i)*SRB(i)*SRB(i)*(Syy(i)*Syy(i)+Sxy(i)*Sxy(i)))/(lamda(i)))-(((1-a(i)-
((3*a(i)*(SRB(i))**4)*((Sxx(i)*Sxx(i))+(Syy(i)*Syy(i))+(2*Sxy(i)*Sxy(i))+(Szz(i)*Szz(i)))))*(Syy(i)))/(lam
da(i)*SRB(i)*SRB(i)))+((1-a(i))/(3*lamda(i)*SRB(i)*SRB(i))))
                    k2yy(i)=h*(-(4*srate*Sxy(i)*(Syy(i)+(k1yy(i)/2)))-
((3*a(i)*SRB(i)*SRB(i)*((Syy(i)+(k1yy(i)/2))*(Syy(i)+(k1yy(i)/2))+Sxy(i)*Sxy(i)))/(lamda(i)))-(((1-a(i)-
((3*a(i)*(SRB(i))**4)*(((Syy(i)+(k1yy(i)/2))*(Syy(i)+(k1yy(i)/2)))+(Sxx(i)*Sxx(i))+(2*Sxy(i)*Sxy(i))+(Szz
(i)*Szz(i)))))*((Sxx(i)+(k1xx(i)/2))))/(lamda(i)*SRB(i)*SRB(i)))+((1-a(i))/(3*lamda(i)*SRB(i)*SRB(i))))
                    k3yy(i)=h*(-(4*srate*Sxy(i)*(Syy(i)+(k2yy(i)/2)))-
((3*a(i)*SRB(i)*SRB(i)*((Syy(i)+(k2yy(i)/2))*(Syy(i)+(k2yy(i)/2))+Sxy(i)*Sxy(i)))/(lamda(i)))-(((1-a(i)-
((3*a(i)*(SRB(i))**4)*(((Syy(i)+(k2yy(i)/2))*(Syy(i)+(k2yy(i)/2)))+(Sxx(i)*Sxx(i))+(2*Sxy(i)*Sxy(i))+(Szz
(i)*Szz(i)))))*((Sxx(i)+(k2xx(i)/2))))/(lamda(i)*SRB(i)*SRB(i)))+((1-a(i))/(3*lamda(i)*SRB(i)*SRB(i))))
                    k4yy(i)=h*(-(4*srate*Sxy(i)*(Syy(i)+(k3yy(i)/1)))-
((3*a(i)*SRB(i)*SRB(i)*((Syy(i)+(k3yy(i)/1))*(Syy(i)+(k3yy(i)/1))+Sxy(i)*Sxy(i)))/(lamda(i)))-(((1-a(i)-
((3*a(i)*(SRB(i))**4)*(((Syy(i)+(k3yy(i)/1))*(Syy(i)+(k3yy(i)/1)))+(Sxx(i)*Sxx(i))+(2*Sxy(i)*Sxy(i))+(Szz
(i)*Szz(i)))))*((Sxx(i)+(k3xx(i)/1))))/(lamda(i)*SRB(i)*SRB(i)))+((1-a(i))/(3*lamda(i)*SRB(i)*SRB(i))))
                    Syyn(i)=Syy(i)+(k1yy(i)+2*k2yy(i)+2*k3yy(i)+k4yy(i))/6

                    k1xy(i)=h*((srate*Syy(i))-(4*srate*(Sxy(i)**2))-
((3*a(i)*SRB(i)*SRB(i)*Sxy(i)*(Sxx(i)+Syy(i)))/(lamda(i)))-(((1-a(i)-
((3*a(i)*(SRB(i))**4)*((Sxx(i)*Sxx(i))+(Syy(i)*Syy(i))+(2*Sxy(i)*Sxy(i))+(Szz(i)*Szz(i)))))*(Sxy(i)))/(lam
da(i)*SRB(i)*SRB(i))))
                    k2xy(i)=h*((srate*Syy(i))-(4*srate*((Sxy(i)+(k1xy(i)/2))**2))-
((3*a(i)*SRB(i)*SRB(i)*(Sxy(i)+(k1xy(i)/2))*(Sxx(i)+Syy(i)))/(lamda(i)))-(((1-a(i)-
((3*a(i)*(SRB(i))**4)*((2*(Sxy(i)+(k1xy(i)/2))*(Sxy(i)+(k1xy(i)/2)))+(Sxx(i)*Sxx(i))+(Syy(i)*Syy(i))+(Szz
(i)*Szz(i)))))*((Sxy(i)+(k1xy(i)/2))))/(lamda(i)*SRB(i)*SRB(i))))
                    k3xy(i)=h*((srate*Syy(i))-(4*srate*((Sxy(i)+(k2xy(i)/2))**2))-
((3*a(i)*SRB(i)*SRB(i)*(Sxy(i)+(k2xy(i)/2))*(Sxx(i)+Syy(i)))/(lamda(i)))-(((1-a(i)-
((3*a(i)*(SRB(i))**4)*((2*(Sxy(i)+(k2xy(i)/2))*(Sxy(i)+(k2xy(i)/2)))+(Sxx(i)*Sxx(i))+(Syy(i)*Syy(i))+(Szz
(i)*Szz(i)))))*((Sxy(i)+(k2xy(i)/2))))/(lamda(i)*SRB(i)*SRB(i))))
                    k4xy(i)=h*((srate*Syy(i))-(4*srate*((Sxy(i)+(k3xy(i)/1))**2))-
((3*a(i)*SRB(i)*SRB(i)*(Sxy(i)+(k3xy(i)/1))*(Sxx(i)+Syy(i)))/(lamda(i)))-(((1-a(i)-
((3*a(i)*(SRB(i))**4)*((2*(Sxy(i)+(k3xy(i)/1))*(Sxy(i)+(k3xy(i)/1)))+(Sxx(i)*Sxx(i))+(Syy(i)*Syy(i))+(Szz
(i)*Szz(i)))))*((Sxy(i)+(k3xy(i)/1))))/(lamda(i)*SRB(i)*SRB(i))))
                    Sxyn(i)=Sxy(i)+(k1xy(i)+2*k2xy(i)+2*k3xy(i)+k4xy(i))/6

                    k1zz(i)=h*(-(4*srate*Sxy(i)*Szz(i))-
((3*a(i)*SRB(i)*SRB(i)*Szz(i)*Szz(i))/(lamda(i)))-(((1-a(i)-
((3*a(i)*(SRB(i))**4)*((Sxx(i)*Sxx(i))+(Syy(i)*Syy(i))+(2*Sxy(i)*Sxy(i))+(Szz(i)*Szz(i)))))*(Szz(i)))/(lam
da(i)*SRB(i)*SRB(i)))+((1-a(i))/(3*lamda(i)*SRB(i)*SRB(i))))
                    k2zz(i)=h*(-(4*srate*Sxy(i)*(Szz(i)+(k1zz(i)/2)))-
((3*a(i)*SRB(i)*SRB(i)*(Szz(i)+(k1zz(i)/2))*(Szz(i)+(k1zz(i)/2)))/(lamda(i)))-(((1-a(i)-
((3*a(i)*(SRB(i))**4)*((Sxx(i)*Sxx(i))+(Syy(i)*Syy(i))+(2*Sxy(i)*Sxy(i))+((Szz(i)+(k1zz(i)/2))*(Szz(i)+(k
1zz(i)/2))))))*((Szz(i)+(k1zz(i)/2))))/(lamda(i)*SRB(i)*SRB(i)))+((1-a(i))/(3*lamda(i)*SRB(i)*SRB(i))))
                    k3zz(i)=h*(-(4*srate*Sxy(i)*(Szz(i)+(k2zz(i)/2)))-
((3*a(i)*SRB(i)*SRB(i)*(Szz(i)+(k2zz(i)/2))*(Szz(i)+(k2zz(i)/2)))/(lamda(i)))-(((1-a(i)-
((3*a(i)*(SRB(i))**4)*((Sxx(i)*Sxx(i))+(Syy(i)*Syy(i))+(2*Sxy(i)*Sxy(i))+((Szz(i)+(k2zz(i)/2))*(Szz(i)+(k
2zz(i)/2))))))*((Szz(i)+(k2zz(i)/2))))/(lamda(i)*SRB(i)*SRB(i)))+((1-a(i))/(3*lamda(i)*SRB(i)*SRB(i))))
                    k4zz(i)=h*(-(4*srate*Sxy(i)*(Szz(i)+(k3zz(i)/1)))-
((3*a(i)*SRB(i)*SRB(i)*(Szz(i)+(k3zz(i)/1))*(Szz(i)+(k3zz(i)/1)))/(lamda(i)))-(((1-a(i)-
```

```
((3*a(i)*(SRB(i))**4)*((Sxx(i)*Sxx(i))+(Syy(i)*Syy(i))+(2*Sxy(i)*Sxy(i))+((Szz(i)+(k3zz(i)/1))*(Szz(i)+(k
3zz(i)/1))))))*((Szz(i)+(k3zz(i)/1))))/(lamda(i)*SRB(i)*SRB(i)))+((1-a(i))/(3*lamda(i)*SRB(i)*SRB(i))))
                        Szzn(i)=Szz(i)+(k1zz(i)+2*k2zz(i)+2*k3zz(i)+k4zz(i))/6

                        k1SRB(i)=h*((srate*SRB(i)*(2*Sxy(i)))-((SRB(i)-1)/(l0s(i)*exp(-v(i)*(SRB(i)-
1)))))
                        k2SRB(i)=h*((srate*(SRB(i)+(k1SRB(i)/2))*(2*Sxy(i)))-
(((SRB(i)+(k1SRB(i)/2))-1)/(l0s(i)*exp(-v(i)*((SRB(i)+(k1SRB(i)/2))-1)))))
                        k3SRB(i)=h*((srate*(SRB(i)+(k2SRB(i)/2))*(2*Sxy(i)))-
(((SRB(i)+(k2SRB(i)/2))-1)/(l0s(i)*exp(-v(i)*((SRB(i)+(k2SRB(i)/2))-1)))))
                        k4SRB(i)=h*((srate*(SRB(i)+(k3SRB(i)/1))*(2*Sxy(i)))-
(((SRB(i)+(k3SRB(i)/1))-1)/(l0s(i)*exp(-v(i)*((SRB(i)+(k3SRB(i)/1))-1)))))
                        SRBn(i)=SRB(i)+(k1SRB(i)+2*k2SRB(i)+2*k3SRB(i)+k4SRB(i))/6

                        txxn(i)=(3*(eta(i)/lamda(i))*SRBn(i)*SRBn(i)*Sxx(i))-(eta(i)*lamda(i))
                        tyyn(i)=(3*(eta(i)/lamda(i))*SRBn(i)*SRBn(i)*Syy(i))-(eta(i)*lamda(i))
                        txyn(i)=(3*(eta(i)/lamda(i))*SRBn(i)*SRBn(i)*Sxy(i))-(eta(i)*lamda(i))
                        tzzn(i)=(3*(eta(i)/lamda(i))*SRBn(i)*SRBn(i)*Szz(i))-(eta(i)*lamda(i))

                        sviscn(i)=(txyn(i))/srate
                END DO                                          !(c)

                svisn=0
                DO k=1, no                                      !(d)
                   svisn=svisn+sviscn(k)
                END DO                                          !(d)
                error=ABS(svisn-svis)
                WRITE(*,*) tn, svisn, error
                WRITE(1,*) tn, svisn, error
        END DO                                                  !(2)

        !*****CLOSING OUTPUT FILE*****
        CLOSE (1, STATUS='KEEP')
        END PROGRAM XPPSHEAR
```

2. Shear Free Flow

```
! XPPELONGATION.f90
!
!**************************************************************************
!
! PROGRAM: XPPELONGATION
!
! PURPOSE:  To obtain elongational viscosity using XPP model.
!
!**************************************************************************

        PROGRAM XPPELONGATION

        IMPLICIT NONE

        !*****VARIABLES*****
        REAL   t, tn                                    !time
        REAL   Sxx(8), Szz(8), Sxxn(8), Szzn(8)         !S tensor components
```

```
REAL   txx(8), tzz(8), txxn(8), tzzn(8)              !Stress tensor components
REAL   SRB(8), SRBn(8)                               !Strech ratio of the backbone
REAL   ls                                            !lamdas: stretch relaxation time
REAL   l0s(8)                                        !lamda0s: stretch relaxation time 0
REAL   v(8)      !measure of the influence of the surroundings polymer chains
REAL   a(8)      !alpha: Material parameter defining the amount of anisotropy
REAL   lamda(8), eta(8)          !discrite relaxation spectrum
INTEGER        no        !Number of elements in the discrete relaxation spectrum
INTEGER        q(8)      !Number of dangling arms in the pom-pom molecule
REAL   h, tol, error, erate, evis, evisn, sumxx, sumzz
REAL   k1xx(8), k2xx(8), k3xx(8), k4xx(8)
REAL   k1zz(8), k2zz(8), k3zz(8), k4zz(8)
REAL   k1SRB(8), k2SRB(8), k3SRB(8), k4SRB(8)
REAL   evisc(8), eviscn(8)
REAL   r(4)
INTEGER                i, j, k, l, m, n
CHARACTER*20           out1

!*****OPENING OUTPUT FILE*****
out1 = 'evisc.dat'
OPEN (1, FILE=out1)

!*****INPUT*****
! Relaxation Spectrum and fitting parameters
WRITE(*,*) 'Number of relaxation elements:  '
READ(*,*)  no

DO k=1, no
        WRITE(*,*) 'Relaxation time'
        READ(*,*) lamda(k)
        WRITE(*,*) 'Relaxation spectrum viscosity'
        READ(*,*) eta(i)
        WRITE(*,*) 'Number of dangling arms in the pom-pom molecule  q', k
        READ(*,*) q(k)
        WRITE(*,*) 'Ratio between relaxation time and stretch relaxation time 0', k
        READ(*,*) r(k)
        WRITE(*,*) 'Material parameter defining the amount of anisotropy   a', k
        READ(*,*) a(k)
!measure of the influence of the surroundings polymer chains on thebackbone tube stretch
        v(k)=2/q(k)
!stretch relaxation time 0
        l0s(k)=lamda(k)/r(k)
END DO

! Extension rate
WRITE(*,*) 'Extension rate'
READ(*,*) erate

! Step
WRITE(*,*) 'Step size'
READ(*,*) h

! Tolerance
tol=0.0000001

!*****SOLVING DIFFERENTIAL EQUATIONS*****
```

```
! Runge-Kutta Method (Fourth Order)
error=tol+1
tn=0
evisn=0
DO i=1, no                                                    !(a)
        Sxxn(i)=0.333333
        Szzn(i)=0.33333333
        SRBn(i)=1
        txxn(i)=0
        tzzn(i)=0
        eviscn(i)=0
END DO                                                        !(a)
DO WHILE (error>tol)                                          !(2)
        t=tn
        evis=evisn
        DO j=1, no                                            !(b)
                Sxx(j)=Sxxn(j)
                Szz(j)=Szzn(j)
                SRB(j)=SRBn(j)
                txx(j)=txxn(j)
                tzz(j)=tzzn(j)
                evisc(j)=eviscn(j)
        END DO                                                !(b)

        tn=t+h
        DO i=1, no                                            !(c)
                k1xx(i)=h*(-(erate*Sxx(i))+(4*erate*Sxx(i)*(Sxx(i)-Szz(i)))-
((3*a(i)*SRB(i)*SRB(i)*Sxx(i)*Sxx(i))/(lamda(i)))-(((1-a(i)-
((3*a(i)*(SRB(i))**4)*((2*Sxx(i)*Sxx(i))+(Szz(i)*Szz(i)))))*(Sxx(i)))/(lamda(i)*SRB(i)*SRB(i)))+((1-
a(i))/(3*lamda(i)*SRB(i)*SRB(i))))
                k2xx(i)=h*(-
(erate*(Sxx(i)+(k1xx(i)/2)))+(4*erate*(Sxx(i)+(k1xx(i)/2))*((Sxx(i)+(k1xx(i)/2))-Szz(i)))-
((3*a(i)*SRB(i)*SRB(i)*(Sxx(i)+(k1xx(i)/2))*(Sxx(i)+(k1xx(i)/2)))/(lamda(i)))-(((1-a(i)-
((3*a(i)*(SRB(i))**4)*((2*(Sxx(i)+(k1xx(i)/2))*(Sxx(i)+(k1xx(i)/2)))+(Szz(i)*Szz(i)))))*((Sxx(i)+(k1xx(i)/2
))))/(lamda(i)*SRB(i)*SRB(i)))+((1-a(i))/(3*lamda(i)*SRB(i)*SRB(i))))
                k3xx(i)=h*(-
(erate*(Sxx(i)+(k2xx(i)/2)))+(4*erate*(Sxx(i)+(k2xx(i)/2))*((Sxx(i)+(k2xx(i)/2))-Szz(i)))-
((3*a(i)*SRB(i)*SRB(i)*(Sxx(i)+(k2xx(i)/2))*(Sxx(i)+(k2xx(i)/2)))/(lamda(i)))-(((1-a(i)-
((3*a(i)*(SRB(i))**4)*((2*(Sxx(i)+(k2xx(i)/2))*(Sxx(i)+(k2xx(i)/2)))+(Szz(i)*Szz(i)))))*((Sxx(i)+(k2xx(i)/2
))))/(lamda(i)*SRB(i)*SRB(i)))+((1-a(i))/(3*lamda(i)*SRB(i)*SRB(i))))
                k4xx(i)=h*(-
(erate*(Sxx(i)+(k3xx(i)/1)))+(4*erate*(Sxx(i)+(k3xx(i)/1))*((Sxx(i)+(k3xx(i)/1))-Szz(i)))-
((3*a(i)*SRB(i)*SRB(i)*(Sxx(i)+(k3xx(i)/1))*(Sxx(i)+(k3xx(i)/1)))/(lamda(i)))-(((1-a(i)-
((3*a(i)*(SRB(i))**4)*((2*(Sxx(i)+(k3xx(i)/1))*(Sxx(i)+(k3xx(i)/1)))+(Szz(i)*Szz(i)))))*((Sxx(i)+(k3xx(i)/1
))))/(lamda(i)*SRB(i)*SRB(i)))+((1-a(i))/(3*lamda(i)*SRB(i)*SRB(i))))
                Sxxn(i)=Sxx(i)+(k1xx(i)+2*k2xx(i)+2*k3xx(i)+k4xx(i))/6

                k1zz(i)=h*((2*erate*Szz(i))+(4*erate*Szz(i)*(Sxx(i)-Szz(i)))-
((3*a(i)*SRB(i)*SRB(i)*Szz(i)*Szz(i))/(lamda(i)))-(((1-a(i)-
((3*a(i)*(SRB(i))**4)*((2*Sxx(i)*Sxx(i))+(Szz(i)*Szz(i)))))*(Szz(i)))/(lamda(i)*SRB(i)*SRB(i)))+((1-
a(i))/(3*lamda(i)*SRB(i)*SRB(i))))

        k2zz(i)=h*((2*erate*(Szz(i)+(k1zz(i)/2)))+(4*erate*(Szz(i)+(k1zz(i)/2))*(Sxx(i)-
(Szz(i)+(k1zz(i)/2))))-((3*a(i)*SRB(i)*SRB(i)*(Szz(i)+(k1zz(i)/2))*(Szz(i)+(k1zz(i)/2)))/(lamda(i)))-(((1-
a(i)-
```

```
((3*a(i)*(SRB(i))**4)*((2*Sxx(i)*Sxx(i))+((Szz(i)+(k1zz(i)/2))*(Szz(i)+(k1zz(i)/2))))))*((Szz(i)+(k1zz(i)/2
))))/(lamda(i)*SRB(i)*SRB(i)))+((1-a(i))/(3*lamda(i)*SRB(i)*SRB(i))))

        k3zz(i)=h*((2*erate*(Szz(i)+(k2zz(i)/2)))+(4*erate*(Szz(i)+(k2zz(i)/2))*(Sxx(i)-
(Szz(i)+(k2zz(i)/2))))-((3*a(i)*SRB(i)*SRB(i)*(Szz(i)+(k2zz(i)/2))*(Szz(i)+(k2zz(i)/2)))/(lamda(i)))-(((1-
a(i))-
((3*a(i)*(SRB(i))**4)*((2*Sxx(i)*Sxx(i))+((Szz(i)+(k2zz(i)/2))*(Szz(i)+(k2zz(i)/2))))))*((Szz(i)+(k2zz(i)/2
))))/(lamda(i)*SRB(i)*SRB(i)))+((1-a(i))/(3*lamda(i)*SRB(i)*SRB(i))))

        k4zz(i)=h*((2*erate*(Szz(i)+(k3zz(i)/1)))+(4*erate*(Szz(i)+(k3zz(i)/1))*(Sxx(i)-
(Szz(i)+(k3zz(i)/1))))-((3*a(i)*SRB(i)*SRB(i)*(Szz(i)+(k3zz(i)/1))*(Szz(i)+(k3zz(i)/1)))/(lamda(i)))-(((1-
a(i))-
((3*a(i)*(SRB(i))**4)*((2*Sxx(i)*Sxx(i))+((Szz(i)+(k3zz(i)/1))*(Szz(i)+(k3zz(i)/1))))))*((Szz(i)+(k3zz(i)/1
))))/(lamda(i)*SRB(i)*SRB(i)))+((1-a(i))/(3*lamda(i)*SRB(i)*SRB(i))))
                Szzn(i)=Szz(i)+(k1zz(i)+2*k2zz(i)+2*k3zz(i)+k4zz(i))/6

                k1SRB(i)=h*(-(2*erate*SRB(i)*(Sxx(i)-Szz(i)))-((SRB(i)-1)/(l0s(i)*exp(-
v(i)*(SRB(i)-1)))))
                k2SRB(i)=h*(-(2*erate*(SRB(i)+(k1SRB(i)/2))*(Sxx(i)-Szz(i)))-
(((SRB(i)+(k1SRB(i)/2))-1)/(l0s(i)*exp(-v(i)*((SRB(i)+(k1SRB(i)/2))-1)))))
                k3SRB(i)=h*(-(2*erate*(SRB(i)+(k2SRB(i)/2))*(Sxx(i)-Szz(i)))-
(((SRB(i)+(k2SRB(i)/2))-1)/(l0s(i)*exp(-v(i)*((SRB(i)+(k2SRB(i)/2))-1)))))
                k4SRB(i)=h*(-(2*erate*(SRB(i)+(k3SRB(i)/1))*(Sxx(i)-Szz(i)))-
(((SRB(i)+(k3SRB(i)/1))-1)/(l0s(i)*exp(-v(i)*((SRB(i)+(k3SRB(i)/1))-1)))))
                SRBn(i)=SRB(i)+(k1SRB(i)+2*k2SRB(i)+2*k3SRB(i)+k4SRB(i))/6

                txxn(i)=(3*(eta(i)/lamda(i))*SRBn(i)*SRBn(i)*Sxx(i))-(eta(i)*lamda(i))
                tzzn(i)=(3*(eta(i)/lamda(i))*SRBn(i)*SRBn(i)*Szz(i))-(eta(i)*lamda(i))
                eviscn(i)=(tzzn(i)-txxn(i))/erate
        END DO                                          !(c)

        evisn=0
        DO k=1, no                                      !(d)
                evisn=evisn+eviscn(k)
        END DO                                          !(d)
        error=ABS(evisn-evis)
        WRITE(*,*) tn, evisn, error
        WRITE(1,*) tn, evisn, error
END DO                                                  !(2)

!*****CLOSING OUTPUT FILE*****
CLOSE (1, STATUS='KEEP')
END PROGRAM XPPELONGATION
```

C. Random Walks

Random walk theory is described in Chapters II and XII. Chapter XII presents some simulations of the random growth of polymer chains, where the starting points were considered as the active sites in the catalyst surface. Here are

presented the codes developed to generate the random walks in one (1-D) and two (2-D) dimensions.

1. 1-D

```
! 1DRW.f90
!
!*****************************************************************************
!
! PROGRAM:  1DRW
!
! PURPOSE:  To obtain the number of junctions between "two chains" ( one
!           random walks). The number of steps in the random walks is
!           given by the user, as well as the number of iterations and the
!           distance between the starting points of the chains.
!
!*****************************************************************************

      PROGRAM RW1D

      IMPLICIT NONE

      !*****VARIABLES*****

      REAL        rA, rB, RAND          !random numbers
      REAL        jun(1500)             !junctions
      REAL        avejun                !average of junctions
      INTEGER     d                     !distance between starting points
      INTEGER     n                     !number of steps
      INTEGER     it                    !number of iterations
      INTEGER     x(500)                !step
      INTEGER     yA(500)               !position of chain A
      INTEGER     yB(500)               !position of chain B
      INTEGER     i, j, k, cont, res, leo   !auxiliary variables
      CHARACTER   archrs6, archrs7      !output files

      !*****OPEN OUTPUT FILES*****

      archrs6 = 'junctions.dat'
      archrs7 = '1DRW.dat'

      OPEN (6, FILE=archrs6)
      OPEN (7, FILE=archrs7)

      !*****INPUT*****

      WRITE(*,*) 'Distance between starting points'
      READ(*,*) d
      WRITE(*,*) 'number of steps'
      READ(*,*) n
      WRITE(*,*) 'number of iterations'
      READ(*,*) it
```

```
DO j=1, it                                    !Iterations loop (1)
        cont=0
        leo=0
        x(1)=0                                !initial position
        yA(1)=0                               !initial position
        yB(1)=d                               !initial position
        WRITE(*,*) x(1), yA(1), yB(1)
        WRITE(7,*) x(1), yA(1), yB(1)
        DO i=2, n                             !Number of steps loop (2)
                x(i)=x(i-1)+1
                rA=rand()                     !random number between 0 and 1
                rB=rand()                     !random number between 0 and 1
                IF (rA<0.3333)  THEN          ! Chain A new position (A)
                                yA(i)=yA(i-1)-1
                        ELSE
                                IF (rA<0.6666)  THEN
                                                yA(i)=yA(i-1)
                                        ELSE
                                                yA(i)=yA(i-1)+1
                                END IF
                END IF                        ! Chain A new position (A)
                IF (rB<0.3333)  THEN          ! Chain B new position (B)
                                yB(i)=yB(i-1)-1
                        ELSE
                                IF (rB<0.6666)  THEN
                                                yB(i)=yB(i-1)
                                        ELSE
                                                yB(i)=yB(i-1)+1
                                END IF
                END IF                        !Chain B new position (B)
                WRITE(*,*) x(i), yA(i), yB(i)
                WRITE(7,*) x(i), yA(i), yB(i)
                res=yA(i)-yB(i)
                IF (res.EQ.0)   THEN
                                leo=1
                        ELSE
                                leo=0
                END IF
                cont=cont+leo

        END DO                                ! Number of steps loop (2)
        jun(j)=cont
END DO      !Number of iterations loop (1)

avejun=cont/it

DO k=1, it
        WRITE(6,*) jun(k)
END DO

!*****CLOSING OUTPUT FILES*****

CLOSE (6, STATUS='KEEP')
CLOSE (7, STATUS='KEEP')

END PROGRAM RW1D
```

The program was used with different distance between starting points (d). Some results are presented in Figure B.1 through Figure B.3.

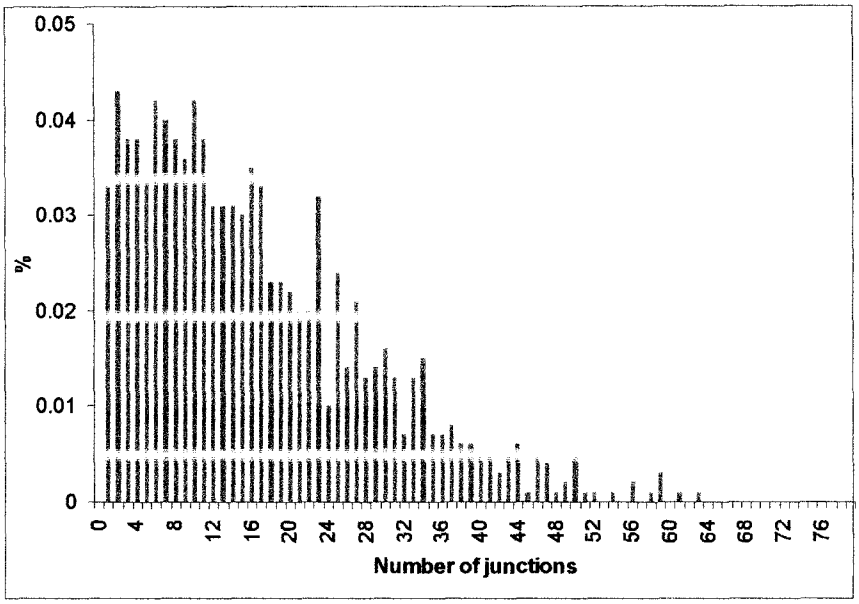

Figure B.1. Number of junctions distribution using d = 0.

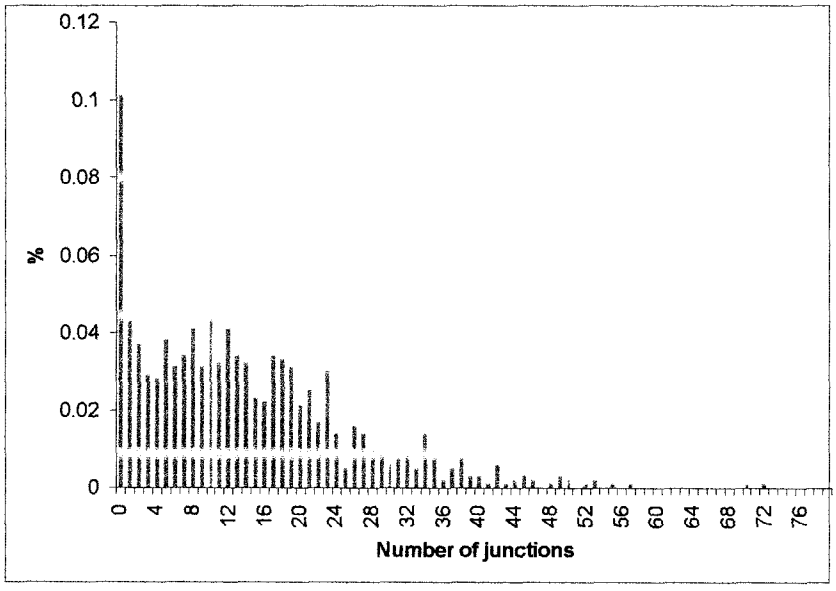

Figure B.2. Number of junctions distribution using d = 3.

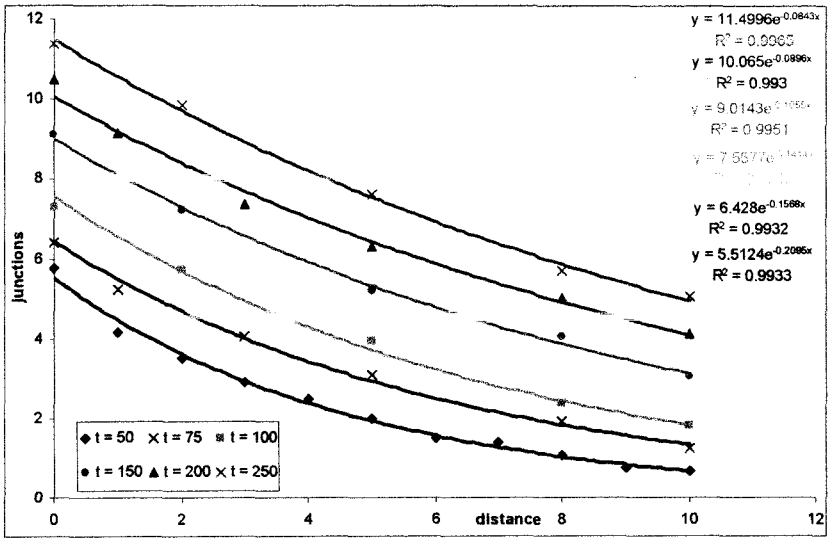

Figure B.3. Relationship between the average of junctions and distance (d) for different number of steps (t).

2. 2-D

```
! 2DRW.f90
!
! FUNCTIONS:
!       2DRW    - Entry point of console application.
!
!*****************************************************************************************
!
! PROGRAM: 2DRW
!
! PURPOSE:  To obtain the number of junctions between "two chains" ( two
!           dimension random walks). The number of steps in the random walks
!           is given by the user, as well as the number of iterations and the
!           distance between the starting points of the chains.
!
!*****************************************************************************************

      PROGRAM RW2D

      IMPLICIT NONE

      !*****VARIABLES*****

      REAL      raA, rbA, raB, rbB, RAND    !random numbers
      REAL      jun(1500)                   !junctions
      REAL      avejun                      !average of junctions
      INTEGER   d                           !distance between strating point
      INTEGER   n                           !number of steps
      INTEGER   it                          !number of iterations
      INTEGER   xA(500)                     !X position in chain A
      INTEGER   xB(500)                     !X position in chain B
```

```
INTEGER      yA(500)                !Y position in chain A
INTEGER      yB(500)                !Y position in chain B
INTEGER      ABx(500,500)           !junctions in X
INTEGER      ABy(500,500)           !junctions in Y
INTEGER      AB(500,500)            !junctions
INTEGER           i, j, k, h, cont, res, leoA, leoB, kjA, kjB
CHARACTER*20      archrs6, archrs7

!*****OPENING OUTPUT FILES*****

archrs6 = 'jun2D.dat'
archrs7 = '2DRW.dat'

OPEN (6, FILE=archrs6)
OPEN (7, FILE=archrs7)

!*****INPUT*****

WRITE(*,*) 'Distance between starting points'
READ(*,*) d
WRITE(*,*) 'Number of steps'
READ(*,*) n
WRITE(*,*)'Number of iterations'
READ(*,*) it

!*****CHAIN GROWTH*****

DO j=1, it                                  !Iteration loop (1)

        cont=0
        xA(1)=0                             !initial position
        yA(1)=0
        xB(1)=0
        yB(1)=d
        !WRITE(*,*) xA(1), xB(1), yA(1), yB(1)
        WRITE(7,*) xA(1), xB(1), yA(1), yB(1)
        DO i=2, n                           !Number of steps loop (2)
                raA=rand()      !Random number to decide the direction of growth in A
                raB=rand()      !Random number to decide the direction of growth in B
                rbA=rand()      !Random number to decide the sense of growth in A
                rbB=rand()      !Random number to decide the sense of growth in B
                IF (raA>0.5)            THEN                    ! (A)
                                                kjA=1
                                        ELSE
                                                kjA=0
                END IF                                          ! (A)
                IF (raB>0.5)            THEN                    ! (B)
                                                kjB=1
                                        ELSE
                                                kjB=0
                END IF                                          ! (B)
                ! kj = 0, movement in X
                ! kj = 1, movement in Y

                !NEW xA
                IF (kjA==0)     THEN                                    ! (2A)
```

```
                                IF (rbA>0.5)    THEN        ! (3A)
                                                            xA(i)=xA(i-1)+1
                                                ELSE
                                                            xA(i)=xA(i-1)-1
                                END IF                      ! (3A)
                        ELSE
                                xA(i)=xA(i-1)
        END IF                                              ! (2A)

        !NEW xB
        IF (kjB==0)     THEN                                ! (2B)
                                IF (rbB>0.5)    THEN        ! (3B)
                                                            xB(i)=xB(i-1)+1
                                                ELSE
                                                            xB(i)=xB(i-1)-1
                                END IF                      ! (3B)
                        ELSE
                                xB(i)=xB(i-1)
        END IF                                              ! (2B)

        !NEW yA
        IF (kjA==1)     THEN                                ! (2A)
                                IF (rbA>0.5)    THEN        ! (3A)
                                                            yA(i)=yA(i-1)+1
                                                ELSE
                                                            yA(i)=yA(i-1)-1
                                END IF                      ! (3A)
                        ELSE
                                yA(i)=yA(i-1)
        END IF                                              ! (2A)

        !NEW yB
        IF (kjB==1)     THEN                                ! (2B)
                                IF (rbB>0.5)    THEN        ! (3B)
                                                            yB(i)=yB(i-1)+1
                                                ELSE
                                                            yB(i)=yB(i-1)-1
                                END IF                      ! (3B)
                        ELSE
                                yB(i)=yB(i-1)
        END IF                                              ! (2B)
        WRITE(7,*) xA(i), yA(i), xB(i), yB(i)
END DO                                          !Number of steps loop (2)

!*****NUMBER OF JUNCTIONS*****
DO k=1, n                                                   !(1)
        DO h=1, n                                           !(2)
                IF (xA(k)==xB(h))       THEN                !X
                                                ABx(k,h)=1
                                        ELSE
                                                ABx(k,h)=0
                END IF                                      !X
                IF (yA(k)==yB(h))       THEN                !Y
                                                ABy(k,h)=1
                                        ELSE
                                                ABy(k,h)=0
```

```
                    END IF                                          !Y
                    AB(k,h)=ABx(k,h)*ABy(k,h)
                    cont=cont+AB(k,h)
                END DO                                              !(2)
            END DO                                                  !(1)
            WRITE(*,*) cont
            jun(j)=cont
    END DO                                                          !Iterations loop (1)
    DO k=1, it
            WRITE(6,*) jun(k)
    END DO

    !*****CLOSING OUPUT FILE*****

    CLOSE (6, STATUS='KEEP')
    CLOSE (7, STATUS='KEEP')

    END PROGRAM RW2D
```

Some results obtained with this program are presented next.

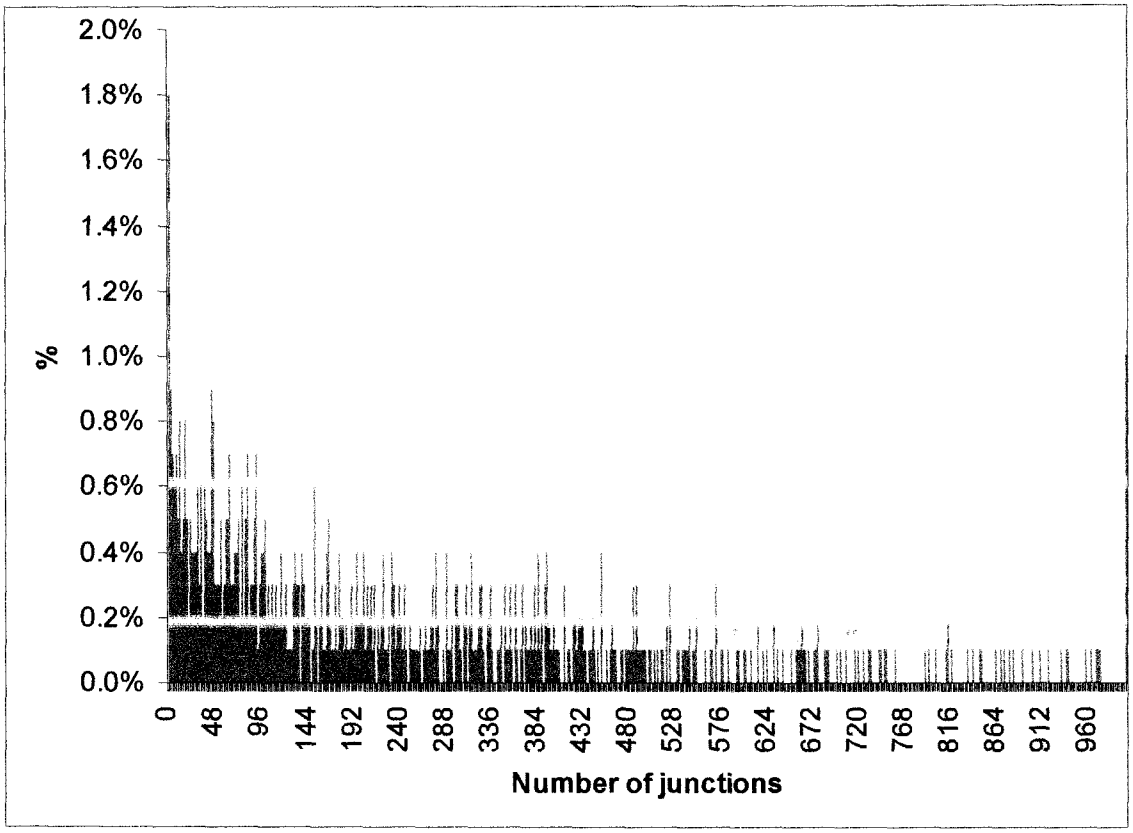

Figure B.4. Number of junctions distribution using d = 0.

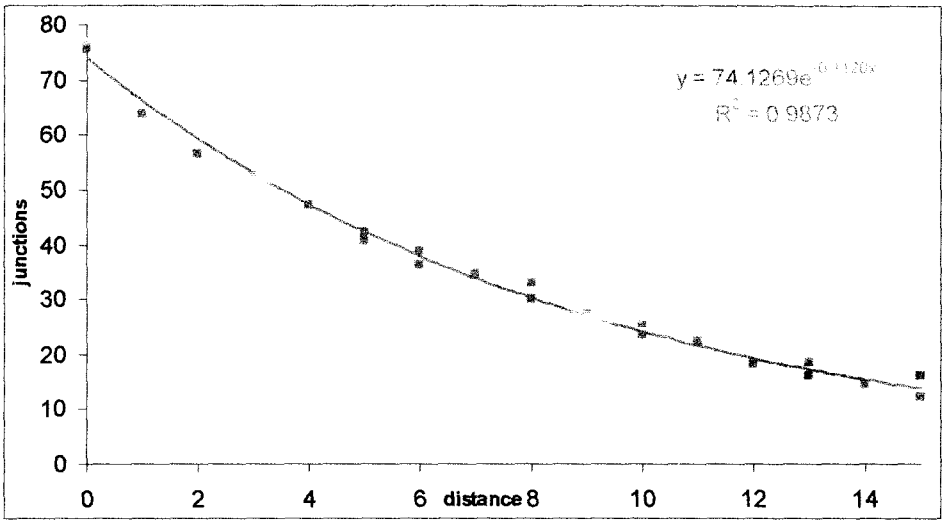

Figure B.5. Relationship between the average of junctions and distance (d) for different number of steps (t).

D. Self-avoiding Random Walks

Self-avoiding random walks are introduced in Chapter II and are used to simulate the random growth of polymer chains in Chapter XII. In this case, as well as in random walks, the starting points were considered as the active sites in the catalyst surface. Here are presented the codes developed to generate the self-avoiding random walks (SAW's) in two (2-D) and three (3-D) dimensions.

1. 2-D

```
! SARW2D.f90
!
! FUNCTIONS:
!       SARW2D     - Entry point of console application.
!
!****************************************************************************
!
! PROGRAM: SARW2D
!
! PURPOSE:  To obtain the number of junctions between "two chains" ( two
!           dimension SAW's). The number of steps in the random walks
!           is given by the user, as well as the number of iterations and the
!           distance between the starting points of the chains..
!
!****************************************************************************
```

```
PROGRAM SARW2D

      IMPLICIT NONE

      !*****VARIABLES*****

      REAL          raA, rbA, raB, rbB, RAND        !random numbers
      REAL          maxX, maxY, minX, minY
      REAL          jun(1500)                       !junctions
      INTEGER       d                               !distance between strating points
      INTEGER       n                               !number of steps
      INTEGER       it                              !number of iterations
      INTEGER       xA(500), nxA(500)               !X position in chain A
      INTEGER       xB(500), nxB(500)               !X position in chain B
      INTEGER       yA(500), nyA(500)               !Y position in chain A
      INTEGER       yB(500), nyB(500)               !Y position in chain B
      INTEGER       ABx(500,500)                    !junctions in X
      INTEGER       ABy(500,500)                    !junctions in Y
      INTEGER       AB(500,500)                     !junctions
      INTEGER       leoxa(500,500), leoxb(500,500)
      INTEGER       leoya(500,500), leoyb(500,500)
      INTEGER       ca(1500), cb(1500)
      INTEGER             conta, contb, i, j, k, h, cont, res, kjA, kjB
      CHARACTER*20  archrs5, archrs6, archrs7

      !*****OPENING OUTPUT FILES*****

      archrs6 = 'junSAW(2).dat'
      archrs7 = 'SAW(2).dat'

      OPEN (6, FILE=archrs6)
      OPEN (7, FILE=archrs7)

      !*****INPUT*****

      WRITE(*,*) 'Distancia entre los puntos de origen'
      READ(*,*) d
      WRITE(*,*) 'numero de pasos (maximo 499)'
      READ(*,*) n
      WRITE(*,*) 'numero de iteraciones (maximo 1499)'
      READ(*,*) it

      !*****LIMITS FOR X AND Y*****

      maxX=n/5
      maxY=n/5
      minX=-n/5
      minY=-n/5

      !*****CHAIN GROWTH*****

      DO j=1, it                                    !Iteration loop (1)
            cont=0
            xA(1)=0                                 !initial position
            yA(1)=0
```

```
xB(1)=0
yB(1)=d
nxA(1)=0
nyA(1)=0
nxB(1)=0
nyB(1)=d
DO i=2, n                                   ! Number of steps loop (2)
        raA=rand()      !Random number to decide the direction of growth in A
        raB=rand()      !Random number to decide the direction of growth in B
        rbA=rand()      !Random number to decide the sense of growth in A
        rbB=rand()      !Random number to decide the sense of growth in B
        IF (raA>0.5)            THEN                            ! (A)
                                    kjA=1
                                ELSE
                                    kjA=0
        END IF                                                  ! (A)
        IF (raB>0.5)            THEN                            ! (B)
                                    kjB=1
                                ELSE
                                    kjB=0
        END IF                                                  ! (B)
        ! kj = 0, movement in X
        ! kj = 1, movement in Y

        !NEW xA
        IF (kjA==0)     THEN                                    ! (2A)
                            IF (rbA>0.5)    THEN                ! (3A)
                                                xA(i)=xA(i-1)+1
                                            ELSE
                                                xA(i)=xA(i-1)-1
                            END IF                              ! (3A)
                        ELSE
                            xA(i)=xA(i-1)
        END IF                                                  ! (2A)
        IF (xA(i)>maxX .OR. xA(i)<minX)     THEN
                                                xA(i)=xA(i-1)
        END IF

        !NEW xB
        IF (kjB==0)     THEN                                    ! (2B)
                            IF (rbB>0.5)    THEN                ! (3B)
                                                xB(i)=xB(i-1)+1
                                            ELSE
                                                xB(i)=xB(i-1)-1
                            END IF                              ! (3B)
                        ELSE
                            xB(i)=xB(i-1)
        END IF                                                  ! (2B)
        IF (xB(i)>maxX .OR. xB(i)<minX)     THEN
                                                xB(i)=xB(i-1)
        END IF

        !NEW yA
        IF (kjA==1)     THEN                                    ! (2A)
                            IF (rbA>0.5)    THEN                ! (3A)
                                                yA(i)=yA(i-1)+1
```

```
                                        ELSE
                                            yA(i)=yA(i-1)-1
                        END IF                                          ! (3A)
                    ELSE
                        yA(i)=yA(i-1)
    END IF                                                              ! (2A)
    IF (yA(i)>maxY .OR. yA(i)<minY)     THEN
                                            yA(i)=yA(i-1)
    END IF

    !NEW yB
    IF (kjB==1)     THEN                                                ! (2B)
                        IF (rbB>0.5)    THEN                            ! (3B)
                                            yB(i)=yB(i-1)+1
                                        ELSE
                                            yB(i)=yB(i-1)-1
                        END IF                                          ! (3B)
                    ELSE
                        yB(i)=yB(i-1)
    END IF                                                              ! (2B)
    IF (yB(i)>maxY .OR. yB(i)<minY)     THEN
                                            yB(i)=yB(i-1)
    END IF

!*****SAW RESTRICTIONS*****

    conta=0
    contb=0
    DO k=1, i-1                                                         !(1)
        IF (xA(i)==xA(k))           THEN
                                        leoxa(i,k)=1
                                    ELSE
                                        leoxa(i,k)=0
        END IF
        IF (yA(i)==yA(k))           THEN
                                        leoya(i,k)=1
                                    ELSE
                                        leoya(i,k)=0
        END IF
        IF (xB(i)==xB(k))           THEN
                                        leoxb(i,k)=1
                                    ELSE
                                        leoxb(i,k)=0
        END IF
        IF (yB(i)==yB(k))           THEN
                                        leoyb(i,k)=1
                                    ELSE
                                        leoyb(i,k)=0
        END IF
        conta=conta+leoxa(i,k)*leoya(i,k)
        contb=contb+leoxb(i,k)*leoyb(i,k)
    END DO                                                              !(1)

        IF (conta>0)                THEN
                                        xA(i)=xA(i-1)
                                        yA(i)=yA(i-1)
```

```
                                        ELSE
                                            xA(i)=xA(i)
                                            yA(i)=yA(i)
                    END IF
                    IF (contb>0)            THEN
                                            xB(i)=xB(i-1)
                                            yB(i)=yB(i-1)
                                        ELSE
                                            xA(i)=xA(i)
                                            yB(i)=yB(i)
                    END IF
END DO                                      !Number of steps loop (2)

        !*****ELIMINATING REPEATED POINTS*****

        h=1
        k=1
        DO WHILE (h<=n)                                         !(2)
                h=h+1
                k=k+1
                IF (xA(h)==nxA(k-1) .AND. yA(h)==nyA(k-1)) THEN
                                                                k=k-1
                                                            ELSE
                                                                nxA(k)=xA(h)
                                                                nyA(k)=yA(h)
                END IF
        END DO                                                  !(2)
        ca(j)=k-1

        h=1
        k=1
        DO WHILE (h<=n)                                         !(2)
                h=h+1
                k=k+1
                IF (xB(h)==nxB(k-1) .AND. yB(h)==nyB(k-1)) THEN
                                                                k=k-1
                                                            ELSE
                                                                nxB(k)=xB(h)
                                                                nyB(k)=yB(h)
                END IF
        END DO                                                  !(2)
        cb(j)=k-1

!*****FINAL SAW*****

DO i=1, ca(j)
        WRITE(7,*) nxA(i), nyA(i), j, 'A'
END DO
DO i=1, cb(j)
        WRITE(7,*) nxB(i), nyB(i), j, 'B'
END DO
!*****NUMBER OF JUNCTIONS*****
DO k=1, ca(j)                                           !(1)
        DO h=1, cb(j)                                   !(2)
                IF (nxA(k)==nxB(h))     THEN            !X
```

```
                                                    ABx(k,h)=1
                                                ELSE
                                                    ABx(k,h)=0
                        END IF                                  !X
                        IF (nyA(k)==nyB(h))     THEN            !Y
                                                    ABy(k,h)=1
                                                ELSE
                                                    ABy(k,h)=0
                        END IF                                  !Y
                        AB(k,h)=ABx(k,h)*ABy(k,h)
                        cont=cont+AB(k,h)
                    END DO                                      !(2)
                END DO                                          !(1)
                WRITE(*,*) cont, ca(j), cb(j)
                jun(j)=cont
END DO                                                          !Iterations loop (1)

DO k=1, it
        WRITE(6,*) jun(k), ca(k), cb(k)
END DO

!*****CLOSING OUPUT FILE*****

CLOSE (6, STATUS='KEEP')
CLOSE (7, STATUS='KEEP')

END PROGRAM SARW2D
```

Figures B.6 to B.8 show results from this program.

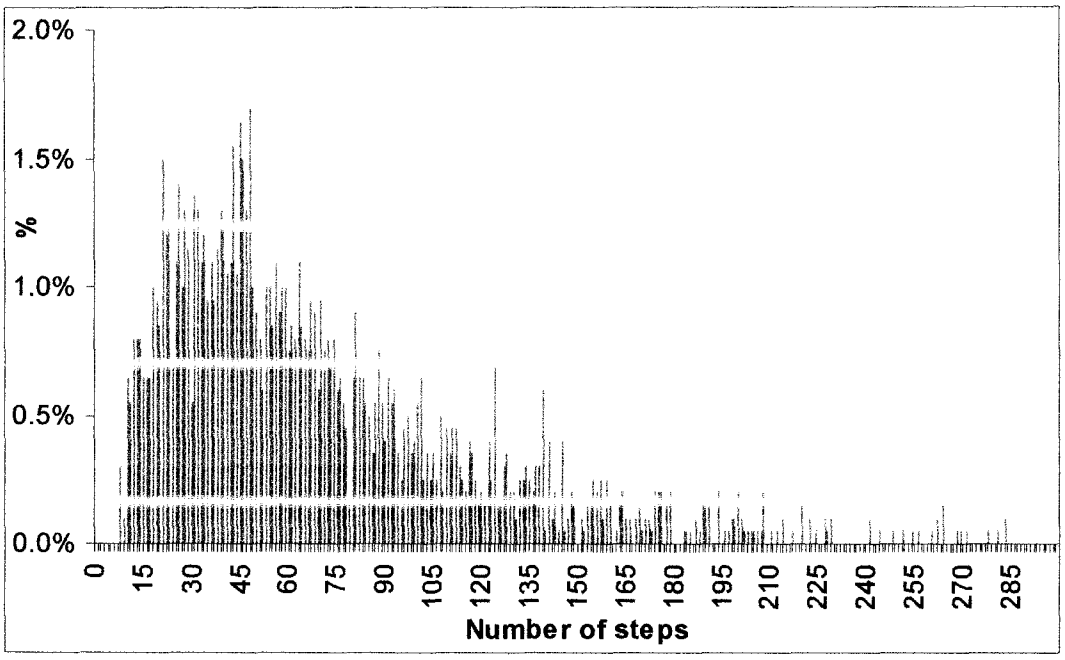

Figure B.6. Chains' length distribution.

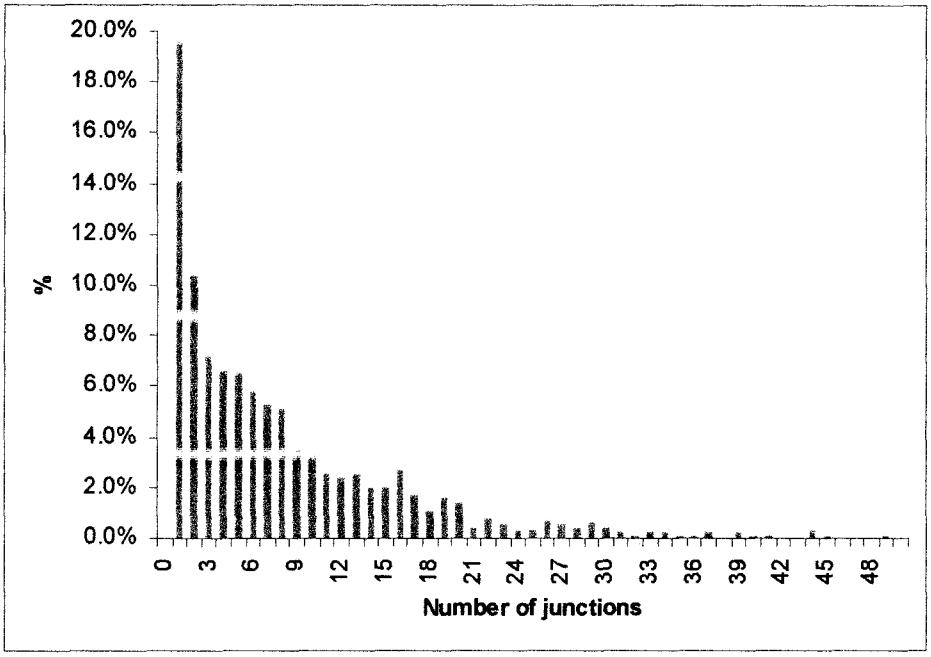

Figure B.7. Number of junctions distribution using d = 0.

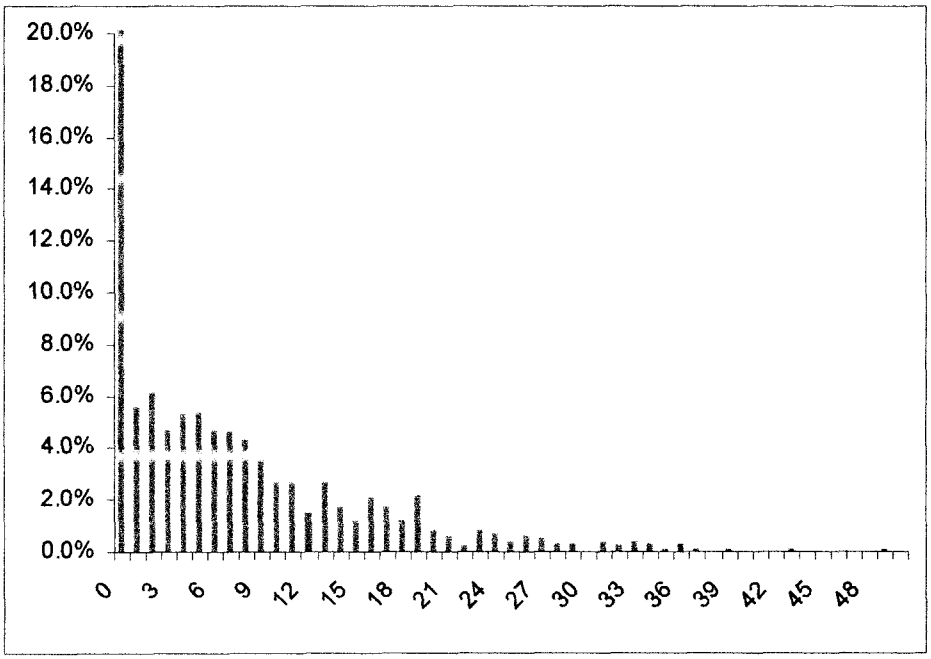

Figure B.8. Number of junctions distribution using d = 3.

2. 3-D

```
! SAW3DV2.f90
!
! FUNCTIONS:
!       SAW3DV2     - Entry point of console application.
!
!****************************************************************************************
!
! PROGRAM: SAW3DV2
!
! PURPOSE:  To obtain the number of junctions between "two chains" ( three
!           dimension self-avoiding random walks). The number of steps
!           in the SAW's is given by the user, as well as the number of iterations
!           and the distance between the starting points of the chains.
!
!****************************************************************************************

PROGRAM SAW3Dv2

      IMPLICIT NONE

      !*****VARIABLES*****

      REAL          raA, rbA, raB, rbB, RAND                    !random numbers
      REAL          maxX, maxY, minX, minY, maxZ, minZ
      REAL          jun(1501)       !junctions
      INTEGER       d               !distance between strating points
      INTEGER       n               !number of steps
      INTEGER       it              !number of iterations
      INTEGER       xA(1501), nxA(1501)   !X position in chain A
      INTEGER       xB(1501), nxB(1501)   !X position in chain B
      INTEGER       yA(1501), nyA(1501)   !Y position in chain A
      INTEGER       yB(1501), nyB(1501)   !Y position in chain B
      INTEGER       zA(1501), nzA(1501)   !Z position in chain A
      INTEGER       zB(1501), nzB(1501)   !Z position in chian B
      INTEGER       ABx(1501,1501)        !junctions in X
      INTEGER       ABy(1501,1501)        !junctions in Y
      INTEGER       ABz(1501,1501)        !junctions in Z
      INTEGER       AB(1501,1501)         !junctions
      INTEGER       leoxa(1501,1501), leoxb(1501,1501)
      INTEGER       leoya(1501,1501), leoyb(1501,1501)
      INTEGER       leoza(1501,1501), leozb(1501,1501)
      INTEGER       ca(1501), cb(1501)
      INTEGER             conta, contb, i, j, k, h, cont, res, kjA, kjB
      CHARACTER*20        archrs6, archrs7

      !*****OPENING OUTPUT FILES*****

      archrs6 = 'junSAW3D(2).dat'
      archrs7 = 'SAW3D(2).dat'

      OPEN (6, FILE=archrs6)
      OPEN (7, FILE=archrs7)

      !*****INPUT*****
```

```
WRITE(*,*) 'Distance between starting points'
READ(*,*) d
WRITE(*,*) 'Number of steps'
READ(*,*) n
WRITE(*,*) 'Number of iterations'
READ(*,*) it

!*****LIMITS FOR X, Y AND Z*****

maxX=n/5
maxY=n/5
maxZ=n/5
minX=-n/5
minY=-n/5
minZ=-n/5

!*****CHAIN GROWTH*****

DO j=1, it                                  !Iteration loop (1)
        cont=0
        xA(1)=0                             !initial position
        yA(1)=0
        zA(1)=0
        xB(1)=0
        yB(1)=d
        zB(1)=0
        nxA(1)=0
        nyA(1)=0
        nzA(1)=0
        nxB(1)=0
        nyB(1)=d
        nzB(1)=0
        DO i=2, n                                   !Number of steps loop (2)
                raA=rand()      !Random number to decide the direction of growth in A
                raB=rand()      !Random number to decide the direction of growth in B
                rbA=rand()      !Random number to decide the sense of growth in A
                rbB=rand()      !Random number to decide the sense of growth in B
                IF (raA>0.6666)         THEN                    ! (A)
                                                kjA=2
                                        ELSE
                                                IF (raA>0.3333)         THEN
                                                                        kjA=1
                                                                ELSE
                                                                        kjA=0
                                                END IF
                END IF                                          ! (A)
                IF (raB>0.6666)         THEN                    ! (B)
                                                kjB=2
                                        ELSE
                                                IF (raB>0.3333)         THEN
                                                                        kjB=1
                                                                ELSE
                                                                        kjB=0
                                                END IF
                END IF                                          ! (B)
```

```
! kj = 0, movement in X
! kj = 1, movement in Y
! kj = 2, movement in Z

!NEW xA
IF (kjA==0)      THEN                                          ! (2A)
                      IF (rbA>0.5)    THEN                     ! (3A)
                                                  xA(i)=xA(i-1)+1
                                      ELSE
                                                  xA(i)=xA(i-1)-1
                      END IF                                   ! (3A)
                 ELSE
                      xA(i)=xA(i-1)
END IF                                                         ! (2A)
IF (xA(i)>maxX .OR. xA(i)<minX)        THEN
                                            xA(i)=xA(i-1)
END IF

!NEW xB
IF (kjB==0)      THEN                                          ! (2B)
                      IF (rbB>0.5)    THEN                     ! (3B)
                                                  xB(i)=xB(i-1)+1
                                      ELSE
                                                  xB(i)=xB(i-1)-1
                      END IF                                   ! (3B)
                 ELSE
                      xB(i)=xB(i-1)
END IF                                                         ! (2B)
IF (xB(i)>maxX .OR. xB(i)<minX)        THEN
                                            xB(i)=xB(i-1)
END IF

!NEW yA
IF (kjA==1)      THEN                                          ! (2A)
                      IF (rbA>0.5)    THEN                     ! (3A)
                                                  yA(i)=yA(i-1)+1
                                      ELSE
                                                  yA(i)=yA(i-1)-1
                      END IF                                   ! (3A)
                 ELSE
                      yA(i)=yA(i-1)
END IF                                                         ! (2A)
IF (yA(i)>maxY .OR. yA(i)<minY)        THEN
                                            yA(i)=yA(i-1)
END IF

!NEW yB
IF (kjB==1)      THEN                                          ! (2B)
                      IF (rbB>0.5)    THEN                     ! (3B)
                                                  yB(i)=yB(i-1)+1
                                      ELSE
                                                  yB(i)=yB(i-1)-1
                      END IF                                   ! (3B)
                 ELSE
                      yB(i)=yB(i-1)
END IF                                                         ! (2B)
```

```
        IF (yB(i)>maxY .OR. yB(i)<minY)        THEN
                                                    yB(i)=yB(i-1)
        END IF

        !NEW zA
        IF (kjA==2)     THEN                                          ! (2A)
                              IF (rbA>0.5)     THEN                   ! (3A)
                                                  zA(i)=zA(i-1)+1
                                               ELSE
                                                  zA(i)=zA(i-1)-1
                              END IF                                  ! (3A)
                         ELSE
                              zA(i)=zA(i-1)
        END IF                                                        ! (2A)
        IF (zA(i)>maxZ .OR. zA(i)<minZ)        THEN
                                                    zA(i)=zA(i-1)
        END IF

        !NEW zB
        IF (kjB==2)     THEN                                          ! (2B)
                              IF (rbB>0.5)     THEN                   ! (3B)
                                                  zB(i)=zB(i-1)+1
                                               ELSE
                                                  zB(i)=zB(i-1)-1
                              END IF                                  ! (3B)
                         ELSE
                              zB(i)=zB(i-1)
        END IF                                                        ! (2B)
        IF (zB(i)>maxZ .OR. zB(i)<minZ)        THEN
                                                    zB(i)=zB(i-1)
        END IF

!*****SAW RESTRICTIONS*****

        conta=0
        contb=0
        DO k=1, i-1                                                   !(1)
              IF (xA(i)==xA(k))          THEN
                                            leoxa(i,k)=1
                                         ELSE
                                            leoxa(i,k)=0
              END IF
              IF (yA(i)==yA(k))          THEN
                                            leoya(i,k)=1
                                         ELSE
                                            leoya(i,k)=0
              END IF
              IF (zA(i)==zA(k))          THEN
                                            leoza(i,k)=1
                                         ELSE
                                            leoza(i,k)=0
              END IF
              IF (xB(i)==xB(k))          THEN
                                            leoxb(i,k)=1
                                         ELSE
                                            leoxb(i,k)=0
```

```
        END IF
        IF (yB(i)==yB(k))       THEN
                                        leoyb(i,k)=1
                                ELSE
                                        leoyb(i,k)=0
        END IF
        IF (zB(i)==zB(k))       THEN
                                        leozb(i,k)=1
                                ELSE
                                        leozb(i,k)=0
        END IF
        conta=conta+leoxa(i,k)*leoya(i,k)*leoza(i,k)
        contb=contb+leoxb(i,k)*leoyb(i,k)*leozb(i,k)
END DO                                                          !(1)

        IF (conta>0)            THEN
                                        xA(i)=xA(i-1)
                                        yA(i)=yA(i-1)
                                        zA(i)=zA(i-1)
                                ELSE
                                        xA(i)=xA(i)
                                        yA(i)=yA(i)
                                        zA(i)=zA(i)
        END IF
        IF (contb>0)            THEN
                                        xB(i)=xB(i-1)
                                        yB(i)=yB(i-1)
                                        zB(i)=zB(i-1)
                                 ELSE
                                        xA(i)=xA(i)
                                        yB(i)=yB(i)
                                        zB(i)=zB(i)
        END IF
END DO                                  !Number of steps loop (2)


!*****ELIMINATING REPEATED POINTS*****

h=1
k=1
DO WHILE (h<=n)                                         !(2)
        h=h+1
        k=k+1
IF (xA(h)==nxA(k-1) .AND. yA(h)==nyA(k-1) .AND. zA(h)==nzA(k-1)) THEN
                                                        k=k-1
                                                                ELSE
                                                        nxA(k)=xA(h)
                                                        nyA(k)=yA(h)
                                                        nzA(k)=zA(h)
END IF
END DO                                                  !(2)
ca(j)=k-1
h=1
k=1
DO WHILE (h<=n)                                         !(2)
        h=h+1
```

```
                k=k+1
            IF (xB(h)==nxB(k-1) .AND. yB(h)==nyB(k-1) .AND. zB(h)==nzB(k-1)) THEN
                                                                    k=k-1
                                                                        ELSE
                                                                    nxB(k)=xB(h)
                                                                    nyB(k)=yB(h)
                                                                    nzB(k)=zB(h)
            END IF
            END DO                                                  !(2)
            cb(j)=k-1

        !*****FINAL SAW*****

        DO i=1, ca(j)
            WRITE(7,*) nxA(i), nyA(i), nzA(i), j, 'A'
        END DO
        DO i=1, cb(j)
            WRITE(7,*) nxB(i), nyB(i), nzB(i), j, 'B'
        END DO

        !*****NUMBER OF JUNCTIONS*****
        DO k=1, ca(j)                                               !(1)
            DO h=1, cb(j)                                           !(2)
                IF (nxA(k)==nxB(h))     THEN                        !X
                                            ABx(k,h)=1
                                        ELSE
                                            ABx(k,h)=0
                END IF                                              !X
                IF (nyA(k)==nyB(h))     THEN                        !Y
                                            ABy(k,h)=1
                                        ELSE
                                            ABy(k,h)=0
                END IF                                              !Y
                IF (nzA(k)==nzB(h))     THEN                        !Z
                                            ABz(k,h)=1
                                        ELSE
                                            ABz(k,h)=0
                END IF                                              !Z
                AB(k,h)=ABx(k,h)*ABy(k,h)*ABz(k,h)
                cont=cont+AB(k,h)
            END DO                                                  !(2)
        END DO                                                      !(1)
        WRITE(*,*) cont, ca(j), cb(j)
        jun(j)=cont
END DO                                                              !Iterations loop (1)

DO k=1, it
        WRITE(6,*) jun(k), ca(k), cb(k)
END DO

!*****CLOSING OUPUT FILE*****

CLOSE (6, STATUS='KEEP')
CLOSE (7, STATUS='KEEP')

END PROGRAM SAW3Dv2
```

Some results from this program are given in Figures B.9 to B.13.

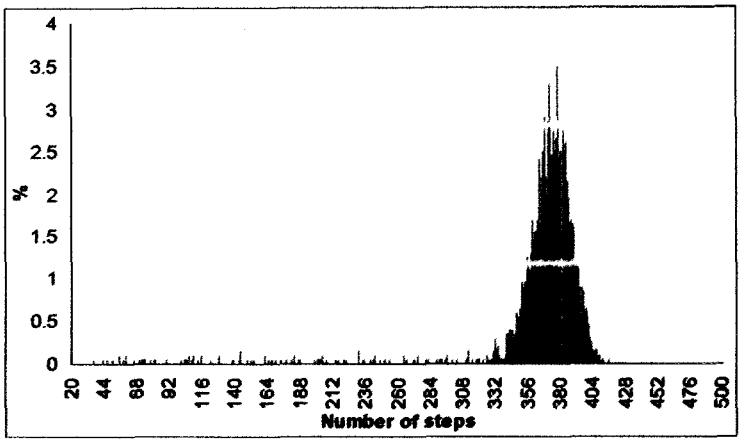

Figure B.9. Chains' length distribution.

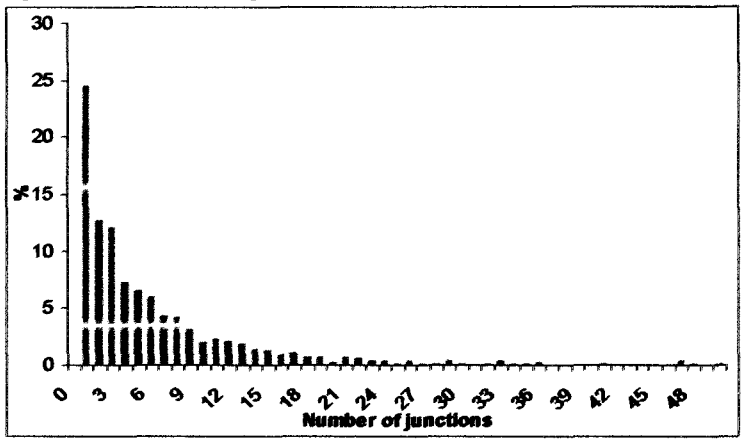

Figure B.10. Number of junctions distribution using d = 0.

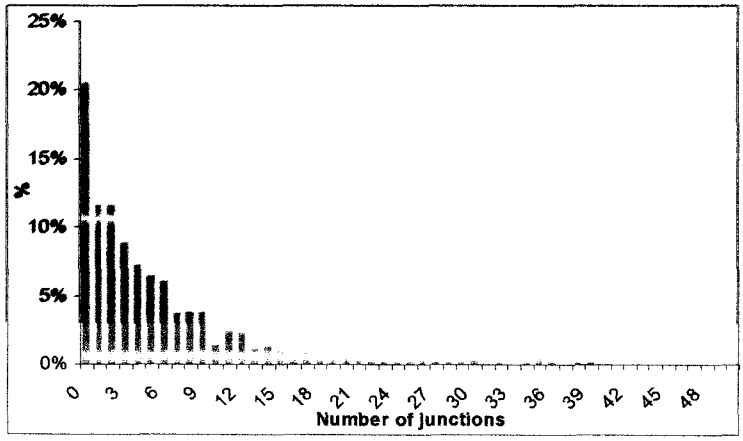

Figure B.11. Number of junctions distribution using d = 1.

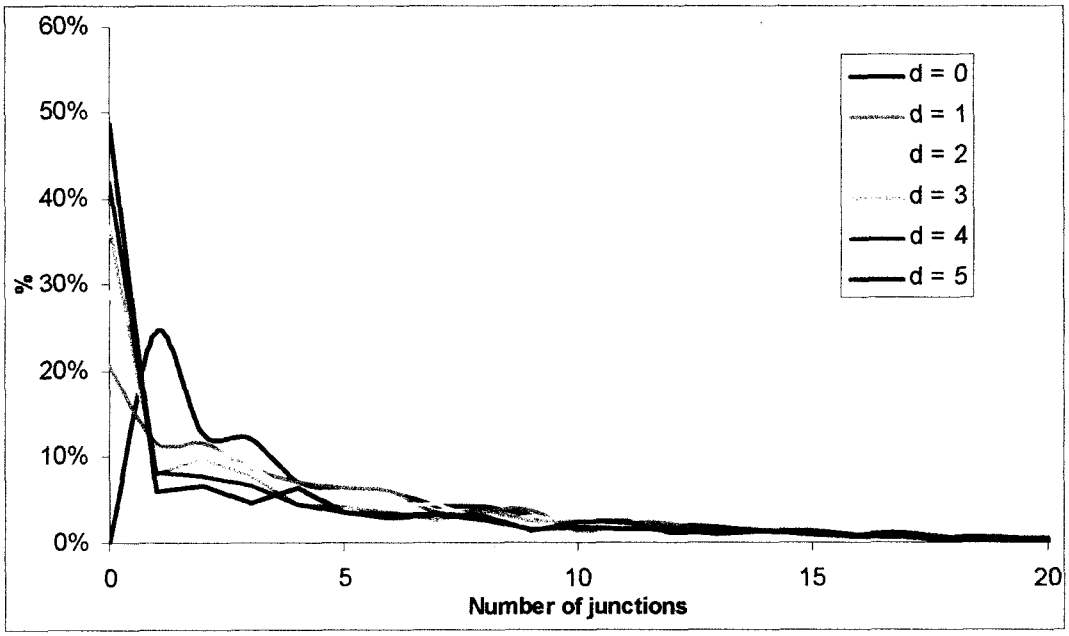

Figure B.12. Percentage of probability of a number of junctions for different distance between starting points.

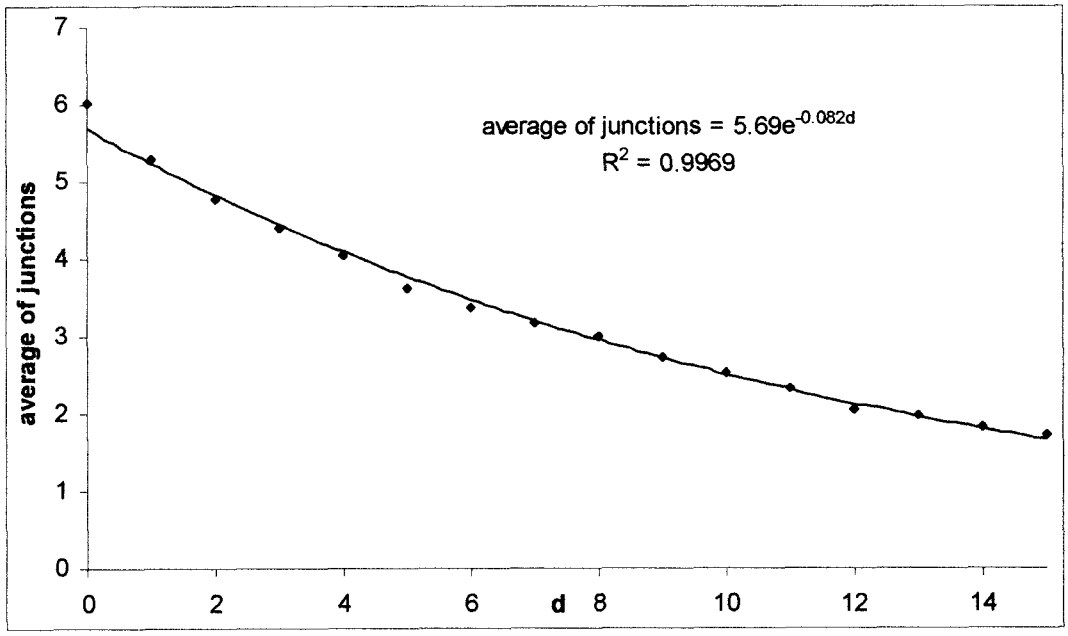

Figure B.13. Relationship between the average of junctions and distance (d) for different number of steps (t).

Appendix C. Rheometers Procedures

A. Parallel Plate Rheometer

1. Equipment description

Constant Strain Rheometer RDA II Rheometrics Dynamics Analyzet.

Rheometrics Scientific (RSI) software.

Configuration: Parallel plates.

Geometry: 25 mm in diameter.

2. Safety precautions

- ⇨ The use of heat resistant gloves is recommended, since the oven and test fixtures are hot when testing at elevated temperatures.
- ⇨ A cryogenic hazard exists, since sub-ambient temperature testing involves the use of liquid nitrogen. Transfer lines, oven chamber and its contents may be extremely cold. Use appropriate gloves when working around these areas.
- ⇨ The torque transducer is sensitive to axial and normal forces and can be damaged if overloaded. Pay close attention to torque and normal force indicators when performing the following:
    1. Turning on motor drive; if a sample is loaded when energizing the motor drive, the torque transducer will be damaged.
    2. Attaching or removing test fixtures.
    3. Loading or unloading test specimens.
    4. Cleaning test fixtures.

3. Sample preparation

a. Weight 30.0 grams of polymer pellets and 0.03 grams of 2-6 di-tert-butyl-p-cresol (BHT) on analytical balance. BHT concentration can be 1000 ppm up

to 2% in weight. Polypropylene fluff samples first need to be stabilized with irganox 1076 in a ratio of 15 grams of fluff to 7 mll of Irganox.

b. Pour polymer pellets and BHT on grinder (coffee mill).
c. Cut two sheets of Mylar and place them over the metal plates.
d. Press mixer bottom for 1 second and then interrupt the mixing by depressing it. Do this 5 times.
e. Place the appropriate (1 or 2 mm) thickness sample plate (mold plate) over one of the metal plates with Mylar over it.
f. Place the mixed pellets over the sample plate holes and square.
g. Place the Mylar sheet and the other metal plate over the mould plate (with polymer pellets poured on it).
h. Mold press 25 mm diameter disks with minimum thickness of 2.5 mm by leaving 2 minutes of pre-heating at 5,000 psi and 375 - 400 °F in mold, then 2 minutes of compression by increasing mold pressure up to 25,000 psi.
i. Using gloves, take away steel plates from the mold press and leave them to bench cooling for 15 minutes.
j. Separate the plates, and take away sampling material from the mold. Cut off sample material.
k. Take away Mylar from the steel plates and clean them using spatula.

4. System start-up

a. Clean parallel plates.
b. Install lower tool thermocouple (sample temperature is monitored by lower tool thermocouple).
c. At the front panel of the rheometer, set thermocouple jumper to "Computer/Tool".
d. Tight upper and bottom fixtures with 25 mm plates correctly (with motor power off). Ensure normal force not to exceed ±10%.
e. Lower plates until contact is made and inspect visually to ensure concentricity (how parallel plates are).

f. Turn the motor off, and freely turn the lower fixture plate to see if gap is changing (no change in gap ensures concentricity).
g. Separate the plates.
h. At the back of the rheometer, check nitrogen pressure settings for the oven (while closed) is at 40 psi and transducer pressure is at 35 psi.
i. Turn main power of the system control on.
j. Turn main power of the control computer on.
k. Checking that no sample is loaded, turn motor power on. Make sure that there is no sample loaded in the fixtures prior to energizing the motor, otherwise damage to transducer will occur.
l. Verify that both, torque and normal indicators are at cero.
m. Being in the RSI software environment, in user login choose the RAA or the RDA II equipment.
n. Configure instrument to control temperature by the oven by selecting in utilities window: service, instrument configuration, temperature control loop, and oven air temperature.
o. Verify status to be ok and in dynamic mode. Otherwise, set motor mode to "dynamic" in control Window (verifying that no sample is loaded and that the parallel plates aren't together).
p. Raise top plate approximately 1 mm to allow for fixture expansion during the heating process.
q. Close the oven, making sure that both upper and lower baffles are in the right position (so that insulation is ensured). Make sure that the upper baffle is not touching the oven, since this would cause a normal force that can damage the equipment.
r. Set temperature in panel icon. At the start of the heating process, the setpoint should be 50 °C more than the test temperature. Once temperature has achieved 5 °C less than the test temperature, the actual setpoint is set to a slightly higher temperature (5°C more) than the desired test temperature.

s. Once temperature has equilibrated (1/2 hour), adjust plates to zero gap by turning knob slowly until parallel plates touch each other (identified by the last zero normal force while approaching parallel plates).

t. Reset gap indicator.

u. In start icon save the test file following the test conditions.

v. Press exit test bottom (do not begin test).

Table C.1. Frequency sweep test conditions

VARIABLE	TEST CONDITIONS
Test type	Frequency Sweep (dynamic mode)
Test name	Frequency Sweep for all Polymers
Location	C:\RSIOrche600\Data\Polymers
Geometry	25 mm Parallel Plate
Gap	1 mm
Strain	10 % (standard)
Sweep type	logarithmic
Sweep range	500 to 0.01 rad/sec
Points per decade	4
Correlation Delay	0.5 cycles
Temperature Loop Control	Oven air temperature
Temperature monitor	Lower tool thermocouple (set jumper to Computer/Tool)

5. Specimen loading

a. Open oven, raise upper plate enough so that specimen can be inserted (3 mm maximum).

b. Place the specimen between the plates. Safety precautions should be taken, since oven is hot).
c. Close the oven.
d. Lower upper plate until contact is made with specimen and close oven. 50% of normal force will ensure full contact.
e. Allow 5 minutes for specimen preheating, then lower upper plate to 1.05 or 2.05 mm gap (depending on the specimen thickness).
f. Allow normal force to diminish to 30% or less before trimming specimen.
g. Open oven and trim excess material away from plates.
h. Lower upper plate to 1.0 or 2.0 mm final gap (final gap should be a little less than the specimen thickness), close oven.
i. Allow additional 5 minutes for temperature equilibrium prior to testing (± 0.2 °C from setpoint).
j. Ensure that the normal force is less than 10% before beginning test.

Note: each time oven is opened, setpoint should be raised 50 °C more than the actual temperature, to achieve testing temperature again. Once the temperature has returned to its setpoint temperature, re-adjust the setpoint to this desired value.

6. Begin test

a. In start icon, verify that the testing conditions are the desired ones. Then press begin test bottom. The start icon (in green) should change to stop icon (in red).
b. The view icon is for choosing between results in graph format or in table format. Display results in a table that shows frequency, G', G", G*, Eta*, Tan Delta, Temperature, and Torque.
c. The torque resolution is more than 2 gr cm, but leave resulting data with torque greater than 0.8 gr cm. Eliminate data with a lower torque.

d. Once test is finished, calculate the point at which G' (storage modulus) and G" (loss modulus) intersect by selecting analysis, then G'/G" crossover, and finally, stamp crossover modulus and frequency on graph option.
e. Once test is finished, fit viscosity data by selecting viscosity curve by double clicking on curve itself, then select curve fit window, followed by fit data to model, viscosity models, carreau model, fit, save fit, and stamp fit on graph.

➔ To save the results file in an ASC II format (*.txt), choose the export option in the file window.

7. Equipment clean up

a. Separate the gap slowly up to 3 mm (check normal force).
b. Open oven, separate still more the plates, and clean plates using a spatula and a brass brush.
c. Clean plates by wiping them with isopropyl alcohol.
d. Close gap to 3 mm and close oven again.
e. If no more tests are to be done, lower the temperature setpoint to 25 °C, then wait until the rheometer cools down. Finally, turn off the system control, the motor, the gap gage, and the control computer.

8. Emergency shut down procedure

a. Turn off the test station motor, system control, and the control computer of the rheometer.
b. Determine if a test specimen is loaded (open oven chamber and visually determine it).
c. Remove test specimen.
d. Open oven chamber.

e. Loosen the top (transducer) and bottom (motor actuator) test fixture clamps (thumbs screws located on the right side of the motor actuator and transducer clamps).
f. Raise the torque transducer platform up with the hand crank located on the right side of the test station and remove the test fixtures. Monitor the normal force meter while raising the torque transducer platform. The control computer should be turned back on to monitor the normal force. If the top fixture clamp is not lose enough to allow the fixture to slide out of the clamp, transducer overloading may occur.
g. Turn off the gas chiller if applicable.
h. Turn off the computer, the nitrogen filters, the printer and plotter.
i. Unplug all electrical cards.
j. Block in the nitrogen supply.
k. Block in liquid nitrogen if applicable.

B. Capillary Rheometer

1. Equipment description

Rosand Capillary Rheometer
Model RH7-2
Double Bore
Barrel Diameter: 15 mm
Available Pair of Capillary Dies:

➔	Diameter:	0.5 mm
	Entrance Type:	90 °
	Short Die Lenght:	0.25 mm
	Long Die Lenght:	8 mm

➔ Diameter: 1.0 mm
Entrance Type: 90 °
Short Die Length: 0.25 mm
Long Die Lenght: 16 mm

➔ Diameter: 1.0 mm
Entrance Type: 180 ° (Flat)
Short Die Lenght: 0.25 mm
Long Die Lenght: 16 mm

➔ Diameter: 0.5 mm
Entrance Type: 90 °
Short Die Lenght: 0.25 mm
Long Die Lenght: 24 mm

2. Safety precautions

⇨ The use of heat resistant gloves is necessary, especially while changing dies and cleaning the barrel and pistons.

⇨ Keep hands clear of crosshead while operating the equipment.

⇨ Care must be taken when initially lowering pistons into barrels so as not to bend the pistons or overload the transducer. Monitor transducer load and ensure that the pistons are properly inserted into the barrels.

3. Test Setup

a. Open the Dr. Rheology software in the computer.

b. Ensure that the proper dies and tranducer are assigned in the software.

c. Indicate the desire temperature and allow enough time to temperature equilibrium.

d. Go to the pretest section, and introduce a preheat-compression-preheat-compression stage to ensure the accuracy of the test.

e. Indicate the velocity range of testing by creating a shear rate schedule.

4. Running tests

a. Ensure that the appropriate transducers are properly installed.
b. Place the short and long dies in the bottom of the barrels.
c. Calibrate and re-zero, using Dr. Rheology software, the pressure transducers.
d. Load the polymer sample into the barrel. Add material in small increments and tamp with the compressing rod.
e. Place the pistons on the crosshead. Lower the crosshead with the pistons until plungers contact the material.
f. Close the crosshead door.
g. Start test.

5. Equipment cleanup

a. Unscrew (turning clockwise) the die fixtures using the iron made plain screw. The fixture will come down, but the capillary die will still be attached to the barrel, since the residual melt holds it to the barrel's walls.
b. Introduce the compressing or tamping brass rod to the barrel's feeding opening and push downwards until the residual melt and capillary die are expunged from the barrel. Care must be taken, since the residual melt and capillary die are extremely hot and can touch your feet when they are expunged. After expunging is done, take away the compressing rod from the barrel. Notice that you can see now through the barrel.
c. In order to clean the barrel as much as possible, introduce the cleaning tube to the barrel's feeding opening using a folded cleaning pad on its tip. After cleaning, take away the cleaning tube from the barrel.
d. See if the barrel is completely clean; if not, repeat previous step as necessary.

C. Controlled Stress Rheometer

1. Equipment description

Constant Stress Rheometer SR5000 Rheometrics.

Rheometrics Scientific (RSI) software.

Configuration: Cone and Plate.

Geometry: 25 mm in diameter.

Cone Angle: 0.0996 radians

Gap: 0.048 mm

Stress limits: 0.239736 to 11,986.77 Pa.

2. Safety precaution

- ⇨ The use of heat resistant gloves is recommended, since the oven and test fixtures are hot when testing at elevated temperatures.
- ⇨ A cryogenic hazard exists, since sub-ambient temperature testing involves the use of liquid nitrogen. Transfer lines, oven chamber and its contents may be extremely cold. Use appropriate gloves when working around these areas.
- ⇨ The torque transducer is sensitive to axial and normal forces and can be damaged if overloaded. Pay close attention to torque and normal force indicators when performing the following:
    1. Attaching or removing test fixtures.
    2. Loading or unloading test specimens.
    3. Cleaning test fixtures.

3. Sample preparation

a. Weight 30.0 grams of polymer pellets and 0.03 grams of 2-6 di-tert-butyl-p-cresol (BHT) on analytical balance. BHT concentration can be 1000 ppm up to 2% in weight.

b. Pour polymer pellets and BHT on grinder (coffee mill).

c. Cut two sheets of Mylar and place them over the metal plates.
d. Press mixer bottom for 1 second and then interrupt the mixing by depressing it. Do this 5 times.
e. Place the appropriate (1 or 2 mm) thickness sample plate (mold plate) over one of the metal plates with Mylar over it.
f. Place the mixed pellets over the sample plate holes and square.
g. Place the Mylar sheet and the other metal plate over the mould plate (with polymer pellets poured on it).
h. Mold press 25 mm diameter disks with minimum thickness of 2.5 mm by leaving 2 minutes of pre-heating at 5,000 psi and 375 - 400 °F in mold, then 2 minutes of compression by increasing mold pressure up to 25,000 psi.
i. Using gloves, take away steel plates from the mold press and leave them to bench cooling for 15 minutes.
j. Separate the plates, and take away sampling material from the mold. Cut off sample material.
k. Take away Mylar from the steel plates and clean them using spatula.

4. System start-up

a. Insure proper nitrogen pressure to air bearing and flow to oven purge. Air bearing regulator should be 80 psi minimum and oven flow meter 20 psi, inlet pressure to filter should be 60 psi.
b. Load Rheometric's Orchestrator Software vis RSI Orchestrator Icon.
c. Turn on heater on rheometer.
d. Set operating temperature on software.
e. Allow 30 minutes for temperature equilibration.
f. Set up desired test conditions at start buttom icon in Rheometrics Software

5. Zeroing the gap

a. Unlock shaft mechanism in the rheometer.
b. Press gap icon in rheometrics software, introduce 0.048 mm of gap.

c. Press *zero* fixture buttom.
d. Verify that the gap reader in the rheometer indicates 0.048.
e. Press exit buttom in the zeroing gap window.

6. Specimen loading

a. Insure that the drive shaft is locked; turn carfuly shaft clockwise until flat face faces the locking mechanism.
b. Move to 1.5 mm gap to load sample.
c. Raise measuring geometry and oven cover, and using tweezers insert specimen on lower plate.
d. Lower measuring geometry until contact with specimen is made, then lower oven cover back into place; lower gap if necessary to about 1.5 mm).
e. Pre-heat specimen for 2 minutes.
f. Lower measuring geometry to specified gap (0.052 mm).
g. Raise oven cover and trim excess polymer away from plates. Use aluminum trimming tool.
h. Lower oven cover back into place.
i. Reduce gap to 0.048 mm if necessary.
j. Unlock drive shaft.
k. Equilibrate temperature for 2 minutes.
l. Start test.

7. Equipment cleanup

a. Separate the gap slowly up to 1.5 mm (check normal force).
b. Insure that the drive shaft is locked.
c. Raise gap to about 0.5 mm
d. Raise oven and measuring geometry.
e. Clean cone and plate using aluminum spatula and special metal brush
f. Clean plates by wiping them with isopropyl alcohol.
g. Close oven again.

h. If no more tests are to be done, lower the temperature setpoint to 25 °C, then wait until the rheometer cools down.